FLUID INCLUSION GEOCHEMISTRY OF SELECTED EPIGENETIC, LOW TEMPERATURE MINERALIZATION IN THE U.K.

MARIA CHRISTOULA

B.Sc., M.Sc., D.I.C.

Thesis submitted for the degree of
Doctor of Philosophy
of the University of London

Imperial College of Science, Technology and Medicine
Royal School of Mines
Department of Geology

August 1992

BIBL LONDON UNIV

To my parents

Στους γονεις μου

Abstract

This thesis is a study of aspects of fluid processes involved in the genesis of Pb-Zn and Cu-Fe epigenetic, sediment-hosted mineralization in Britain. Areas studied include the North and South Pb-Zn-fluorite Pennine orefields, the Cu-rich Ecton Hill deposit and the Fe-mineralization at Llanharry, South Wales. Comparative studies on the granite-related, fluorite mineralization at South Crofty, Cornwall are also carried out. The main aim of the research has been to provide an understanding of the physical and chemical conditions under which the ore-fluids associated with these deposits originated and evolved. These aspects are investigated using evidence from detailed microthermometric and chemical analyses of fluid inclusions in fluorite and calcite samples. The Decrepitation-ICP and destructive Neutron Activation Analysis methods were used for the determination of the Na-K-Li and Cl-Br contents of fluid inclusions. Apart from the microthermometry and chemical analysis of fluid inclusions, a sulphur isotope study in samples from the Ecton Hill deposit was also undertaken.

The fluid inclusion microthermometric evidence for the Pennine, Ecton Hill and, to a lesser extend, the Llanharry samples demonstrates the remarkable uniformity of the key features, such as temperature, salinity and Na/Ca ratios, of the ore fluids in these areas. The ore-fluids can be described as low-temperature, high salinity Na-Ca-Cl brines similar to those associated with the classical Mississippi Valley-Type (MVT) mineralization. Similar low-temperature high salinity fluids were also encountered in fluorite samples from the late, chlorite stage of the paragenesis at South Crofty, Cornwall. Evidence from the alkali metal concentrations is used as a means to trace the importance of fluid-rock interactions in modifying the chemistry of the ore-forming fluids. The higher K and Li contents of the North Pennine inclusion fluids compared to those of the South Pennines and also of modern day basinal brines, are interpreted as the result of temperature-controlled, fluid-rock interactions with the underlying Weardale granite. This view is further supported by the high K and Li contents of inclusion fluids of the South Crofty samples.

Evidence on the halogen (Cl-Br) signature of the inclusion fluids is used as a means of tracing the origin and evolution of the ore-fluids and to further explore previously proposed similarities between inclusion fluids and modern-day basinal brines. The Cl/Br ratios of the Pennine, Ecton Hill, and Llanharry fluids are well constrained and are generally lower than the seawater ratio of 298. The overall lack of regional variations of the relative Cl-Br fluid contents in the Pennines, Ecton Hill and Llanharry, provide new evidence highlighting the

general homogeneity of ore-fluids associated with both Pb-Zn and Cu-Fe-dominant mineralization. The Cl-Br patterns of inclusion fluids in these areas do not indicate interaction of fluids with halite (i.e. evaporite leaching). They are generally more consistent with a marine source for the fluids with subaerial evaporation as the cause of their high salinity. The low-temperature, high salinity inclusion fluids in late fluorite from South Crofty have Cl/Br ratios comparable with those encountered in the Pennine samples. The results indicate the presence of basinal-brine type fluids at the late stages of the complex hydrothermal events in the region.

The sulphur isotopic composition of sulphide and sulphate samples from the Cu-dominant mineralization at Ecton Hill indicates that seawater of Carboniferous age is the main source of sulphate. The sulphate-sulphide sulphur isotope data are generally consistent with a bacterial sulphate reduction process for the precipitation of sulphides. Overall, the sulphur isotope results are consistent with the patterns defined by the composition of fluid inclusions and they do not indicate interaction of the ore-fluids with the Triassic evaporites of the adjacent Cheshire basin.

Acknowledgments

The present study was undertaken with financial support from the Greek State Scholarships Foundation. Partial financial support during the last year of the study was provided by the British Council. I am grateful to both institutions for providing this opportunity.

This study could not have been made possible without the support from my supervisors Dr. Andy Rankin and Dr. Michael Ramsey. Thank you both for your invaluable academic advice, patience and encouragement throughout the last few years.

My sincere thanks to Dr. Chris Stanley (Natural History Museum) for providing some superb fluorite samples. Many thanks are also due to Mr. Geoff Cox of the Mineral Industry Manpower Unit, and to his wife Elizabeth for the opportunity of sampling at Ecton mine and for their hospitality.

The research has benefited throughout from the advice and technical assistance received from the staff and fellow students at Imperial College. Especially I would like to thank Dr. Chris Halls for initiating my interest and for his advice on the perplexing South Crofty mineralization. I would also like to thank Mick Moser, Drs Jamie Wilkinson, Chris Farmer, Shawn Mulshaw, Ben MacNeilI, and Richard Herrington, for their help and co-operation during the long working hours in the fluid inclusion laboratory. Especially, I owe much to my room-mates, Adrian King, Khurshid Hasan and Rujian Zhao for their support, friendship and for putting-up with me during the last few years.

I would like to thank Mr. Barry Coles and Mr. Alban Doyle for their patient technical assistance and advice for the ICPAES analysis of fluid inclusions. Miss Lizz Morris and Miss Gill Ragg are also thanked for preparing the excellent polished thin wafers used in fluid inclusion microthermometry. Many thanks are also due to Mr. Adolpho Cash from the photography section for his willingness to help even at very short notice.

The sulphur isotopic analyses were carried out at the Stable Isotope Laboratories of the NERC Isotope Geosciences Laboratory, Keyworth. Without the support and invaluable academic advice provided by Dr. Baruch Spiro, the study could not have been undertaken.

The Neutron Activation Analysis was undertaken at the Imperial College Reactor Center, Silwood Park. The experiments could not have been carried out without the guidance and support provided by Dr. Susan Parry, Mr. Brian Bennett and Mrs. Georgina Coe.

To my friends, Antonis, Cleo, George, Nana, and Stella for being there during the ups and downs of the last few years, thank you all. To Andreas, just thanks is not enough, somehow we made it.

To my parents for their love and continuous support throughout my studies, I dedicate this thesis.

List of Figures 6

List of Tables 13

List Of Plates 14

Chapter 1 Introduction 15

1.1 Introduction 15

1.2. Aims and Objectives of Research 16

1.3. Thesis Outline 17

Chapter 2

Review of the main geological characteristics and genetic models for carbonate-hosted epigenetic mineralization with special reference to UK examples 19

2.1. Introduction 19

2.2. Geological Setting of Mississippi Valley-Type Deposits 20

2.2.1. Host Rocks 20

2.2.2. Ore Mineralogy 20

2.2.3. Isotope Geochemistry 22

2.2.4. Nature of Ore Fluids 24

2.3. Models for Ore Genesis 25

2.3.1. Dynamics of Fluid Flow 25

2.3.2. Ore-Transport and Deposition 28

2.4. Epigenetic Sediment-Hosted Mineralization in the U.K. 31

2.4.1. Geological Setting of the Pennine Orefields 31

2.4.1.1. The North Pennine Orefields (Alston and Askrigg) 33

2.4.1.1.1. Host Rock Geology 33

2.4.1.1.2. Igneous Rocks.....36

2.4.1.1.3. Ore Mineralogy.....38

2.4.1.1.4. Isotope studies.....39

2.4.1.2. The South Pennine Orefield.....40

2.4.1.2.1 Host-Rock Geology.....42

2.4.1.2.2. Volcanics.....42

2.4.1.2.3. Ore Mineralogy.....43

2.4.1.2.4. Isotope Studies.....44

2.4.1.3. Cu-dominant Mineralization.....45

2.4.2. Theories for ore-genesis in the Pennines.....46

2.4.2.1. Models involving rising juvenile fluids.....46

2.4.2.2. Descending brines from Triassic evaporites.....47

2.4.2.3. Brines Expelled from Sedimentary Basins.....48

2.4.3. The Llanharry Iron Deposit, South Wales.....51

2.5. Granite-Related, Fluorite Mineralization South Crofty, Cornwall....53

2.6. Summary.....57

Chapter 3 Development and evaluation of experimental methods for the chemical analysis of ionic species in fluid inclusions.....58

3.1. Introduction.....58

3.2. Samples Studied.....59

3.3. The Decrepitation ICP (D-ICP) method.....60

3.3.1. Experimental System and Sample Preparation.....61

3.3.2. Calibration, Sensitivity and Detection limits.....61

3.3.3 Review of mechanisms of material transfer into the plasma . 64

3.3.4. Time resolved D-ICP 64

3.3.5. Quality Control 65

3.3.5.1. Alkali Metals and Alkaline Earths 66

3.3.5.2. Analysis Of Variance (ANOVA) 73

3.3.5.3. Base Metals and Sulphur 73

3.3.6. Time-Resolved Profiles 77

3.4. Neutron Activation Analysis (NAA) 83

3.4.1. Experimental System and Sample Preparation 85

3.4.2. Experimental Procedure 86

3.4.3. Appraisal of the Results 88

3.5. Summary and general conclusions 90

Chapter 4 Fluid Inclusion Microthermometry 92

4.1. Introduction 92

4.1.1. Aims of microthermometric analysis 92

4.1.2 Nomenclature 100

4.2. Previous Work 100

4.2.1. Previous work in the Pennines and South Wales 101

4.2.2. South Crofty 102

4.3. Equipment for microthermometry 104

4.4. Methodology 104

4.5. Microthermometric Results 108

4.5.1. Pennines 108

4.5.2. Llanharry, South Wales 117

4.5.3. South Crofty, Cornwall 121

4.5.4. Temperature-Salinity Relationships..... 126

4.5.5. $NaCl/CaCl_2$ ratios..... 131

4.6. Summary of results and conclusions..... 138

Chapter 5 Alkali and Halogen Geochemistry of Fluid Inclusions..... 141

5.1. Introduction 141

5.2. Summary of previous work 142

5.3 Methodology of present work 142

5.4. The Na-K-Li contents of fluid inclusions 143

5.4.1. Interpretation of Results..... 146

5.4.2. Factors controlling the concentration of Li in subsurface waters and inclusion fluids. 149

5.4.3. Alkali Geothermometry 152

5.5. Cl-Br contents of sedimentary brines and fluid inclusions..... 156

5.5.1. Controls on the Cl/Br ratios of sedimentary brines 156

5.5.2. Cl-Br relationships in Fluid Inclusions..... 160

5.5.2.1. Pennines and South Wales..... 161

5.5.2.2. South Crofty, Cornwall 165

5.6. Cation-Bromide relationships 168

5.7. Summary of results and general discussion 174

5.8. Implications for the source and evolution of mineralizing fluids in the

Pennine orefields 175

Chapter 6 A Sulphur Isotope Study on the Ecton Hill Cu Deposit..... 181

6.1. Introduction 181

6.2. Geological Background 181

6.3. Previous work..... 185

6.3.1 North Pennines 185

6.3.2. South Pennines 186

6.3.3. Red Bed Cu-mineralization in the Cheshire Basin..... 187

6.4. Sulphur isotope distribution in the Ecton Hill deposit. 188

6.4.1. Experimental procedure 188

6.4.2. Results and Discussion. 189

6.5. Concluding Remarks 194

Chapter 7 Conclusions and recommendations for further work 196

7.1 Concluding Remarks 196

7.2. Recommendations for further work..... 200

References..... 202

Appendix A 223

Appendix B 229

Appendix C 250

List of Figures

Fig.2.1.	Sketch-map of the U.S.A. showing the location of Mississippi Valley-Type (MVT) Lead-Zinc districts and their spatial relationship with major sedimentary basins (after Cathles & Smith 1983).	21
Fig.2.2.	Diagram showing the $\delta^{18}O$-δD isotopic composition of seawater, meteoric, magmatic, and metamorphic waters, selected oil-field brines and inclusion fluids from MVT deposits (after Taylor 1974).	23
Fig.2.3a.	Schematic representation of conceptual model for gravity-driven fluid flow in sedimentary basins (after Garven & Freeze 1984).	27
Fig.2.3b.	Schematic representation of conceptual stratigraphic model showing overpressured sandstones and siltstones in overpressured shale sequences near basin margins (after Fowler & Anderson 1991).	27
Fig.2.4.	Sketch-map showing the major Dinantian carbonate-hosted orefields in Britain (after Plant et. al. 1988).	32
Fig.2.5.	Sketch-map showing the main geological formations, structural features, mineral veins and subdivisions of the North Pennine (Alston) orefield (Tyne to Stainmore), (after Dunham 1992).	34
Fig.2.6.	Sketch-map of the North Pennine (Askrigg) orefield (Stainmore to Craven) showing the main geological formations and subdivisions of the field (after Dunham & Wilson 1985).	35
Fig.2.7.	Sketch-map illustrating the spatial relationship between buried granites and fluorite mineralization in the two North Pennine orefields (after Colman et. al. 1989a).	37
Fig.2.8.	Sketch-map showing the major geological formations in the South Pennine (Derbyshire) orefield (after Aitkenhead et. al. 1985).	41
Fig.2.9a.	Schematic representation of proposed genetic model for mineralization in the South Pennines (after Worley & Ford 1977).	49

Fig.2.9b. Schematic representation of proposed genetic model for mineralization in the North Pennines (after Solomon et. al. 1971). 49

Fig.2.10. Sketch-map showing the location, general morphology and geological setting of the Llanharry-iron deposit in South Wales (after Rankin & Criddle 1985). 52

Fig.2.11. Location map of the South Crofty Mine, Cornwall (after Farmer & Halls 1992). 54

Fig.3.1. Schematic representation of the Decrepitation-ICP furnace system used in the present study. 62

Fig.3.2. Frequency distribution of the K/Na and Li/Na weight ratios of fluid inclusions obtained from replicate D-ICP analyses in two fluorite samples. 70

Fig.3.3. Control charts showing the variation of the K/Na weight ratios obtained from replicate D-ICP analyses of fluid inclusions in five fluorite samples. 71

Fig.3.4. Control charts showing the variation of the Li/Na weight ratios obtained from replicate D-ICP fluid inclusion analyses in five fluorite samples. 72

Fig.3.5. Comparison of K/Na and Li/Na weight ratios obtained from D-ICP and crush-leach ICP analysis of fluid inclusions. Error bars corresponding to one standard deviation are given for data points representing means of replicate analyses. 74

Fig.3.6. Representative profiles showing the morphology and time-intervals of the Na, Ca, K and Li responses obtained from time-resolved D-ICP analysis of fluid inclusions in fluorite. 78

Fig.3.7. D-ICP time-resolved profiles showing the morphology of the Pb and S peaks obtained from a trial contamination D-ICP run in speck pure silica smeared with PbS grains. 80

Fig.3.8. Comparison of time-resolved profiles for Na and Pb obtained from D-ICP analysis of ordinarily washed and electrolytically-cleaned fluorite samples. 81

Fig.3.9. Comparison of time-resolved profiles for Na and sulphur obtained from D-ICP analysis of ordinarily washed and electrolytically cleaned samples. 82

Fig.3.10. Flow-chart showing the experimental procedure followed in the present study for the determination of Cl, Na, and Br in fluid inclusions by Neutron Activation Analysis. 87

Fig.3.11. Comparison of the a) Cl/Br and b) Na/Br weight ratios obtained from destructive Neutron Activation Analysis (RNAA) and a combination of ion-chromatography with crush-leach ICP and Cl-selective electrode. Error bars corresponding to one standard deviation are given for data points representing means of replicate analyses. 89

Fig.4.1. Schematic representation of idealized distribution of primary, secondary and pseudosecondary fluid inclusions (after Shepherd et. al. 1985a) 93

Fig.4.2. Sketch-map showing the outline of the fluorite zone, the major structural features, veins and main sample sites in the Alston orefield, North Pennines (map redrawn from Dunham 1992). 95

Fig.4.3. Sketch-map showing the outline of fluorite-dominant areas, major structural features and mineral veins and sample sites in the Askrigg orefield, North Pennines (map redrawn from Dunham & Wilson 1985). 96

Fig.4.4. Sketch-map showing the main geological formations, mineral veins and main sample sites in the South Pennine (Derbyshire) orefield. 97

Fig.4.5. Schematic representation of heating-freezing cycles followed in microthermometric analysis of fluid inclusions. 107

Fig.4.6. Histograms showing the frequency distribution of fluid inclusion homogenization temperatures (T_H) in samples from the three Pennine orefields. 110

Fig.4.7. Histograms showing the frequency distribution of a) homogenization (T_H), b) first melt (T_{FM}), c) hydrate ($T_M h$) and d) ice melting (T_{LM}) temperatures of fluid inclusions in calcites from Ecton Hill. 111

Fig.4.8. Histograms showing the frequency distribution of first melting temperatures (T_{FM}) of fluid inclusions in samples from the three Pennine orefields. 114

Fig.4.9. Histograms showing the frequency distribution of hydrate melt temperatures ($T_M h$) of fluid inclusions in samples from the three Pennine orefields. 116

Fig.4.10. Histograms showing the frequency distribution of last ice melting temperatures (T_{LM}) of fluid inclusions in samples from the three Pennine orefields. 118

Fig.4.11. Histograms showing the frequency distribution of total salinities (eq. wt% NaCl) of fluid inclusions in samples from the three Pennine orefields. 119

Fig.4.12. Histograms showing the frequency distribution of a) homogenization (T_H), b) first melt (T_{FM}), c) hydrate ($T_M h$) and d) ice melting (T_{LM}) temperatures of fluid inclusions in quartz and calcite samples from the Llanharry Fe-deposit, South Wales. 122

Fig.4.13. Histograms showing the frequency distribution of a) homogenization, (T_H), b) first melt, (T_{FM}), c) hydrate ($T_M h$) and d) ice melting (T_{LM}) temperatures of fluid inclusions in fluorite samples from the late chlorite stage of mineralization at South Crofty, Cornwall. 125

Fig.4.14. Bivariate, homogenization temperature-salinity plots for fluid inclusions in samples from the a) Alston, b) Askrigg, c) South Pennines and Ecton Hill mineralized districts. 127

Fig.4.15. Bivariate, homogenization temperature- total salinity plot for fluid inclusions in quartz and calcite samples from the Llanharry Fe-rich deposit in South Wales. 129

Fig.4.16. Bivariate, homogenization temperature-total salinity plot for fluid inclusions in fluorite from the late, chlorite stage of mineralization at South Crofty, Cornwall. 130

Fig.4.17. Triangular plots showing the range of the relative NaCl-$CaCl_2$ contents of fluid inclusions from the North Pennine orefields (Alston and Askrigg) as estimated from paired hydrate ($T_M h$) and ice (T_{LM}) melting temperatures. Isotherms for the H_2O-NaCl-$CaCl_2$ system, after Oakes et. al. (1990). 135

Fig.4.18. Triangular plots showing the range of the relative NaCl-$CaCl_2$ contents of fluid inclusions in samples from the Derbyshire and Ecton Hill orefields as estimated from paired hydrate ($T_M h$) and ice (T_{LM}) melting temperatures. Isotherms for the H_2O-NaCl-$CaCl_2$ system, after Oakes et. al. (1990). 136

Fig.4.19. Triangular plots showing the range of the relative NaCl-$CaCl_2$ contents of fluid inclusions in samples from a) Llanharry, S. Wales and, b) Late, fluorite mineralization at South Crofty, Cornwall. Isotherms for the H_2O-NaCl-$CaCl_2$ system, after Oakes et. al. (1990). 137

Fig.5.1. Bivariate plots showing the variation of Na/K and Na/Li atomic rations of inclusion fluids in samples from a) the North Pennines (Alston and Askrigg), Derbyshire, Ecton Hill, and Llanharry, b) Alston and South Crofty 145

Fig.5.2. Bivariate plots showing the relationship between fluid inclusion homogenization temperatures and ,the a) Na/K and b) Na/Li atomic ratios of inclusion fluids in samples from the North Pennines (Alston and Askrigg), Derbyshire, Ecton Hill, Llanharry and South Crofty. 148

Fig.5.3. Bivariate LogLi-LogNa plots showing the Li-Na relationships in a) fluid inclusions studied in the present work and b) sedimentary basin brines, saline minewaters and spring waters (data from: 1) Carpenter et. al. 1974, 2) Edmunds 1975, 3) Edmunds et. al. 1987, and 4) Manning and Struit 1990) 151

Fig.5.4. Bivariate plot showing the relationship between fluid inclusion homogenization temperatures (T_H°C) and temperatures (°C) calculated using the a) Fournier b) Truesdell Na/K and c) Fouillac & Michard Na-Li geothermometers. 154

Fig.5.5. Halogen (Br/Cl, I/Cl) ratios of some representative surface and subsurface waters (after Bohlke & Irwin 1992). 157

Fig.5.6. Concentration trends of a) Cl and b) Ca, K, Mg in seawater relative to Br during the evaporation of seawater and the precipitation of evaporite minerals (After Carpenter 1978). 159

Fig.5.7. Bivariate logarithmic plots showing the Cl-Br concentrations, relative to the seawater evaporation trajectory, of a) fluid inclusions analyzed in the present work and b) sedimentary brines, thermal waters and spring waters; Sources of data: 1) Carpenter et. al. (1974), 2) Kharaka et. al. (1985), 3) Edmunds (1975), 4) Edmunds et. al. (1987), Manning & Struit (1990) 162

Fig.5.8. Bivariate logarithmic plots showing the Na-Br concentrations, relative to the seawater evaporation trajectory of a) fluid inclusions analyzed in the present work and, b) sedimentary basin brines and thermal waters, sources of data 1) Carpenter et. al. (1974), 2) Edmunds (1975), 3) Edmunds et. al. 1987, and 4) Manning & Struit (1990). 164

Fig.5.9. Br/Cl and I/Cl ratios of inclusion fluids in samples from the St. Austell granite and selected volcanic fumarole condensates. (after Bohlke & Irwin 1992). 167

Fig.5.10. Bivariate logarithmic plots showing the K-Br concentrations relative to the seawater evaporation trajectory of a) inclusion fluids analyzed in the present work and b) sedimentary basin brines and thermal waters (sources of data as in Fig.5.8). 169

Fig.5.11. Bivariate logarithmic plot showing the Li-Br concentrations, relative to the seawater evaporation trajectory of a) inclusion fluids and analyzed in the present work and b) sedimentary basin brines and thermal waters (sources of data as in Fig.5.8). 171

Fig.5.12. Bivariate logarithmic plot showing the Ca-Br concentrations relative to the seawater evaporation trajectory of a) inclusion fluids analyzed in the present work and b) sedimentary basin brines and thermal waters (sources of data as in Fig.5.8). 173

Fig.5.13. Schematic representations of proposed genetic models for mineralization in the a) South Pennines (modified from Worley & Ford 1977) and b) North Pennines (modified from Solomon et. al. 1971). 176

Fig.6.1. Sketch-map showing the Dinantian formations in the Peak District (South Pennines) (after Aitkenhead et. al. 1985) 182

Fig.6.2. Schematic representation of the lateral and vertical relationships between Carboniferous formations in the Ecton Hill and adjacent areas (After Aitkenhead & Chisholm 1982). 184

Fig.6.3. Sulphur isotopic composition of sulphide and sulphate samples from the Ecton Hill Cu-mineralization. 191

Fig.6.4. Sulphur isotope age curve for sulphate (After Claypool et. al.1980) 193

List of Tables

Table.3.1. Averages of the K/Na, Li/Na, Sr/Na, Mg/Na and Ba/Na weight ratios obtained from replicate D-ICP analyses in five fluorite samples. 68

Table.3.2. K/Na and Li/Na weight ratios obtained from replicate D-ICP analysis in two fluorite samples. 69

Table.3.3. Comparison of the Sulphur, Pb, Zn, Cu, Fe, Mn, K and Li weight ratios to Na obtained from the D-ICP analysis of ordinarily washed and electrolytically-cleaned samples. 76

Table.3.4. Absolute Cl, Br, Na values and Cl/Br and Cl/Na weight ratios obtained from replicate Neutron Activation Analysis of fluid inclusions in fluorite. 90

Table.4.1. Ranges of published homogenization temperatures of fluid inclusions in samples from the Pennine Orefields. 101

Table.4.2. Averages of fluid inclusion homogenization temperatures obtained in the present work in samples from the Pennine Orefields. 112

Table.5.1. Ranges of Na/K and Na/Li atomic ratios of fluid inclusions in samples from the three Pennine orefields, Ecton Hill, Llanharry and South Crofty. 144

Table.5.2. Ranges of Cl/Br weight ratios of fluid inclusions in samples from the three Pennine orefields, Ecton Hill, Llanharry and South Crofty. 161

Table.6.1. Published sulphur isotope data from the Pennine Pb-Zn ores, the Cheshire Basin copper mineralization, and selected Carboniferous Pb-Zn vein deposits in the British Isles. 188

Table.6.2. Sulphur isotope composition of chalcopyrite, galena and barite from the Ecton Hill deposit. 190

List Of Plates

Plates 4.1a-d.	Fluorite samples from the Pennine orefields. a) yellow vuggy fluorite crystals, Scordale mine, b) banded purple-colorless fluorite, Dirtlow Rake, c) Light purple fluorite crystals, Boltsburn mine, d) dark purple fluorite crystals, Odin Mine.	98
Plates 4.2a-d.	Fluorite samples from the Pennine orefields. a) green fluorite crystals, Blackdene mine, b) massive banded fluorite, Whiteheaps Mine, c) colorless fluorite crystals + PbS inclusions, Ladywash mine, d) fluorite associated with massive PbS, Millclose mine..	99
Plates 4.3a-b.	Typical, two-phase aqueous, liquid-vapour inclusions in fluorite from the North Pennine orefield.	109
Plates 4.4a-b	Representative fluid inclusions in samples from the Llanharry Mine, South Wales. a) Swarms of monophase secondary inclusions in calcite b) Rare primary two-phase inclusions in calcite.	120
Plates 4.5a-d.	Fluid Inclusions in fluorite from South Crofty mine.	124
	a) and b) Multiple generations of two-phase inclusions in late fluorite c) Two-phase aqueous inclusions with variable degrees of fill d) Three-phase liquid-vapour-solid inclusions in fluorite from the early, pegmatite stage of the paragenesis.	132
Plates 4.6a-d	Phase changes observed in aqueous inclusions during a typical freezing cycle.	133
	a) T=25°C Liquid+Vapour	
	b) T=-90°C inclusion completely frozen	
	c) T=-59°C, a few degrees above first melt (T_{FM}), liquid+solid	
	d) T=-30°C, massive melt, ice+hydrohalite+liquid.	
Plates 4.7a-c	Phase changes during a freezing cycle (continued.)	
	a) T=-26°C, ice+hydrate+liquid+vapour temperature approaching $T_M h$.	
	b) T=-24°C, Ice+liquid+vapour, $T_M h$	
	c) T=-20°C Ice+liquid+vapour, very close to T_{LM}	

Chapter 1

Introduction

1.1 Introduction

Numerous studies of the geological and geochemical characteristics of epigenetic, carbonate-hosted, Pb-Zn mineralization of the Mississippi Valley-Type (MVT), (reviewed by Bastin 1939, Heyl et. al. 1974, Ohle 1980, White 1974, Sverjensky 1986, Anderson & MacQueen 1982), have established that the deposits formed from hot, saline, aqueous solutions sometime after the lithification of host rocks. However, despite these extensive investigations, important aspects of the origin of these deposits remain unresolved. Particularly controversial are aspects of the timing of mineralization, the source of fluids, metals and sulphur, as well as, the mechanisms of ore-transport and deposition.

The epigenetic, predominantly carbonate-hosted lead-zinc mineralization of the English Pennines has an equally long history of research covering most aspects of geological and structural setting, ore mineralogy and geochemistry (reviewed by Dunham 1983, 1992, Dunham & Wilson 1985, Atkinson et. al. 1982, Colman et. al. 1989a). Broad similarities between the classical MVT and Pennine mineralization, based on geological and geochemical evidence, have been inferred by several authors and have recently been emphasized by Dunham (1983). Apart from the Pennines, similar comparisons have also been proposed for other sediment-hosted deposits in the UK, such as the Ecton Hill Cu-rich mineralization and the Llanharry Fe-ores of South Wales (Masheder & Rankin 1988, Rankin & Criddle 1985). However, despite the general agreement on the overall framework of ore-genesis, unresolved questions encountered in the study of MVT mineralization also apply to the above mentioned deposits in Britain.

The present work is concerned with an understanding of the character and evolution of ore-forming fluids associated with the Pb-Zn-fluorite mineralization in the Pennines, the Cu-dominant mineralization of Ecton Hill, the Llanharry Fe-deposit of South Wales together with additional observations of comparable phenomena during the late stage of the granite-related fluorite mineralization at South Crofty, Cornwall. This chapter outlines the main aims of the project and gives a summary of the methodology employed during the study.

1.2. Aims and Objectives of Research

The aims of the present work can be summarized as follows:

1) To further develop and assess analytical techniques for the determination of major and trace ionic species in fluid inclusions.

2) To investigate previously proposed genetic similarities between epigenetic sediment-hosted deposits in Britain and the MVT mineralization, as well as, to further examine the affinity of the ore-forming fluids with modern-day basinal brines. The possible links to the classical MVT, basinal-brine-related mineralization are investigated primarily for the English Pennines but also extend to the Ecton Hill, Llanharry and South Crofty areas.

3) To compare the character of the ore-forming fluids in the separate areas of study and to investigate the possibility of separate fluid sources and evolutionary paths for fluids involved in Pb-Zn and Cu-Fe dominant mineralization.

4) To highlight the effects of fluid-rock interaction with different lithologies in modifying the chemistry of the ore-forming fluids.

5) To unravel the provenance of the ore-forming fluids and the cause of their high salinities.

6) To investigate the origin of sulphur and the mechanisms of sulphide deposition in the Cu-rich mineralization of Ecton Hill, in comparison to the rest of the Pennine deposits.

These aspects are investigated mostly through extensive fluid inclusion studies. Evidence from the physical and chemical properties of fluid inclusions is used as a means of establishing the provenance and evolution of the ore-forming fluids and of examining their affinity to modern-day basinal brines. The study concentrates on data from the chemical composition of inclusion fluids. Oxygen-hydrogen isotopic analysis of the fluid inclusions was not undertaken in the present study. Such investigations are common practice in the study of modern-day basinal brines. However, the techniques required for oxygen-hydrogen isotopic analysis of fluid inclusions were not available to the author during the present study.

Comparative studies of inclusion fluids in samples from Pb-Zn and Cu-Fe dominant sediment-hosted mineralization in the British Isles, as well as, the granite-related mineralization at South Crofty, provide a means of assessing the possible importance of

basinal brine-type fluids in ore genesis. Variations of the alkali metal contents of fluid inclusions from the separate areas of study are used as a means of tracing the importance of temperature-controlled, fluid-rock interactions with different lithologies in modifying the chemistry of the ore-forming fluids. Furthermore, the halogen (Cl-Br) signature of the inclusion fluids is used in an attempt to unravel the origin of the fluids, and to further investigate similarities with modern-day basinal brines. Particular emphasis is also given to the application of the Cl-Br systematics as a means of investigating the causes of high salinity which is a key, common feature of inclusion fluids in the areas of study and in MVT mineralization in general. Sulphur isotope investigations in sulphide and sulphate samples from the Ecton Hill Cu-rich deposit are also undertaken in order to trace the origin of the sulphur species and to draw comparisons with the Pb-Zn-dominant mineralization of the Pennines.

1.3. Thesis Outline

Chapter 2 of the thesis sets the background of the present work and is devoted to a review of the general geological framework and also to an appraisal of the current theories for the genesis of MVT mineralization. Existing knowledge on the geology and mineralization of the areas under study is also reviewed, whereas, questions on the applicability of existing models for ore-genesis in these areas are also addressed in that chapter.

Chapter 3 is concerned with the development and critical appraisal of experimental methods for elemental analysis of the aqueous phase in fluid inclusions. Extensive fluid inclusion analysis was carried out using the Decrepitation-ICP (D-ICP) and Neutron Activation Analysis (NAA) techniques. The methods were developed particularly for the destructive analysis of single generation fluid inclusions in fluorite and calcite samples. Questions on statistical errors inherent in the analysis of fluid inclusions are also considered.

Results from microthermometric analysis are presented in Chapter 4. Detailed microthermometric work was undertaken in order to identify the fluid inclusion populations present in the samples, and to further refine previously published temperature-salinity data with the aid of more accurate, paired measurements on a large number of inclusions. Furthermore, new data on the relative Ca-Na contents of fluid inclusions, based on detailed phase equilibria at sub-zero temperatures, were obtained in the present study.

Chapter 5 consists of extensive investigations of the chemical composition of the ore-forming fluids trapped in the inclusions. Comparative data on the alkali metal and halogen

concentrations of inclusion fluids are used in an attempt to unravel fluid-rock interaction processes and to highlight aspects of the provenance and chemical evolution of the ore fluids. Chapter 6 is concerned with results on the sulphur isotope composition of sulphide and sulphate samples from the Ecton Hill deposit.

Finally, the main conclusions of the study, the value and limitations of the methodology used together with recommendations for further work are presented in Chapter 7.

Chapter 2

Review of the main geological characteristics and genetic models for carbonate-hosted epigenetic mineralization with special reference to UK examples

2.1. Introduction

Sedimentary basins host some of the most important base-metal sulphide deposits in a variety of lithologies including the red bed copper, submarine exhalative, as well as the sandstone and carbonate hosted lead-zinc deposits. The basins are dynamic, open systems, where both energy and mass transfer generate fluids which, under favorable conditions, can become ore-forming. These saline fluids, the so called basinal brines, are envisaged as the link between the base-metal, sedimentary basin-related deposits (Ohle 1980, Gustafson and Williams 1981, Bjórlykke and Sangster 1981, Sangster 1983, 1990). Of all sediment-hosted mineralization, the Pb-Zn, carbonate-hosted, ores, the so called Mississippi Valley-Type (MVT), are possibly the most extensively studied and yet most enigmatic class. Particularly, aspects of the timing of mineralization, the patterns of fluid flow, and the mechanisms of ore transport and deposition are still under debate (Sverjensky 1984, 1986, Sangster 1986, Anderson 1983, Barnes 1983).

The present work is concerned with aspects of ore genesis and particularly fluid evolution of Pb-Zn and Cu-Fe sediment-hosted mineralization in Britain. Field areas studied include the North and South Pennine orefields, the Cu-rich mineralization of Ecton Hill, west Derbyshire and the Llanharry Fe-deposit of South Wales. Especially for the Pennines, existing geological evidence reveals a strong resemblance to the classical MVT mineralization (Dunham 1983), whereas similar comparisons have also been drawn for the Ecton Hill and Llanharry deposits (Masheder & Rankin 1988, Rankin & Criddle 1985). Thus, in order to set the background of the present work, the first part of the present chapter will be devoted to a review of the main geological features, as well as, of the current theories for ore-genesis in the Mississippi Valley-Type deposits. In the second part, emphasis will be placed to the geological setting of the above mentioned sediment-hosted deposits in the UK, which, each to a different extent, have aspects in common with the MVT ores.

2.2. Geological Setting of Mississippi Valley-Type Deposits

The following summary is largely based on detailed review papers by Ohle (1980), Anderson & Macqueen (1982), Anderson (1978), Sverjensky (1986), Sangster (1983, 1986, 1990) and Russell & Skauli (1991) which incorporate information acquired over decades of active research. However, as noted previously, despite the vast amount of information concerning the geological setting, mineralogy, structural evolution. and fluid chemistry, many aspects of ore-genesis are still controversial. As pointed out by Anderson & Macqueen (1982), a fact that is often overlooked is the diversity of the MVT mineralization. Apart from the general features which define the MVT class, each district has its own characteristics, some of which may have a bearing upon modelling ore genesis. Doubts on the definition of a unifying genetic model for all MVT ores were also expressed by Sangster (1983) who suggested that "when these differences are taken into account, perhaps finding a common genetic model is akin to searching for a common tree that will grow apples, oranges, and peaches".

2.2.1. Host Rocks

Most MVT ores are found in carbonate rocks with dolomites being the dominant hosts to mineralization. The age of the hosts range from Proterozoic to Cretaceous with a dominance towards the Cambrian, Ordovician to Carboniferous time span. They most usually occur at or near the edges of sedimentary basins, or on arches between basins (Fig.2.1). The carbonate hosts are relatively undisturbed platformal carbonates or foreland fold and thrust belts. In most districts, igneous rocks are not common, or when present, they are not contemporaneous with mineralization. Stratigraphic evidence suggests that mineralization took place at shallow depths ranging from a few to a 1000m and thus, the pressures involved might not have exceed several hundred atmospheres. There is a tendency for deposits to be associated with unconformity related structures such as paleokarsts and/or facies fronts between platformal carbonates and basinal shales (Anderson & Macqueen 1982).

2.2.2. Ore Mineralogy

The ore-paragenesis is relatively simple with galena, sphalerite, pyrite and marcasite the most common sulphides. Barite and fluorite are the most common gangue minerals. Mineralization is epigenetic with sulphides occurring in pre-existing pore spaces. There is always evidence of dissolution of the carbonate hosts, expressed by slumping, collapse, and brecciation giving proof of the epigenetic nature of the mineralization (Sverjensky 1986).

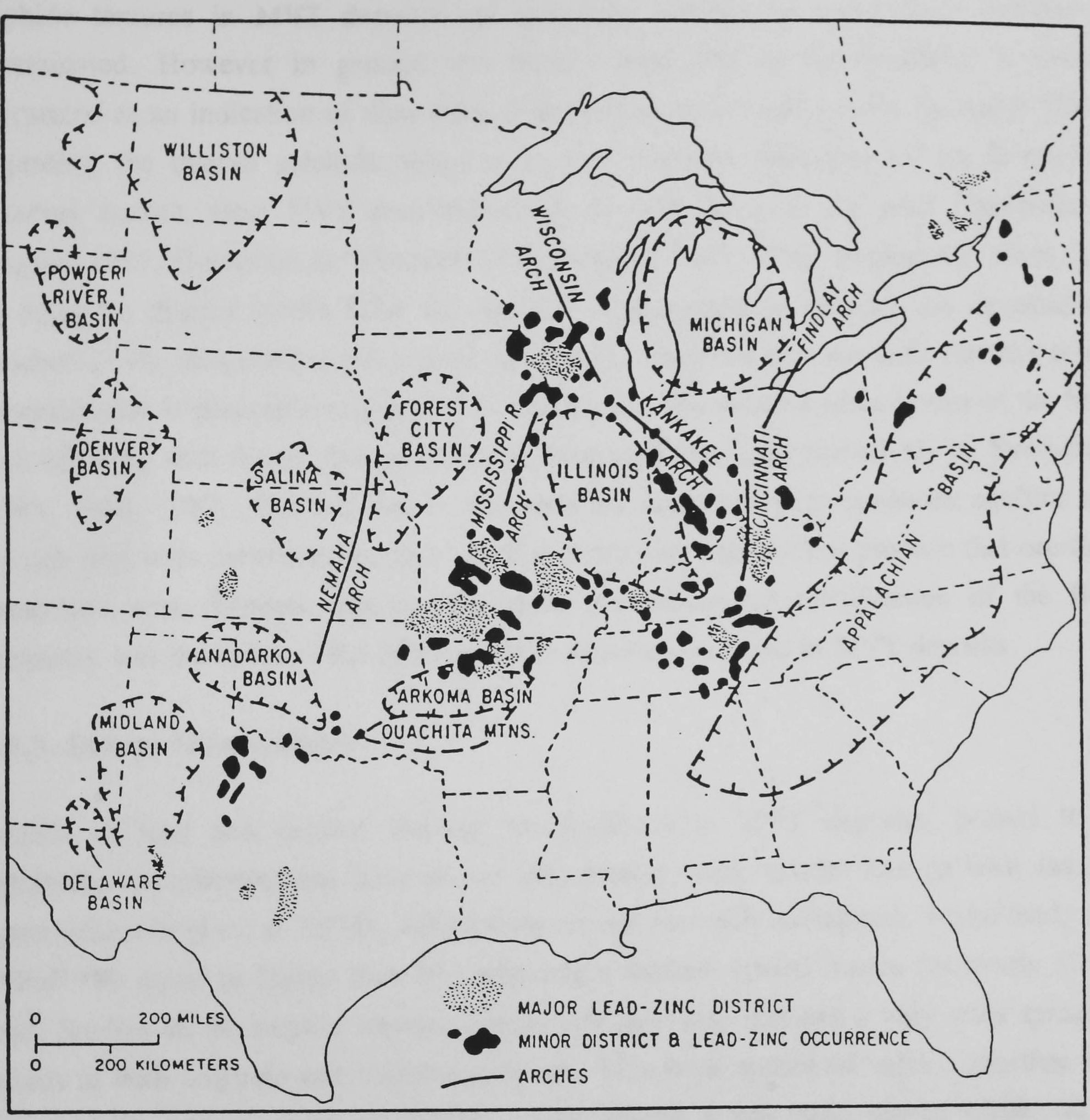


Fig.2.1. Sketch-map of the U.S.A. showing the location of Mississippi Valley-Type Lead-Zinc deposits and their spatial relationship with major sedimentary basins (after Cathles & Smith 1983).

Sulphide textures in MVT deposits are extremely varied and range from massive to disseminated. However in general, the large crystal size of the sulphides is usually interpreted as an indication of slow rates of deposition and crystal growth (Sangster 1990). Regarding the overall sulphide abundances, and with the exception of the South-East Missouri district, most MVT ores tend to be Zn-rich and very Cu poor (Bjorlykke & Sangster 1981, Gustafson & Williams 1981, Sangster 1983, 1990, Sverjensky 1986). The SE Missouri district in the USA and the Laisvall deposits in Sweden are anomalously enriched in Pb compared to the typical MVT ores. They are also the only districts where mineralization is predominantly hosted in sandstones. The possible associations of the host-rock lithology with the sulphide paragenesis have been examined extensively by Sverjensky (1984, 1986, 1987). The fact that Pb-rich ores are associated with sandstone aquifers and Zn-rich ores with carbonate aquifers has lead Sverjensky (op. cit.) to propose that ore-fluid interaction with different aquifer lithologies and subsequent modification of the fluid chemistry was the cause of the different metal ratios encountered in MVT deposits.

2.2.3. Isotope Geochemistry

Results of lead and sulphur isotopic investigations in MVT deposits, proved to be extremely complicated and have shown that almost every district has its own isotopic systematics (Heyl et. al. 1974). All deposits contain markedly radiogenic, J-type lead, with $^{206}Pb/^{204}Pb$ equal or higher than 20, indicating a shallow crustal source for nearly all the lead. Studies on the sulphur isotopic distribution have also revealed a very wide spread of values in both sulphide and sulphate minerals. This large spread of values, together with the generally heavy nature of sulphur, argues against a magmatic source while, on the contrary, favours a shallow crustal source for the sulphur. Syngenetic sulphide minerals, shales, evaporites and connate seawater have all been considered as possible sources of sulphur (Heyl et. al. 1974, Sasaki & Krouse 1969, Powell & Macqueen 1984).

Information on the oxygen-hydrogen isotopic composition of fluid inclusions from the MVT ores is limited (Fig.2.2). Only δD can be measured directly in the fluids whereas ^{18}O values are deducted form the isotopic composition of oxygen-bearing host minerals such as quartz and barite. Work by Hall & Friedman (1963, 1969) and Pinckney & Rye (1972) revealed that the $^{18}O/\delta D$ signature of fluid inclusions is very similar to that of the nearby oil-field brines. Although oil field brines are largely thought to represent connate or originally trapped seawater, their ^{18}O-δD composition showed that they possibly contain a meteoric water component (Taylor 1974). As can be seen from Fig.2.2, these waters have a very wide range of ^{18}O-δD values. Within a given basin, the highest $\delta^{18}O$ values are

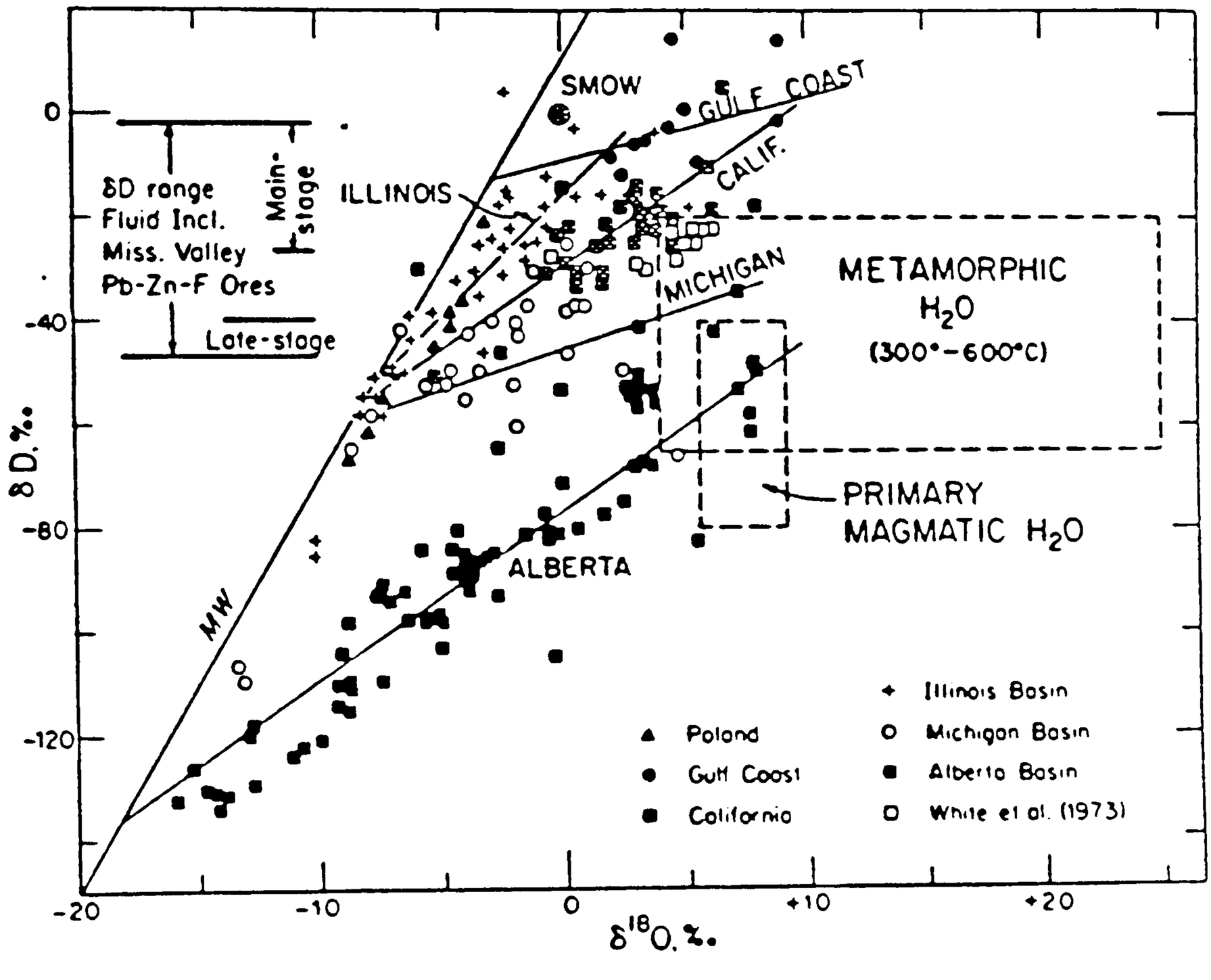


Fig.2.2. Diagram showing the $\delta^{18}O$-δD isotopic composition of seawater, meteoric, metamorphic and magmatic waters and inclusion fluids from Mississippi Valley-Type (MVT) deposits (after Taylor 1974).

associated with the highest temperatures and salinities. δD values also show an increasing trend with increasing salinity and $\delta^{18}O$. That considerable scatter of ^{18}O and δD values was interpreted as a result of mixing with "true" connate waters, exchange with hydroxyl-bearing clay minerals or fractionation effects such as membrane filtration and reactions involving hydrocarbons (Taylor 1974). In general, due to the widespread range of the sulphur isotopic values, the radiogenic nature of lead, as well as, the limited and yet inconclusive information on the ^{18}O-δD distribution of inclusion fluids, isotope geochemistry alone cannot provide a conclusive answer to the problem of ore-genesis and source of fluids in most MVT districts.

2.2.4. Nature of Ore Fluids

Evidence from the physical and chemical properties of fluid inclusions in minerals from MVT ores provide some of the most important constraints on the origin of these deposits. Fluid inclusions in sphalerite, carbonates, fluorite, and to a lesser extend barite, have been studied in MVT deposits more extensively than in any other ore deposit type. Possibly the most striking feature of MVT mineralization is the uniformity of environmental conditions in the various districts. As emphasized by Roedder (1976, 1979), the fluid inclusion data (temperature-salinity) are remarkably uniform in most MVT deposits despite the differences in ore-paragenesis (from almost pure Pb, to Zn and fluorite dominant), isotope geochemistry, structural setting, age and host rock type.

The inclusion fluids are dense, highly saline brines with total salinities always higher than 15 and often exceeding 20% salts, up to five to ten times the salinity of seawater. Daughter minerals (i.e. halite) are not present, indicating the occurrence of other than Na and Cl ions in solution. Very low freezing temperatures of the inclusion fluids indicate that they are dominated by Na-Ca chlorides with lesser amounts of K and Mg. Organic matter is also common either as methane, immiscible oil droplets or in solution within the brines. Homogenization temperatures fall in the range between 80 and 200°C, but most commonly between 100-150°C. Total pressures are always greater than the vapour pressure of the original brine, showing that boiling has not taken place (Roedder 1984).

Analogies between inclusion fluids and modern oil-field brines have long been noted and discussed in the literature (e.g. Roedder 1979, Sverjensky 1984, Anderson 1978, Carpenter et. al. 1974, Hanor 1979a). Interaction of the ore-forming fluids with different lithologies together with different degrees of fluid-rock equilibration have been called upon to explain the higher K/Na ratios of the inclusion fluids compared to modern-day sedimentary brines

(Sverjensky 1984). The ultimate origin of the brines themselves is not clear although individual brines have been assumed to represent connate seawater, compaction or formation waters. Another area of debate involves the mechanism through which the fluids acquired their high salinities. Proposed mechanisms include subaerial evaporation, membrane filtration and increase of salinity with depth, interaction with evaporites and contribution from interstitial evaporite brines generated in sabkha-type environments. Similarly, as noted in the previous section, the source of the ore-forming constituents (metals and sulphur), is also not clearly defined.

None of these theories on the source of fluids, ore-metals and sulphur has gained uniform acceptance for all MVT ores; the geological and geochemical characteristics of each district have led to the acceptance or dismissal of none of the above mechanisms. The question of whether the uniform composition of the fluids is a result of a single process or a combination of phenomena all leading to the same conclusion is still under debate.

2.3. Models for Ore Genesis

During the last 20 years the basinal fluid expulsion model has become the most popular as the principal mechanism for ore-genesis in the MVT deposits. Several authors have expressed their doubts, which originate mainly from the lack of conclusive evidence linking individual deposits to specified source-basins (Ohle 1980, Sangster 1990, Russell & Skauli 1991). The affiliation of the ores with sedimentary basins, however, is too strong to be ignored and, consequently, whichever the ore-forming mechanisms are, they have to be found within, or closely associated with the basinal environment. It is mainly due to the complexity of the sedimentary basin environment itself that answers are not easily reached. The most controversial aspects of ore-genesis in the MVT deposits are those of fluid flow, ore transport and deposition.

2.3.1. Dynamics of Fluid Flow

As noted by Sverjensky (1986) a very important constraint on any model involving the migration of MVT ore-fluids out of sedimentary basins lies on the fact that the fluids are able to reach the sites of deposition at relatively shallow depths and at temperatures consistent with those established by fluid inclusion studies. Four models have been proposed to account for the movement of ore fluids from their source through the aquifers and to the site of ore-deposition: a) basin compaction b) episodic basin dewatering c) gravity driven fluid flow and d) a proximal source model involving geopressured, shale-

dominated sequences.

a) Steady compaction of sediments containing fluids under hydrostatic pressures was proposed as a driving mechanism for fluid flow at the Pine Point deposit by Noble (1963), and Jackson & Beales (1967). However more recent, advanced fluid flow modelling has shown that flow rates resulting from simple compaction under normal subsidence will be far too low to transport temperatures in excess of 100°C into a near surface environment (Cathles & Smith 1983). Thus, in order to overcome the temperature conservation problem, three additional models were proposed.

b) Episodic release of fluids under lithostatic pressures was proposed by Sharp (1978) and more recently by Cathles & Smith (1983). Their model involves rapid fluid loss from the mid-basin and fast transport over hundreds of km along permeable aquifers. Episodicity was envisaged as a result of a continuous built-up of fluid pressures until lithostatic pressures were reached. The formation of ores might have been the result of multiple dewatering pulses, enhanced by faulting by a process similar to seismic pumping (Sibson et. al. 1975).

c) Cross-formational gravity driven fluid flow was proposed by Garven & Freeze(1984a,b) and Garven (1985) as an important energy source for fluid transport. This model is seen as a large scale process requiring an uplift at the distal portion of the basin creating a topographically high groundwater recharge zone (Fig.2.3a). During uplift the fluids are driven down across the section to a lower permeable aquifer. It is obvious that permeability is then the most critical factor in the resulting velocity of fluid transport. Given the fact that the system is not perturbed significantly and because the fluids are continuously recharged at one edge of the basin and discharged at the other, large volumes of fluids could pass through the basin.

d) A proximal source model was proposed by Fowler & Anderson (1991) in order to overcome the permeability constraints associated with long distance migration models particularly in shale-dominated basins. The model involves geopressured zones (sediments that contain fluids at pressures higher than hydrostatic), and it is mainly applicable for deposits in close proximity of shale-dominated sequences (Fig.2.3b). Temperature gradients associated with geopressured zones have been shown to be significantly steeper than those in normally pressured sediments. Rapid expulsion of the overpressured fluids along pre-existing faults or hydraulic fracturing leads to hydrothermal mineralization. Thick shale-rich sequences are considered ideal for the development and maintenance of high fluid pressures, whereas the proximity of the source and the high flow rates of expulsion can account for the

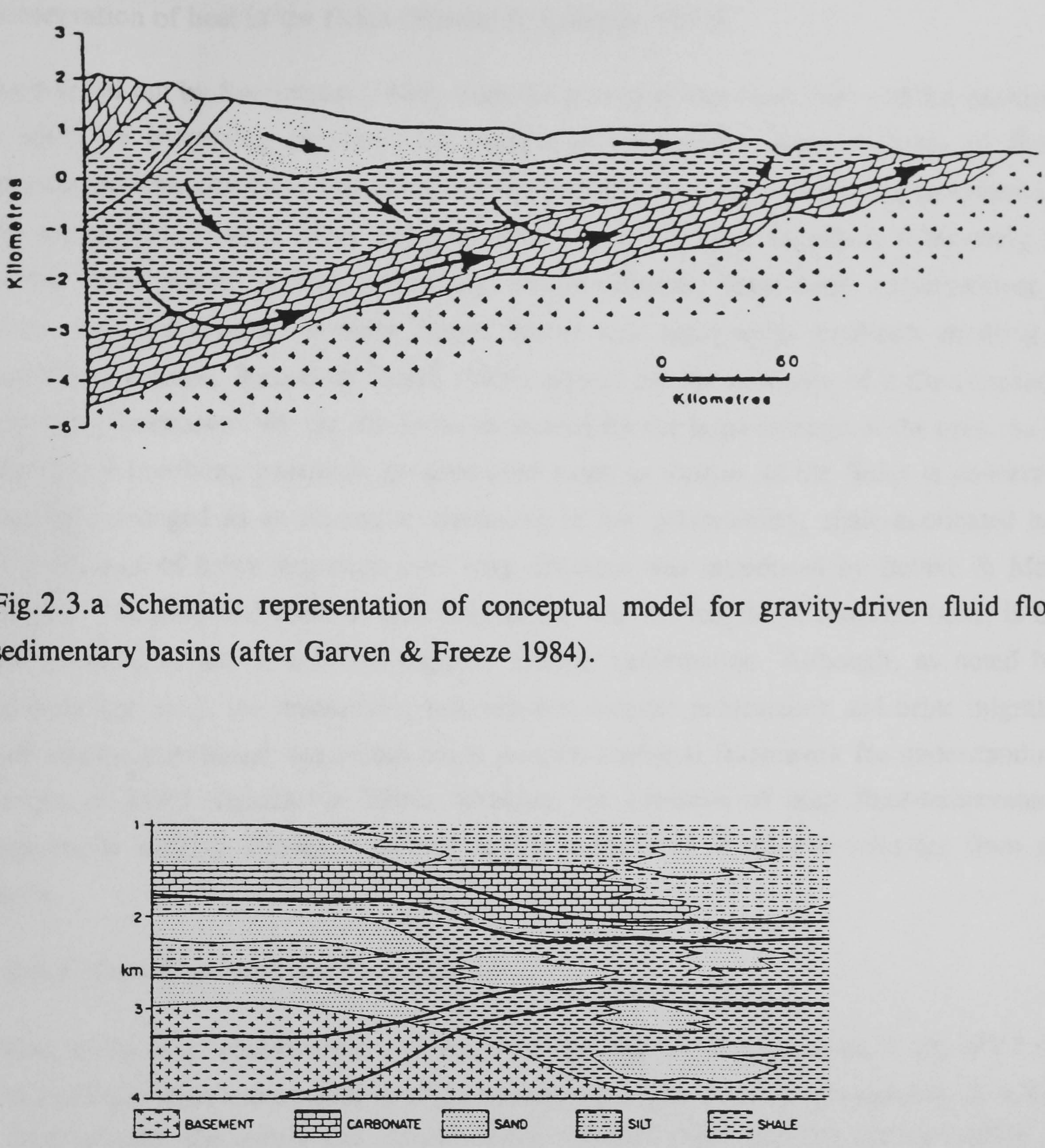


Fig.2.3.a Schematic representation of conceptual model for gravity-driven fluid flow in sedimentary basins (after Garven & Freeze 1984).

Fig.2.3.b Schematic representation of conceptual stratigraphic model showing overpressured sandstones and siltstones in overpressured shales near the basin margin. Isotherms (heavy lines) converge in geopressure zone producing an area of steep geothermal gradient (after Fowler & Anderson 1991).

conservation of heat in the fluids (Fowler & Anderson 1991).

As pointed out by Sverjensky (1986), both the gravity-driven fluid flow and the expulsion as a result of increasing pressure, are capable of transporting large volumes of fluids at elevated temperatures and thus, they are not mutually exclusive. According to Hanor (1979) the generation of fluids under high pressures is probably more important at the early stages of the development of deep sedimentary basins whereas, basin-wide, gravity-driven fluid flow, may predominate in more mature basins with topographic gradients resulting from uplift and erosion. Russell & Skauli (1991) argued for the necessity of a fluid-recharge or recycling mechanism for the ore fluids to account for the large tonnage of the ores. As far as the model involving proximal, geopressured zones as sources of the fluids is concerned, it can be envisaged as an attractive alternative in low permeability, shale-dominated basins. The concept of brine migration over long distances was introduced by Bethke & Marshak (1990). The proposed scale of brine migration, over the lengths of orogenic belts, is that of plate tectonics, and a result of regional tectonic deformation. Although, as noted by the authors (op. cit.), the mechanistic link between tectonic deformation and brine migration is not clearly understood, the model could provide a general framework for understanding the origin of MVT deposits in North America, the presence of high fluid-temperatures in apparently shallow sediments as well as the occurrence of oil-reservoirs far from source beds.

2.3.2. Ore-Transport and Deposition

One of the most controversial and hotly debated aspects of ore-genesis in the MVT ores is the identification and modelling of the transport and precipitation mechanisms. It is still not clear whether the metals and reduced sulphur species (H_2S and HS^-) are transported in the same brine, or the metals are carried in H_2S deficient brines and precipitation is a result of the addition of H_2S at some later stage. Both experimental and theoretical calculations support ore-metal transport by sulphur deficient brines. However, it has also been argued that a single fluid model may be applicable in some cases (Sverjensky 1981, 1984). In general there are three models for transport and deposition in the MVT ores (Anderson & MacQueen 1982, Barnes 1983, Anderson 1983, Sverjensky 1986).

a) *Mixing model*. According to that model the base metals are transported in H_2S-free brines and deposition occurs as a result of either mixing with a H_2S bearing fluid, or by the release of reduced sulphur by thermal degradation of organic compounds, or by reduction of sulphate at or near the site of deposition.

b) *Sulphate reduction model.* The base metals are transported together with sulphate in the same solutions and sulphate reduction is the cause of deposition.

c) *Reduced sulphur or single brine model.* Base metals and reduced sulphur are carried in the same brine and precipitation occurs as a result of changes in pH, dilution or cooling.

The main factor controlling the applicability of these models is the solubility of metal sulphides in Na-Cl brines in the presence or absence of reduced sulphur. The major barrier in establishing which of the above processes leads to ore-formation is the lack of knowledge regarding the pH, and oxidation state of the ore forming solutions, both of which constrain the solubility of metal sulphides. Temperature and pressure changes are not likely to be of controlling importance in the MVT mineralization, since there is no evidence of significant temperature drop nor boiling of the fluids (Anderson 1983, Lydon 1986). Compositional controls, mainly expressed as the concentration of reduced sulphur, pH and Eh, are considered as the most important factors in the transport and precipitation of sphalerite and galena (Anderson 1973, 1975, 1983, Anderson & Macqueen 1982, Sverjensky 1984, 1986). The pH of the fluids is closely linked with the concentration of reduced sulphur, as can be seen by the following reaction:

$PbS + 2H^+ \rightarrow Pb^{+2} + H_2S$ (1) for which the equilibrium constant is:

$$K = aPb^{+2} \times aH_2S / (aH^+)^2 \times aPbS \quad (2)$$

Since the activity a for galena is 1 and the activities aPb^{+2} and a H_2S are approximated by the concentration values mPb^{+2} and mH_2S respectively, equation (2) becomes:

$$K = mPb^{+2} \times mH_2S/(aH^+)^2 \quad (3)$$

From equation (3) it is clear that the value of the equilibrium constant K and consequently the concentration of reduced sulphur and acidity (aH^+) have opposite effects to the metal sulphide solubilities. At constant mH_2S an increase in acidity will raise mPb^{+2}, whereas at constant acidity an increase in mH_2S will lower mPb^{+2} (Anderson 1983).

Taking into account the very low solubilities of sulphides at near neutral pH and at moderate temperatures, a transport problem is created when metals and sulphur are carried in the same brine. The low pH values required for the reduced sulphur model to be active are considered not realistic by many authors (e.g. Anderson 1973, 1975, 1983, Barret & Anderson 1982).

There are no clear-cut limits regarding the required metal and sulphur concentrations of a potentially ore-forming brine. Roedder (1960) argued that a combination of parameters, including flow rates, fluid volumes and ore-metal concentrations is needed for a fluid to become ore-forming. It has been considered that metal concentrations have to exceed the value of 1ppm and should preferably be in the order of tens to hundreds of ppm for the solution to become ore-forming (Anderson 1983). Thus, for a fluid carrying both metals and reduced sulphur and in order to overcome the low concentration problem, large quantities of fluid, long periods of time and/or high flow rates are required

The problem of transport ceases to exist if the sulphur species are in the form of sulphate ($SO_4^=$) because metal sulphates are much more soluble than sulphides (Anderson 1983). In such a case however, a sulphate reduction mechanism has to be active at the site of deposition. Sverjensky (1984, 1986) argued strongly in favour of the single brine, reduced sulphur model, at least for some districts. According to his arguments some modern oil-field brines with pH as low as 4.5 are possible carriers of low concentrations (of the order of 1ppm) of metals and reduced sulphur to the sites of ore formation. The presence of barite in many MVT ores adds further complications to the identification of transport and precipitation mechanisms. Ba^{+2} is virtually insoluble in the presence of even minor concentrations of $SO_4^=$. Therefore Ba^{+2} has to be transported in a $SO_4^=$-deficient brine with barite deposition taking place as a result of mixing with a $SO_4^=$-bearing fluid or by oxidation of a reducing, H_2S-bearing fluid which also contains Ba^{+2} (Barnes 1983, Anderson 1983). Fluorite, which is also present in some MVT deposits such as the Illinois-Kentucky district can also be deposited from Na-Ca-Cl brines. As proposed by Anderson (1983), if the hydrothermal brine is near saturation with respect to CaF_2, it will precipitate fluorite as a result of sulphide deposition due to an increase in the Ca contents of the fluid. However, fluorite can also be deposited by other means such as cooling, or by carbonate dissolution unrelated to sulphide precipitation (Barnes 1983).

It is still not clear which of the above mentioned models is active and leading to ore-genesis in the MVT districts. The main barrier in resolving these strongly debated arguments is the lack of knowledge regarding the pH, metal, and sulphur concentrations of both modern oil field brines, and most importantly, of fluid inclusions. It is also possible that the yet poorly understood organic complexing effects are important and active during ore transport and deposition (Giordano & Barnes 1981).

As expressed by all students of MVT mineralization, still the questions outnumber the answers. There is no shortage of intriguing problems to study. Research yet has a lot to

gain from studies regarding mainly the timing of mineralization, ore-fluid chemistry, the importance of organic matter, and the hydrogeological modelling of the MVT basinal systems.

2.4. Epigenetic Sediment-Hosted Mineralization in the U.K.

A number of base metal deposits in Britain have many aspects in common with the classic Mississippi-Valley Type mineralization (Fig.2.4). Most of all, the Pb-Zn-F-Ba ores of the three Pennine orefields (Alston, Askrigg and Derbyshire), which are regarded by Dunham (1983) as a 'fluoritic subtype' of the MVT class in terms of mineralogy, host rock lithology, as well as orefluid temperature and chemistry. However as noted previously, apart from the Pennines, ,orefields such as the Cu-rich mineralization of Ecton Hill and the goethite, hematite ores of Llanharry, South Wales, are similar to the MVT mineralization in terms of their affiliation with sedimentary basins, and their formation from hypersaline brines. Questions regarding the genesis of MVT ores also apply to their possible counterparts in the UK. Some of these aspects will be addressed in the present work in the view of new evidence from fluid inclusion composition as a means of delineating the origin and chemical evolution of the mineralizing fluids. However, in order to set the background of the present work it is considered necessary to review the well established facts on the geological framework of these deposits.

For the English Pennines there is a particularly extensive literature covering most aspects of geological setting, structural evolution and ore mineralogy. The following summary is based mainly on reviews by Dunham (1983, 1992), Ford (1976), Ineson (1976), Ineson & Ford (1982), Dunham & Wilson (1984), Mostaghel & Ford (1986) and Colman et. al. (1989a). Knowledge accumulated over decades of research will be paired with new evidence of the present work in an attempt to clarify some aspects of ore genesis which are still poorly understood.

2.4.1. Geological Setting of the Pennine Orefields

In the three Pennine orefields (Alston, Askrigg and Derbyshire) mineralization occurs as long, thin oreshoots in brittle host rocks (limestone, siliceous sandstone) of predominantly Asbian and Brigantian age, confined by shales and argillized volcanics (Dunham 1983, Colman et al 1989a). In contrast to the Irish carbonate-hosted deposits, mineralization in the Pennines is clearly epigenetic and there is no evidence of any syn-Carboniferous activity (Dunham 1983).

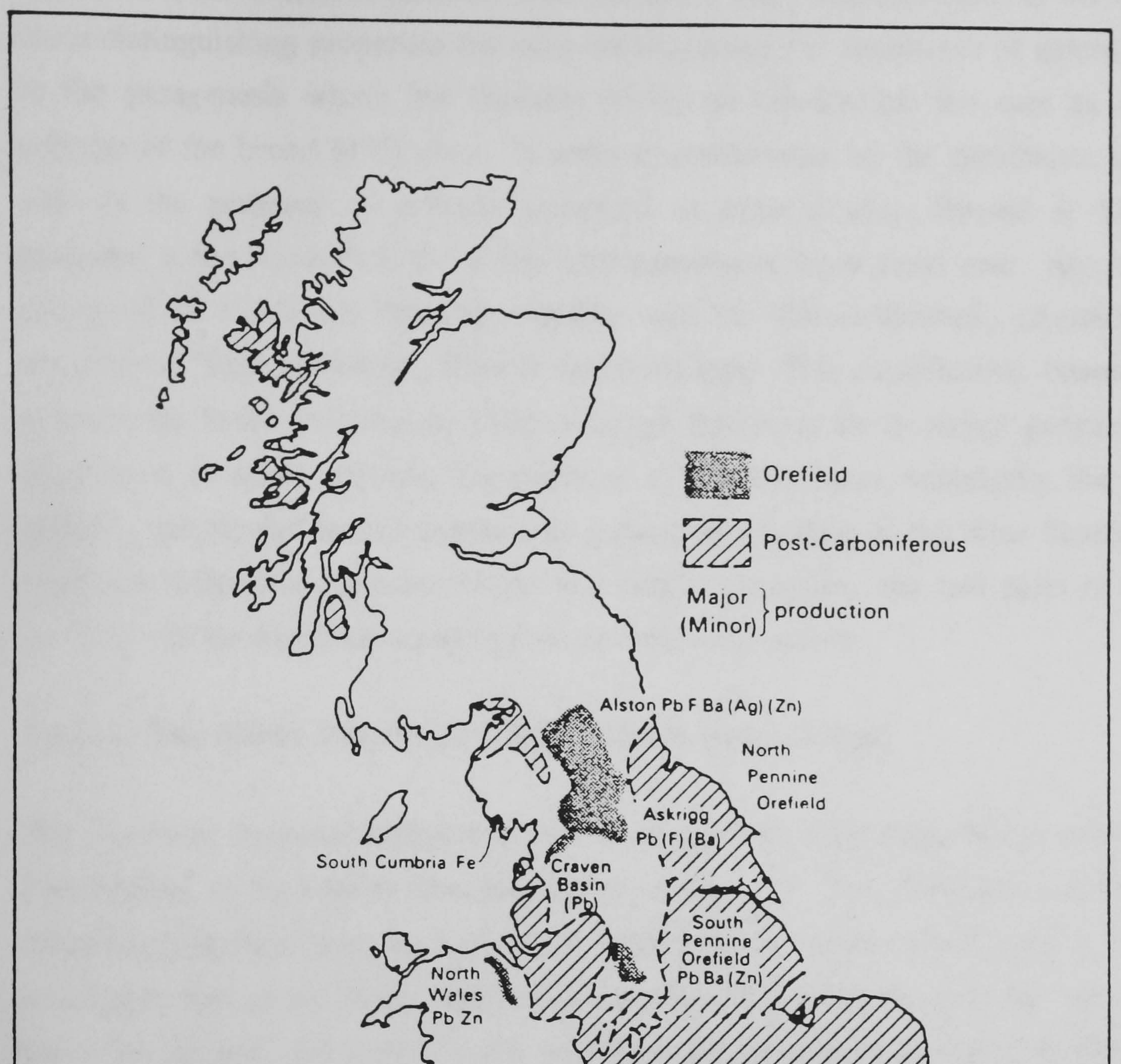


Fig.2.4. Sketch-map showing the major Dinantian Carbonate-hosted orefields in Britain (after Plant et. al. 1988).

Apart from the overall similarities with the MVT ores, mineralization in the Pennines has some distinguishing properties, the most obvious being the dominance of galena and fluorite in the paragenesis which led Dunham (1983) to characterize the ores as a "fluoritic" subtype of the broad MVT class. In order to compensate for the dominance of fluorite as well as the presence of granitic intrusions in some districts, Russell & Skauli (1991) proposed a new classification of the carbonate-hosted base metal ores. According to this classification the North Pennines together with the Illinois-Kentucky (Rossiclare) district comprise a "high enthalpy", fluorite dominant type. This classification however does not mention the South Pennines in which although fluorite is the dominant gangue, there is no conclusive evidence proving the presence of granitic rocks underlying the orefield. In general, despite the overall comparable geological signature of the three Pennine orefields, there are differences between North and South. Therefore, the two parts of the Pennine orefield will be described separately in the following section.

2.4.1.1. The North Pennine Orefields (Alston and Askrigg)

The Northern Pennine orefields extend from south of the Roman Wall, north of the main Tyne valley, to the Craven limestone uplands (Figs. 2.5, 2.6). The field is divided into two almost symmetrical parts by the pass of Stainmore; the Alston block lying in the north and Askrigg to the south. Both orefields are bounded by fault systems to the north, south and west. To the east, the Alston block sediments disappear beneath the Coal Measures which are overlain by Permian strata, whereas the Askrigg sediments dip beneath the Permo-Triassic and Jurassic of the vale of York and North Yorkshire moors (Dunham 1948 1992, Dunham and Wilson 1984).

2.4.1.1.1. Host Rock Geology

The sedimentary sequence in the two orefields is comparable. Lower Palaeozoic (Ordovician-Sil urian), highly folded slates and turbidites form the basement on which Carboniferous rocks rest unconformably. The Lower Palaeozoic basement of both orefields has been intruded by two Devonian granites. In the Alston orefield mineral deposits occur in strata ranging from Palaeozoic (Ordovician and Sil urian slates and Devonian granite), to Permian age. However, the main hosts of mineralization are the Visean and Namurian strata. Of particular importance as hosts to mineralization are the Yoredale cyclothems, best developed during the Brigantian stage. They consist of rhythmic units of limestone, shale, sandstone and often coal horizons, being repeated seven to ten times. The effect of this rhythmic sedimentation was to give alternations of brittle limestone, compact

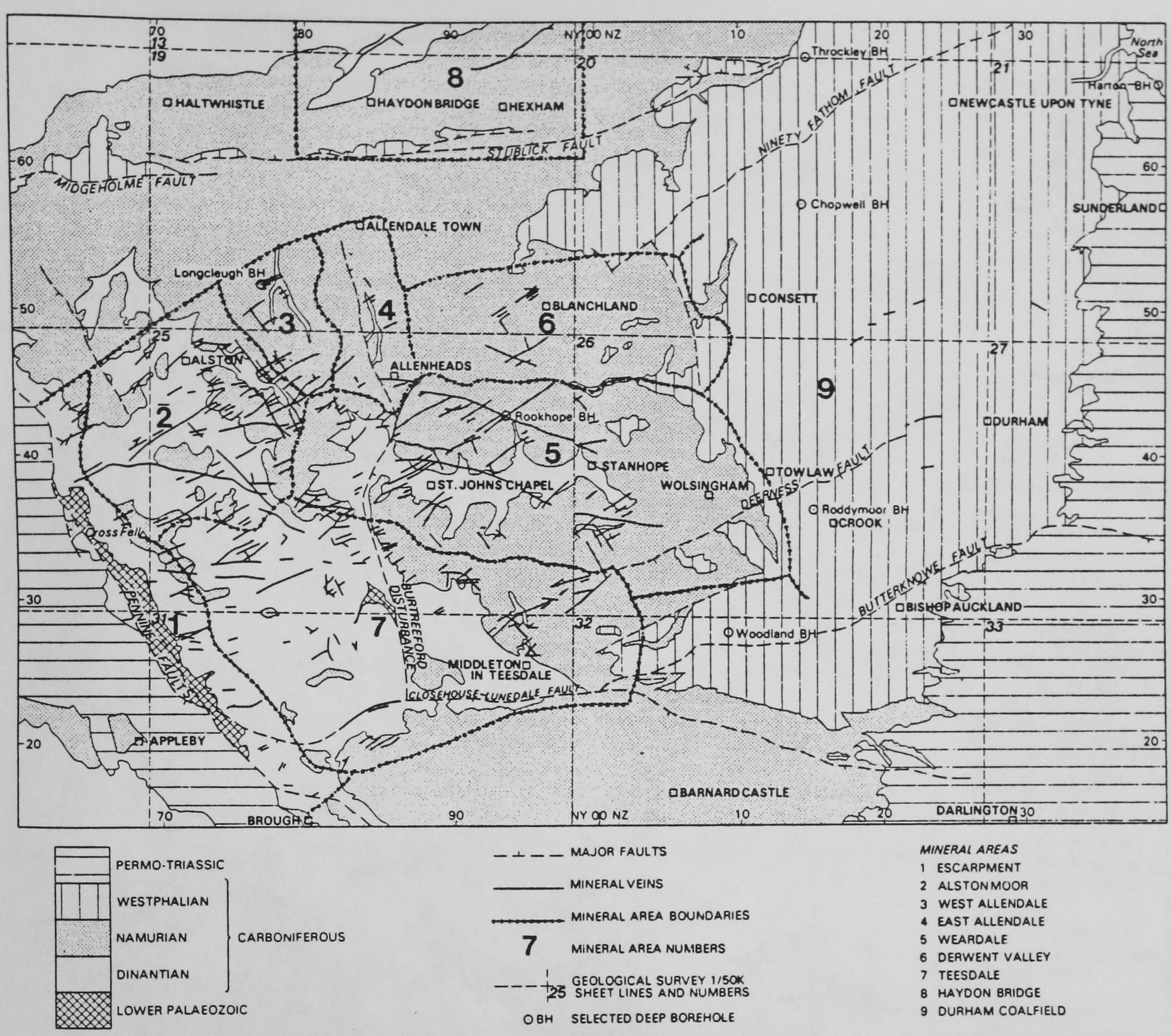


Fig.2.5. Sketch-map showing the main geological formations, mineral veins, major structural features and subdivisions of the Northern Pennine (Alston) Orefield (Tyne to Stainmore) (after Dunham 1992).

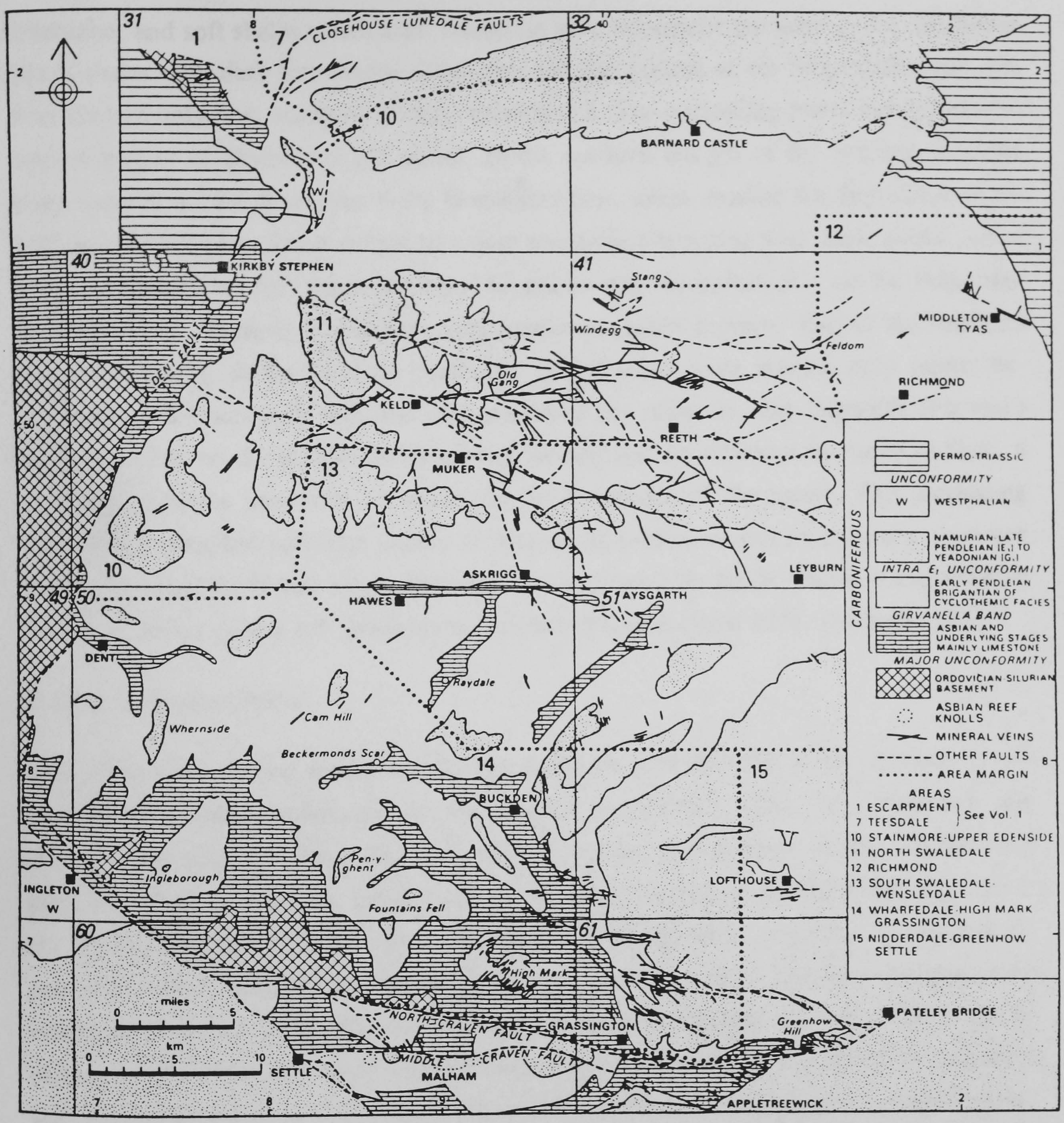


Fig.2.6. Sketch-map of the Northern Pennine (Askrigg) Orefield (Stainmore to Craven) showing the main geological formations and subdivisions of the field (after Dunham & Wilson 1985).

limestone, and soft shales which after fracturing have influenced the form of the oreshoots. Black shales with dark bituminous limestones are also present at the Brigantian stage, but they contain only few, scattered mineral occurrences. The succeeding Namurian formations consist mainly of sandstones and shales. In the southern margin of the Askrigg field the basal member of the Namurian is the Grassington Grit, which marked the deposition of the Millstone Grit facies. These consist of coarse sandstones alternating with thick shales. Apart from the Grassington Grit where the basal limestone rests unconformably on the Brigantian limestones, the Millstone Grit strata rarely contain workable deposits. East of the Northern Pennine orefield, at the Durham coalfields, Westphalian strata contain only minor Ba-dominant oreshoots with scattered occurrences of ore minerals. Rot liegendes (Permian) dune sands rest on the eroded Carboniferous surface, and are followed by the Marl Slate, a dolomitic siltstone less than 1m thick (the Kupfershiefer of Germany). The succeeding Zechstein formations comprise mainly of Magnesian Limestone and an evaporite sequence that has reached the bittern stage. Extensive but non-economic barite-fluorite mineralization with only minor galena and sphalerite is found at that stage (Ford 1976, Dunham 1983).

2.4.1.1.2. Igneous Rocks

One of the most striking features of the two North Pennine orefields is the presence of two Caledonian granites underneath the mineralized sedimentary rocks. The Weardale and Wensleydale granites form the core of the Alston and Askrigg blocks respectively (Fig.2.7). Both granites are members of a post-orogenic suite of granite complexes within the Caledonide belt in Lower Devonian times. Although both intrusions are chemically evolved, recent geochemical evidence (Brown et. al. 1987) indicates compositional contrasts reflecting differences in melt affiliation and evolution. Having been emplaced during Lower Devonian times (390-410Ma), they clearly predate the carbonate sequence and mineralization by at least 100Ma. Hence, although a direct influence on mineralization in terms of rising juvenile fluids, as proposed by previous authors (Sawkins 1966a, Russell and Smith 1979), is not considered likely, the intrusions may have provided local hot spots focusing the migrating fluids during increased tectonism and mantle heat flow during Lower Permian times (Brown et. al. 1987). Petrographic and geochemical evidence indicate that the Weardale granite underwent extensive hydrothermal alteration and mineral reequilibration during its emplacement into the relatively hydrous Caledonian basement (greywacke-shale sequence). The smaller, less altered and less fractured Wensleydale granite was emplaced into a less hydrous basement (magnetite-rich mudstones siltstones and greywacke sandstones), resulting in a much less clear-cut relationship between mineral zonation and the geophysically inferred form of the buried granite. Preliminary data from

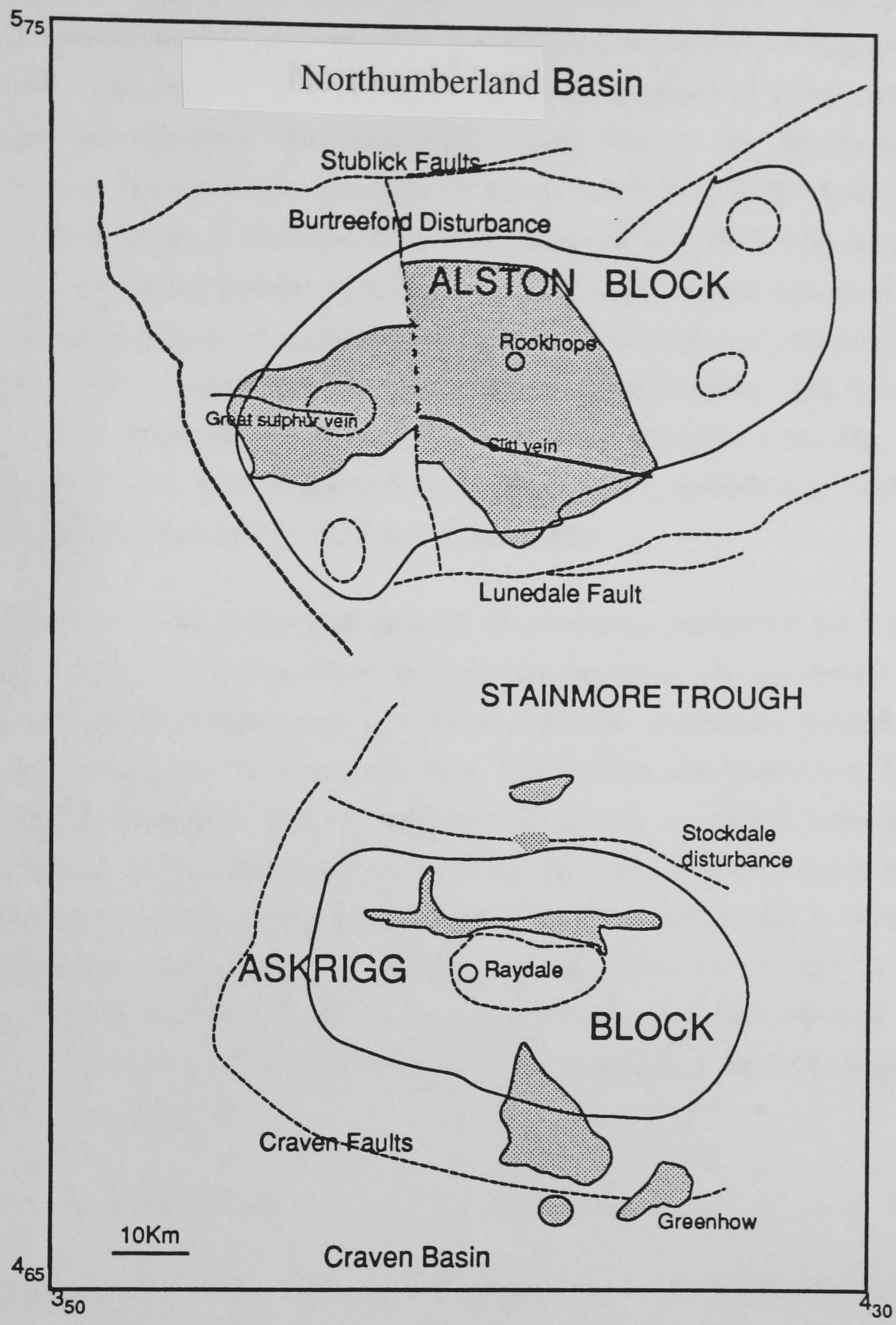


Fig.2.7. Sketch-map showing the spatial relationship between buried granites and fluorite mineralization in the North Pennine orefields (modified from Colman et. al. 1989a)

the Raydale borehole have shown that the Wensleydale granite is mainly non-porphyritic, and unfoliated medium grained rock, in contrast to the coarser, strongly foliated Weardale intrusion. The kind of alteration that would be expected if brines responsible for the Pennine mineralization had penetrated, is not seen in the Wensleydale granite core (Dunham & Wilson 1984). The more extensive contribution of the Weardale granite to the mineralizing fluids is indicated by a wide variety of As, Sb Bi Mo, Sn and REE bearing minerals around the granite cupolas (Brown et al 1987). In the Alston orefield, apart from the Devonian granite, a quartz-dolerite sill, the Whin Sill and associated dykes have also intruded the Carboniferous sequence prior to mineralization. The Whin Sill has been extensively altered and metasomatized lo sing large amounts of Fe, Mg, Ca; it cuts strata ranging from the basal Brigantian to the Westphalian, extends over 5000Km2 and has a maximum thickness of 75m (Colman et. al. 1989a).

In terms of tectonic setting both granites are subduction-related but the Wensleydale granite exhibits more within-plate characteristics. The extensive LIL enrichment of the Weardale granite could be interpreted as a result of water-rock interaction, possibly associated with its emplacement to a more hydrous crust. The Wensleydale granite was further away from the site of subduction and as noted by Brown et. al. (1987) crystallized in a dryer environment a fact that may account for its "within plate" character. The different properties of the two granitic intrusions have influenced the overall evolution and given rise to distinctive zonal patterns in the two orefields. Their contribution to the mineralizing events will be further discussed in the present work, and their influence onthe ore fluids will be assessed in terms of differences in the composition of fluid inclusions in minerals from the two orefields.

2.4.1.1.3. Ore Mineralogy

Mineralization in Alston block has a central fluorite zone (600Km2) which is giving way abruptly outwards to a barium dominated zone (Dunham 1948, 1992). A detailed study of the sulphide mineralogy in the North Pennines by Vaughan & Ixer (1980) revealed significant differences between Alston and Askrigg. North of Stainmore the sulphide assemblages show much greater diversity. The earliest phase is the ankeritization of the limestone and the carbonatization on the dolerite. There follows a quartz-pyrite-pyrrhotite Sn-bearing chalcopyrite assemblage, accompanied by minor amounts of Co-Ni-Fe arsenides and sulpharsenides and trace amounts of bismuthite, cassiterite, REE and Ag-bearing minerals. Major gangue minerals during this stage are quartz and fluorite. Galena and sphalerite occur at a later stage of epigenetic mineralization. Fluorite and barite are

now the dominant gangue minerals but quartz is also present (Vaughan and Ixer 1980). In general, both the gangue and sulphide mineral zonation reflects the presence of two hot spots above the Rookhope and Tynehead cupolas where the mineralization includes the characteristic high-temperature quartz-pyrite-pyrrhotite assemblage (Vaughan and Ixer 1980, Brown et. al. 1987). These quartz-copper mineral localities, believed to mark feeder centers, are also characterized by high Y values in fluorite (Smith 1974).

The patterns of mineral zonation are different in the Askrigg block, where there are no clear concentric, gangue mineral zones. Fluorite is generally associated with barite in centered areas, surrounded by barite and calcite-dominant peripheral zones. Only at the outer North Western part of the orefield there is a poorly defined quartz-pyrite chalcopyrite zone, which, however lacks the characteristic pyrrhotite of the Alston Block (Vaughan and Ixer 1980, Brown et. al. 1987). In general, the sulphide assemblage in Askrigg consists of a sequence of bravoite, pyrite, marcasite, chalcopyrite, galena and sphalerite. Ni and Co-bearing phases are sulphides rather than arsenides and sulpharsenides, Sb and As-minerals are generally rare, and no Bi or REE phases have been recorded (Brown et. al. 1987).

2.4.1.1.4. Isotope studies

The first study on the isotopic composition of North Pennine sulphides was undertaken by Moorbath (1962); his results on the Pb isotopes of galena gave ages identical to those from the lead bearing outer zone of the Cornubian tin-copper Permian mineralization. However, because of the radiogenic nature of the leads, typical of J-type Pb encountered in most MVT regions, determination of the timing of mineralization based on Pb isotope distribution is of questionable validity. Later work by Dunham et. al. (1968), based on $^{39}Ar/^{40}Ar$ measurements on clay alteration minerals adjacent to the mineralized veins, indicated 284 ± 40 Ma for the onset of mineralization with further hydrothermal activity at 230 and 170Ma. In general, as noted by Dunham (1983), there is no evidence for Syn-Carboniferous activity such as in the Irish deposits. Recent work by Halliday et. al. (1990), based on K/Ar and Sm/Nd isotopic composition of fluorite suggests that at least some part of the mineralizing events took place at Mesozoic rather than Paleozoic times, whereas, metallogenic events were active at intervals between 290 and 180Ma.

The isotopic composition of sulphur in both sulphide and sulphate minerals has been widely used as a means of tracing the origin of sulphur species, as well as, the nature of the sulphide precipitation mechanisms. In the Alston Block, work by Solomon et. al. (1971) revealed a very wide range for the sulphide (galena) sulphur isotopic composition, with

$\delta^{34}S$ values ranging from -5.9‰ to +15‰. Mitchell and Krouse (1971) reported a narrow range of sulphur isotopic values for 16 galena samples from the Greenhow-Skyreholme area. However in general, the overall spread of the sulphide sulphur isotopic values in the North Pennine orefields is wide and similar to the range observed in most MVT ores. Barite shows a much more uniform sulphur isotopic composition with a mean $\delta^{34}S$ of +19‰, interpreted by Solomon et. al. (1971) as characteristic of Carboniferous connate seawater. A more detailed review and discussion on the sulphur isotopic characteristics of both the North and South Pennine orefields will be given in Chapter 6 which is devoted to a sulphur isotope study in samples from the Ecton Hill Cu-rich mineralization.

Strontium isotope studies in fluorites were undertaken by Shepherd et. al. (1982). The $^{87}Sr/^{86}Sr$ data were paired with the results of a fluid inclusion Rb-Sr isochron study in samples from the Great Sulphur Vein (Shepherd & Darbyshire 1986), in an attempt to resolve the age and origin of the ore-forming fluids. Assuming a 206Ma age (calculated from the Rb-Sr isochron), the basement granite appears too radiogenic to be compatible with the uniform tight-spread $^{87}Sr/^{86}Sr$ ratios of the fluorites (0.71003-0.71134). On the basis of the strontium isotopic distribution, the Carboniferous shale and/or the limestone sequences were favoured by Shepherd et. al. (1982) as potential fluid sources. The distribution of $\delta^{18}O$ values in quartz and barite coupled with the Deuterium-Hydrogen isotopic signature of inclusion fluids in fluorite, quartz and barite from the Alston orefield are similar to those of MVT ores and strongly favour a basin brine rather than a juvenile origin of the fluids (Moore 1980). The inclusion fluids are strongly depleted in δD, with values ranging from -106 to +8‰. A process involving expulsion of fluids through semipermeable shale-membranes was proposed by Moore (1980), as the principal cause of the observed δD depletion of the North Pennine fluids. However, as noted by Roedder (1979) and Kharaka et. al. (1985), the original isotopic composition of the fluids is rarely preserved as it is readily affected by fluid-rock interaction processes. Therefore, the isotope signature alone cannot provide conclusive evidence on the provenance of the ore-forming fluids. The provenance of the ore-fluids in the Pennines will be further examined in the present study with the aid of new data from the chemical analysis of fluid inclusions.

2.4.1.2. The South Pennine Orefield

The South Pennine (Derbyshire) orefield lies at the southern end of the North-South trending Pennine hills, in Central England (Fig.2.8). It consists of a plateau of about 90Km^2 of Lower Carboniferous (Dinantian) limestones, often bituminous with dolomite, chert and interbedded volcanics. Overall, the geological setting of the ores is similar to that

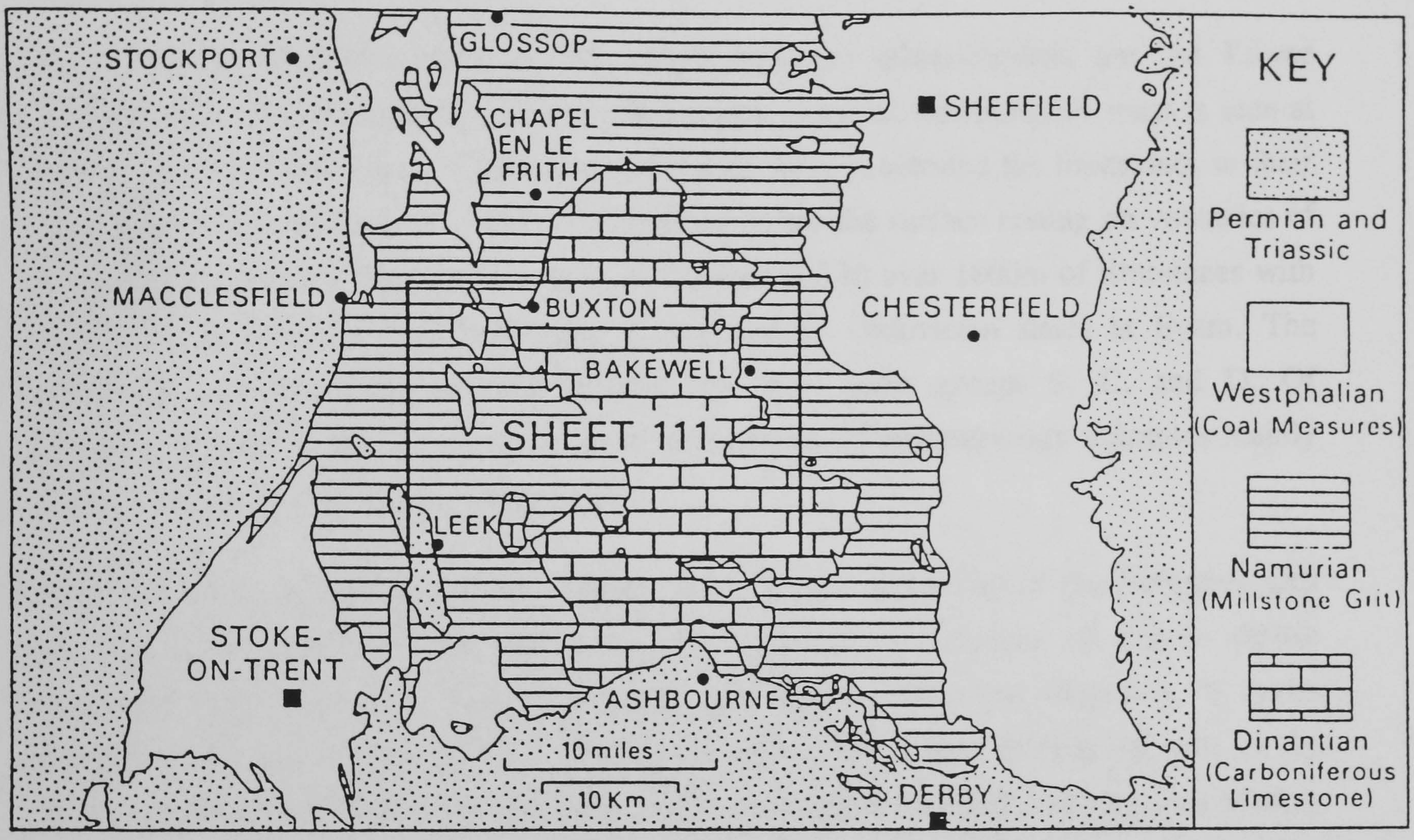


Fig.2.8. Sketch-map showing the main geological formations of the South Pennine Orefield (after Aitkenhead et. al. 1985).

of the Northern field. However, there are some differences mainly regarding the mineral zonation, and the presence of igneous rocks. The following summary of the main geological features of the orefield is based mainly on publications by Dunham (1983), Ford (1976), Ineson and Ford (1982), Mostaghel and Ford (1986), MacDonald et. al. 1984, Colman et. al. (1989a).

2.4.1.2.1 Host-Rock Geology

Similar to the Northern Pennines, the major hosts to mineralization are the Lower Carboniferous (Brigantian) limestones; however, only a part of the limestone mass is seen at the surface. Two boreholes, at Woodale and Eyam have penetrated the limestones to their base, and have encountered a) 500m of limestone below the surface resting on volcanics of uncertain but probably Precambrian age at Woodale and b) over 1800m of limestones with anhydrites towards the base resting on a basement of Ordovician slates at Eyam. The exposed limestone sequences were divided into three main groups S, C, and D. Of particular interest is the D-zone because of the presence of contemporary volcanics mainly lavas and tuffs, known locally as toadstones.

The limestones are overlain by the Upper Carboniferous succession of the Millstone Grit and the Coal measures. The Millstone Grit comprises a sequence of coarse deltaic sandstone alternating with Namurian shales, followed by the Coal Measures, a cyclic sequence with less limestones and many coal seams. The Lower lithological unit of the Millstone Grit in Derbyshire, is the Edale shales. The shales although varying in thickness throughout the orefield, they are sufficiently continuous and have formed a seal over most of the limestone area at the time of mineralization. This is further supported by the presence of only traces of mineralization in the Millstone Grit and Coal Measures (Ford 1976).

2.4.1.2.2. Volcanics

There are no granitic intrusions in the South Pennine orefield. However, characteristic is the presence of basic volcanics within the limestone sequence, with volcanism reaching a peak during the Dinantian. Poor exposure and lack of continuous outcrop make the regional correlation of individual basalt units difficult. Two centers of eruption have been recognized at Matlock and Miller's Dale and overall 30 distinct lava and tuff horizons have been identified (MacDonald et. al. 1984).

The lavas are highly altered, fine grained olivine basalts containing amygdales of

carbonate, chlorite, chalcedony or albite. The primary igneous mineralogy is altered and replaced by secondary minerals. The close association of sub-aerially erupted lavas with submarine flows is a notable feature of the Derbyshire volcanicity and supports the alternation of submergence and emergence recorded in the Carboniferous limestone sequence (Aitkenhead et. al. 1985). Tuffs are less extensive at outcrop than lavas and their presence in association with paleokarsts, suggests that they had an air-fall origin. Thin greenish-grey clay wayboards in the self limestones are also of volcanic origin and they represent periodic accumulations of fine airborne volcanic dust resting on emergent limestone surfaces. As suggested by MacDonald et. al. (1984) in a detailed geochemical and petrographical analysis of the lavas, the Dinantian volcanism in Derbyshire was associated with minor phases of isostatic uplift of a shallow carbonate platform on the Northern margin of St. Georges E-W land mass. The magmas were generated by varying degrees of partial melting of heterogeneous mantle sources followed by fractional crystallization and final equilibration mainly in the lower crust.

2.4.1.2.3. Ore Mineralogy

Roughly defined gangue mineral zones are present in the South Pennine orefield. However, instead of concentric, the zones are North-South trending with fluorite dominant at the East, barite in the center, and calcite at the western part of the orefield. Galena is the dominant sulphide throughout the orefield, with subordinate sphalerite mainly across the eastern part of the orefield (Ford 1976). The only exception from the general Pb-Zn-dominant pattern, is the Cu-rich district of Ecton Hill at the South Western margin of the orefield, which will be described separately in the following section. In general, the primary sulphide mineralogy is uniform and displays a consistent paragenetic sequence with a characteristic widespread occurrence of small amounts of Ni-bearing sulphides. The main sulphide paragenetic sequence in Derbyshire comprises of bravoite, pyrite (nickel-rich and nickel-poor) marcasite, chalcopyrite, galena and sphalerite (Ixer and Townley 1979).

Similar to the Northern Pennine districts, mineralization has the form of veins and metasomatic replacements or cavern fillings. The veins consist of calcite-fluorite-barite and occasionally quartz gangue, with smaller amounts of galena and sphalerite minor amounts of Fe-Ni and Cu sulphides. The sulphides have two main styles of crystallization, either as small inclusions within the gangue minerals or, less commonly, as mixed sulphide ore. In terms of geographical distribution, Fe-Ni sulphides are the most widespread phases, generally as bravoite, pyrite and marcasite. Galena is almost as widespread, and much more abundant, with sphalerite and chalcopyrite less common. There is a general increase

in sulphide abundance towards the eastern margin of the orefield, but no other regional variation was detected (Ixer and Townley 1979).

2.4.1.2.4. Isotope Studies

As in the North Pennines, Moorbath (1962) studied the lead isotopic ratios of a small number of galena specimens and deduced ages of mineralization as 280±20Ma and 180±40Ma. Later work by Coomer and Ford (1975) has shown that the leads are radiogenic J-type, and represent negative model ages. Their work on Pb isotopes revealed a remarkable homogeneity of the Pb isotope distribution. K/Ar dating on clays from altered lavas and tuffs was undertaken by Ineson and Mitchell (1972) who suggested that mineralization was active between 270±7 and 235±5Ma with continuous but minimal activity until 180±2Ma (Late Carboniferous, Late Permian and Late Triassic). However, Mitchell & Krouse (1971) criticized previous $^{40}Ar/^{39}Ar$ isotope work on fine grained clay minerals in the North Pennines (Dunham et. al. 1968), and suggested that the late peaks represent argon loss.

Sulphur, oxygen and carbon isotope analyses in barite-calcite-limestone-sulphide samples are reported by Robinson & Ineson (1979). The $\delta^{13}C$ values of vein calcites and limestones are relatively constant and group around +3‰, a value typical of marine carbonates. Therefore, carbon in the veins appears to have been supplied from the limestones. Most of the $\delta^{18}O$ values of the calcites group around +20‰, whereas the values in barite show a larger spread, from +9 to +26‰. Oxygen isotope fractionation factors between calcite and barite are low and only the barite with the more positive values is thought to approach equilibrium with a fluid of high $\delta^{18}O$ values, or in other words evolved connate water (Robinson & Ineson 1979). Sulphur isotope studies in the area have shown that $\delta^{34}S$ values of barite exhibit a wide spread ranging from +4‰ to -23‰, which was interpreted by the those authors (op. cit.) as a result of a dual source for the sulphur, and mixing of low $\delta^{34}S$ fresh water sulphate with high $\delta^{34}S$ connate water sulphate. Sulphide (galena) sulphur isotopic values are also widespread ranging from -23‰ to +7‰. Similarly to the North Pennines, the sulphur isotope values are not conclusive on the origin of sulphur, but they preclude any contribution of magmatic sulphur (Robinson & Ineson 1979).

More information on the isotopic composition of both sulphides and sulphates together with the subsequent genetic implications for the Pennine orefields in general will be given in Chapter 6, which is devoted to sulphur isotope investigations on the Cu-rich mineralization of Ecton Hill.

2.4.1.3. Cu-dominant Mineralization

Although the dominant sulphides throughout the Derbyshire orefield is galena with minor sphalerite, mineralization at Ecton Hill, the south-western corner of the Peak District, is dominated by copper. The geology of the area has been described by Critchley (1979), Aitkenhead et. al. (1985) and Astrop (1987) on which the following summary is mainly based.

Mineralization is more restricted to the central parts of two major structures, the Ecton and Mixon-Morridge anticlines, where Dinantian limestones are flanked by younger mudstones. Ecton Hill is composed mainly of muddy, thinly bedded limestones belonging to the Milldale and Ecton formations of Lower Carboniferous age. The oldest rocks cropping-out in the Ecton area belong to the Chadian and Arundian stages of the Lower Carboniferous. Contemporary volcanics produced abundant wayboards during the Arundian and Asbian, but no intrusive rocks have been found in the area.

The Ecton and Mixon limestone formations were deposited in a basinal environment, to the west of a migrating reef margin which separated the region from the shallower water environment of the Peak District limestones. These bioclastic and conglomeratic beds were deposited by turbidity currents, presumably flowing from a rising self area to the east. The Namurian in the area is represented by the Millstone Grit facies of sandstones, siltstones, mudstones, derived from landmasses to the South and North-East. The area has undergone E-W compression, which produced a faulted anticlinorium, plunging some 10° to the NW. Mineralization has the form of numerous veins and two large laterally extensive pipe-like bodies, known as the Ecton and Clayton pipes. Dominant vein directions are NNW and ENE with minor E-W and NW trends (Aitkenhead et. al. 1985).

The principal sulphides at Ecton are chalcopyrite, chalcocite and bornite. Chalcopyrite appears to have formed linings to several large cavities, but today is found mainly as small inclusions in clear calcite. Galena is the most abundant sulphide in the presently accessible workings, and sphalerite, although not found underground, is fairly abundant in the mine dumps. Calcite with minor barite and rare fluorite are the main gangue minerals. Large scale zoning of the sulphide minerals has been suggested because of the predominance of galena in the upper levels with Cu-sulphides becoming more abundant as we move downwards in the mine. However, since at present the larger part of the underground workings is flooded, it is not possible to establish that hypothesis any further.

The location of the orebodies, and the Cu-dominant ore paragenesis, links them to the

stratabound occurrences of copper at or near the edge of the Triassic basins of Staffordshire and Cheshire (Aitkenhead et. al. 1985). A different source for the orefluids has been invoked for the Ecton mineralization (Masheder & Rankin 1989). Mineralization at Ecton Hill is a very interesting case study of the basinal brine related mineralization because it provides an insight to the role and the ability of basinal brines to form both Pb-Zn and Cu-dominant sulphide ores. Thus, the ore-fluid chemistry of the Ecton Hill mineralization, together with the sulphur isotopic composition of sulphide and sulphate minerals will be investigated in more detail in the present work.

2.4.2. Theories for ore-genesis in the Pennines

Several genetic models have been proposed for the Pennine orefields over decades of active research in the area. Earliest theories favoured igneous sources for the fluids and ore forming constituents. However in the light of new geochronological, structural, geochemical and fluid inclusion evidence, models involving sedimentary, diagenetic processes have become widely acceptable. Most of the previous and current ideas were reviewed in detail by Dunham (1983), and Colman et. al. (1989b). However since the present work provides new evidence on the chemistry of the ore forming fluids, and consequently aims to further examine these models, a summary of previous theories is essential in order to set the context and background of the research.

2.4.2.1. Models involving rising juvenile fluids.

Ore transport and deposition by rising juvenile fluids was proposed by Dunham (1934), and was generally acceptable in the early days of research. It was mainly the concentric mineral zonation in the North Pennine orefield, and the lack of knowledge on the age of both mineralization and that of the underlying granites which led to the conclusion that mineralization in the Pennines was closely associated with igneous activity, and similar to the outer zones around the Hercynian granites in Devon and Cornwall. However on the basis of both structural and isotopic evidence, it has now become evident that the granites clearly predate the mineralizing events by at least 100Ma (Dunham 1983, 1992, Dunham & Wilson 1985).

Apart from the timing of mineralization, fluid inclusion studies have shown that in terms of both temperature and composition, the mineralizing fluids do not have any magmatic-juvenile signature. In a recent review of the Carbonate-hosted base-metal mineralization in general, Russell & Skauli (1991) argued in favour of a granitic source of the fluorine in the Northern Pennines. Although the source(s) of fluorine has not been positively traced, and

some contribution from the granites cannot be ruled out in the Northern fields, an alternative source has to be found for the South Pennines where there are no granitic intrusives. In general, although the granites may have provided the heat source and the channels for the mineralizing fluids, a more direct influence in contributing ore-fluids, metals and sulphur seems highly unlikely.

A different theory proposed by Sawkins (1966a), involved mixing of granite-derived metal-bearing fluids with Ba-rich cooler brines. That model was aiming mainly to explain the widespread occurrence of barite at the Eastern part of the Northern Pennine orefield. However, the feasibility of such a model is questionable since, apart from the preclusion of granite-derived fluids as ore-forming solutions, the role of Ba-rich brines in mineralization is still not clear. As pointed out by Solomon et. al. (1966), the wall-rocks of the roots of barite deficient mineralized veins, are enriched in Ba, showing that the mineralizing fluids carried that element. Modern barium-bearing, coalfield brines studied by Edmunds (1975) could have been ore forming on a local scale, but their salinities are much lower than those reported for the fluid inclusions. The main barrier in tracing the role, if there is any, of distinct Ba-rich brines to the mineralization lies to the limited information on fluid inclusion composition in barite. Fluid inclusions in barite are extremely difficult to examine due to common phenomena of stretching and leakage. Therefore, the fluid inclusion data from barite samples are of questionable validity.

2.4.2.2. Descending brines from Triassic evaporites

Triassic evaporites were regarded by Davidson (1966) as the cause of the high salinity of mineralizing fluids. According to his theory, the mineralizing solutions were dense brines, derived from the diagenesis of Triassic evaporite sequences, and which acquired the ore forming constituents from the limestones and other rocks through which they passed. However, the isotopic composition of sulphate sulphur in the North Pennines lies in a very restricted range averaging +19.2‰ (Solomon et. al. 1971), while the accepted figure for the Upper Permian is near 10 (Thode & Monster 1965, Claypool et. al. 1980).

In the South Pennine orefield the spread of sulphate sulphur isotopic values is greater, leading Robinson & Ineson (1979) to suggest that both Carboniferous and Triassic brines were involved in mineralization. In the South Pennine orefield the presence of scattered mineralization in Permian and Triassic rocks, may indicate that the Permian rocks rested directly on an eroded surface of the Carboniferous limestones, which led Robinson & Ineson (1979) to propose a Permian start for the mineralization with complex mixing of

separate fluids. However, in the Northern fields the situation is quite different since the large thicknesses of shale-dominated Namurian and Westphalian rocks clearly separated the Permian unconformity from the highest mineralized strata (Dunham 1983).

2.4.2.3. Brines Expelled from Sedimentary Basins

Various versions of the basinal fluid expulsion model have been proposed for ore genesis in the Pennine orefields. Overall, the general concepts of the model are widely acceptable and supported by many authors (Dunham 1983, Ford 1976, Ineson 1976, Worley and Ford 1977, Colman et. al. 1989b, Mostaghel and Ford 1986, Plant et. al. 1988). Schematic representations of the proposed genetic models for the North and South Pennine mineralization are shown in Figs.2.9a and 2.9b.

Brines are expelled from sedimentary basins as a result of pressure rise with increasing burial, towards the margins of the basins. The Namurian shale sequences have been proposed as possible sources of the ore-fluids. As noted by Jones & Plant (1989), the shales are enriched in trace elements and they also have high contents of Rb and U which may account for the enrichment of the ores in radiogenic Sr and Pb isotopes. Also, recent work by Fowler and Anderson (1991), argues that the overpressured shale horizons may account for the high temperatures of the mineralizing fluids, since their heat production can reach values similar to those of the buried granites. However, application of this model to the Pennines where the shales lie on top and not underneath of the mineralized sequences, is not clear.

As suggested by previous authors, there are indications that the overall chemical composition of the mineralizing fluids in the Pennines strongly resembles that of the MVT fluids which have an undisputed oilfield brine affinity (Atkinson et. al. 1982, Roedder 1976). However, despite the overall similarities, the dominance of fluorite and galena in the paragenesis distinguishes the Pennine mineralization from the typical MVT deposits and calls for some additional controls in the mineralizing events. The source of fluoride has to be accounted for in any genetic model for the Pennine mineralization. As suggested by Colman et al. (1989b), rocks most likely to have high F contents are the organic, phosphatic black shale horizons. However, still, the source of fluorine is not clear and a contribution from the granites cannot be ruled out (Russell & Skauli 1991).

As proposed by Colman et. al. (1989b), possible explanations for the Pb dominance generally include a) the preferential complexing of Pb by organic solvents, b) stabilization of Zn-bearing phases in the source rocks and c) control of fluids by diagenetic phase

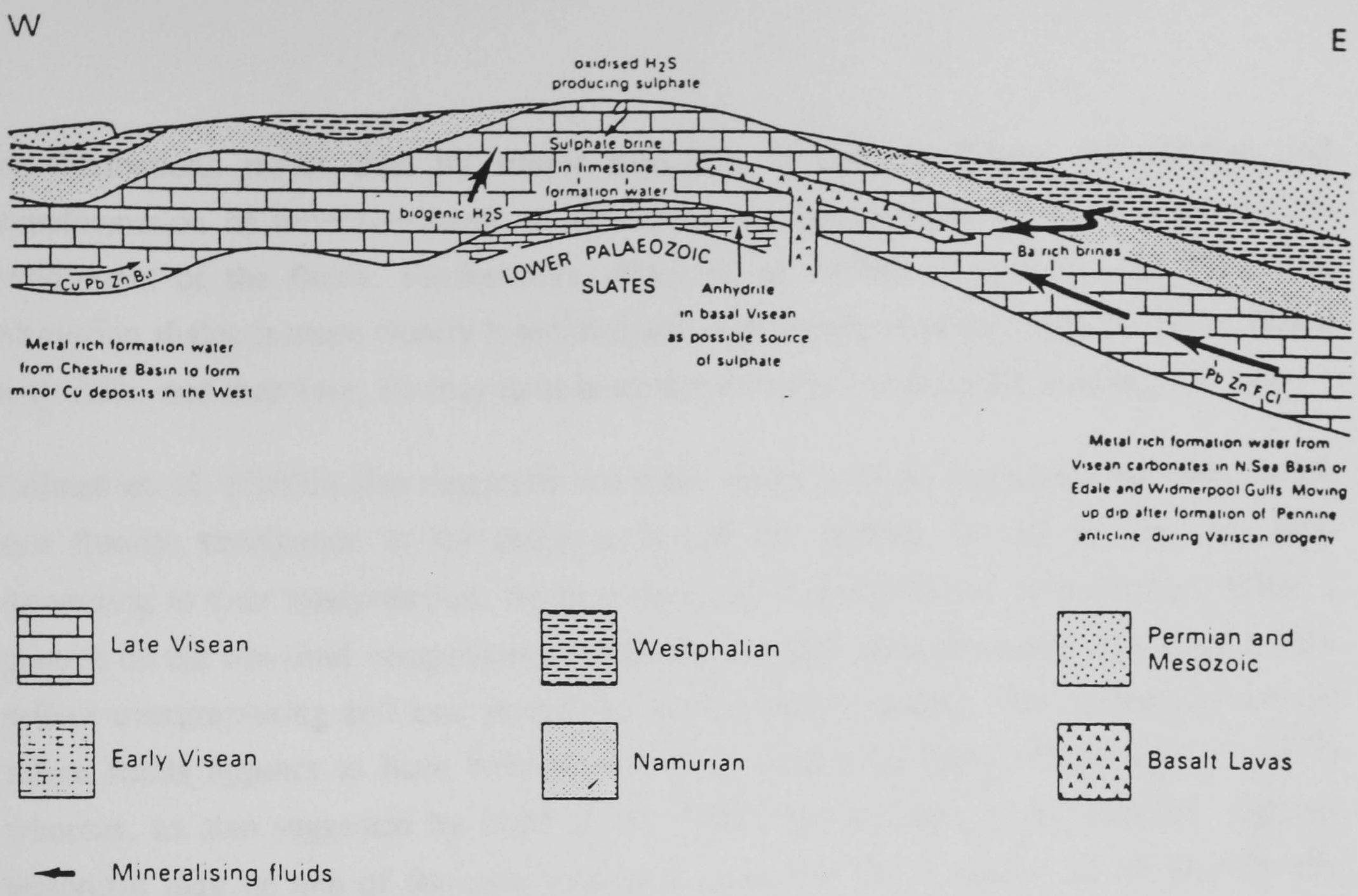


Fig.2.9a. Schematic representation of proposed genetic model for mineralization in the South Pennines (after Worley & Ford 1977).

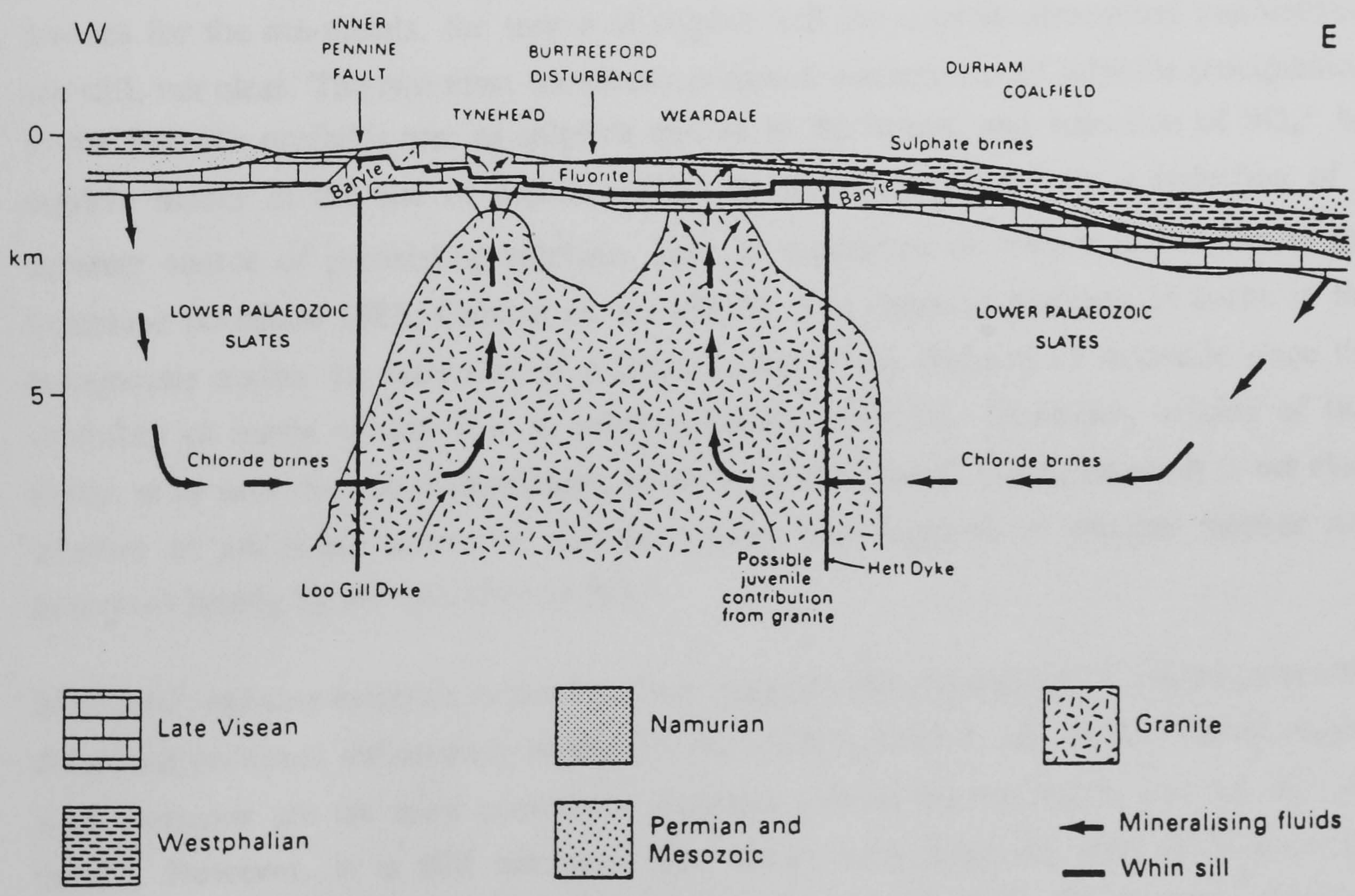


Fig.2.9b. Schematic representation of proposed genetic model for mineralization in the North Pennines (after Solomon et. al. 1971).

BIBL
LONDON
UNIV

transformations rather than by simple solubility in chloride brines. Dehydration and transformation of montmorillonite to illite is a possible explanation for the Ba and Pb enrichment of the fluids. Furthermore, Plant et. al. (1988) alleged that the Pb in the Namurian shales is more closely associated with the organic fraction whereas, Zn is related with illite, and therefore, Pb may have been more readily available for leaching than Zn.

Colman et. al. (1989b) also suggested that there seems to be an association between the Pb and fluorite dominance in the paragenesis and the fracture control of the orebodies. According to their interpretation, the dominance of Pb and F in the Pennines may reflect a control of the ore-fluid composition by diagenetic phase transformations that may in turn reflect overpressuring and heat production by the shale horizons. The episodic release of saline fluids appears to have been depended on seismic pumping (Sibson et. al. 1975) whereas, as also suggested by Plant et. al. (1988) and Colman et. al. (1989b), regional tectonism may be one of the most important factors in the formation of Pb and fluorite dominant MVT deposits in general.

As in all MVT deposits, the problem of ore-transport and deposition in the Pennines is still not clear. Although the shales and possibly the limestones are considered as possible sources for the ore-metals, the source of sulphur and the sulphide-deposition mechanisms are still, not clear. The two most commonly proposed mechanisms of sulphide precipitation in the Pennine orefields are: a) sulphate carried in the brines, and reduction of $SO_4^=$ by organic matter at the site of deposition and b) derivation of H_2S by a reduction of a separate source of preexisting sulphate, such as evaporites or formational fluids in the limestone (Dunham 1983, Colman et. al. 1989b). The common presence of barite in the paragenesis makes the reduction of sulphate in the brines difficult to reconcile since the solubility of barite is very low in sulphate-bearing solutions. Therefore, mixing of two fluids, at or near the site of deposition, needs to be considered. Furthermore, It is not clear whether an additional source of reduced sulphur was required or whether sulphur was generated locally by the reduction of $SO_4^=$.

In general, existing evidence in the Pennines suggests that the sources of fluids can be both distal and proximal sedimentary basins (Dunham 1983, Plant et. al. 1988). The Namurian shale horizons are the most commonly proposed sources for the fluids and for the ore-metals. However, it is still not clear how these fluids acquired such high salinities. Tectonism seems to have played a more important role in the Pennine mineralization than in the typical MVT districts. Evidence from fluid inclusions from all three Pennine orefields strongly supports a sedimentary rather than a magmatic affinity for the ore-fluids.

Further evidence on the physical and chemical properties of the ore-fluids will be provided in the present work with greater emphasis on the halogen and alkali metal contents of fluid inclusions as a means of further tracing the origin and chemical evolution of the fluids. Theories on the genesis of the Pennine ores will be further discussed in the following chapters under the light of the new geochemical evidence obtained from fluid inclusion analysis.

2.4.3. The Llanharry Iron Deposit, South Wales

The Llanharry iron deposit is one of those hematite-goethite deposits with a history of mining tracing back to Roman times. The orebody is confined almost entirely to the *Dibunophyllum* zone of Carboniferous (Avonian) limestone and is capped by Triassic (Keuper) breccias and marls. There are no major non-ferrous orefields in the area; only small tonnages of galena were raised from Dinantian limestones on the southeastern rim of the coalfield near Machen, north of Cardiff. There are however important replacement deposits of iron in the Carboniferous Limestone, where it crops-out along the southern edge of the coalfield. The geology of the Llanharry mine was reviewed by Williams (1958) and more recently by Gayer and Criddle (1970), and Rankin & Criddle (1985) on which the following summary is based .

The ore in the upper levels of the mine has the form of a relatively continuous sheet, conformable with the top of the limestone and leans against black, Namurian shales. Below the 320ft level the orebody splits into six roughly cylindrical orebodies, almost parallel to the dip of the limestone, whereas, still remains in contact with the shales. At greater depths the orebodies plunge more steeply and away from the shales, with limestone becoming the hanging wall. The foot-wall in that case being one or more of a series of grey shale horizons within the limestone (Fig.2.10).

The dominant ore type consists of layers or bands (1mm to 1m thickness) of colloform and crystalline goethite, with minor amounts of hematite. The bands are separated by cavities which are partly or entirely filled by stalactitic goethite, hematite, calcite and quartz. Calcite is the most common cavity filling mineral and at that stage clearly post-dates the crystallization of iron minerals. In cavities that are partially filled, euhedral calcite and quartz may enclose the iron minerals or are encrusted within them, indicating several stages of mineralization. Quartz, although abundant, is not distributed as uniformly as calcite. Pyrite is not common at Llanharry. It is present mainly as small inclusions in calcite, and as nodular clusters in cavities at the foot-wall grey shale. It is usually partly or totally

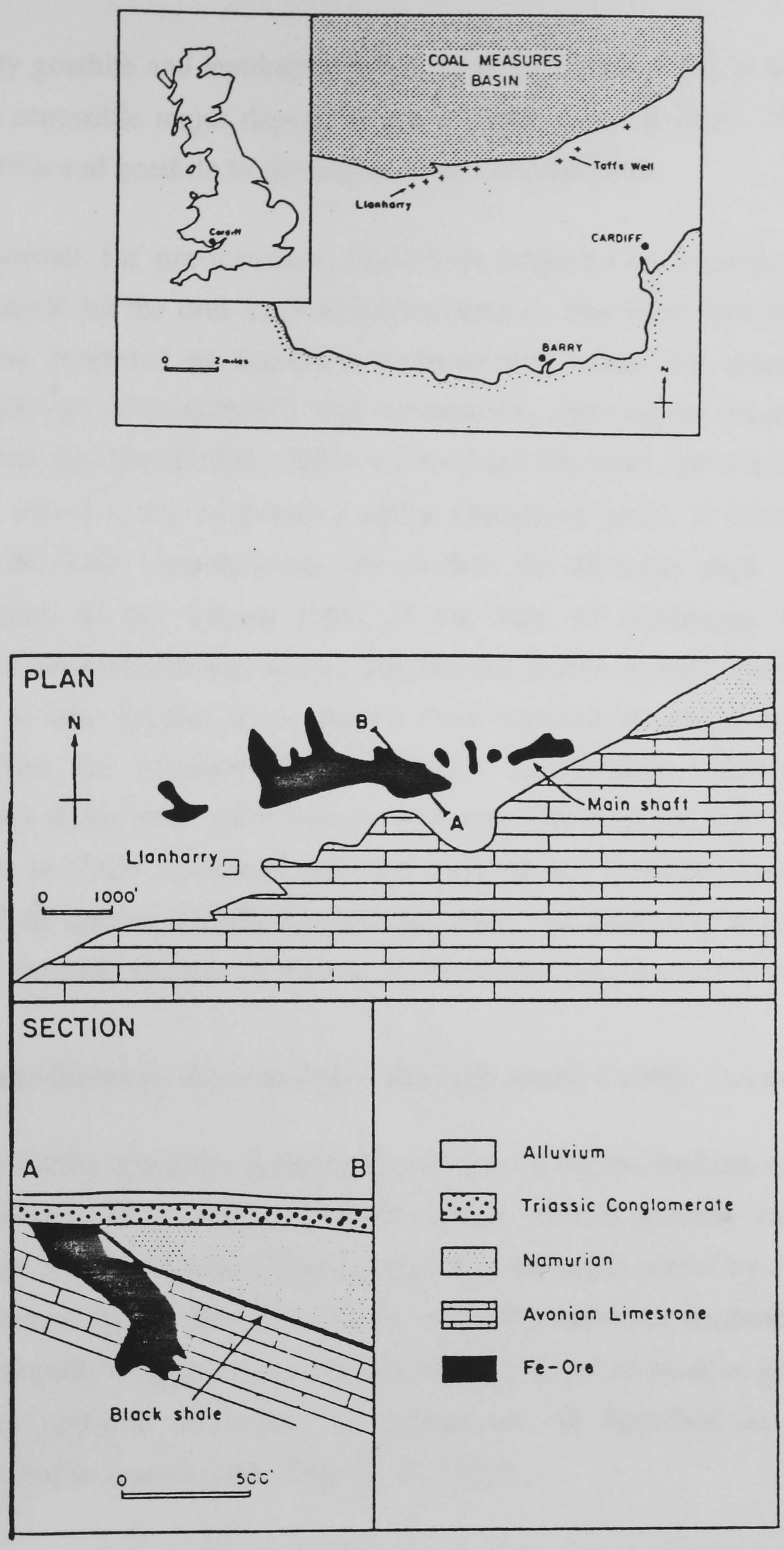


Fig.2.10. Sketch-maps showing the location, general morphology and geological setting of the Llanharry-Fe deposit in South Wales (after Rankin & Criddle 1985).

replaced by goethite and lepidocrocite. Barite is not common at Llanharry but it is abundant at the last accessible major deposit of the orefield, Garth at Taffs Well, mainly associated with hematite and goethite to the east and west of Llanharry.

Several theories for ore-formation have been proposed by previous authors. The earlier models considered the ores as of supergene origin. This view was challenged by Williams (1958) who proposed an ascendant hydrothermal model for mineralization during the Miocene period. This approach was subsequently opposed by Gayer and Criddle (1970) who showed that the orebody follows Hercynian fractures down the dip of the limestone sequence, and it is cut by possibly alpine (Miocene) faults. It follows that the ore must post-date the Late Carboniferous and predate the Miocene stage. The absence of iron mineralization at the Liassic strata of the Vale of Glamorgan and the presence of fragmented hematite ore and broken bipyramidal quartz crystals, indicates that the ore was emplaced at Late Keuper times. Recent fluid inclusion studies in both calcite and quartz samples from the Llanharry deposit (Rankin and Criddle 1985) have shown that the mineralizing fluids were saline brines, with appreciable amounts of Ca^{+2}, indicating broad similarities to fluids associated with the classical MVT mineralization. Additional, more detailed fluid inclusion studies in samples from the Llanharry deposit, were undertaken during the present research in order to further investigate that possibility.

2.5. Granite-Related, Fluorite Mineralization South Crofty, Cornwall

The South Crofty mine lies in the middle of the Camborne-Redruth mining district in West Cornwall (Fig.2.10). It is part of the Cornubian orefield spatially associated with the roof of an S-type, high-heat-production monzogranite batholith hosted by a deformed and lightly metamorphosed Upper Paleozoic marine mudstone-sandstone sequences. The Carnmenellis granite is broadly circular and is surrounded by a series of satellite granites. Although there are internal textural variations, the granite can be described as a coarse porphyritic muscovite-biotite granite (Leveridge et. al. 1990).

The current workings at South Crofty are situated on lode structures within the Carn Brea granite ridge which intrudes the metamorphosed slates and greenstones of the Devonian Mylor Slate formation, commonly known as "Killas". The Carn Brea granite is a two-mica monzogranite having many features in common with the other evolved granites of the Cornubian batholith (Farmer & Halls 1992). The timing of emplacement is generally assumed to be the same as the adjacent Carnmenellis pluton, around 285$\pm$9Ma, as determined by Darbyshire and Shepherd (1985) on the basis of Rb/Sr whole rock isotopic

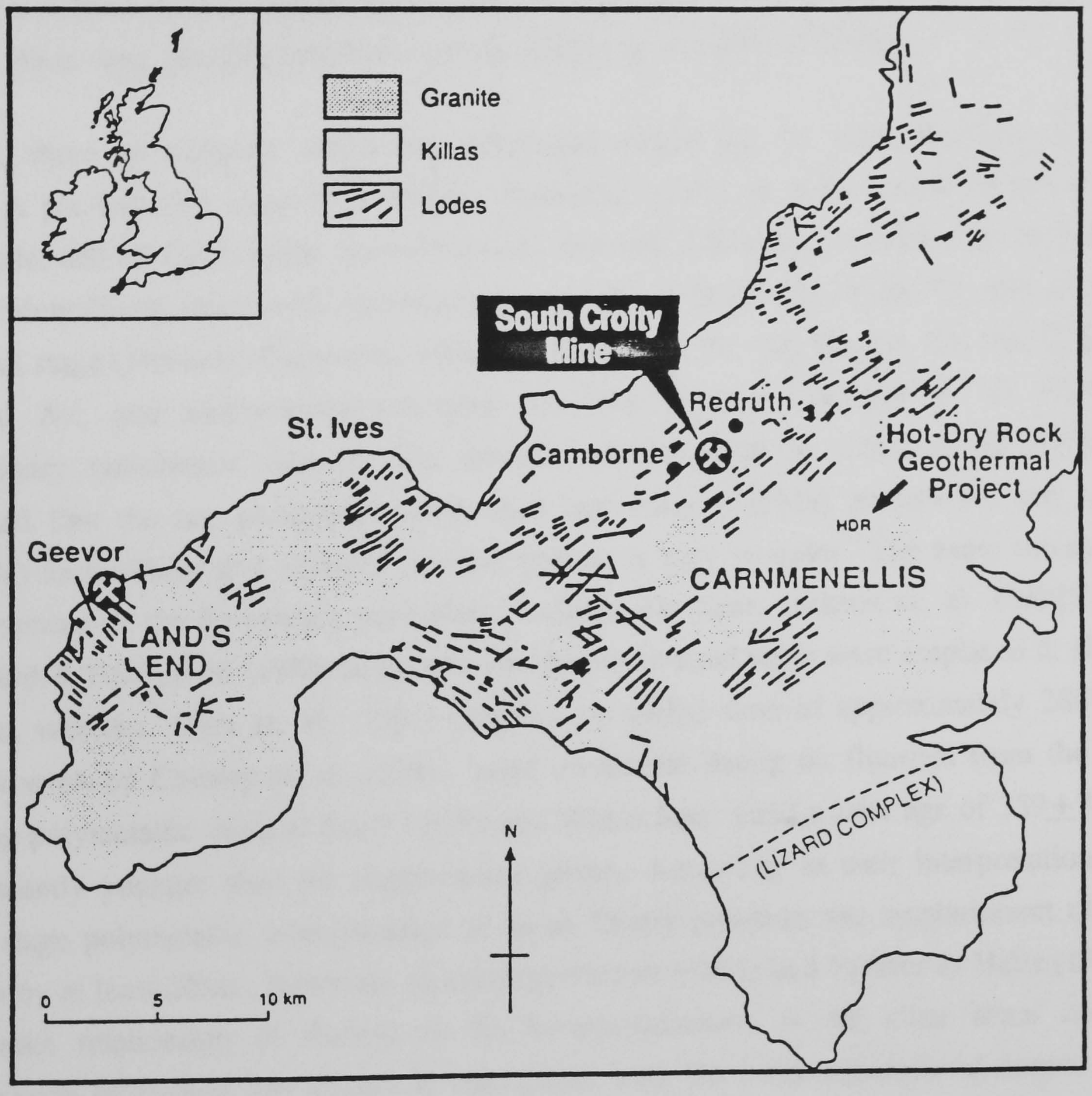


Fig. 2.11. Location map of the South Crofty Mine, Cornwall (after Farmer & Halls 1992).

dating. In a more recent work by Chen et. al. (1991), $^{40}Ar/^{39}Ar$ age spectra for magmatic micas and K-feldspar in the Carnmenellis and Carn Brea granites defined the following chronology:

i) emplacement and rapid cooling of the now exposed surfaces at 288-290Ma, with further cooling at 286Ma, ii) emplacement of the feldspar porphyry dikes (South Crofty) at $>$283Ma, iii) local emplacement of biotite-rich, fine grained granite at 276Ma, iv) cooling of present surface of the Carnmenellis pluton to $<$110°C at 267Ma and v) further cooling of the 2.3Km-deep (present-day) Carnmenellis pluton to $<$110°C at 203Ma.

Overall, three metallogenic stages are recognized within the ore field (Jackson et. al. 1989). A pre-batholith stage (300-400Ma) consisting mainly of strata-bound Fe-Mn oxy-hydroxide, and Fe-Cu sulphide syn-sedimentary deposits. Follows a syn-batholith, or main-stage, mineralizing event with hydrothermal deposits of Sn-Cu-As-Fe-Zn-Pb, and a post batholith stage (Mesozoic-Cainozoic) with vein deposits of Pb, Ag, Sb, Ba, Zn, Fe, U, Co, Ni and Au, and hydrothermal-supergene kaolinite deposits (Jackson et. al. 1989). Preliminary radiometric data for the metallic mineralization by Chen et. al. (1991), indicated that the ore paragenesis subdivided into early (285Ma) greisen-W, and later (270Ma) tourmalinite and chloritic (Sn-Cu) phases, is very complex. The exact timing of emplacement of the Sn-bearing mineralized lodes is not clear. Jackson et. al. (1982) and Shepherd & Darbyshire (1986) suggested that the mineralized veins were emplaced at about 270Ma, whereas, Chen et. al. (1991) proposed an earlier time of approximately 280Ma. Recent work by Chesley et. al. (1991) based on Sm-Nd dating on fluorites from the Sn-bearing polymetallic veins at South Crofty and Wheal Jane, yield a later age of 259$\pm$7Ma, significantly younger than the Carnmenellis pluton. According to their interpretation the main stage polymetallic mineralization at South Crofty postdates the emplacement of the pluton by at least 20Ma. However, as noted by Farmer (1991) and Farmer & Halls (1992), the exact relationship of fluorite to the Sn-mineralization is not clear since several generations of fluorite are present in association with the main mineralizing event. It is therefore possible that the Sm-Nd fluorite ages obtained by Chesley et. al. (1991), represent a later event, separate from the earlier, hypothermal Sn-mineralization (C. Halls 1992).

The principal lodes at South Crofty have a NE trend with minor veins trending to a E-W direction. Several stages of mineralization have been recognized on the basis of both structural and mineralogical evidence. The earliest stage consists of quartz, K-feldspar, wolframite, lollingite/arsenopyrite, in the form of swarms or flat-lying veins, commonly

known as floors. The bulk of cassiterite mineralization is found in later stages, in a series of steeply dipping subparallel lodes which exhibit a very composite structure. Cassiterite in the lodes is associated with two paragenetically distinct stages. The first, having a tourmaline-dominant gangue mineralogy, is called the "tourmaline stage". It is followed by a paragenetic association in which chlorite forms the main gangue, and it is therefore called "chlorite stage". Generally, the higher grades of tin mineralization are associated with blue tourmaline in the above mentioned tourmaline-stage of the paragenesis, whereas, in the chlorite-stage, tin appears to be evenly precipitated in open spaces which have undergone little structural deformation (Farmer & Halls 1992). The latest stage of mineralization at South Crofty is confined in a series of wrench faults, known as cross-courses. They are either quartz, quartz-fluorite, or quartz-hematite-bearing veins, which cut across the tin-bearing veins throughout the mine workings.

Combined geological, mineralogical, structural, isotopic, and fluid inclusion evidence indicates that mineralization in the Cornubian orefield in general, is a product of multiple hydrothermal events (Jackson et. al. 1989). The earliest mineralization events associated with the batholith are related to the emplacement and crystallization of the roof rocks. As suggested by Jackson et. al. (1989), most of the mineralization was formed where fluids of meteoric origin mixed with metal and sulphur-bearing fluids of magmatic origin However, later hydrothermal events, as indicated by the presence of polymetallic (Pb-Zn-Cu-F-Ba-U) veins, are possibly not directly associated with the granite plutons, and are characterized by a distinctive fluid chemistry. The low temperature high salinity of the inclusion fluids from that later stage of mineralization has led many authors to suggest that they were formed by basinal brines expelled from the Mesozoic sedimentary basins flanking the peninsula (Alderton 1975, 1978, Shepherd & Scrivener 1987). The presence of low-temperature, high-salinity fluids has also been reported in the South Crofty fluorites (Farmer 1991).

The possibility that fluids with a basinal brines affiliation were involved at some later stage of mineralization at South Crofty is further examined in the present work by the means of detailed fluid inclusion studies. Evidence from both the temperature and chemical composition of fluid inclusions will be used to assess the previously invoked role of basinal brines in the mineralizing events, the influence of the granitic intrusives, as well as draw comparisons with the base-metal mineralization in the Pennines and MVT-deposits in general.

2.6. Summary

Deposits of the MVT class have long been recognized as a distinct and economically important class of base-metal mineralization. The basic characteristics of these deposits have been summarized by many investigators and include the following. The deposits are closely associated with sedimentary sequences and they commonly occur at or near the edges of sedimentary basins with dolomite being the most common host-rock, whereas, igneous rocks are relatively unimportant in most areas. Mineralization is clearly epigenetic with sphalerite and galena being the main sulphides, whereas, barite and fluorite are also present in certain areas. Fluid inclusion investigations have established that the ores were deposited from highly saline brines of moderate temperatures ranging from 80 to about 150^{o}C. However, apart from these general features that define the MVT class, each district has its own characteristics. Overall, models involving the expulsion of saline brines from sedimentary basins are favoured for ore-genesis in the MVT deposits. Nevertheless, after decades of active research, no unifying genetic model has been established for all MVT deposits. Puzzling problems centre around the timing of mineralization, the origin of the fluids, as well as the ore-transport and sulphide precipitation mechanisms.

Broad similarities between the Pb-Zn-fluorite mineralization of the English Pennines and the classical MVT deposits have also been noted and discussed in the literature. The dominance of fluorite in the paragenesis, as well as the possible influence from the underlying granites in the North Pennines, highlight the main differences between the Pennine and the classical MVT mineralization. Sedimentary basin evolution models have also been favoured for ore genesis in the Pennines. Regional differences, however, between the three Pennine orefields, mainly in terms of the importance of igneous rocks in the mineralization, may have a bearing on genetic models for the Pennine mineralization in general.

Similar comparison with the general sedimentary basin-related mineralization have also been made for other deposits such as the Ecton Hill Cu-dominant mineralization and the Llanharry Fe-ores of South Wales. The possibility that basinal oil-field brines are involved in the formation of deposits in a variety of lithologies and of variable ore paragenesis is further investigated here through detailed fluid inclusion investigations. The study also extends to investigations of comparable phenomena during the late stages of fluorite mineralization at South Crofty, Cornwall.

Chapter 3

Development and evaluation of experimental methods for the chemical analysis of ionic species in fluid inclusions

3.1. Introduction

The main objective of fluid inclusion analysis is to provide an insight to the fluid processes that have taken place in the rock or mineral host and, on how they varied in different geological environments and throughout time. Especially in the field of ore-genetic studies, information on the physical and chemical properties of fluid inclusions has provided very important constraints regarding the origin and evolution of ore-forming fluids.

Several methods have been developed for the chemical analysis of fluid inclusions. These methods are described by Roedder (1984), Shepherd et. al. (1985a) and, more recently, in a comprehensive review by Roedder (1990). In the case of a typical two-phase, liquid-vapour, aqueous inclusion the ideal method would be one that enables determination of all fluid inclusion constituents, major and trace, anions and cations, together with the volatile content, pH and Eh of the inclusion solution. However, no such technique has yet been developed and usually more than one methods have to be employed to obtain a complete chemical analysis of the inclusion fluids.

Fluid inclusions can be analyzed either by "bulk" or "point" methods following destructive or non-destructive procedures. In the case of bulk methods the analyses refer to a large number of inclusions whereas, in point methods individual inclusions are analyzed. In general, fluid inclusions are far from simple analytical samples and a number of problems have to be overcome during their chemical analysis. These problems are caused by the microscopic size of inclusions (individual inclusions are typically less than a few microns in size and contain around 10^{-9} g of material for analysis) and their low abundance in the host mineral. High sensitivity methods are therefore a prerequisite for the determination of both major and trace elements in the inclusions. Difficulty in extraction and interference from the host also have to be readily dealt with, in both destructive and non-destructive methods. Especially when bulk methods are employed, standard reference materials for fluid inclusions are not readily available. This lack of real fluid inclusion "standards" makes the calibration and validation of analytical techniques problematical. Considerable progress is currently been made in that field with the use of synthetic fluid inclusions (Banks & Yardley 1992) for validation, however yet, the procedure is far from routine.

Apart from microthermometry other non-destructive techniques for fluid inclusions include the electron microprobe, proton microprobe, nuclear magnetic resonance, synchrotron x-ray microprobe, instrumental neutron activation (INAA) and the Laser Raman spectroscopy which recently has become the most valuable tool for the identification and quantitative analysis of polyatomic gas species such as CH_4, CO_2, N_2 and H_2 in the inclusions (Roedder 1990). Bulk, destructive methods require extraction and separation of the inclusion contents (either by crush-leach or decrepitation) from the host. Atomic absorption spectrometry, flame atomic emission spectrometry, ion chromatography, inductively coupled plasma atomic emission spectrometry (ICP-AES) and neutron activation analysis (NAA), have all been used for the analysis of fluid inclusion extracts with varying success (Roedder 1990).

Point, non destructive methods are generally more desirable because they offer information on individual inclusions, as well as, the opportunity of "true" replicate measurements. However, it is non always possible to obtain valid results without extraction of the inclusion fluid. Most problematic is the *in situ* analysis of fluid inclusions in complex minerals such as fluorite and calcite where interference from the host can be severe and has a masking effect to the elements of interest in the fluid. Bulk methods are valid when all fluid inclusions in a sample belong to a single generation regarding both their compositional and physical characteristics. Sample size is also important and methods with small sample size requirements are particularly useful.

3.2. Samples Studied

The present study is concerned with the chemistry of the aqueous phase of fluid inclusions in fluorite and to a lesser extent calcite samples from the English Pennine Pb-Zn-fluorite deposits, the Ecton Hill Cu-dominant mineralization and the Llanharry Fe-ores of South Wales. Selected fluorite samples from the late stage of mineralization at South Crofty, Cornwall, were also analyzed. The geological setting of these deposits is described in Chapter 2; a more detailed description of the samples studied in the present work is given in Chapter 4, whereas, all sample numbers, description and localities are listed in Appendix A. The chemical analysis results were combined with data from microthermometry presented in the following chapter. Efforts, outlined in the present chapter are oriented towards the development of a robust scheme of analysis for the determination of both cationic and anionic species in a large number of samples. The decrepitation-ICP method (D-ICP) proved to be very appropriate for the measurement of cations whereas, destructive Neutron Activation Analysis (RNAA), was used for the determination of Cl and Br.

Extraction of the inclusion fluid was necessary for both methods in order to overcome large scale interference from the host. The experimental procedures followed during the present work together with current developments and evaluation of the results will be presented here.

3.3. The Decrepitation ICP (D-ICP) method

In the standard ICP-AES method a nebulized test solution is injected into a toroidal plasma formed in a stream of argon. The nebulized solution is then subjected to a temperature of about 9000K and is completely atomized. The atomic emissions are examined in a region just above the plasma where the background signal is low (Thomson & Walsh 1988).

The linked decrepitation-Inductively Coupled Plasma-Atomic Emission Spectroscopy (D-ICP) method is based on the fact that rapid heating of mineral fragments containing fluid inclusions normally induces decrepitation during which, the sudden rise in the internal fluid pressure is sufficient to break the host crystals. Upon decrepitation the fluid inclusion contents are rapidly released into the surrounding atmosphere. This phenomenon is utilized by transmitting the ejected decrepitate material directly into the plasma in a stream of argon carrier gas. The temperature at which decrepitation takes place depends mainly on the trapping temperature and pressure of the inclusion but also on other variables such as the composition, size, shape and the position of the inclusion within the crystals (Chryssoulis & Rankin 1988). In general, temperatures substantially higher than the trapping temperatures may be necessary to cause decrepitation.

The D-ICP method has been widely used for the analysis of major and trace cations in fluid inclusions for over a decade now (Thomson et. al. 1980, Chryssoulis 1983, Alderton et. al. 1982, Rankin et. al. 1987 Lindblom et. al. 1989). Most of the current developments and applications of the method are reviewed in a recent publication by Rankin et. al. (1992). Only small changes have been made in the equipment since the method was first used by Thomson et. al. (1980). Most of the efforts were concentrated towards applying the method to various minerals and inclusion types and minimizing interferences. In the present study emphasis is also given to the reproducibility of the results, as well as, to the application of the method to the analysis of fluid inclusions in complex minerals such as fluorite and calcite, which have not been studied widely so far. Furthermore, questions on the validity of the method and the reproducibility of the results are also examined with the aid of replicate analyses and through comparison of results obtained by the D-ICP and the conventional crush-leach analysis.

3.3.1. Experimental System and Sample Preparation

Most of the information on the D-ICP equipment is presented in Rankin et. al. (1992) and only a summary will be given here. The equipment used is shown schematically in Fig.3.1. The spectrometer is an Applied Research Laboratories 34000C 1m vacuum spectrometer equipped with lines for 40 elements and operating conditions as described by Ramsey & Thomson (1985).

The sample, typically 0.3-0.5g of 1-2mm sized fragments, is heated in small Pyrex test tubes to the point of decrepitation within about a minute. The sample tube is connected to the inlet of the ICP by a short (0.5m) clear PVC silicone tubing. A stream of humidified argon carrier gas is passed through the test tube prior to and during decrepitation. The flow rate through the sample container is kept constant throughout the run since the plasma sensitivity depends critically on the carrier-gas flow. A bench mounted, ten-port Teflon valve is an essential part of the system. It facilitates a rapid sample change in less than a minute by ensuring that, in by-pass mode, there is a continuous argon flow into the plasma without introducing air into the system. Rapid heating of the sample is essential in order to cause effective decrepitation. Thus the sample is placed in a preset position within a small electric buncen burner held at a temperature of 700°C. The temperature in the tube rises at rate of approximately 600°C/min causing audible, and occasionally visible decrepitation of the sample.

Fluid inclusions in fluorites and calcites were analyzed in the present study. Sample preparation was simple and involved crushing of the sample in a porcelain pestle and mortar followed by sieving to obtain the fraction between 1 and 2mm. The mineral chips were then picked under the binocular microscope in order to obtain a clean fraction, free from adherent mineral phases such as sulphides and iron staining. Acid cleaning could not be undertaken because calcite is readily and fluorite slightly soluble in both HCl and HNO_3. Hand picking, which was the most time consuming part of sample preparation, was therefore necessary to select moderately clean sample chips for analysis. A restricted number of samples were electrolytically cleaned following a procedure outlined by Roedder (1958). Results obtained from these samples will be discussed in detail in the following sections.

3.3.2. Calibration, Sensitivity and Detection limits

Effective calibration is one of the most problematic aspects of the D-ICP analysis. Most of the problems arise from the fact that the total volume of the analyzed solution is not

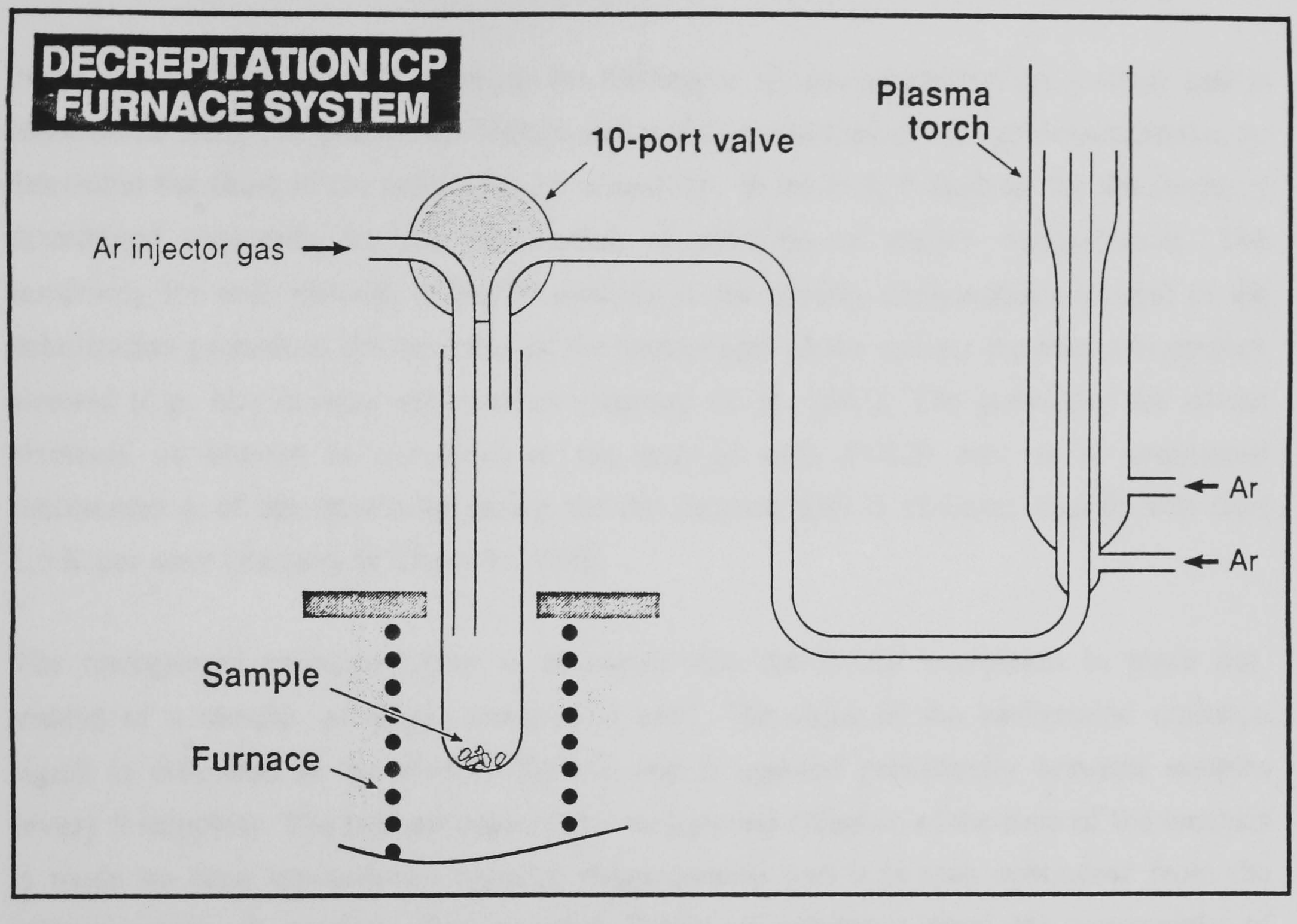


Fig.3.1. Schematic representation of the Decprepitation ICP (D-ICP) furnace system used in the present study.

known, which makes the conversion of each sensitivity (mV) output to an exact concentration value impossible. Therefore, instead of concentration in ppm units, the terms "pseudoconcentration" and "equivalent ppm"(eppm), are considered more appropriate.

In the conventional ICP-AES analysis the calibration at low concentrations is linear and is constructed using two points, the background and a standard point of high concentration, to determine the slope of the calibration or sensitivity. In the D-ICP analysis the sensitivity is determined separately by the nebulization of solutions of known concentration. The sensitivity for each element in D-ICP analysis is not directly comparable with that in the nebulization procedure but the ratio of the sensitivities of the analyte element and another element (e.g. Na) is relatively constant (Ramsey et. al. 1992). The sensitivity for all the elements of interest is measured at the end of each D-ICP run; it is considered representative of the sensitivity during the run because drift is minimal, usually less than 1.5% per hour (Ramsey & Thomson 1985).

The background emission signal is measured with the D-ICP equipment in place but instead of a sample, an empty test-tube is used. The value of the background emission signal is measured at the start of the run and is updated periodically between samples (every 5 samples). The best estimate of the background emission at the time of the analysis is made by time interpolation between measurements and it is then subtracted from the measurements on samples. The detection limits are estimated from the uncertainty of replicate concentration measurements made on blank tubes. These measurements are interpreted over the entire D-ICP batch and they therefore represent the full uncertainty due to background drift, as well as random instrumental noise. However, due to the lack of true blank fluid inclusion samples and random measurement errors, the detection limit estimate is only approximate($\pm$30%).

By using the calibration procedures outlined above it is possible to estimate "pseudoconcentration", "eppm" units for each element in the decrepitate. Absolute concentrations are practically impossible to determine because as noted previously, both the number of inclusions which decrepitate and the mass of material released into the plasma are not known. Therefore, the results are preferably expressed as ratios to Na. It is however possible to convert these pseudoconcentration semiquantitative values to quantitative, concentration values if total salinity data from microthermometry are available for the same samples and if it is established that the same inclusions, of one generation, are present in the two data sets.

3.3.3 Review of mechanisms of material transfer into the plasma

There are various mechanisms for transfer of components from the sample into the plasma. Recognition of these mechanisms is of great importance to understanding the limitations of the analyses and their successful interpretation. Uncertainties arise when more than mechanism predominates. Overall, four mechanisms are recognized (Rankin et. al. 1992).

a) Release of small droplets (aerosol) from inclusions during total decrepitation.

b) Volatilization of components from fluid inclusions which have only partially leaked their components onto the surface of the sample, or from daughter minerals which adhere to the walls of the decrepitated inclusions.

c) Mechanical release of small fragments of the host mineral.

d) Mechanical introduction of fragments of, or volatilization from components, of admixed contaminant grains.

Ideally mechanism (a) should be optimized to the exclusion of all the others. It is however impossible to avoid at least some volatilization from mechanism (b). This is however usually minimized through rapid heating and also by avoiding samples which contain daughter minerals. Introduction of fragments from the host mineral is also unavoidable. This means that it is not possible to determine those components of fluid inclusions that are also present in the host mineral.

For quartz samples mechanism (c) does not cause a serious problem since Si is not usually one of the major constituents of inclusion fluids. The problem is more severe when dealing with calcite and fluorite samples. Decrepitation causes introduction of small fragments of the host mineral into the plasma and consequently, results in a very high Ca signal. It is therefore not possible to determine the Ca levels of the inclusion fluids. Spectral interferences on other elements due to high Ca values are largely overcome by on-peak interference corrections.

3.3.4. Time resolved D-ICP

Time-resolved D-ICP analysis involves multiple short integrations of emissions over a 5 second period followed by a null 3 second period. These integrations are usually measured over a 4 min interval (total time 260s). Because the time-temperature characteristics of the furnace and the time-temperature variations in the sample tube can be measured, the time-

emission profiles can be converted into temperature-emission profiles. Such emission profiles have been previously published (Shepherd et. al. 1985a) using raw emission intensity (mV) units. Current software developments permit processing of large amounts of raw data and therefore enable the presentation of time-resolved plots in terms of "pseudoconcentration" units (Rankin et. al 1992). These are much more meaningful because they are corrected for spectral interference and enable direct calculation of element ratios.

The time-temperature plots are important for establishing the time/temperature interval over which bulk decrepitation occurs. They can also be important in evaluating sources of contamination, as well as, effects of selective volatilization/sublimation of different components. In the course of the present work numerous time resolved D-ICP analyses were undertaken mainly in fluorite but also in calcite samples. Results obtained from these analyses will be presented in the subsequent section which is devoted to the overall evaluation of the D-ICP analysis data.

3.3.5. Quality Control

One of the most serious problems encountered in the D-ICP method, as in all bulk fluid inclusion analyses, is the problem of "within sample" variability. Apart from random analytical error "within sample" variability is caused by the fact that the results represent the average composition of all the analyzed inclusions. It is not possible to overcome this problem when the analyzed samples contain multiple inclusion generations, each with different chemical characteristics. In that case the results from chemical analysis represent only an average composition of all generations present and they are not considered geochemically meaningful.

In the present study and as will be demonstrated in Chapter 4, evidence from microthermometry has shown that, in the majority of the samples, the fluid inclusions belong to a single generation of tightly constrained temperature-salinity patterns. In the present section the question of whether the bulk analysis results are valid is given further consideration. Multiple replicate analyses were undertaken in the same samples in order to examine the extent and effects of the "within sample" variability. Up to 22 separate analyses were performed in selected samples. It was not possible to do the same for all the samples analyzed in the present study because of the lack of adequate sample material, as well as, of the considerable time involved in sample preparation and analysis. However, representative samples from most of the areas of study were selected for replicate analyses

in order to examine whether the differences in fluid inclusion chemistry were real and not just a result of analytical and /or "within sample" variability.

With the D-ICP method it is possible to determine simultaneously up to 40 elements including Na, K, Ca, Mg, Sr, Ba and Li, as well as, Pb, Zn, Cu, Fe, Mn and total sulphur. Information on the concentration of all these elements in fluid inclusions is highly desirable. However due mainly to very low concentration levels and interference from the host mineral, reliable information could be obtained only for a small number of these elements.

3.3.5.1. Alkali Metals and Alkaline Earths

For the purposes of the present study of special interest are the elements Na, Ca, K, Li and also Sr, Mg and Ba. For reasons stated previously Ca could not be determined by chemical analysis. As far as the other cations are concerned, it is essential to examine the reproducibility of their ratios to Na before proceeding to any interpretation of the results.

The basic statistics of the K/Na, Li/Na, Mg/Na, Sr/Na and Ba/Na ratios were calculated from replicate analyses and they are presented in Table 3.1. As can be seen from Table 3.1., the K/Na and Li/Na ratios exhibit adequate reproducibility with coefficient of variation ranging from 5 to 20% (extreme case). The Sr/Na ratios are also fairly reproducible with coefficient of variation from 4 to 20%. The Mg/Na and Ba/Na ratios are problematic and, as it can be seen from their statistics, they are extremely variable in the same sample. Especially for the Ba/Na ratios, coefficients of variation can reach values higher than 100%. Substitution of Mg for Ca is not uncommon in fluorite (Deer et. al. 1962). That is most probably the reason of the very high variability in the Mg/Na values of the decrepitates which possibly reflect contribution from the host mineral phase. The presence of trace quantities of Mg in the fluorite was confirmed by whole-rock ICP analysis following a procedure outlined by Thomson & Walsh (1988). Ba does not substitute for Ca in fluorite, but barite is a very common accessory mineral in the paragenesis of the samples studied. Thus, the possibility that small fragments of barite were present in the analyzed samples cannot be ruled out. The problem could not be solved even with very careful hand picking of the sample chips under the binocular microscope, since barite and colorless fluorite grains have very similar appearance. Appreciable quantities of Ba were also found in the fluorites. The results of whole-rock ICP analysis of fluorites are listed in Appendix C. Consequently, because of their non-reproducible nature, values for both Mg and Ba cannot be used any further as it is not certain whether the elements are

actually present in the fluid inclusions or they are a result of contamination and contribution from the host mineral phase.

For two of the studied samples more than 20 separate analyses were undertaken. The results are shown in Table 3.2. The K/Na and Li/Na values obtained through these replicate analyses are presented in the form of histograms in Fig.3.2. The sample size is not large enough to show with accuracy the form of distribution, however, the ratios are constrained by moderately narrow limits and in the case of sample AL/10/F, exhibit an approximate normal distribution. The relative contributions of pure analytical uncertainty and that from "within sample" heterogeneity to the total variance can be estimated approximately following the calculations by Ramsey et. al. (1992). As can be seen from Table 3.1., precisions in the order of 4% (Na/Li ratio of sample AL/10/F) can be achieved, whereas the most common values of precision are around 10%. If we take the minimum value as representative of the analytical variance and the maximum value as representative of the total variance the following simplistic calculation can be made.

$$\sigma^2 \text{ total sample} = \sigma^2 \text{"within sample"} + \sigma^2 \text{ analytical}$$

Substitution of the corresponding values in the above equation would suggest that the sample heterogeneity although small, accounts for approximately 80% of the total sample variance.

Apart from these two samples for which more than 20 analyses were performed, replicates were also obtained for other samples. Similarly, the results for Na/K and Na/Li showed remarkable homogeneity confirming the microthermometric evidence for the presence of one dominant fluid inclusion generation and consequently, proving the validity of the bulk chemical analysis results. K/Na and Li/Na values obtained through multiple analyses of sample separates are presented as control charts in Fig.3.3. and 3.4. These charts show that during the several D-ICP runs, outliers were not encountered and that all values lie within the limits of two standard deviations.

Table 3.1. Averages of major and trace cation (X/Na) weight ratios obtained from replicate D-ICP analyses in five fluorite samples.

Sample	K/Na mean	standard deviation (s)	coefficient of variation (CV%)	n
AL/10/F	0.095	0.0064	6.73	22
AL/6/F	0.098	0.0098	10.00	20
AS/1/F	0.034	0.0075	22	9
DR/7/F	0.0182	0.0023	12.63	5
DR/9/F	0.0237	0.0016	6.75	5
Sample	Li/Na mean	standard deviation (s)	coefficient of variation (CV%)	n
AL/10/F	0.0039	0.00015	3.96	22
AL/6/F	0.0028	0.00027	9.64	20
AS/1/F	0.00069	0.00019	27	7
DR/7/F	0.00040	0.000021	5.20	5
DR/9/F	0.00050	0.000027	5.40	5
Sample	Sr/Na mean	standard deviation (s)	coefficient of variation (CV%)	n
AL/10/F	0.019	0.0014	7.14	22
AL/6/F	0.019	0.0038	20.00	18
AS/1/F	0.0117	0.0013	11.11	7
DR/7/F	0.0125	0.0005	4.00	4
DR/9/F	0.020	0.0017	8.50	5
Sample	Mg/Na mean	standard deviation (s)	coefficient of variation (CV%)	n
AL/10/F	0.012	0.010	86.37	8
AL/6/F	0.010	0.0047	47	11
AS/1/F	0.014	0.00053	3.78	5
DR/7/F	0.0085	0.0048	56.47	4
DR/9/F	0.016	0.0048	30	5
Sample	Ba/Na mean	standard deviation (s)	coefficient of variation (CV%)	n
AL/10/F	0.017	0.0038	22.87	22
AL/6/F	0.052	0.093	17.5	14
AS/1/F	0.019	0.023	122	7
DR/7/F	0.021	0.018	85.7	4
DR/9/F	0.26	0.22	84.6	5

Table 3.2. K/Na and Li/Na weight ratios from replicate D-ICP analyses in two fluorite samples.

Sample AL/6/F		Sample AL/10/F	
K/Na	**Li/Na**	**K/Na**	**Li/Na**
0.114	0.0033	0.080	0.0039
0.107	0.0031	0.098	0.0042
0.110	0.0031	0.085	0.0038
0.106	0.0030	0.088	0.0038
0.089	0.0029	0.089	0.0037
0.095	0.0031	0.090	0.0038
0.095	0.0030	0.096	0.0037
0.092	0.0031	0.097	0.0039
0.090	0.0027	0.098	0.0040
0.088	0.0028	0.098	0.0039
0.113	0.0030	0.092	0.0038
0.109	0.0030	0.098	0.0038
0.102	0.0026	0.092	0.0036
0.100	0.0024	0.098	0.0038
0.094	0.0026	0.091	0.0040
0.099	0.0028	0.099	0.0039
0.078	0.0024	0.100	0.0039
0.092	0.0026	0.108	0.0042
0.085	0.0026	0.096	0.0038
0.095	0.0027	0.103	0.0039
		0.091	0.0036
x=0.098	x=0.0028	x=0.095	x=0.0039
std=0.0098	std=0.00027	std=0.0064	std=0.00018

Over the last decade the D-ICP method has become a routine technique for the analysis of fluid inclusions in a variety of minerals. Nevertheless, there is still criticism surrounding the quality of the results. In the present study and despite the fact that the precision of the results has been demonstrated through replicate analyses and statistical calculations, it was considered necessary to further validate the accuracy of the method by analyzing a number of samples using both the D-ICP and the conventional crush-leach methods. Similar comparisons have been made in the past by Rankin & Graham (1988) and Rankin et. al. (1992), mainly concerning the Na/K ratios which proved to be comparable especially for samples which did not contain daughter minerals.

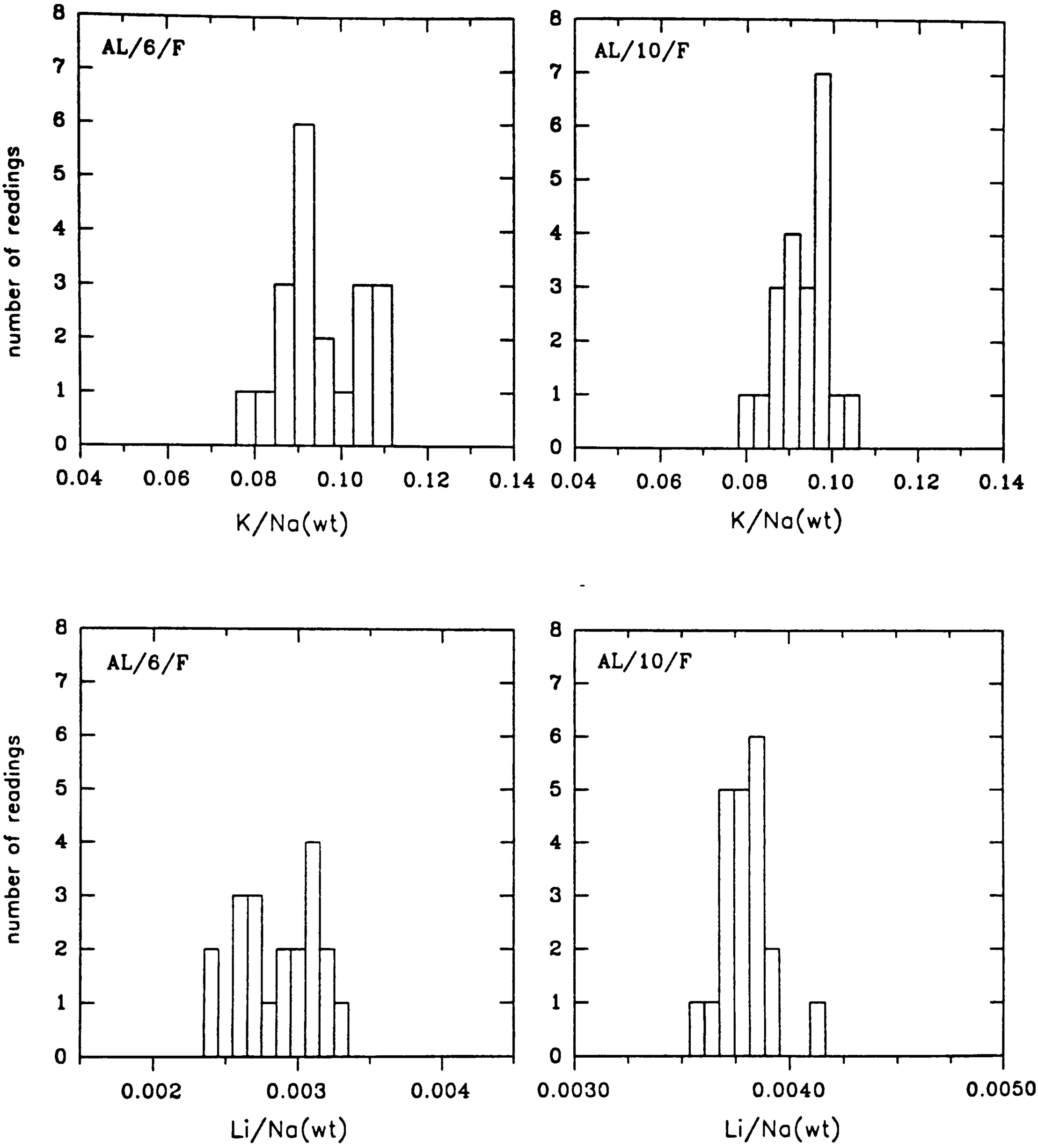


Fig.3.2. Frequency distribution of the K/Na and Li/Na weight ratios of fluid inclusions obtained from replicate D-ICP analyses in two fluorite samples (data presented in Table 3.2).

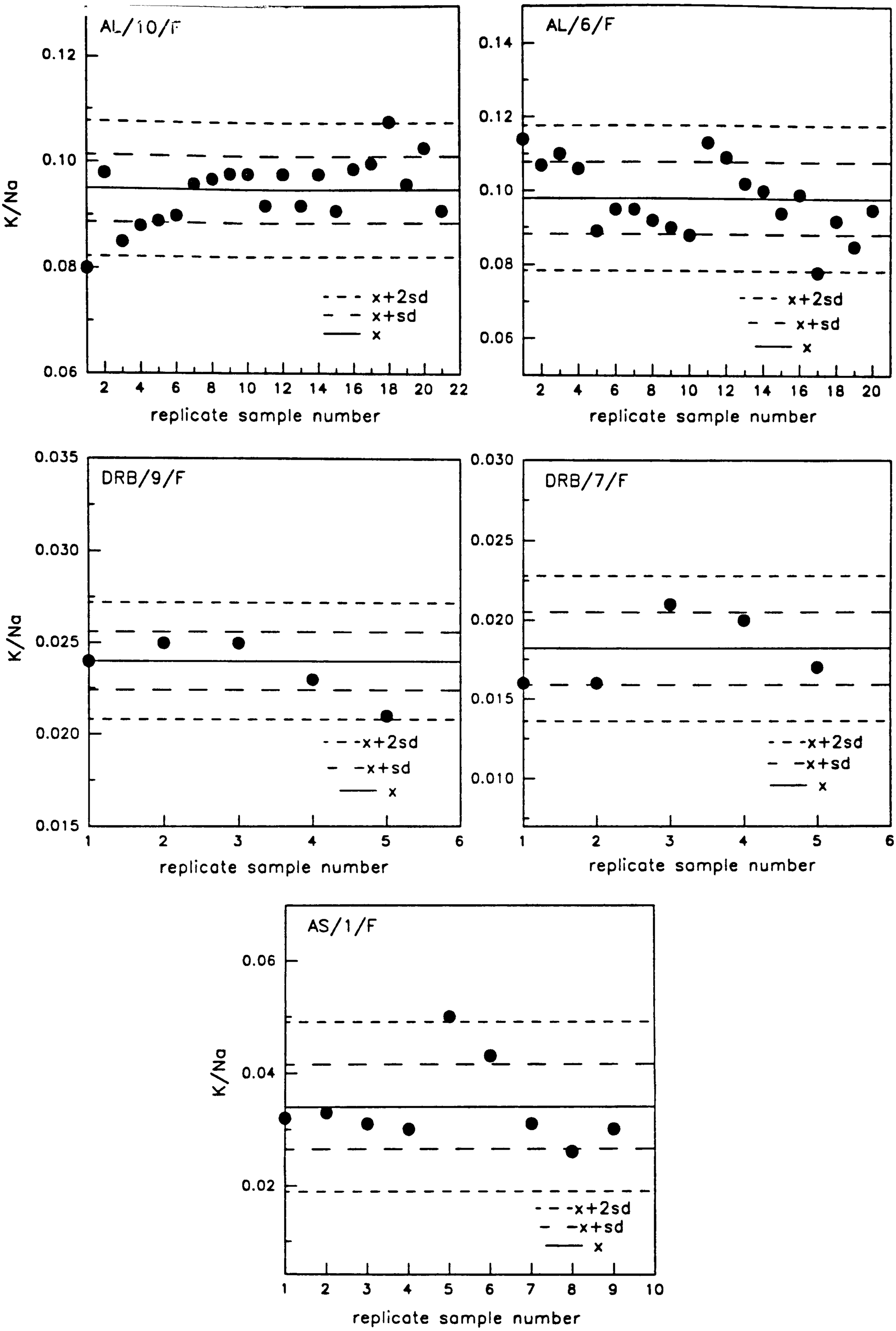


Fig.3.3. Control charts showing the variation of the K/Na weight ratios of fluid inclusions obtained from replicate D-ICP analyses of five fluorite samples.

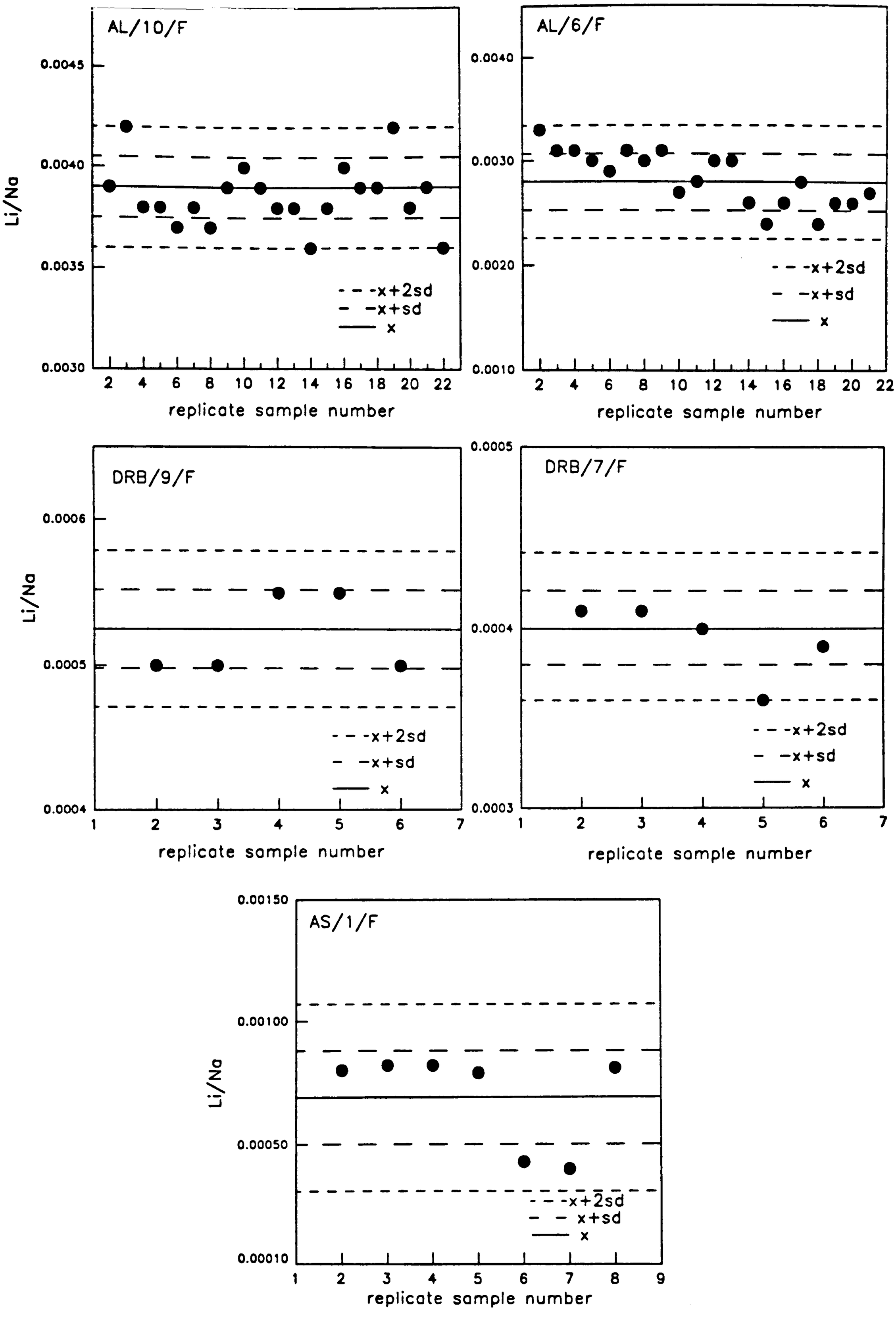


Fig.3.4. Control charts showing the variation of the Li/Na weight ratios of fluid inclusions obtained from replicate D-ICP analyses of five fluorite samples.

Values of K/Na and Li/Na obtained by crush-leach ICP and D-ICP are presented in bivariate plots (Fig.3.5), with error bars representing the standard deviation for samples where multiple analyses were done. Overall, the two sets of data are quite comparable. Most of the observed differences are within the limits of the total uncertainty caused by "within sample" variability. Also, in the early stages of the present work contamination from the agate mortar during the crushing-leaching procedure caused the higher crush-leach K values. Lithium could not be detected in all samples with the crush-leach method due to the dilution required for the extraction of the leachate. This was not a problem in the D-ICP method because no dilution is required. Therefore, using smaller amounts of sample (0.2-1.00g) it was possible to determine trace elements such as Li in most of the samples.

3.3.5.2. Analysis Of Variance (ANOVA)

An important part of the present study is concerned with the variation and significance of the Na/K and Na/Li ratios of inclusion fluids in samples from different localities. Therefore, it is considered essential to establish that the between-sample or geological variation is greater than the "within-sample" variation. Thus, analysis of variance (ANOVA) was performed in order to identify the different sources of variance and to evaluate their extent in selected samples.

Three samples representative of three different localities with characteristic fluid inclusion chemistry mainly in terms of K and Li contents (low, medium and high) were selected for this purpose. The detailed ANOVA calculations and tables are presented in Appendix C. From the calculations and the F-test at the 0.05 probability level, it became clear that the "between" sample variation is much higher than the "within" sample one. For the Na/K ratios the calculated "within" and "between" sample variance is 2.8% and 97.2% of the total variance respectively. For the Na/Li ratios, the calculated percentages of the total variance are 16.3 and 83.7 for the "within" and "between" sample variance respectively. Therefore the observed differences in the chemistry of these representative samples are indeed a result of true sample variation and not an artifact arising from the uncertainties of bulk fluid inclusion analysis.

3.3.5.3. Base Metals and Sulphur

Efforts were made to determine the levels of base and heavy metals and sulphur in the inclusion fluids. This proved to be a very difficult task. Problems were caused due to the very low levels of these elements in the fluids, as well as, due to contamination from sulphide grains in the samples. Even though the analyzed samples were very carefully

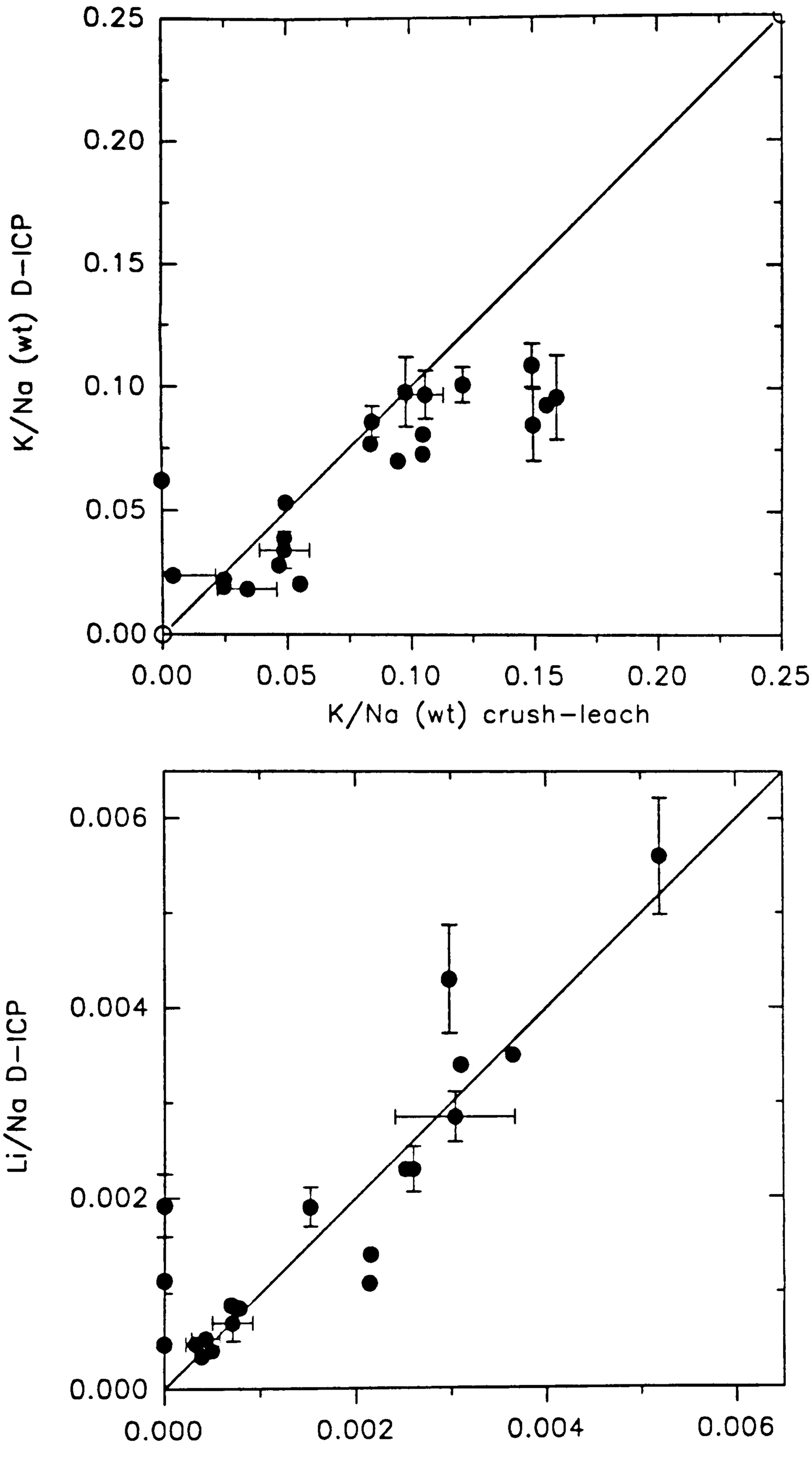


Fig.3.5. Comparison of K/Na and Li/Na weight ratios obtained from D-ICP and crush-leach ICP analysis of fluid inclusions. Error bars corresponding to one standard deviation are given for data points representing means of replicate analyses.

picked and selected under the binocular microscope it proved impossible to avoid contamination from microscopic and submicroscopic sulphide grains and inclusions. In order to overcome the problem of contamination some of the samples were electrolytically cleaned following the procedure by Roedder (1958). Only a small number of samples could be electrolytically cleaned because the considerable lengths of time required (up to 6 weeks for a sample). The relative concentrations of the electrolytically-cleaned samples together with the ones obtained for the same samples without electrolytic cleaning are presented in Table 3.5. In the cases where replicate analyses were undertaken, the ranges of the obtained ratios are given.

As it is clear from the values in Table 3.5., electrolytic cleaning caused a dramatic decrease of the metal and sulphur values in most of the samples. This decrease confirmed that contamination from sulphide grains or iron staining must have been the cause for the high metal and sulphur values as well as for the extremely wide range of the ratios in replicate analyses. Unlike the metal and sulphur values, the Na/K and Na/Li ratios do not differ between ordinarily washed and electrolytically clean samples. Unfortunately the electrolytic cleaning cell was obtained only during the final stages of the present work and because of the length of time involved in sample preparation only 10 samples have undergone electrolytic cleaning treatment. The very non-reproducible nature of the metal and sulphur values in most of the non-cleaned samples and their high levels compared with the ones from the cleaned samples, makes them non-valid as they are a result of contamination and do not represent true fluid inclusion concentrations. Further consideration to the problem of contamination will be given in the following section which is devoted to the use of time-resolved D-ICP analysis as a means of distinguishing signals from contamination and fluid inclusion decrepitation.

Table 3.3. Comparison of sulphur, Pb, Zn, Cu, Fe, Mn, K and Li weight ratios to Na obtained from D-ICP analysis in ordinarily washed and electrolytically-cleaned samples shown as -C

Sample	Pb/Na	Zn/Na	Cu/Na	Fe/Na	Mn/Na	S/Na	K/Na	Li/Na
AL/10/F	0.043-0.019	0.312-0.0222	0.019-0.0030	0.055-0.0026	0.010-0.0041	0.16-0.067	0.11-0.083	0.0042-0.0036
AL/10/F-C	0.0025	*	*	0.011	0.0032	*	0.081	0.0039
AL/6/F	1.43-0.0093	0.014-0.001	0.016-0.0008	0.125-0.016	0.017-0.0021	0.625-0.034	0.11-0.078	0.0033-0.0024
AL/6/F-C	0.0033	0.0006	<0.0001	0.015	0.0027	<0.014	0.085	0.0025
AL/1/F	0.0079-0.0062	0.0014-0.0013	<0.0001.	0.051-0.031	0.0064-0.0053	0.77-0.34	0.109-0.097	0.0053
AL/1/F-C	0.018	0.0021	<0.00055	0.034	0.011	<0.045	0.096	0.0063
AL/9/F	0.0083-0.0062	0.013	<0.0001	0.055-0.016	0.005-0.0043	3.33	0.085-0.081	0.003
AL/9/F-C	0.0082-0.0071	*	<0.00016	0.038-0.022	0.0034-0.0029	*	0.079	0.0032
AL/12/F	0.083-0.031	0.0094-0.0076	<0.0005	0.024	0.0023-0.0021	0.032	0.11-0.092	0.0023-0.0018
AL/12/F-C	<0.022	<0.0007	<0.0008	0.020	0.002	0.028	0.081	0.0017
AL/15/F	<0.020	0.078-0.072	0.0046-0.0028	0.023-0.22	0.0043-0.0033	<0.20	0.12-0.090	0.0044-0.0035
AL/15/F-C	<0.0046	0.0011	<0.0005	0.018	0.0021	0.17	0.084	0.005
AL/5/F	0.035-0.02	0.019-0.0081	0.0054-0.0026	0.24-0.23	0.042-0.037	<0.20	0.09	0.0021-0.0018
AL/5/F-C	0.0068	<0.0003	0.0068	0.027	<0.00008	0.18	0.079	0.0018
AL/2/F	0.1-0.03	0.012-0.0036	0.0042-0.00018	0.33-0.015	0.022-0.0034	0.30-0.047	0.104-0.068	0.0026-0.0021
AL/2/F-C	<0.0085	<0.00028	<0.00032	0.012	0.0024	0.057	0.081	0.0021
AS/1/F	0.053-0.017	0.014-0.0007	0.0007-0.00032	0.43-0.0049	0.014-0.00014	0.5-0.0015	0.043-0.026	0.0008-0.0004
AS/1/F-C	0.00044	0.00017	<0.00003	0.0019	<0.000001	<0.0034	0.030	0.00081

* Indicates that no measurements could be taken because the system was saturated due to the very high response from Ca (>12000mV)

(C) Indicates electrolytically-cleaned sample.

3.3.6. Time-Resolved Profiles

As noted previously, the main purpose of the time-resolved D-ICP is to establish the exact time/temperature interval over which maximum decrepitation takes place. The second objective of the time resolved D-ICP concerns the evaluation and recognition of the temperature domains of the various mechanisms of material transfer to the plasma. The time and temperature over which fluid inclusions decrepitate is not constant and it depends on the trapping temperature of the inclusions and the internal properties of the host mineral phase. Therefore, as noted in Rankin et. al. (1992), decrepitation of fluorite and calcite-hosted fluid inclusions occurs at a slightly earlier time and lower temperature compared to inclusions hosted in the much harder quartz.

In the present study time resolved D-ICP was undertaken for numerous fluorite and calcite samples (60 samples including duplicates). Representative time resolved profiles for the major and trace cations are presented in Fig.3.6. As can be seen from the Ca and Na profiles, maximum decrepitation occurs at the time interval between 35 and 40 seconds and at temperatures 150-500°C. The very high Ca signal is an unavoidable consequence of the introduction of host-mineral fragments (fluorite or calcite) into the system following the eruption of fluid inclusions. This has a masking effect on the Ca content of the fluid inclusions which therefore cannot be determined. The extent of the Ca response strongly depends on the number of fluid inclusions present in the sample. It was observed than not only the number but the size also of fluid inclusions influence the size of the Ca signal. Samples which contained numerous small inclusions produced very high Ca peaks, which occasionally caused saturation of the system (Ca emission intensity higher than 12000 mV).

Problems caused by the very high Ca response impeded previous investigators (Lindblom et. al. 1989) from analyzing fluorite and calcite-hosted fluid inclusions by the D-ICP method. One cannot deny that analysis of fluid inclusions in fluorite and calcite samples involves far more problems than that for quartz. However, at present software developments (Thompson et. al. 1992) on interference corrections enable us to analyze fluid inclusions in those minerals with comparable success to the analysis in quartz hosts. One problem which could not be solved is the separation of the host mineral Ca signal from the fluid inclusion signal resulting in our inability to determine the Ca content of the fluid inclusions by chemical analysis.

As can be seen from the various profiles (Fig.3.6), Na is the most abundant cation in the fluid inclusions. The timing of the Na, and unavoidably Ca peaks, mark the onset and

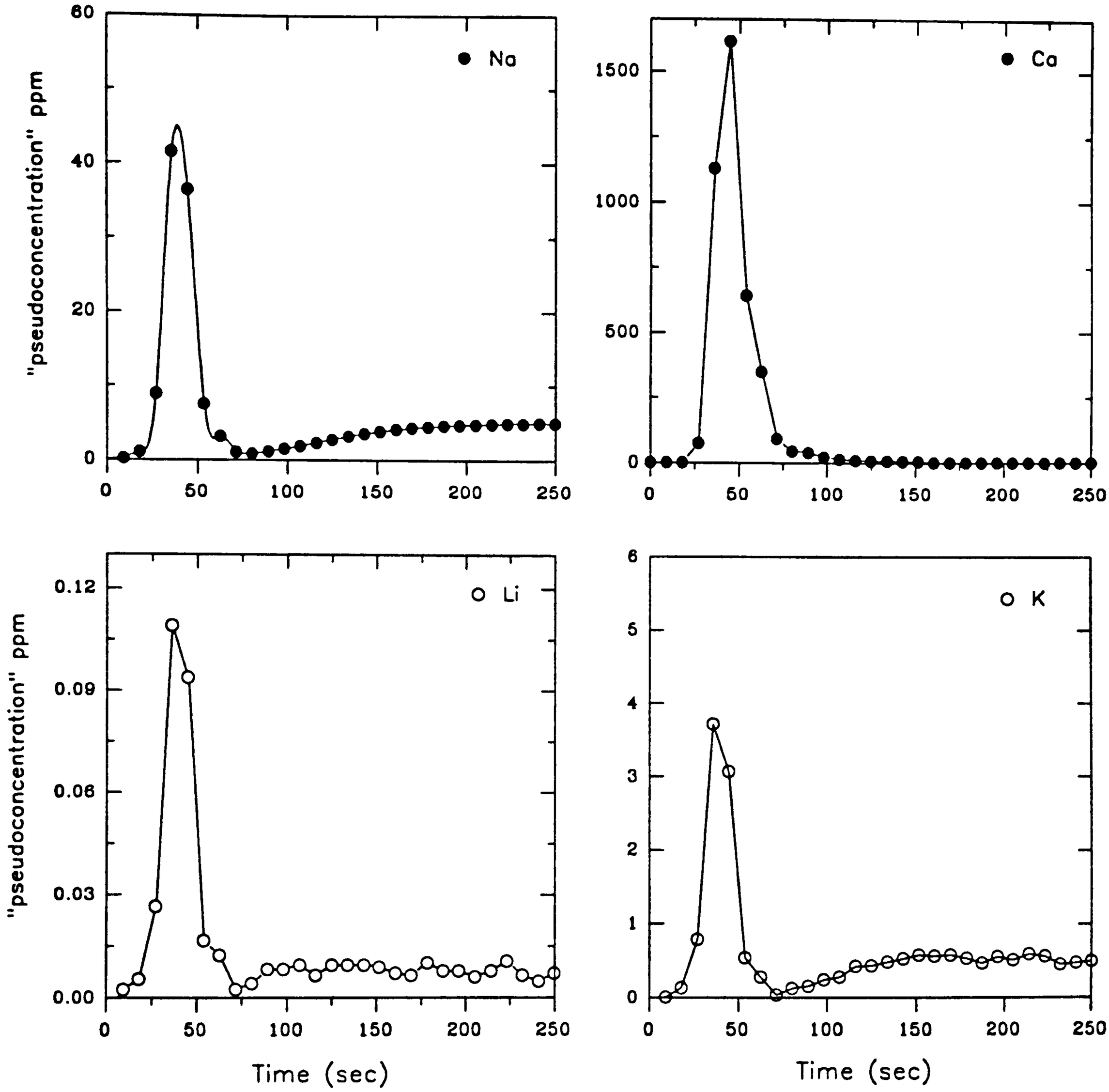


Fig.3.6. Profiles showing the morphology and time-intervals of the Na, Ca, K and Li responses obtained from time-resolved D-ICP analysis of fluid inclusions in fluorite.

termination of bulk decrepitation. As far as other elements such as K, Li are concerned, it can be seen from their profiles that their peaks coincide with those of Na and Ca, showing that they too are released during bulk decrepitation.

As mentioned previously, contamination from adherent sulphide grains and inclusions proved to be the major barrier in measuring the base metal and sulphur contents of the inclusion fluids. Time-resolved analysis was undertaken in an attempt to separate the signals from contamination from "true" fluid inclusion responses. Grains of high purity silica were smeared with tiny galena fragments and treated as a normal sample for D-ICP analysis. The time-resolved profiles for Pb and S from this trial contamination run are presented in Fig.3.7. From these profiles it can be seen that the response for sulphur is much higher than that of lead, with values not comparable with those outlined by the stoichiometric composition of galena. The fact that sulphur is more volatile than lead is the most possible explanation for this phenomenon. Furthermore, the shape of both the lead and sulphur peaks is far from simple. The Pb profile consists of two peaks, one early followed by a second very high broad response. Sulphur shows a similar profile which also consists of two peaks. Sublimation of galena after the initial heating might be the cause of the second, high Pb and S peaks.

Lead and sulphur profiles of similar appearance with those obtained from the contamination run were observed in most of the examined natural fluorite samples. Therefore, it was considered that both responses were a result of contamination from admixed galena grains which could not be avoided even after very careful and extremely time consuming hand picking. As emphasized in the previous section values for base metals and sulphur obtained from replicate normal, non-time resolved D-ICP runs were extremely variable due to the effect of contamination. These values dropped dramatically when the samples were subjected to electrolytic cleaning prior to analysis. Time resolved D-ICP analysis was done on a selection of these samples in order to examine the morphology of the profiles for a variety of elements and most importantly for lead and sulphur.

The Pb, Na and S profiles for ordinarily prepared and electrolytically-cleaned samples are presented in Figs.3.9 and 3.10. In two of the three sample profiles Pb is lower in the cleaned samples. In all three samples the decrease in the sulphur peaks is much more extensive and is not accompanied by a similar reduction of the Na signal. In sample DR/18/F sulphur decreases from 300 to 12 "eppm", in AL/10/F from 70 to 4 "eppm" and in AL/6/F, from 12 to 2 "eppm". Nevertheless, despite this decrease, the shape of the peaks does not change significantly. Two peaks are also present in the electrolytically

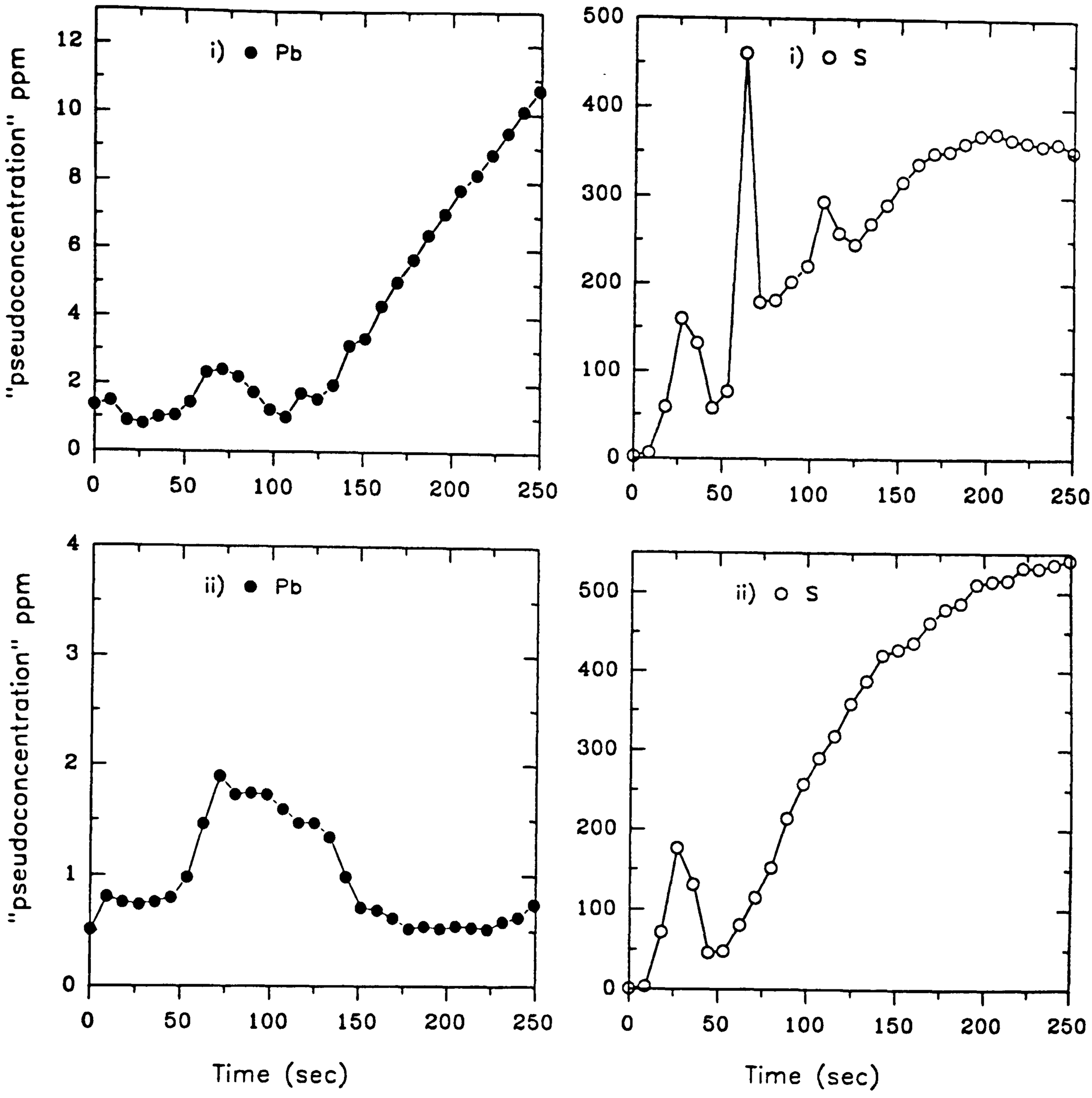


Fig.3.7. D-ICP time-resolved profiles illustrating the morphology of the lead and sulphur peaks obtained from trial contamination D-ICP run using speck pure silica smeared with PbS grains.

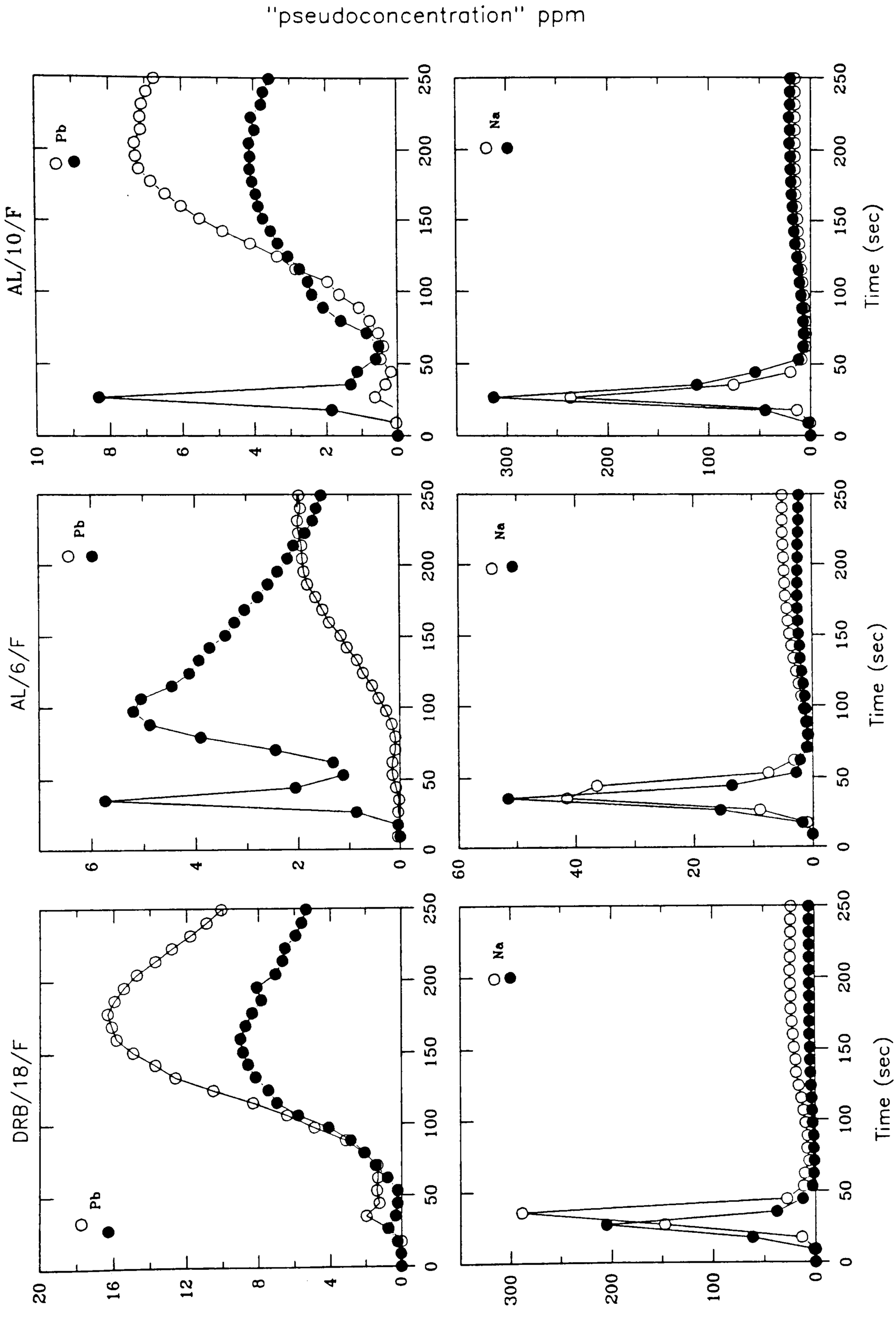


Fig.3.8. Comparison of lead and sodium time-resolved profiles obtained from D-ICP analysis of ordinarily-washed (filled circles) and electrolytically-cleaned (open circles) fluorite samples.

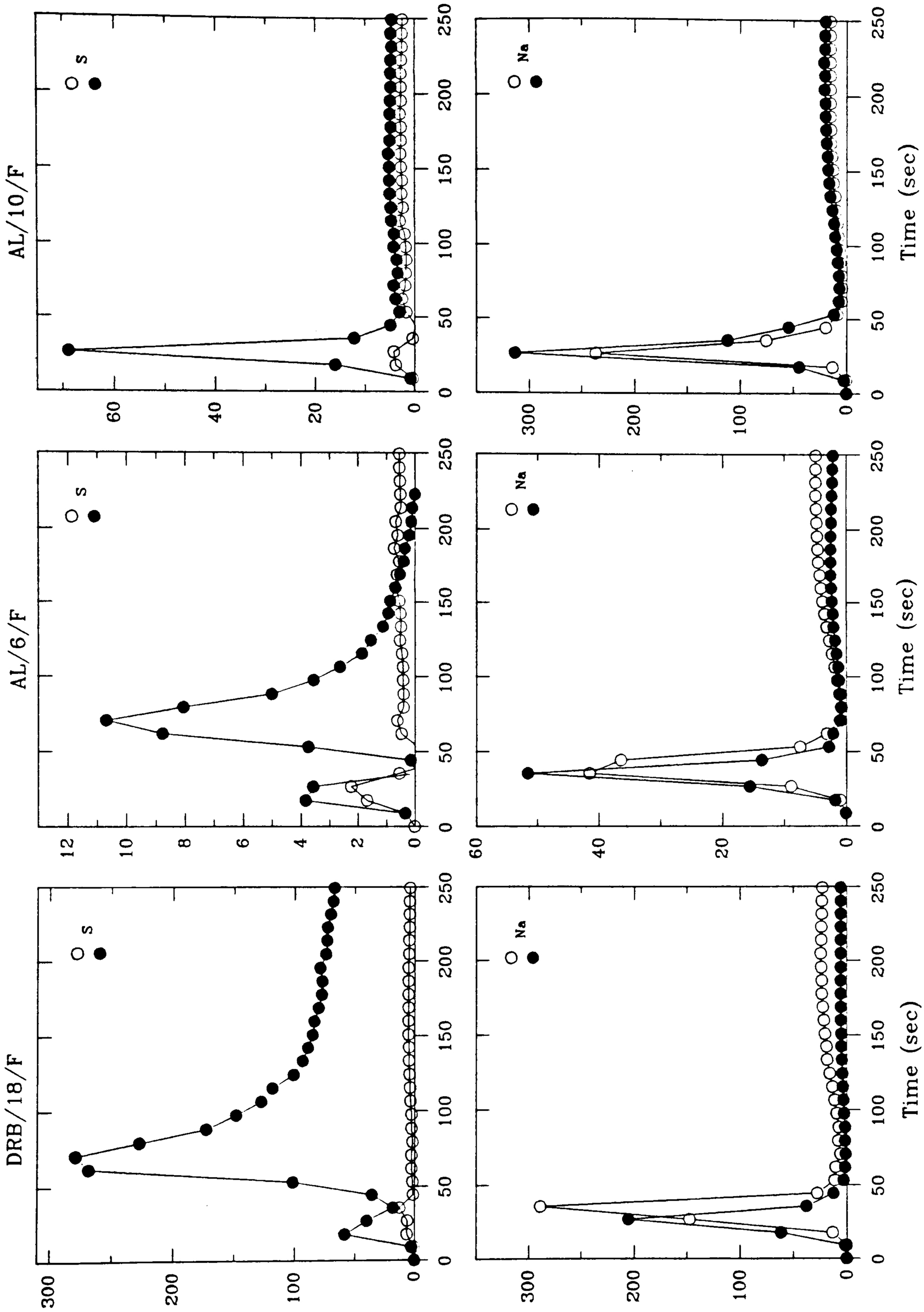


Fig.3.9. Comparison of sulphur and sodium time-resolved profiles obtained from D-ICP analysis of ordinarily-washed (filled circles) and electrolytically-cleaned (open circles) fluorite samples.

cleaned samples but the second response is not as high as in the non-cleaned samples. The response for Na does not change, neither in form nor in size, in the two separately prepared samples. As far as Pb is concerned, the decrease in the size of the peaks is not so obvious. For example, in sample DR/18/F, the Pb peak of the cleaned sample is even higher than that of the non cleaned one but is also accompanied by a higher Na signal. The morphology of the Pb peaks is also similar in the cleaned and non-cleaned fractions. In both sample separates a small, early peak is followed by a broad late response. In sample AL/6/F the Pb peak in the clean fraction shows a two fold decrease and is not accompanied by a similar decrease in Na. For sample AL/10/F, Pb also shows a two fold decrease in the clean fraction. However in that case, similarly to sample AL/6/F and unlike sample DR/18/F, it is the first peak that disappears in the clean fraction whereas the late response remains present.

The mechanisms under which both lead and sulphur are released into the plasma during time-resolved analysis are not easily understood. There is no clear profile pattern to enable us to distinguish between contamination-derived and fluid inclusion sources for Pb and S, even with the aid of electrolytically clean samples. Nevertheless, thorough electrolytic cleaning results in a decrease in both lead and sulphur values. Since the shape of the peaks did not change considerably in the clean fractions, it is not possible to distinguish between contamination-derived and fluid inclusion responses. The use of synthetic fluid inclusions has great potential in resolving these questions in the future.

3.4. Neutron Activation Analysis (NAA)

Because of its low detection limits, multielement capability and small sample requirements the potential of Neutron Activation Analysis for fluid inclusions has been recognized since the early days of fluid inclusion research. A large number of elements can be determined by NAA including the anions Cl^-, Br^- and I^- which cannot be measured by spectroscopic techniques such as atomic absorption, flame atomic emission spectrometry and inductively coupled plasma spectrometry (Touray 1976).

Neutron Activation for the analysis of fluid inclusions was first used by Czamanske et. al. (1963) for the determination of Cu, Mn and Zn contents of inclusion fluids in fluorite and quartz. Later, various modifications of the method following both destructive and non-destructive procedures, have been applied in a variety of minerals (Puchner & Holland 1966, Sabouraud 1974, Wickman & Khattab 1972, Grappin et. al. 1979, Luckscheiter & Parekh 1979, Norman et. al. 1989, Bohlke & Irwin 1992). As mentioned previously non-

destructive analysis of fluid inclusions has several advantages, such as preservation of the sample and subsequent potential for multiple measurements. Contamination from the crushing-leaching procedure is avoided and the time required for sample preparation is minimized. However, non-destructive Neutron Activation Analysis (INAA) although desirable, is mainly successful in minerals like quartz which are free from components which may interfere with the elements of interest in the fluid inclusions.

Irradiation of the sample prior to extraction of the inclusion fluid and analysis was one of the major developments of the method (Puchner & Holland 1966), as it provides a way to avoid any contamination during the leaching stage. A similar procedure was used by Sabouraud (1974) and Grappin et. al. (1979) for the determination of Cl, Na, Br and K in fluid inclusions in gypsum and quartz respectively. In both the above cases the elements of interest were separated with the aid of an inactive carrier and the extracted liquid evaporated to dryness prior to counting. Non-destructive neutron activation (INAA) was used by Luckscheiter & Parekh (1979). In that case the clean matrix of quartz provided the opportunity to obtain good results by the non destructive procedure. INAA was also used for the analysis of fluid inclusions in a single fluorite sample by Wickman & Khattab (1972). However since only one sample was analyzed it is not possible to assess the quality of the results obtained by these authors.

In the present study both non-destructive (INAA) and destructive (RNAA) neutron activation were used for the determination of the Cl, Na and Br contents of fluid inclusions in fluorite and calcite samples. In the early stages of the work efforts were concentrated towards the non-destructive analysis. However, because of the complex nature of both fluorite and calcite, it was not possible to obtain valid results. Br could not be detected by non-destructive analysis. For both fluorite and calcite the activity of Ca produced high background values with a masking effect to the elements of interest. Problems were also caused by the high REE content of the fluorites (especially Eu) as well as the presence of Sr, Mg and Mn in the calcite samples. No REE analysis of the fluorites was undertaken in the present study. However the high REE content of the Pennine fluorites has been demonstrated by previous authors (Shepherd et. al. 1982). Although no quantitative measurements were made in the present work, extensive REE peaks were recognized in the NAA runs.

Therefore, analysis by radiochemical separation of the inclusion fluids (RNAA) was used for the determination of Cl, Br and Na. Instead of evaporating the extracted fluid prior to counting, the liquid itself was counted in order to avoid any loss of material during

evaporation. A relatively simple procedure involving separate irradiations and counting for Br and Cl was developed during the present study (Bennett et. al. 1992). The method enabled us to determine both Cl and Br in the same sample leachate and to achieve very low detection limits.

In the early stages of the present work and prior to the development of the Neutron Activation analysis scheme, ion chromatography was used for the determination of Cl and Br in fluid inclusion leachates using a Dionex 2010i system. Only a small number of samples was analyzed and the method was soon abandoned in favour of neutron activation. The leachates were prepared following the standard crush-leach procedure. Since a minimum of 2ml leachate (non-recoverable) was required for each injection and measurement, sample size requirements were high compared to those of Neutron Activation. Ideally both Cl and Br can be determined in the same leachate by ion chromatography. This could not be achieved in the present work because the levels of Cl are much higher than Br. Hence, at a sensitivity high enough to detect Br, the Cl peak was driven out of range and consequently, Cl had to be determined separately using a Cl-selective electrode. Results obtained from the ion chromatograph and ion-selective electrode will be compared in the following sections. Overall the neutron activation analysis was found much superior since it enables determination of Cl, Br and Na in the same inclusion extract, has much smaller sample size requirements and offers better detection limits.

3.4.1. Experimental System and Sample Preparation

The mineral samples weighing 100mg or less were prepared as doubly polished wafers of chips. They were weighed into polyethylene capsules (6 x 15mm diameter.) ready for irradiation. Multielement chemical standards were prepared from NaCl and NaBr stock solutions. The solutions were combined and diluted to give a standard solution containing 12.96 μg of Na, 20 μg of Cl and 1 μg of Br per ml of solution in high purity water. The carrier was a NaCl solution containing 100mg of Cl per ml.

All the irradiations were made in the Consort Mark II thermal nuclear reactor at Imperial College Reactor Centre. The reactor operates at 100 kW and has irradiation sites for long or short irradiations with thermal neutron fluxes up to 2.4 $x10^{16}$ $nm^{-2}s^{-1}$. The short irradiations were made through a pneumatic device (ICIS) at the centre of the reactor core with a thermal neutron flux of 2.4 $x10^{16}$ $nm^{-2}s^{-1}$, whereas the long irradiations were made at the side of the reactor core with a thermal neutron flux of 10^{16} $nm^{-2}s^{-1}$.

All the counting was done with a pure Ge semiconductor detector (20% efficiency and 1.8 keV FWHM resolution at 1.33MeV). All measurements were made at 2cm distance from the detector end cap. The gamma ray energies measured for quantitative analysis on a ND6700 were at 1368KeV of ^{24}Na, 1642KeV of ^{38}Cl and 617KeV of ^{82}Br and 554KeV of ^{80}Br for long irradiation.

3.4.2. Experimental Procedure

The complete scheme of analysis is shown schematically in Fig.3.10. and it consists of several stages. These are, instrumental analysis for chlorine, radiochemical analysis for chlorine, bromine and sodium followed by the determination of the yield. The samples were first irradiated in sequence with the chlorine standards in ICIS . After a 10min irradiation and a 15 minute decay, the samples were counted for 14min. This 15min decay time was necessary in order to suppress the background caused by the high activities of short lived elements such as F and Ca. Safety precautions were also taken throughout the sample preparation procedure by allowing the radioactive samples to decay sufficiently prior to further handling and leachate-extraction, and by regular monitoring the activity of both samples and equipment.

Once the samples have been counted for Cl instrumentally, they are repacked in clean capsules and placed together with multielement standards in an outer irradiation container and irradiated for 7.5.h at the edge of the reactor core. The following day, after a 16h overnight decay, the samples and standards are transferred to individual irradiation containers and irradiated sequentially for 10min each in order to reactivate the chloride which has decayed overnight. The active samples are transferred immediately after this second irradiation to a clean agate mortar and crushed with 1.5.ml of carrier. Blanks from the agate were also regularly prepared to ensure that the extracted liquid was free of contamination. Approximately 1ml of leachate solution is pipetted to a polythene capsule and then transferred with a filtered syringe to a clean polythene capsule after a 14min decay and counted for a duration of 14min each in order to measure the short-lived nuclides Cl and Na. Filtering of the leachate greatly improved the results as it minimized the amount of non-desirable active radionuclides such as Ca and Eu present in the host mineral phase. Once all the samples and standards have been measured the leachates were allowed to decay in order to allow the chlorine and sodium activity together with any remnant short-lived interferences from the matrix to reduce. After several hours the samples are recounted for a duration of 3 hours each for bromine.

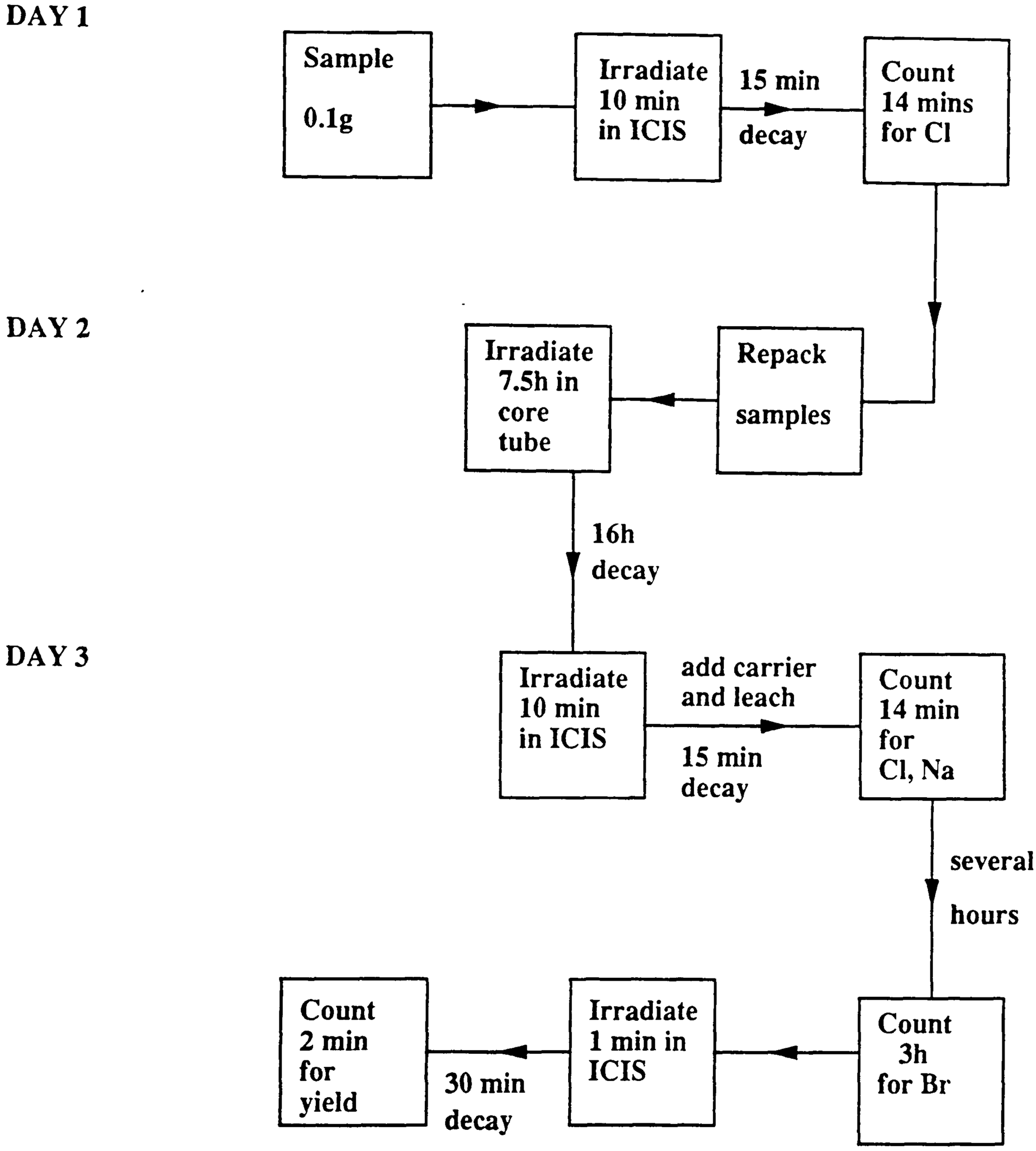


Fig.3.10. Flow-chart showing the experimental procedure followed in the present study for the determination of Cl, Na and Br in fluid inclusions by Neutron Activation Analysis.

It is also important to determine the recovery of the elements during the crushing and leaching stages since the volume of the solution recovered during leaching and filtering can be variable. It is measured by the pre-irradiation of the carrier. Since the Na and Cl contents of the carrier are greatly in excess of the values extracted from the inclusions, re-activation will result in major activity from the carrier only. A 1min irradiation, 30min decay and 1min count of the carrier is required.

3.4.3. Appraisal of the Results

The detection limits for the instrumental, non-destructive neutron activation analysis (INAA) were poor, 2-4 μg for Cl and Na and around 50ng for Br. The complex nature of both fluorite and calcite hosts paired with large scale interference from Ca, REE and in the case of calcite Mn made the detection of both Cl and Na, and especially Br which is present in trace quantities only, impossible. Valid results could only be obtained through radiochemical separation of the inclusion fluids. Indeed the separation procedure greatly improved the detection limits of Cl and Na to 1 μg and 0.50 to 5 ng for Br which could be detected successfully in the majority of the samples.

As in the D-ICP analysis, the total volume of the analyzed inclusions is not known and therefore the results are only valid in the form of ratios to Na or Cl. The reproducibility of the ratios was also examined by the means of replicate analyses of separates from the same sample. However, since the procedure is more complicated than the D-ICP, only a restricted number of replicates could be obtained. Apart from sample chips, doubly polished wafers were also analyzed. Fluid inclusions present in the wafers were previously examined using microthermometric analysis and it was established that they belong to a single population in terms of both temperature and total salinity. As can be seen from Table 3.4., reproducible values were obtained from replicate analyses in both wafers and chips of the same sample.

Cl/Br and Na/Br ratios obtained from neutron activation and those from the combination of ion chromatography, Cl-selective electrode and crush-leach ICP are presented as bivariate plots in Figs.3.11a-b. As noted previously, only a small number of samples was analyzed by ion chromatography and Br could not be detected in all of them. As can be seen from Fig.3.11, the Cl/Br and Na/Br ratios obtained by the two methods were fairly similar especially at higher Br levels. Nevertheless, reproducibility was poorer in the chromatographic method. At low Br concentrations, the obtained Br values were not constant even in cases where splits of the same leachate were analyzed.

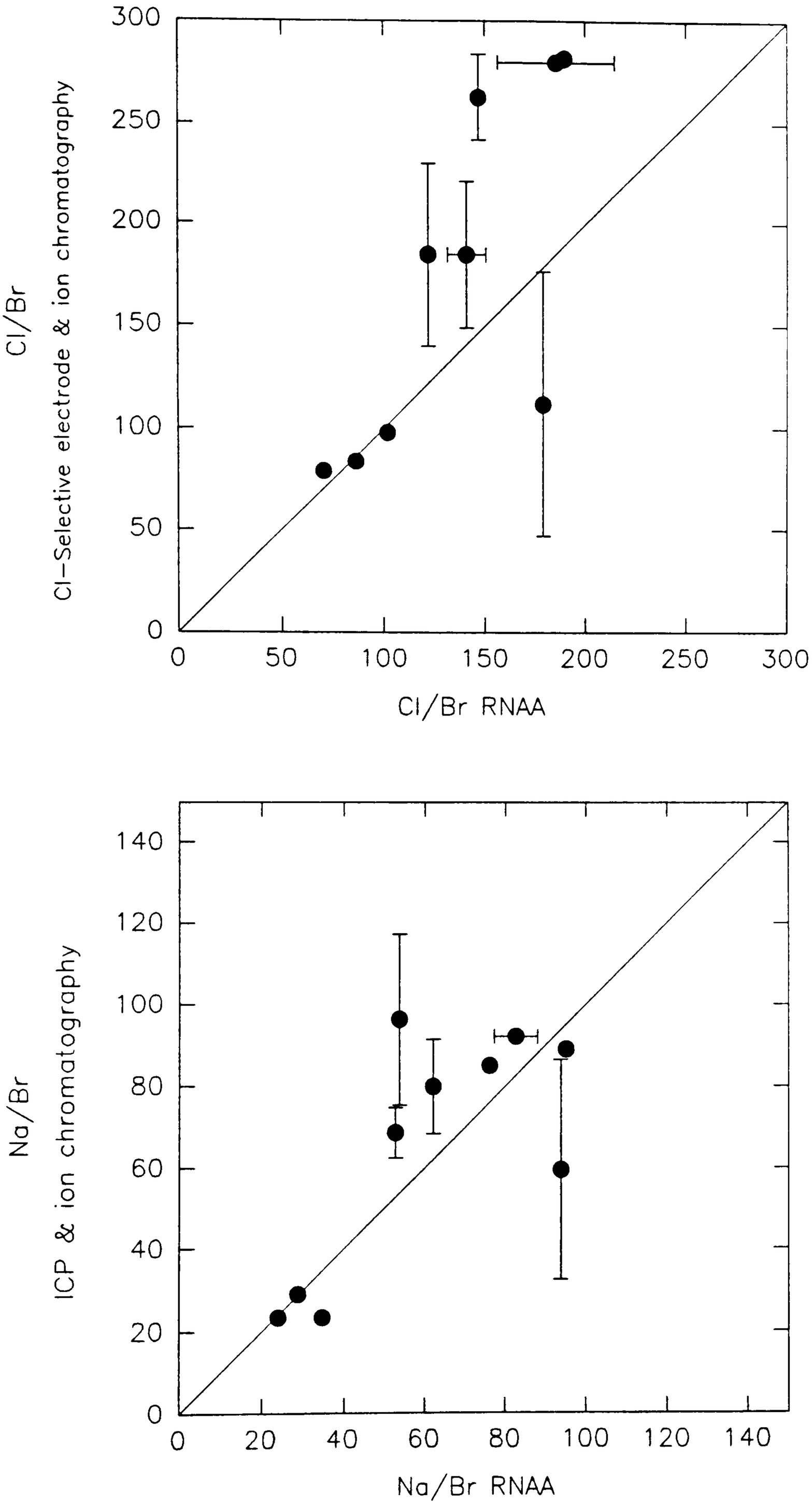


Fig.3.11. Comparison of Cl/Br and Na/Br weight ratios obtained from destructive neutron activation analysis (RNAA) and a combination of ion-chromatography with crush-leach ICP and Cl-selective electrode.

In general the Na/Cl ratios of the fluid inclusions obtained by RNAA are reproducible and are in agreement with results from microthermometry (Chapter 4) which indicate that Na and Cl are the dominant ions in solution. As can be seen from Table 3.6, the Cl/Br ratios also exhibit remarkable reproducibility. The accuracy could not be tested in the present work since no synthetic fluid inclusions were analyzed. Overall the method outlined above is superior to the instrumental neutron activation for the analysis of fluid inclusions in fluorite and calcite samples. It provides a relatively simple, robust procedure for the simultaneous determination of very low levels of Cl, Na and Br in fluid inclusions, while it also has very small sample requirements and simple sample preparation.

Table 3.4. Absolute values and Cl/Br and Cl/Na weight ratios obtained from replicate RNAA analyses of fluid inclusions in fluorite samples. (w indicates that the analyzed sample is a doubly polished wafer).

Sample	Cl (μg)	Br (μg)	Na (μg)	Cl/Br	Cl/Na
AL/6/F	5.83	0.0309	2.23	188.7	2.6
AL/6/F	9.50	0.0456	3.56	208.5	2.7
AL/6/F	9.51	0.0567	4.27	167.6	2.2
AL/11/F	5.66	0.0286	2.79	197.8	2.03
AL/11/F	7.34	0.0399	3.55	183.6	2.06
AL/11/Fw	1.45	0.0087	0.657	167.2	2.21
AL/10/F	20.45	0.2169	9.26	94.3	2.21
AL/10/F	22.84	0.2230	8.15	102.4	2.8
AL/10/Fw	14.55	0.1564	6.07	93.0	2.39
AL/13/F	7.16	0.0732	3.35	97.9	2.13
AL/13/F	9.87	0.1130	4.89	87.1	2.02
AL/13/Fw	3.67	0.0319	1.79	115	2.05
AL/2/F	6.37	0.0284	1.93	224.3	3.29
AL/2/F	12.64	0.0434	3.69	291.2	3.43
DR/1/F	2.34	0.0374	0.69	62.6	3.41
DR/1/F	2.14	0.0304	0.725	70.4	2.95
DR/10/F	8.23	0.0612	3.77	134.5	2.18
DR/10/F	8.62	0.0584	3.64	147.7	2.37

3.5. Summary and general conclusions

Overall, both the D-ICP and RNAA methods have proved very appropriate for the chemical analysis of single generation, aqueous fluid inclusions in both fluorite and calcite samples. One problem which could not be resolved is the selective determination of elements such as Ca, which are also present in the host mineral phase. Still, the main

disadvantage of both methods lies on the fact that they are limited to the analysis of fluid inclusions in samples were only one dominant generation of inclusions is present. Combination of the two methods provides a very robust scheme capable of rapid determination of both cations and anions in fluid inclusions. Apart from major elements (Na, Cl), traces such as Li and Br can also be measured effectively. In the present work it was possible to firmly establish the validity of the results through replicate analyses and quantification of the effects of "within sample" variability. The accuracy of the methods cannot be directly tested since synthetic fluid inclusions of known compositions were not analyzed in the present work. However, comparison of results obtained through D-ICP and RNAA with data from the conventional crush-leach ICP and ion-chromatographic methods respectively, has shown that the data sets are comparable. The use of time resolved D-ICP on electrolytically cleaned samples did not, at present, provide conclusive evidence for distinguishing between contamination-derived and fluid inclusion metal and sulphur contents. However, the D-ICP data obtained from electrolytically cleaned samples showed that high Pb and S values can be caused from contamination from adherent sulphide grains in the samples. In Neutron Activation Analysis, the ability to irradiate and count the filtered liquid extract provides a means to overcome large-scale interferences from the host mineral phase and to avoid any loss of material. The small sample requirements and the simple sample preparation procedures involved in both D-ICP and RNAA methods, enable the routine analysis of large numbers of samples.

Chapter 4

Fluid Inclusion Microthermometry

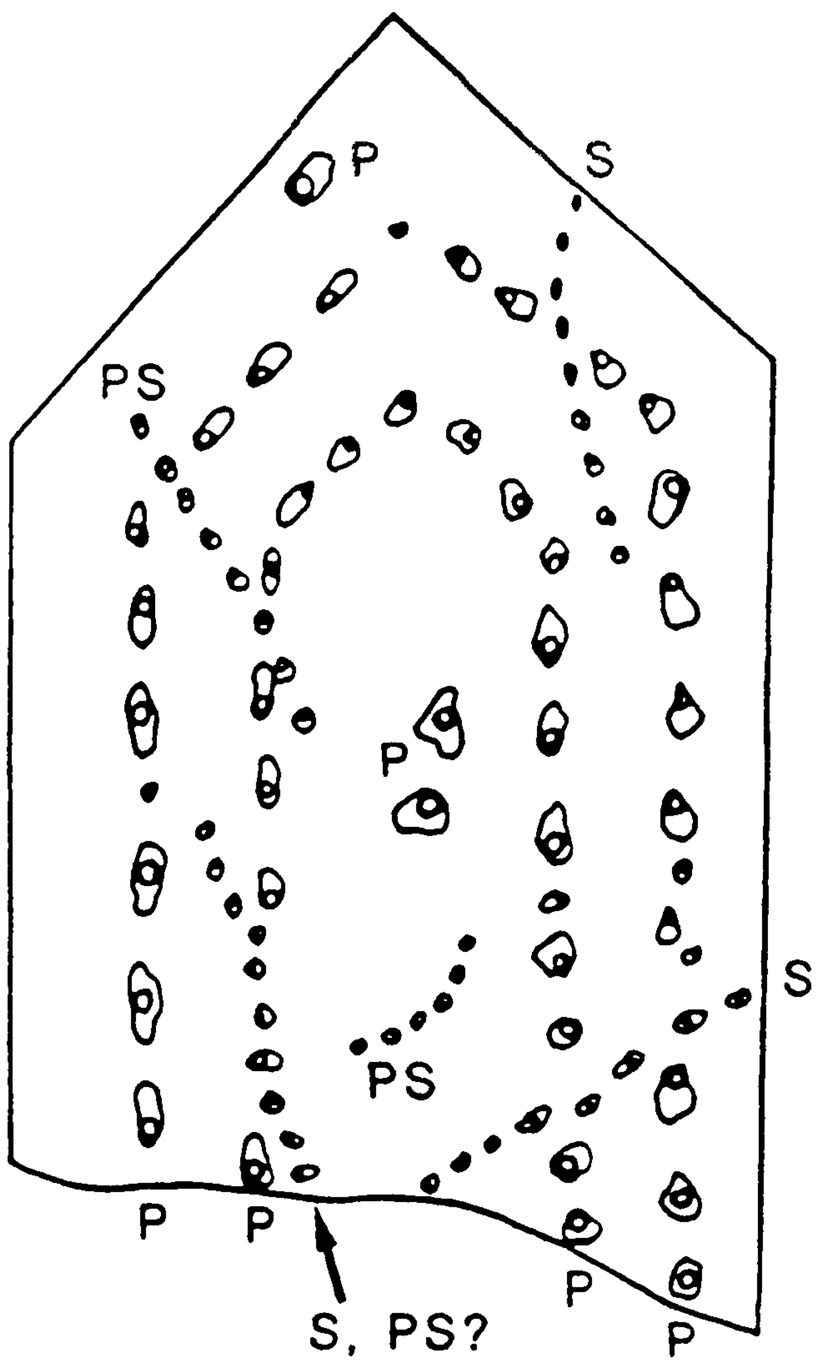
4.1. Introduction

Microthermometry is the most widely used non-destructive technique in the study of fluid inclusions. It is based on the observation and recognition of the phase changes during heating and freezing of fluid inclusions. By accurately measuring the temperatures at which liquid-solid-vapor transformations take place it is possible, with reference to known, simple fluid systems, to derive estimates of the physical and chemical properties of the fluids at the time of trapping. Combined information from a variety of chemical systems has set the background of microthermometric analysis. Comprehensive reviews of the theoretical and practical aspects of fluid inclusion microthermometry are provided by Shepherd et. al. (1985a), Roedder (1984) and Crawford et. al. (1981).

Fluid inclusion microthermometry is based on two assumptions, a) the inclusions are representative of the fluids present during primary growth or recrystallization and b) they behaved as constant volume-composition systems after trapping. However, not all inclusions have remained sealed through time; recent experimental evidence has shown that bulk leakage and non-elastic stretching is not uncommon in soft, easily cleaved minerals (MacLimans 1987, Shepherd et. al. 1985a). It is therefore important that leaked inclusions are recognized and excluded from further measurements since their microthermometric properties are most probably erroneous. Also essential is the distinction of primary from secondary inclusions. Ideally, only primary inclusions should be used for most geological interpretations, since secondary inclusions form at a latter stage and they are not related to primary crystal growth. An idealized distribution of primary secondary and pseudosecondary fluid inclusions is illustrated in Fig.4.1. However, in natural samples which have undergone multiple stages of fracturing and re-healing it is often not possible to separate primary from secondary inclusions by the means of optical examination alone.

4.1.1. Aims of microthermometric analysis

The present study is concerned with the examination of fluid inclusions in minerals (fluorite and to a lesser extend calcite) from the Pb-Zn mineralization of the North and South Pennine orefields and the Cu-rich deposits of Ecton Hill, Staffordshire. Sample sites for these areas are shown in Figs 4.2, 4.3 and 4.4. Several types of fluorite (classified mainly



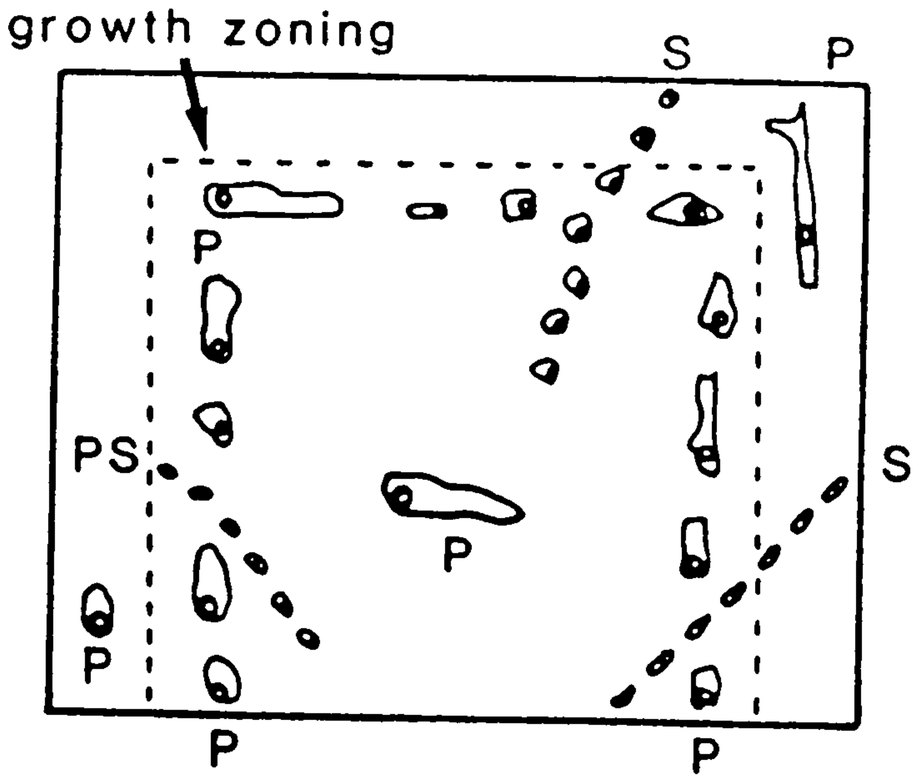


Fig.4.1. Schematic representation of idealized distribution of (P) primary, (S) secondary and (PS) pseudosecondary fluid inclusions (after Shepherd et. al. 1985a).

in terms of colour and texture) have been identified in the Pennine region. However, as will be shown in the subsequent sections and chapters, the overall fluid inclusion characteristics are extremely uniform and do not appear to be closely associated with the colour, or texture of the host fluorites. The lack of variations of the fluid inclusion signature on a single sample or separate crystal scale was recognized during the early stages of the present work. Therefore, broad, regional coverage of the fluorite mineralization in the Pennines was the main basis of sample selection. Due to the inaccessibility of most fluorite mines and in order to avoid sampling from mine dumps, a large number of excellent fluorite samples from precisely documented localities were provided by the Natural History Museum, London. Representative fluorite samples studied in the present work are illustrated in Plates 4.1.a-d and 4.2.a-d. These mainly include, purple, colourless, green, pink and yellow, vuggy fluorite crystals, as well as, massive banded and brecciated fluorite. Fluorite is rare at Ecton Hill; therefore, fluid inclusions in calcite which is the dominant gangue mineral in the area were studied in the present work.

The study also extends to calcite and quartz samples from the Fe-rich mineralization of the Llanharry mine in South Wales. Also, for reasons stated in Chapter 2, fluorites from the late stage of the granite related Sn-W-CaF_2 mineralization at South Crofty, Cornwall are also examined. All sample numbers and corresponding localities are listed in Appendix A.

The processes of hydrothermal mineralization in the Pennines have been studied extensively in the past (i.e. Sawkins 1966a, Dunham 1983, 1992, Mostaghel & Ford 1986), whereas information on the genesis of the Llanharry mineralization is more limited (Rankin & Criddle 1985). Mineralization at South Crofty consists of several separate events with various degrees of affinity to the underlying granite cupola. Most previous fluid inclusion studies at South Crofty focused towards the early mineralizing events responsible for tin-tungsten mineralization (Farmer 1991). Here emphasis is given to the late, chlorite stage of the paragenesis.

In recent years the use of more sophisticated equipment has improved the quality of the microthermometric measurements. Also, evidence from experimental studies on more complicated chemical systems has greatly enhanced our understanding of fluid inclusion behavior under both low and high temperatures (Borisenko 1977, Davis et. al. 1990, Oakes et. al. 1990). Therefore, especially for the Pennine samples, despite the fact that microthermometric studies have been carried out in the past (i.e. Sawkins 1966a, Rogers 1977, 1978, Atkinson et. al. 1982, Moore, 1980), additional results were obtained in the present work in order to further examine the previously reported values and to provide a

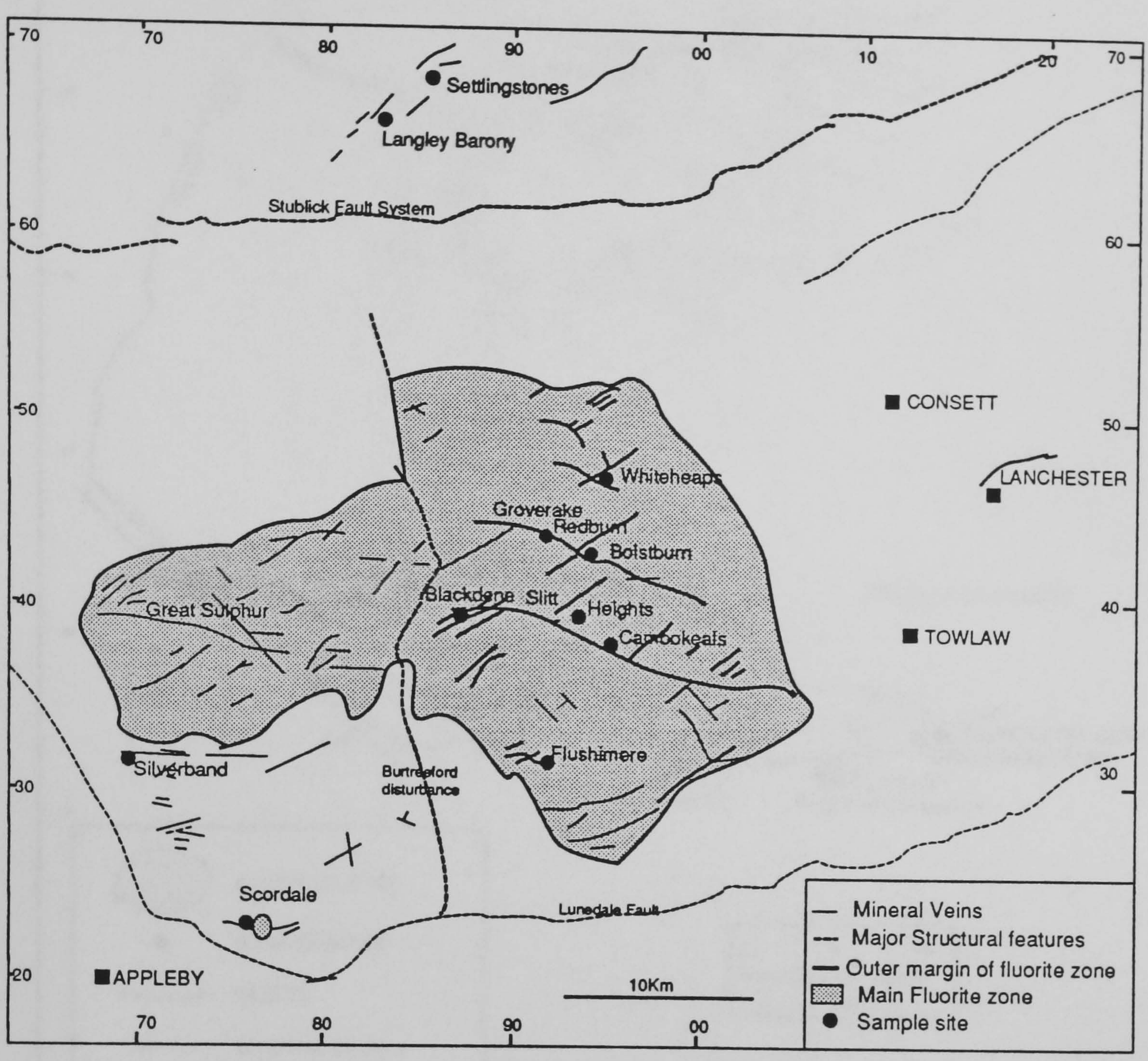


Fig.4.2. Sketch-map showing the outline of the fluorite zone, structural features, mineral veins and main sample sites in the Alston orefield, North Pennines (map redrawn from Dunham 1992). The complete list of sample numbers, NGR, and mineral association is given in Appendix A.

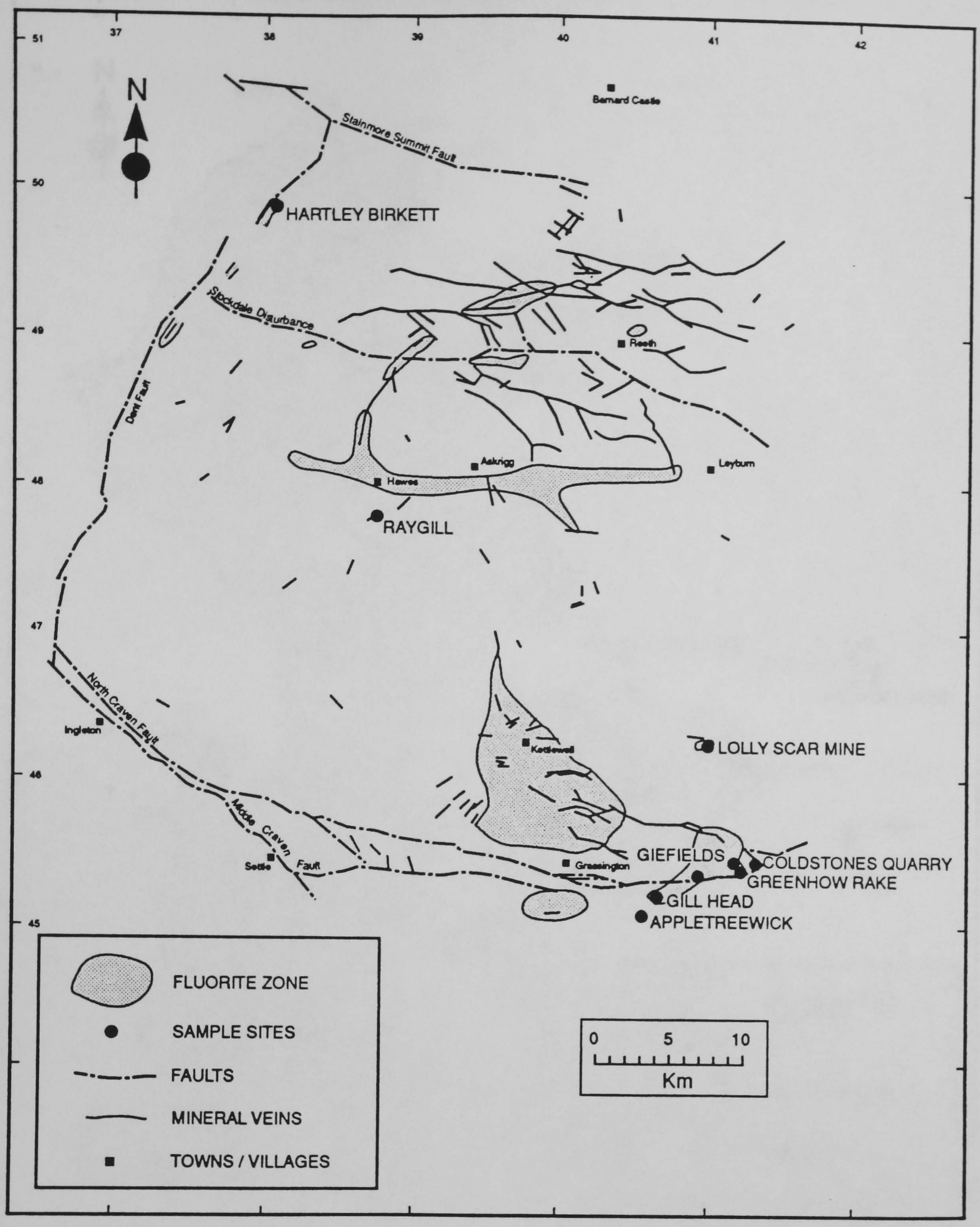


Fig.4.3. Sketch-map showing the outline of fluorite-dominant areas, structural features, mineral veins and sample sites in the Askrigg orefield, North Pennines (map redrawn from Dunham & Wilson 1985). The complete sample list is given in Appendix A.

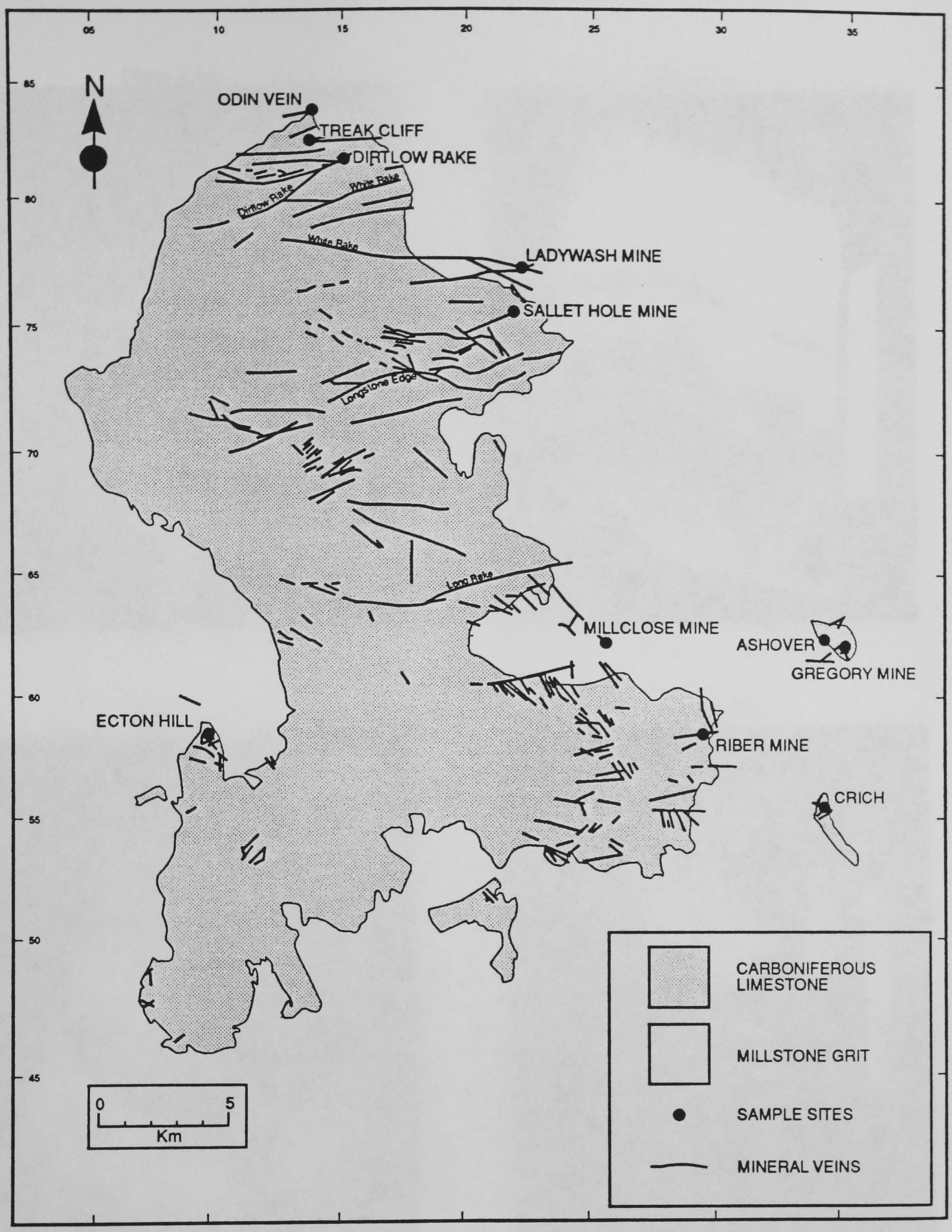


Fig.4.4. Sketch-map showing the main geological formations, mineral veins and sample sites in the South Pennine orefield. The complete sample list is shown in Appendix A.

Plate 4.1a



Plate 4.1b



Plate 4.1c

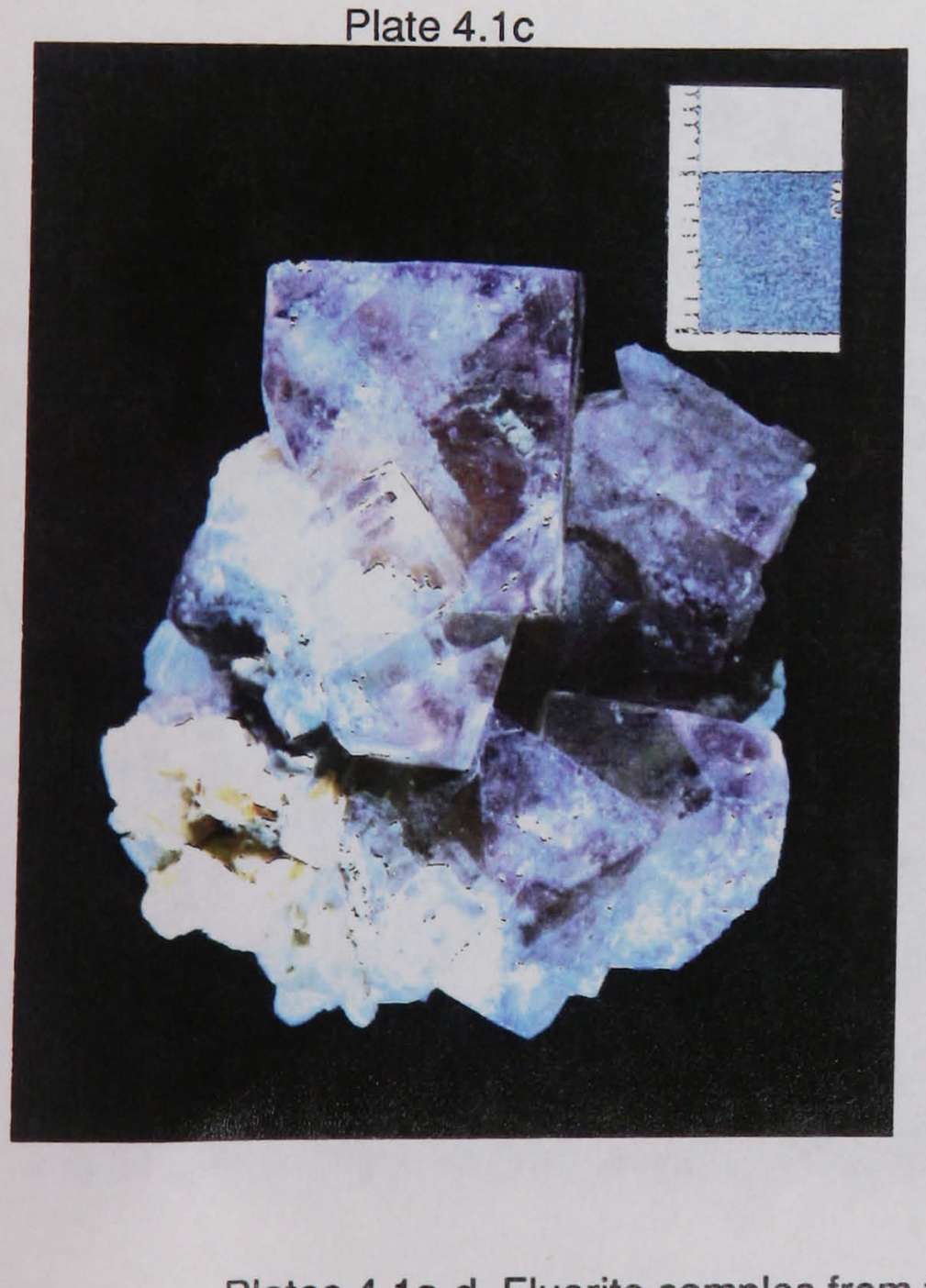
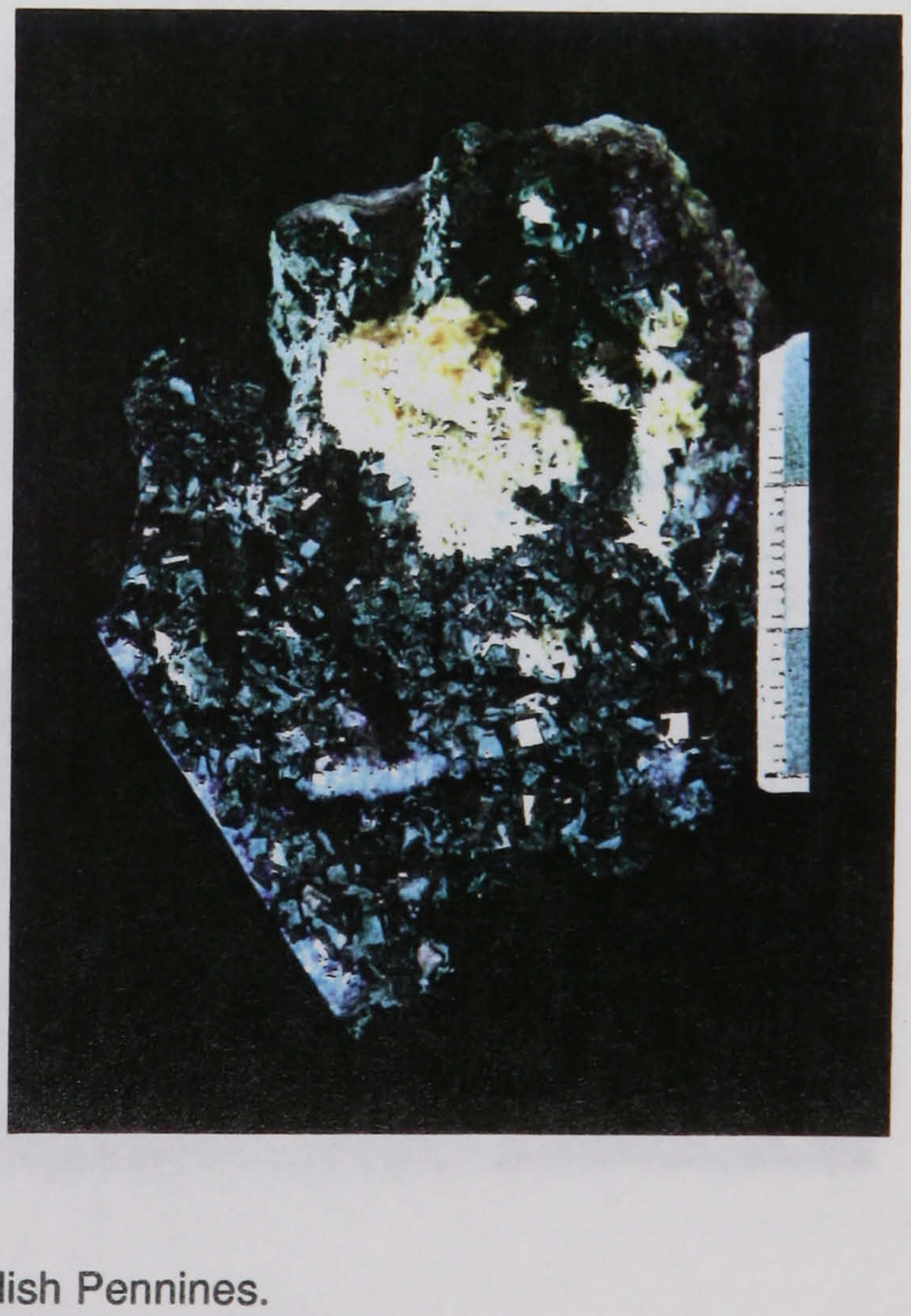


Plate 4.1d



Plates 4.1a-d. Fluorite samples from the English Pennines.
4.1a. Yellow fluorite crystals, Scordale Mine, N.Pennines
4.1b. Banded purple-colourless fluorite, Dirtlow Rake, S. Pennines
4.1c. Light purple fluorite crystals, Bolstburn Mine, N.Pennines
4.1d. Dark purple fluorite crystals (+barite), Odin Mine, S.Pennines

Plate 4.2a



Plate 4.2b



Plate 4.2c



Plate 4.2d



Plates 4.2.a-d. Fluorite samples from the Pennine orefields.
4.2a. Green fluorite crystals (+quartz), Blackdene Mine, N.Pennines
4.2b. Massive banded, colourless-green fluorite, Whiteheaps Mine, N.Pennines
4.2c. Colourless fluorite crystals+PbS inclusions, Lolly Scar Mine, Askrigg
4.2d. Colourless fluorite crystals +PbS, Millclose Mine, S.Pennines

more complete data-base combining information from all three Pennine orefields. Furthermore, as emphasized in Chapter 3, microthermometry is an essential part of the present work, since it enables identification of the dominant fluid inclusion generations in the examined samples. Also important is the use of microthermometric results in conjunction with fluid inclusion chemical analysis as a means of transforming the semiquantitative results and ratios to quantitative values. Nevertheless, although microthermometry occupied a relatively "auxiliary" role in the present work, new data were also obtained. These mainly consist of paired homogenization-salinity measurements and estimates of the Ca-Na contents of the fluids. Prior to the presentation of data obtained in the present work, results from previously published microthermometric analyses in samples from the Pennines, South Wales and South Crofty areas will be reviewed separately in the following sections.

4.1.2 Nomenclature

In order to avoid confusion, a list of the most commonly used abbreviations for the various temperatures recorded during microthermometric analysis is given below.

T_H	Temperature of homogenization (°C)
T_{FM}	Temperature of first melting (°C)
T_M	Temperature of last ice melting (°C)
T_Mh	Temperature of salt-hydrate melting (°C)
T_T	Temperature of trapping (°C)

4.2. Previous Work

Published microthermometric work on the Pennines consists mainly of measurements of homogenization and last melting temperatures (Sawkins, 1966a, Smith 1974, Rogers 1977, 1978, Small 1978). Information on T_{FM} and especially T_Mh is more limited (Masheder & Rankin 1988). Unpaired fluid inclusion homogenization and ice melting temperatures in samples from the Llanharry mine were reported by Rankin & Criddle (1985). More microthermometric work on calcite and quartz samples was carried out in the present work; however, a more extensive study was seriously impeded by the small size and low abundance of fluid inclusions in the mineral samples.

As far as the South Crofty samples are concerned, recent work by Farmer (1991) provided

extensive petrographic, geochemical andmicrothermometric information mainly concerning the Sn-dominant, early stage of the paragenesis. Of main interest for the present study are fluid inclusions from the late fluorite stage of the paragenesis as a means to assess possible links between sedimentary and granite-related, ore-formation environments.

4.2.1. Previous work in the Pennines and South Wales

Most of the previous studies concentrated on the measurement of homogenization and last melt temperatures providing information on minimum trapping temperature and salinity of the fluids. A summary of published homogenization temperatures is given in Table 4.1.

Table 4.1. Summary of published homogenization temperatures in samples from the Pennine and Llanharry ore deposits.

Locality	Mineral	T_H°C (range)	Reference
Alston Block	Fluorite	104-179	Sawkins (1966a)
	Fluorite	90-166	Smith (1974)
	Quartz	132-205	Sawkins (1966a)
	Quartz	115-190	Smith (1974)
	Calcite	67-73	Sawkins (1966a)
	Barite	<129	Sawkins (1966a)
Askrigg Block	Fluorite	91-143	Smith (1973)
	Fluorite	104-158	Rogers (1978)
S. Pennines	Fluorite	92-154	Rogers (1977)
	Fluorite	120-158	Atkinson (1982)
	Fluorite	74-76	Atkinson (1982)
	Fluorite	76-92	Atkinson et. al (1982)
	Fluorite	77-87	Atkinson et. al. (1982)
Ecton Hill	Calcite	58-90	Masheder & Rankin (1988)
Llanharry	Calcite	62-98	Rankin &
	Quartz	55-98	Criddle (1985)

Last ice melting temperatures for the Alston block inclusions were in the range of -16 to -23°C corresponding to salinities between 18-23 eq.wt.%NaCl whereas for Askrigg, reported last ice melting temperatures fall between -10 and -25°C indicating similar overall salinities. For the Derbyshire fluids the distribution of both homogenization temperatures and salinities is more complicated. The dominant fluid inclusion signature is the one characterized by low temperature and high salinity, similar to that of the Northern

orefields. There is however a limited number of inclusions characterized by higher temperatures and very low salinity values, which are commonly associated with hydrocarbon inclusions (Atkinson et. al. 1982, Moser et. al. 1992).

In a fluid inclusion study in calcite samples from the Ecton Hill Cu-rich mineralization, Masheder & Rankin (1988) showed that first melt are much lower than the -22°C eutectic of the NaCl system. First melt temperatures as low as -60°C were encountered confirming the presence of other than NaCl salts in solution. Such low eutectics are characteristic of Ca-rich fluids which was considered by the authors (op.cit.) to be the second most abundant cation, after sodium, in solution. More emphasis on the first and hydrate melt temperatures of inclusion fluids from the Pennine and Ecton Hill mineralization will be given in the following section in conjunction with results obtained during the present work.

4.2.2. South Crofty

Several fluid inclusion studies have been undertaken in the past on a variety of settings in SW England. (Sawkins 1966b Rankin and Alderton 1982, Jackson et. al 1982., Shepherd et al 1985b). The presence of multiple fluid inclusion generations of varying temperatures and salinities has been confirmed from these studies. For the Sn mineralization at the Cornubian orefield in general, microthermometric data from quartz associated with cassiterite suggest that boiling of NaCl-KCl solutions at temperatures between 300 and 400°C and moderate to high salinities (18-28eq.wt%NaCl) were responsible for the cassiterite mineralization (Bromley and Hall 1987).

Vein samples from the Pryces, North, and Tincroft lodes in South Crofty were examined by Scrivener et. al. (1986). The fluid inclusions showed a wide range in homogenization temperatures (123-344°C) and salinities (<1-35eq.wt.%NaCl). Also recognized was a population of low temperature (150-220°C), $CaCl_2$-bearing, high salinity (20eq.wt.%NaCl) fluids. Fluid inclusions from the Tryphena lode at Wheal Pendarves which typically contains a quartz-chlorite-cassiterite paragenesis, have a low T_H range (150-240°C) and restricted salinity (6-11eq.wt.%NaCl) (Scrivener et al 1986).

Studies by Jackson (1977) and Jackson et. al. (1989) on samples from the Levant and Geevor Mines at the St.Just mining district showed that tin mineralization is associated with high temperature fluids (250-380°C) of moderate salinity (15-20eq.wt.%NaCl), with a tendency for a decrease in salinity towards lower temperatures. However an additional group of low temperature, high salinity fluids was also present. Further studies were carried out by Shepherd et al (1985b) in samples from the Birch Tor Sn-tourmaline-quartz

and Sn-hematite-quartz mineralization. Again three populations of fluids were observed. One of high temperature (>300°C) and low to moderate salinity (<20eq.wt.%NaCl), followed by a second lower temperature (200-300°C), high salinity fluid characterized by the presence of NaCl and KCl daughter minerals in the inclusions. As in the case studies mentioned above, a low temperature (120-220°C), $CaCl_2$-bearing fluid with salinity up to 25eq.wt.%NaCl was also recognized.

Shepherd and Scrivener (1987) studied fluid inclusions in samples from the Sn-W-Cu and base metal sulphide fluorite veins in the Kitt-Hill Gunnislake area. Tungsten mineralization was interpreted as associated with high temperature (>300°C), low salinity (<8 eq.wt.%NaCl), CO_2-bearing fluids. A second population of lower temperature (200-310°C), higher salinity fluids (12-20 eq.wt.%NaCl) with eutectics showing the presence of $CaCl_2$ was also identified. Such a distribution was interpreted as representative of partial mixing between two end member fluids. The later, base metal-bearing veins indicated mixing between the low salinity, moderate temperature (300°C) fluids and a $CaCl_2$-bearing fluid of lower temperature (<300°C) and higher salinity (20 eq.wt.%NaCl).

Pb-Zn-dominant mineralization is commonly hosted in a series of late veins throughout the Cornubian orefield. Since their occurrence is more restricted through time, it is possible to assess their constraints with more confidence than for the tin mineralization. Studies by Alderton (1978) in a number of Pb-Zn veins from Devon and Cornwall showed that mineralization is associated with two fluids of characteristic T_H-salinity relationships. Fluid inclusions in samples from veins with similar strike direction to the main stage lodes had a wide range of homogenization temperatures (180-370°C) and salinities (0-13 eq.wt.%NaCl). On the other hand, fluid inclusions from cross-courses had lower temperatures (100-170°C) and much higher salinities between 20 and 26 eq.wt.%NaCl. Similar trends were observed by Shepherd et al (1985b) in samples from North-South bearing cross-courses in the Tamar Valley west of the Dartmoor granite and by Scrivener et. al. (1986) in cross -courses from the South Crofty mine.

Several generations of fluids are present in the hydrothermal veins of the South Crofty mine. Recent work by Farmer (1991) revealed that the early, pegmatite and tourmaline-cassiterite stages of mineralization are characterized by a variety of fluids exhibiting a wide range of both homogenization temperatures and salinities. The dominant trend however in that early stage is the one of decreasing salinity with decreasing temperature.

A quite different trend was observed in samples from the later chlorite stage of the

paragenesis. Here the dominant trend is the one of increasing salinity with decreasing temperature. However, apart from the two end members, a considerable number of readings fall in between these temperature-salinity values. A mixing mechanism was proposed by Farmer (1991) involving three end members. A low temperature (200-250°C) saline fluid (15-20 eq.wt.%NaCl), a second low temperature (200-250°C) and very low salinity fluid (<2 eq.wt.%NaCl) and a third high temperature (300-400°C) and low to moderate salinity fluid (5 eq.wt.%NaCl)

Further fluid inclusion studies on fluorite samples from the late, chlorite stage of mineralization have been carried out in the present work. The main objective is to further examine the low temperature population in terms of both salinity and $CaCl_2$ content and to identify possible similarities with the Pennine fluids.

4.3. Equipment for microthermometry

A Linkam THM600 heating-freezing stage attached to a Leitz petrological microscope was used for all microthermometric analyses. The microscope is equipped with long working distance objective lenses (L32 and L20) and condenser (type Leitz PI 1/0.04), used in combination with binocular x16 eyepieces. The equipment enables inclusions down to 5μm to be studied. The THM600 stage is coupled with a Linkam TMS90 microprocessor controlled system which maintains a pre-set heating and cooling rates during heating and freezing runs. A Linkam CS196 cryogenic pump is required to cool the sample during freezing experiments. A VTO232 Linkam video text overlay superimposes the display on the control unit and under the field of view, onto a video camera linked to a TV monitor. A P613 Mitsubishi Video Copy processor is used to capture the image.

Regular calibration of the heating-freezing stage was undertaken by measuring the melting temperature of high purity melting point standards which were placed in the same position on the stage as the samples. A calibration curve was constructed from the measured and standard melting points of the calibration substances. All subsequent sample measurements were corrected by referring to this curve (Shepherd et. al 1985a). A list of the substances used for the stage calibration and their melting points, is given in Appendix B.

4.4. Methodology

Optical examination of the fluid inclusions using standard polished wafers (1mm thick) was undertaken prior to any microthermometric analysis. This procedure enables separate fluid

inclusion generations with different morphologies and liquid to vapour ratios, to be distinguished and classified. The subsequent microthermometric analysis typically consists of two cycles. A high-temperature cycle for the determination of homogenization temperatures, and a low-temperature, freezing cycle (down to -120°C) for the determination of total salinity, as well as, the relative Na-Ca levels of the inclusion fluids. In most cases the high temperature runs were undertaken prior to freezing in order to avoid possible leakage caused by the expansion of ice in frozen inclusions (Shepherd et. al. 1985a). Care was taken to measure the inclusions with lower homogenization temperature prior to those with high temperature in order to further eliminate any possibilities of leakage. To ensure accuracy low heating rates were normally employed reaching down to 0.5°C/min on approaching homogenization, and 0.2°C/min when recording last melting temperatures.

It has long been recognized that homogenization temperatures generally represent only a minimum estimate of the fluid trapping temperature. The difference between T_H and T_T, commonly known as "pressure correction", is a function of the trapping pressure and fluid composition. Only in the case of fluid inclusions which show signs of boiling (i.e. the pressure of the fluid is equal to the vapour pressure), the homogenization is truly representative of the trapping temperature. In all other cases it is assumed that the fluid pressure is greater than the vapour pressure. In order to estimate the pressure, both the composition and the PVT properties of the fluid need to be known. Due to the uncertainty regarding exact timing and depth of mineralization in the areas of study, no pressure correction was applied to the homogenization temperature values reported here. This subject will be discussed in more detail for the individual areas of study.

For aqueous salt-water systems the temperatures marking three phase changes in the inclusion are very important, i) the temperature of first melt (T_{FM}), ii) the temperature of salt hydrate melt (T_Mh), and iii) the temperature of ice melt (T_{LM}). The temperature of first melt marks the first appearance of liquid after complete freezing and usually corresponds to the eutectic temperature. Where there is no solid solution between the solid phases the eutectics are invariant points and are a function solely of the composition of the fluid regardless of the concentration of the solutes. For a pure NaCl-H_2O system the eutectic is -20.8°C, whereas for NaCl-$CaCl_2$-H_2O it is -52°C (Shepherd et. al. 1985a). Identification of the composition of the inclusion fluid by recording of the first melting temperature is the first and possibly the most important step of low-temperature microthermometric analysis, since it enables the use of the appropriate phase diagrams for further estimates of total salinity and element ratios. However, the first melting temperature

is the most difficult to record as it is marked by the formation of only tiny amounts of liquid. As noted by Roedder (1984) at least 10% melt of the solid-frozen inclusion is required for the first melt to be identifiable.

In fairly concentrated inclusions, salt hydrates may develop in addition to ice. Hydrohalite ($NaCl \cdot 2H_2O$) and antarcticite ($CaCl_2 \cdot 6H_2O$) are the most common. Ice is usually the last phase to disappear in a frozen inclusion. The temperature marking last ice melt (T_{LM}) is an estimate of the freezing point depression and a function of the overall salinity of the inclusion fluid. However, in more concentrated systems, the last phase to melt is the salt-hydrate instead of ice. Optical distinction between hydrohalite and antarcticite crystals is very difficult. As noted by Shepherd et. al. (1985a), unless the fluid has a Ca/Na weight ratio higher than 15, the hydrate formed after ice melting can be assumed to be hydrohalite. For the inclusions examined in the present work independent evidence (chemical analysis of inclusions in quartz (Rankin & Graham 1988) and charge balance calculations) indicates that Na rather than Ca is the most abundant cation in solution. Therefore, the reported T_Mh are considered to represent final hydrohalite melting. Paired T_{LM} and T_Mh measurements plotted on appropriate phase diagrams (Borisenko 1977, Oakes et.al. 1990), provide more accurate estimates of both salinity and element ratios of the inclusion fluids. In the present work the more recent phase diagram of Oakes et.al.(1990) was used for the calculation of the relative Na-Ca contents of the inclusions.

A procedure outlined by Shepherd et. al. (1985a) was followed in order to record more easily the phase changes during the heat-cool cycle. The temperature of the frozen inclusion was slowly raised until only one ice crystal remained. Then the temperature was rapidly lowered again, causing the ice crystal to grow further. With further freezing, salt hydrates crystalized and usually occupied a corner of the inclusion. This sequential freezing procedure enables the separation of the frozen phases (ice and hydrate) and makes the recording of the phase changes on melting easier. Both the ordinary and sequential freezing cycles are schematically illustrated in Fig. 4.5.

Efforts were made to record all four temperatures (T_H, T_{FM}, T_Mh, T_{LM}) of main phase changes of individual inclusions. Approximately 900 individual inclusions were studied in the present work, resulting in a total number of approximately 3500 measurements. All measurements from microthermometry are listed in Appendix B.

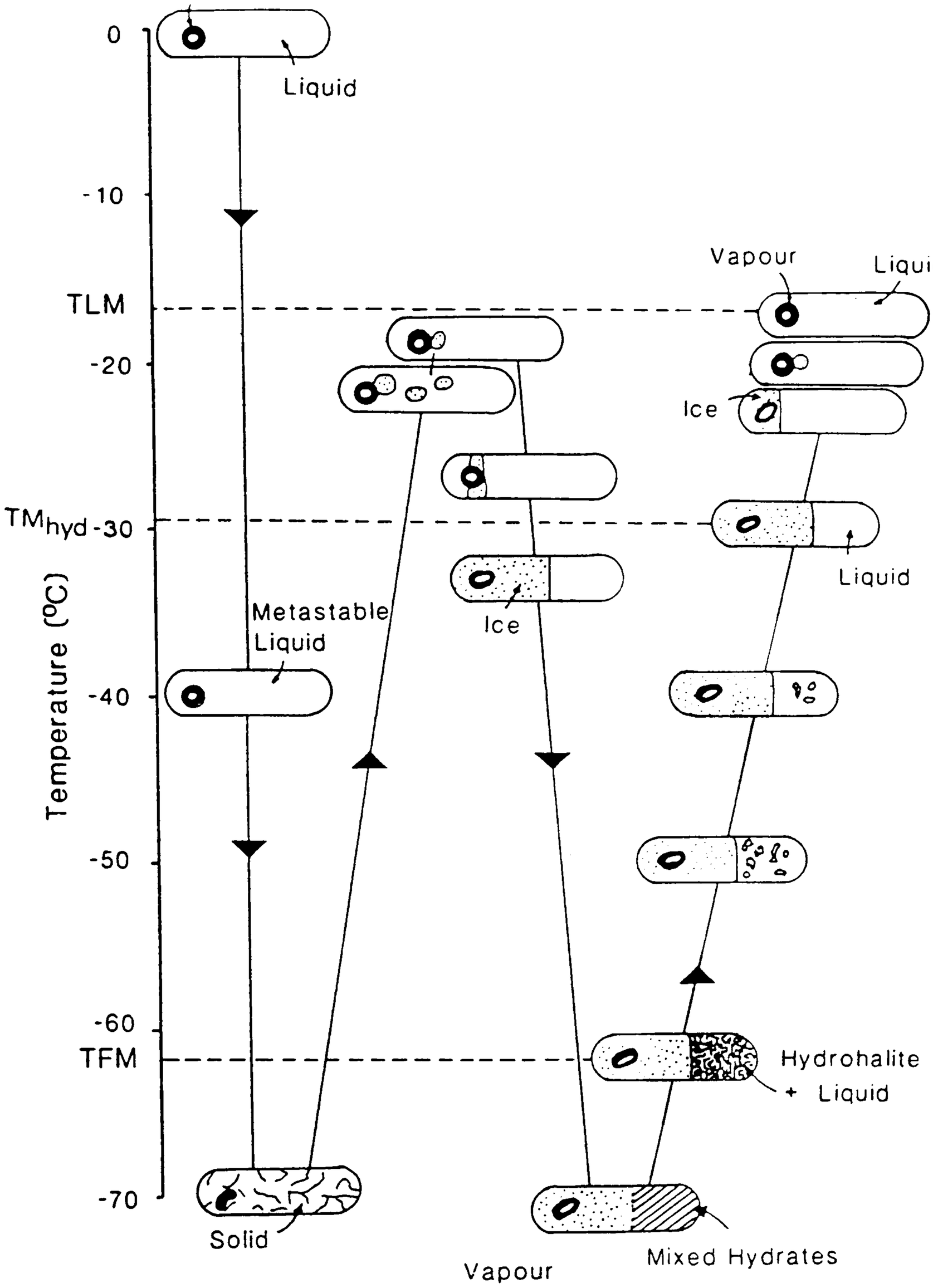


Fig.4.5. Schematic representation of typical heating-freezing cycles followed during microthermometric analysis of fluid inclusions.

4.5. Microthermometric Results

As noted previously, most of the emphasis in the present study is focused towards the recording of paired T_{FM}, T_Mh and T_{LM} temperatures as a means of estimating the fluid inclusion composition. However, homogenization temperatures will also be reported here. Results from the areas of study (Pennines, Llanharry an South Crofty) will be presented separately in the following section.

4.5.1. Pennines

All studied inclusions from the Pennine samples are two phase liquid-vapour inclusions with high degrees of fill in the range between 0.90-0.95 (Plates 4.3a, 4.3b). On heating, they all homogenized in the liquid state with gradual disappearance of the vapor bubble.

Fluid inclusion homogenization temperatures in samples from the three Pennine orefields are presented in the form of histograms in Fig.4.6. For the Alston block inclusions, homogenization temperatures fall in the range between 73 and 212°C. As can be seen from Fig.4.6a, the values exhibit a normal distribution with a mean of 125°C. The Askrigg block inclusions have temperatures in the range of 74-128°C. Their distribution is also normal with a mean of 100°C. Compared to the T_H values from the two Northern Pennine fields, there is a further decrease of homogenization temperatures in the Derbyshire inclusions. As can be seen from Fig.4.6c, the majority of the readings fall in the range between 60 and 120°C, with a mean of 80°C. However, apart from these low temperature fluids, a small number of inclusions homogenized at higher temperatures reaching values up to 160°C. These values were obtained from two specific localities, in the northern part of the Derbyshire orefield (Dirtlow Rake and Blue John Cavern, samples DR/1/F, DR/2/F). Fluid inclusions in calcites from the Ecton Hill Cu-deposit exhibit homogenization temperatures in the range between 57 and 90°C (Fig.4.7a.). Their spread is within the range defined by the low-temperature group of the Derbyshire fluids.

As can be seen from Figs.4.6a-c, homogenization temperatures obtained from the three Pennine orefields exhibit a well defined decreasing trend from north to south. In order to further establish this trend, and examine the significance of the observed differences in T_H between Alston, Askrigg and Derbyshire, a simple statistical test was performed.

Plate 4.3a

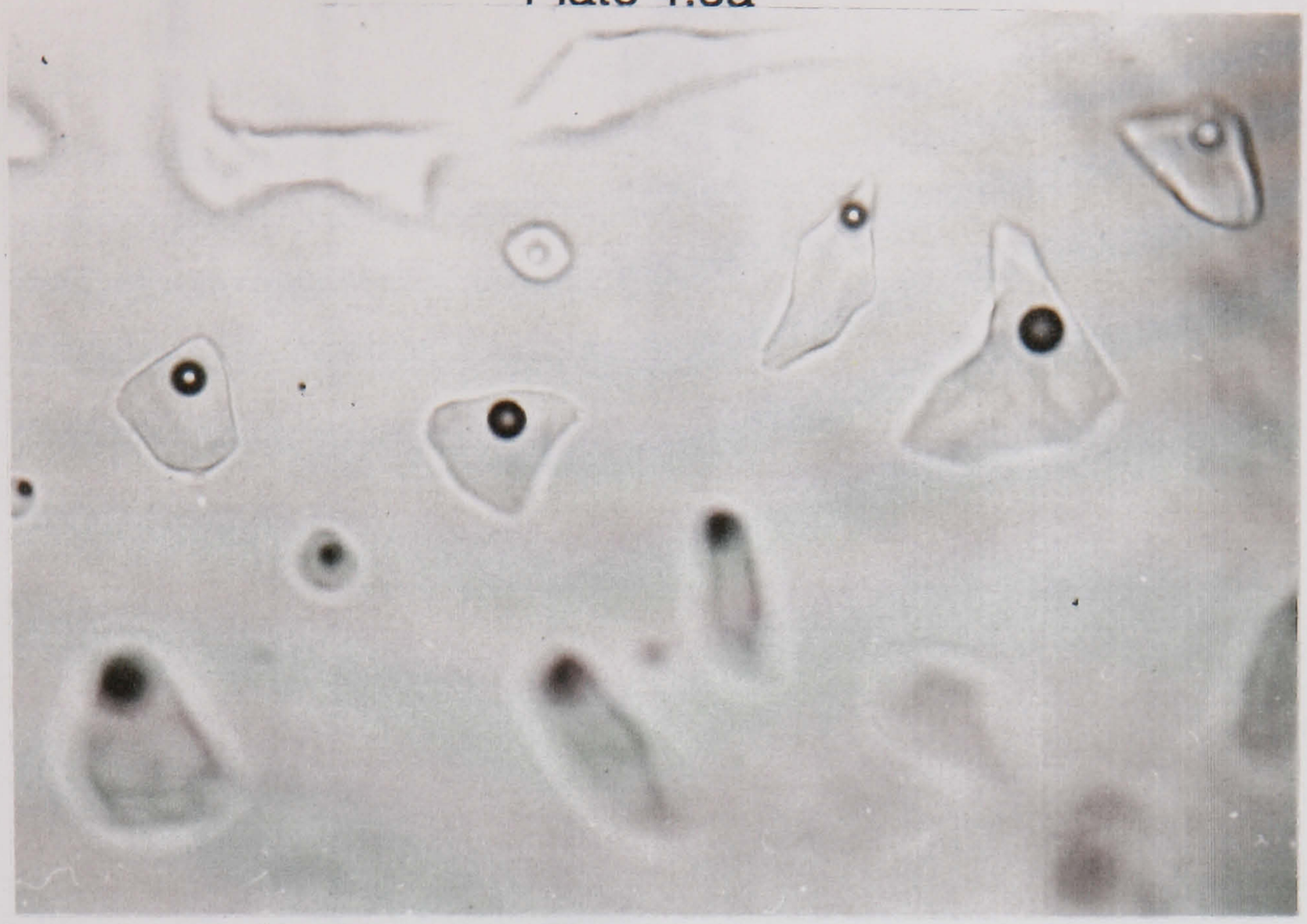
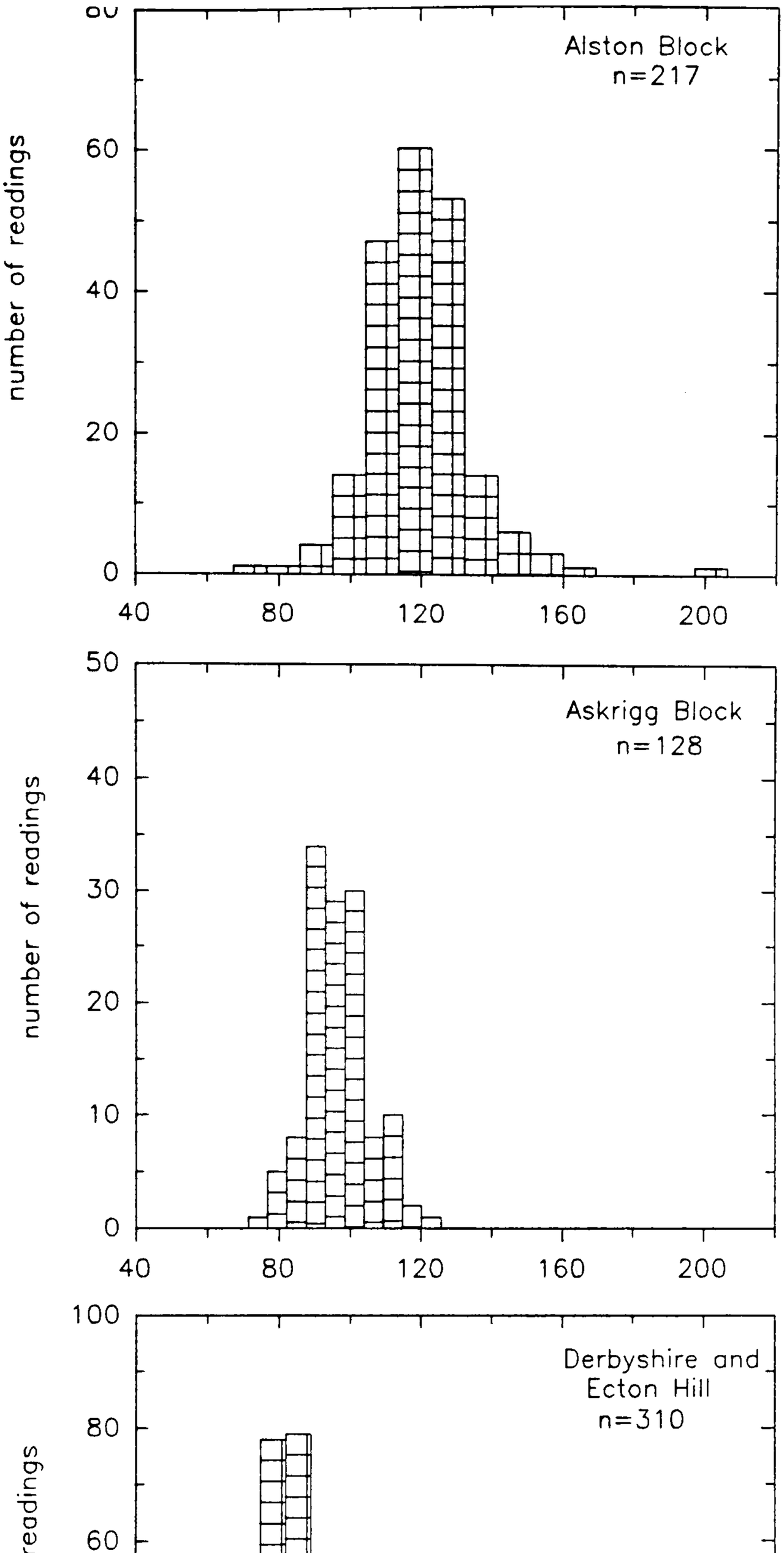


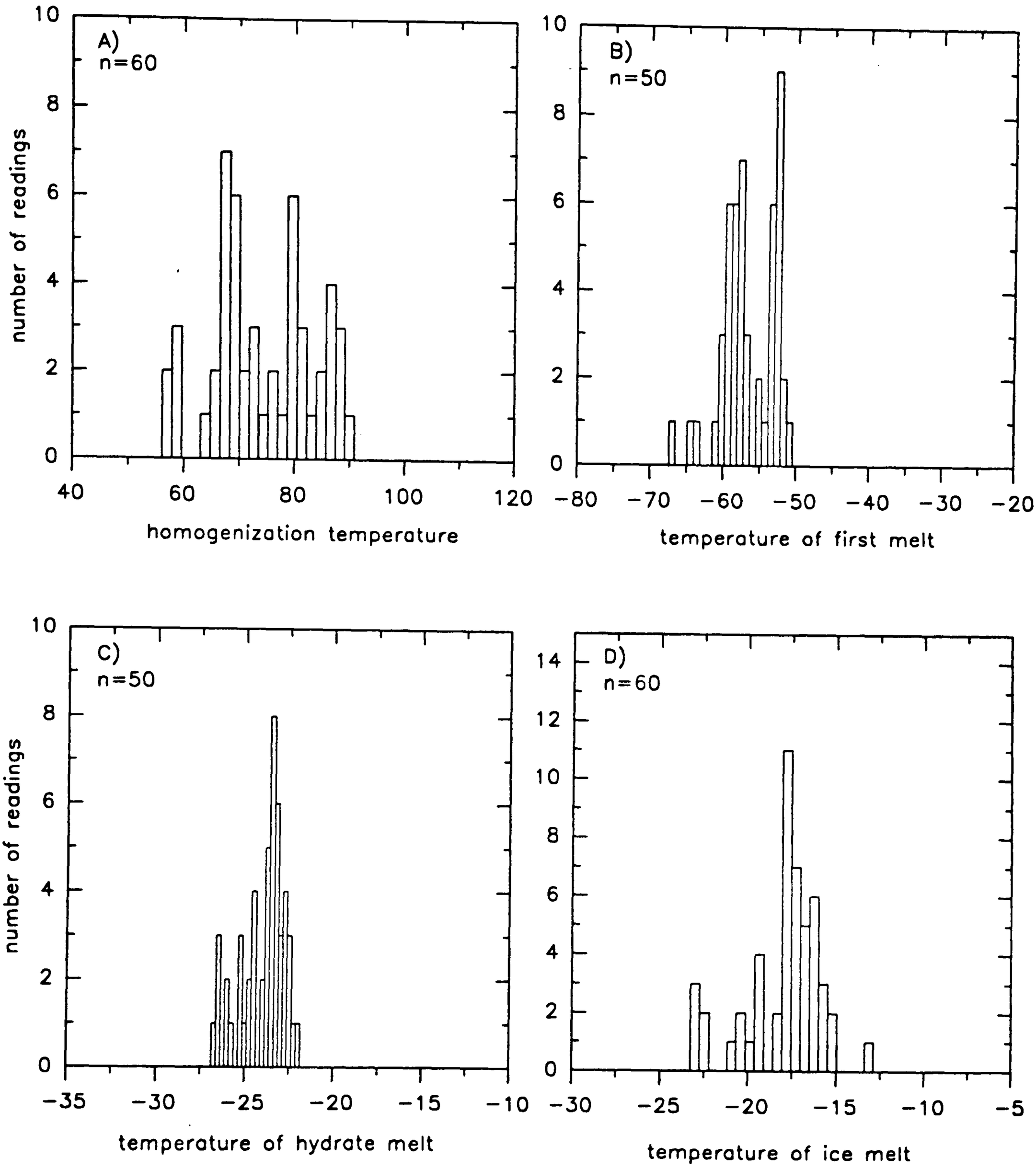
Plate 4.3b



Plates 4.3a and 4.3b. Typical two-phase, aqueous Liquid-Vapour fluid inclusions in fluorite from the Pennine orefields (field of view= 120x90μm)



Figs.4.6a-c. Histograms showing the frequency distribution of homogenization temperatures (T_H) of fluid inclusions from the three Pennine orefields.



Figs.4.7a-d. Histograms showing the frequency distribution of a) homogenization (T_H), b) first melt (T_{FM}), c) hydrate ($T_M h$) and d) ice (T_{LM}) melting temperatures of fluid inclusions in calcite samples from Ecton Hill.

Table 4.2. Average T_H values from the three Pennine orefields

Alston Block	Askrigg Block	Derbyshire
T_H mean (x_1)= 125	T_H mean(x_2)=99.5	T_H mean(x_3)=92.2
std (s1)=14.5	std (s2)=8.9	std (s3)=19.9
min.T_H=72.8	min T_H=74	min T_H=59.7
max.T_H=212	max T_H=128	max T_H=164
number of readings (n_1)=217	number of readings (n_2)=128	number of readings (n_3)=164

The statistical test is based on the calculation of a "pooled estimate" (s) of standard deviation (Miller & Miller 1988). The following equations are used.

$$s^2= \{(n_1-1)s_1^2 + (n_2-1)s_2^2\}/(n_1+n_2-2) \quad (1)$$

$$t= (x_1-x_2) / s \{(1/n_1+n_2)\}^{1/2} \quad \text{where t has } n_1+n_2-2 \text{ degrees of freedom} \quad (2)$$

Substitution of the Alston and Askrigg T_H statistics to the above equations yields a value for t_{calc}=42. For 343 degrees of freedom, and 0.05 probability the tabulated value for t is 1.96. Therefore, since $t_{calc} > t_{tab}$ the null hypothesis that $x_1-x_2=0$ is rejected, and the difference between the two sets of data is significant at the 0.05 probability level. The same conclusion can be drawn for the comparison of the Askrigg and Derbyshire values for which t_{calc}=8.4. As can be seen from Table 4.2. both the low and high-temperature populations of the Derbyshire fluids are included in the calculations.

As noted in the previous section, no pressure correction is applied to the T_H data presented here. Several attempts have been made in the past towards calculating the depth and hence, the pressure and temperature of the fluids at the time of trapping. In general, the most serious barrier in accurately calculating the depth of mineralization is the lack of knowledge of the exact timing of mineralization. Hydrostatic rather than lithostatic pressures are more likely since, as noted by Hanor (1979b) derivation from hydrostatic pressures occurs at depth greater than 1.4-4.5Km. For the Northern Pennine orefield, a maximum cover of 1100m was postulated by Sawkins (1966a) on the basis of stratigraphic evidence. If such a depth is assumed, the resulting pressures are in the range between 100-200bars and the subsequent corrections between 10-20°C (Sawkins 1966a). For the Derbyshire orefield, Rogers (1977) applied a 11°C positive, pressure correction by assuming that mineralization took place at pre-Permian times, underneath an approximate 1000m cover. However, in a

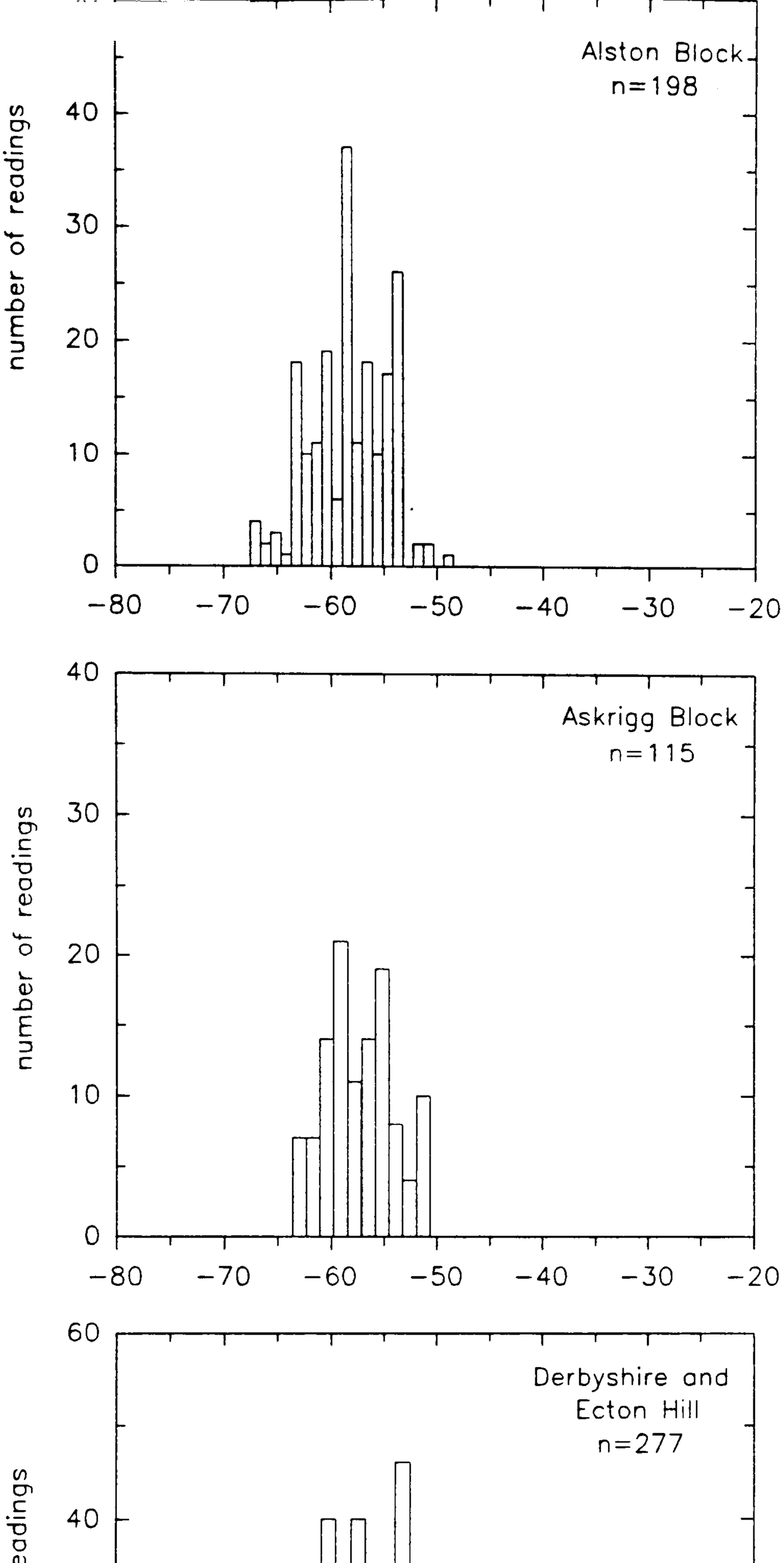
recent publication Mostaghel & Ford (1986) proposed the presence of a more extensive sediment cover at the time of mineralization in Derbyshire. This general uncertainty regarding the timing and consequently the depth of mineralization in the Pennines does not permit an accurate determination of the pressure correction. However, available information (op. cit), indicates that most possibly the pressure correction does not exceed 20°C.

Following the procedure outlined in section 4.2. and after the measurements of T_H, phase changes of frozen inclusions were recorded. Low temperature measurements in most of the Pennine fluorites were facilitated by the great abundance of large, isolated, primary fluid inclusions with high degrees of fill (0.95). Supercooling phenomena were very common and rapid lowering of the temperature was required in order to freeze the inclusions.

On reheating the completely frozen inclusions, first melt commonly occurred at temperatures in the range of -65 to -50°C. Temperatures of first melt are presented in a histogram form in Figs.4.8a-c. These temperatures are much lower than the eutectic temperatures of -20.8°C of the system NaCl-H_2O and -22.9°C for the system NaCl-KCl-H_2O (Potter et. al. 1978, Hall et. al. 1988). Such low temperatures are much closer to the eutectic temperatures of between -49.5 and -57°C of $CaCl_2$ ($\pm MgCl_2$)-NaCl-dominant systems (Crawford et. al. 1981, Davis et. al. 1990).

The relatively large spread of T_{FM} values is mainly a result of the problems surrounding the precise determination of the temperature marking the appearance of the first liquid. First melts at temperatures as low as -70°C were also observed. As noted by Davis et al (1990), phase changes at temperatures as low as -85°C and -60°C may be a result of metastable $CaCl_2$-hydrate melting, as well as, of the melting and recrystallization of ice. Therefore, first melt temperatures are not always representative of the true eutectics. This ambiguity regarding the first and eutectic melts was also noted by Roedder (1984). He pointed out that in apparently unfrozen inclusions, crystals do form but are submicroscopic and cannot be observed. On warming, the inclusions show rapid crystal growth and deformation of the vapour bubble. In the case that crystals are not observed, the vapor deformation is a result of the thermal expansion of the liquid (Roedder 1984).

Despite the problems surrounding the accurate determination of T_{FM}, recorded first melts in the Pennine inclusions occurred at consistently low temperatures. This phenomenon can only be interpreted as an indication of $CaCl_2$ ($\pm MgCl_2$) together with NaCl-salts in solution. (Shepherd et. al. 1985a, Davis et. al. 1990). For reasons discussed in Chapter 3,



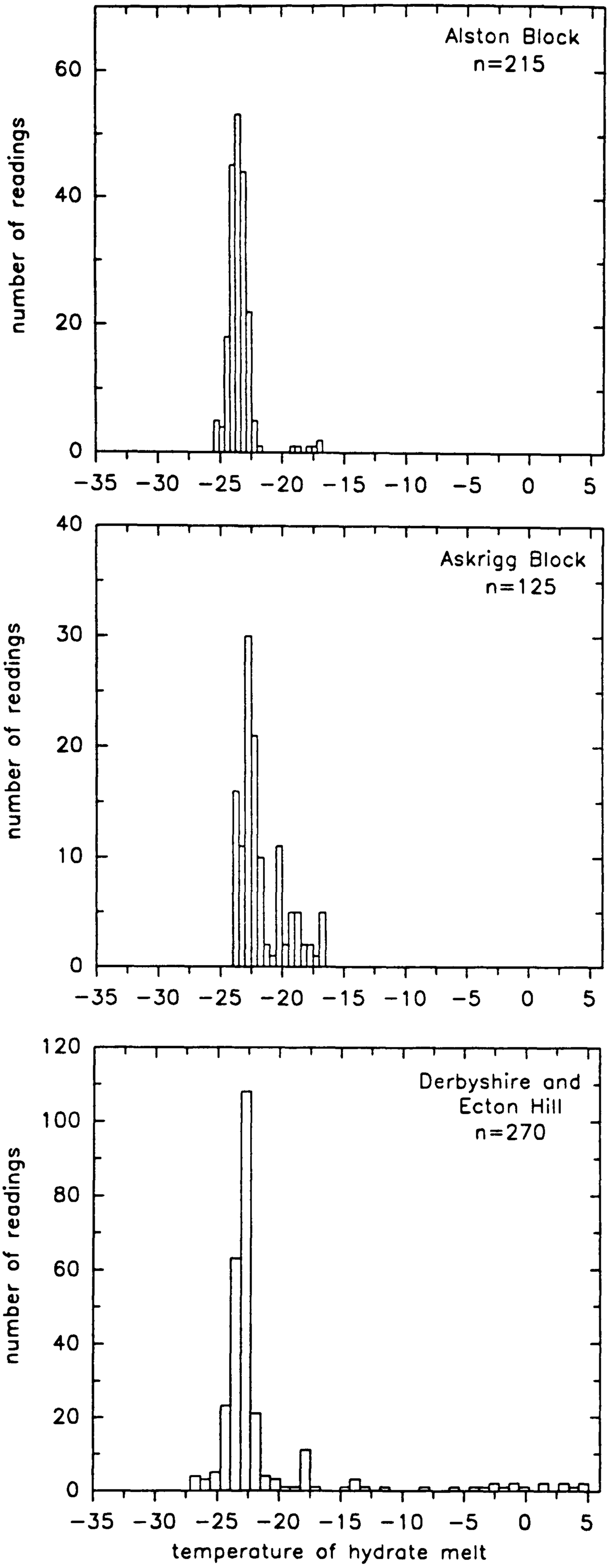
Figs.4.8a-c. Histograms showing the frequency distribution of first melting temperatures (T_{FM}) of fluid inclusions in samples from the three Pennine orefields.

the Ca and Mg contents of fluid inclusions in fluorite and calcite samples could not be determined by chemical analysis. However, chemical analysis of fluid inclusions in quartz (Rankin & Graham 1988) has shown that Na and Ca are the major cations in solution. Therefore, although small quantities of $MgCl_2$ may be present in the fluids, it is conceivable to interpret the freezing results in terms of the simple $NaCl-CaCl_2-H_2O$ system for which experimental data are more readily available (Oakes et. al. 1990, Borisenko 1977). Overall, for the majority of the Pennine samples, the low temperatures of first melt, indicate the dominance of Na and Ca chlorides in solution since Br, I, F, SO_4, NO_3, HCO_3 and CO_3 -dominant systems have much higher eutectic temperatures (data for these systems are summarized in Shepherd et. al. 1985a).

For the Derbyshire fluids, not all recorded first melts are low. First melts for a small number of inclusions occurred at temperatures as high as -22°C (Fig.4.8c). These values were obtained from the relatively high-temperature fluid inclusions mentioned previously. Consequently, in terms of both homogenization and first melting temperatures, these inclusions can be envisaged as members of a separate generation of fluids. Their high first melt temperatures indicate that NaCl, and possibly KCl, are the dominant salts in solution.

After recording the first melt temperature and identification of the fluid system, the next step is the measurement of hydrate and ice melting temperatures. For the majority of the samples from Alston and Askrigg, the hydrate (hydrohalite) phase melted prior to ice. However, in some samples of higher salinity hydrohalite was the last phase to melt. Hydrohalite melt temperatures obtained from samples from the three Pennine orefields are presented as histograms in Figs.4.9a-c.

For Alston Block T_Mh show a narrow spread between -26 and -22°C with a mean value of -23.2°C. Only a small number of values, between -19 and -16°C, lie outside this range. These values mark the fact that hydrohalite melted after ice. The Askrigg fluids show a wider spread of T_Mh values ranging from -24 to -18°C. Similarly to the Alston fluids, the higher values represent hydrohalite melting after ice. Hydrate melt in the Derbyshire inclusions occurs at temperatures between -27 and -15°C. However, in a limited number of inclusions the hydrates melted at temperatures up to +5°C. Such high melting temperatures can be caused by the presence of hydrocarbon-clathrates which usually have the form of irregular plates and have a tendency to occur close to the vapour bubble (Shepherd et. al. 1985a). However, in the inclusions mentioned above the last melting phases had the form of isolated individual crystals and therefore, they were interpreted as salt-hydrates. Such high T_Mh values are most possibly caused by the metastable behavior of hydrohalite



Figs.4.9a-c. Histograms showing the frequency distribution of hydrate melting temperatures ($T_M h$) of fluid inclusions from the three Pennine orefields.

crystals which at low heating rates can persist up to positive temperatures (Davis et al 1990). Salt hydrates were not observed in fluid inclusions in the two samples from Dirtlow Rake and Blue John Cavern.

Ice melting temperatures for the three Pennine orefields are presented as histograms in Fig.4.10. For the Alston block inclusions most of the T_{LM} values lie in the range between -23.9 and -16.5°C (Fig.4.10a). Only a small number of readings fall below this range and correspond to ice melting prior to hydrohalite. The same observations are made for the Askrigg fluids which similarly show ice melting temperatures between -24 and -17°C (Fig.4.10b). For the Derbyshire inclusion fluids, ice melts show a larger spread between -27 and -15°C. Hydrohalite melting after ice is more common in the Derbyshire samples than in the Northern fields. Fluid inclusions in the Blue John and Dirtlow Rake samples have high ice melt values, in the range between -4 to -1°C, indicating very low salinity values. This values are in agreement with results obtained by Moser et. al. (1992) from mixed aqueous-hydrocarbon inclusions which are also common in these samples.

Last hydrohalite or ice melting temperatures were used to calculate the overall salinity of the fluids using equations derived from experimental data for simple chemical systems. Curves and equations by Potter et. al. (1978) for the NaCl-H_2O system were used to calculate overall salinities which are expressed as equivalent wt.%NaCl. These are presented as histograms in Fig.4.11. The Alston and Askrigg fluids show similar salinity trends ranging between 19 and 23 eq.wt%NaCl. The Derbyshire fluids show a larger spread with the majority of the readings falling between 17 and 26 eq wt% NaCl and a low salinity population with values between 1 and 5 eq. wt% NaCl.

4.5.2. Llanharry, South Wales

Previous work on fluid inclusions in quartz and calcite samples from the Llanharry Fe ore deposit in South Wales was undertaken by Rankin & Criddle (1985). Problems caused by the small size and scarcity of fluid inclusions in both quartz and calcite samples, mentioned by Rankin & Criddle (1985), were also encountered in the present work. Of the 10 examined samples, more detailed, paired results could be obtained only from four samples.

Unlike the Pennines, monophase liquid inclusions, typical of low-temperature environments predominate in the Llanharry samples (Plate 4.4a). Measurements were taken on the scarce two-phase inclusions (Plate 4.4b), as well as on a restricted number of initially monophase inclusions which developed a vapour bubble after freezing, following a procedure outlined by Rankin & Criddle (1985). Homogenization temperatures obtained in the present work

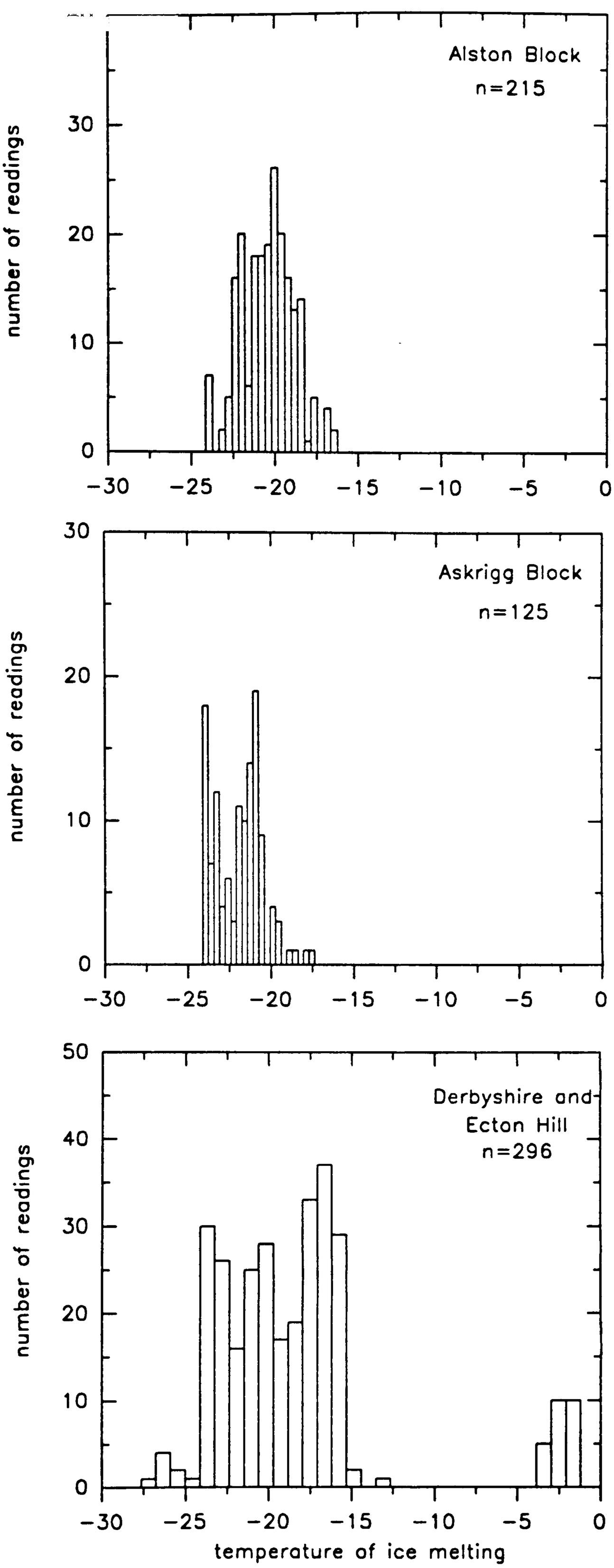
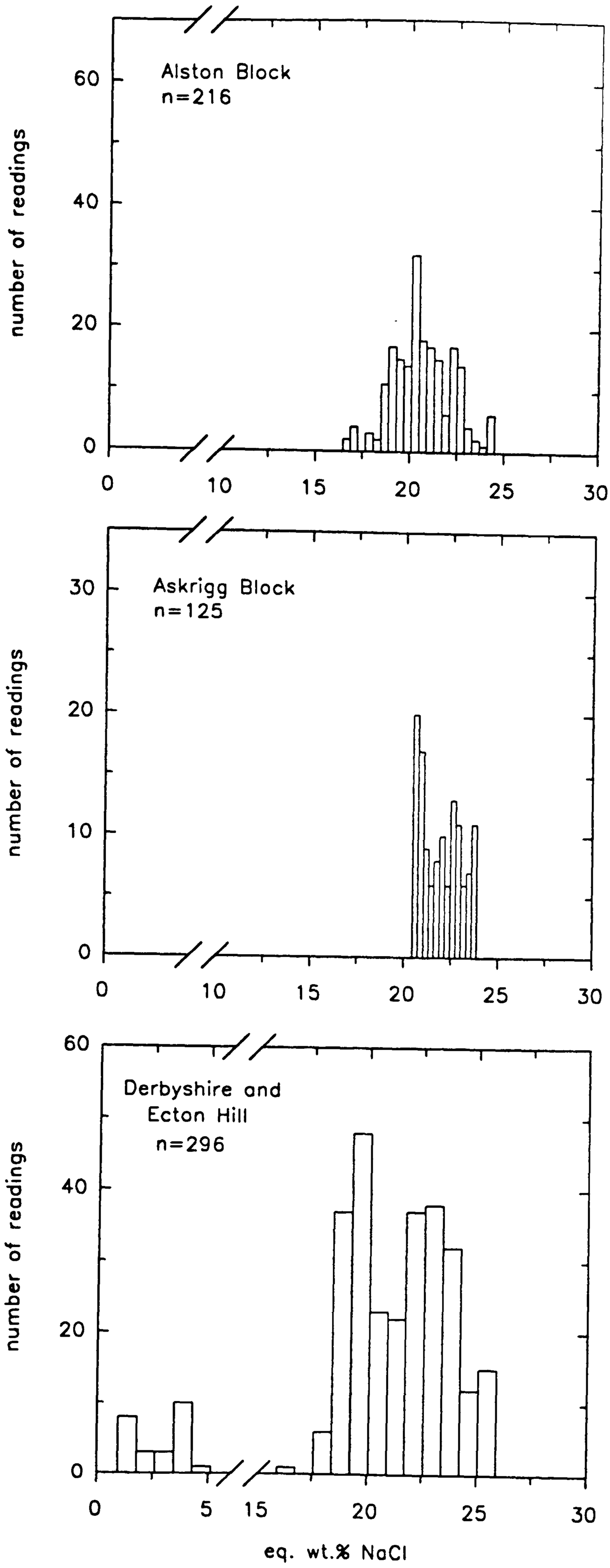


Fig.4.10. Histograms showing the frequency distribution of last ice melting temperatures (T_{LM}) of fluid inclusions in samples from the three Pennine orefields.



Figs.4.11a-c. Histograms showing the frequency distribution of total salinities of fluid inclusions (expressed as eq.wt.%NaCl) of fluid inclusions from the three Pennine orefields.

Plate 4.4a

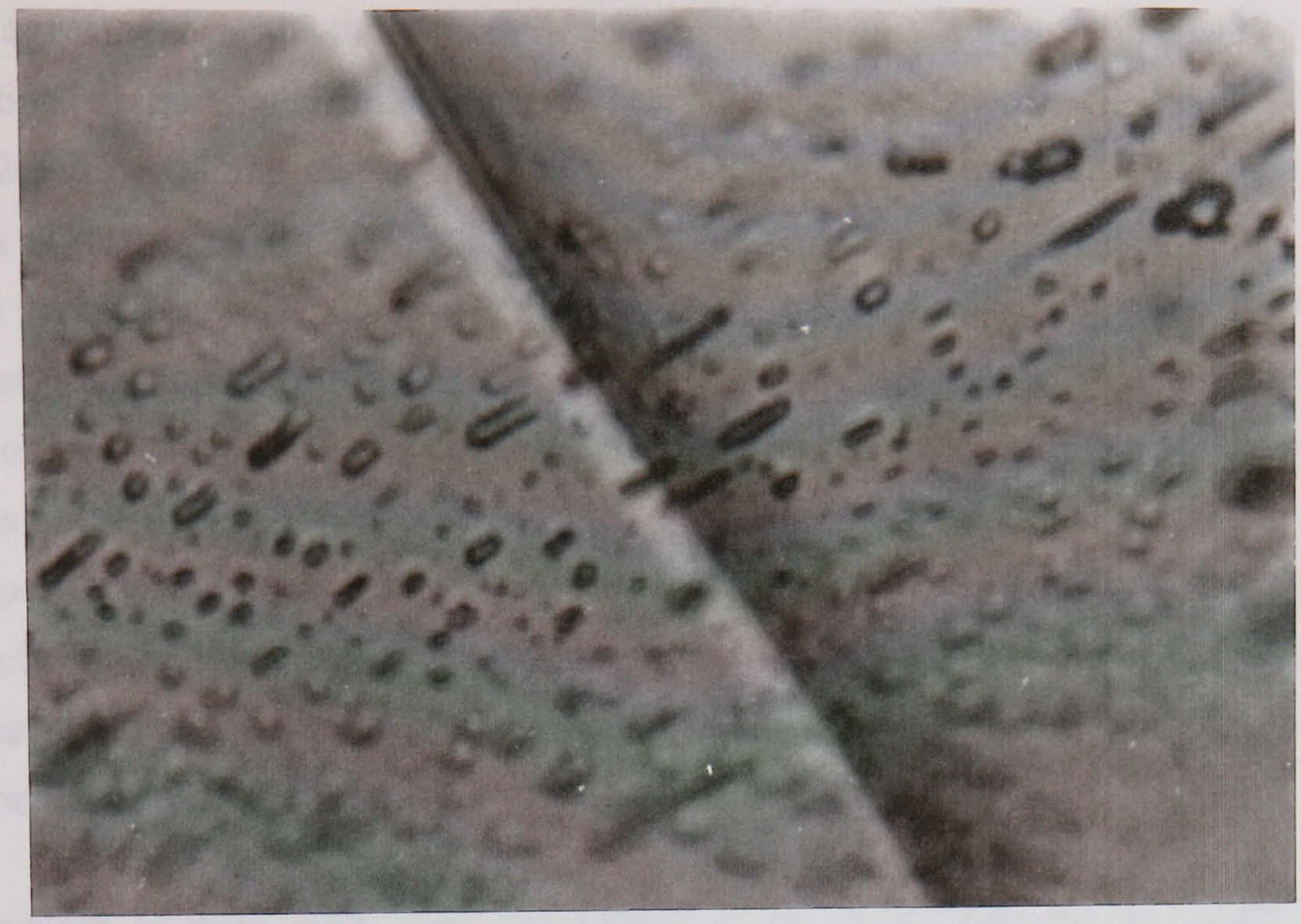
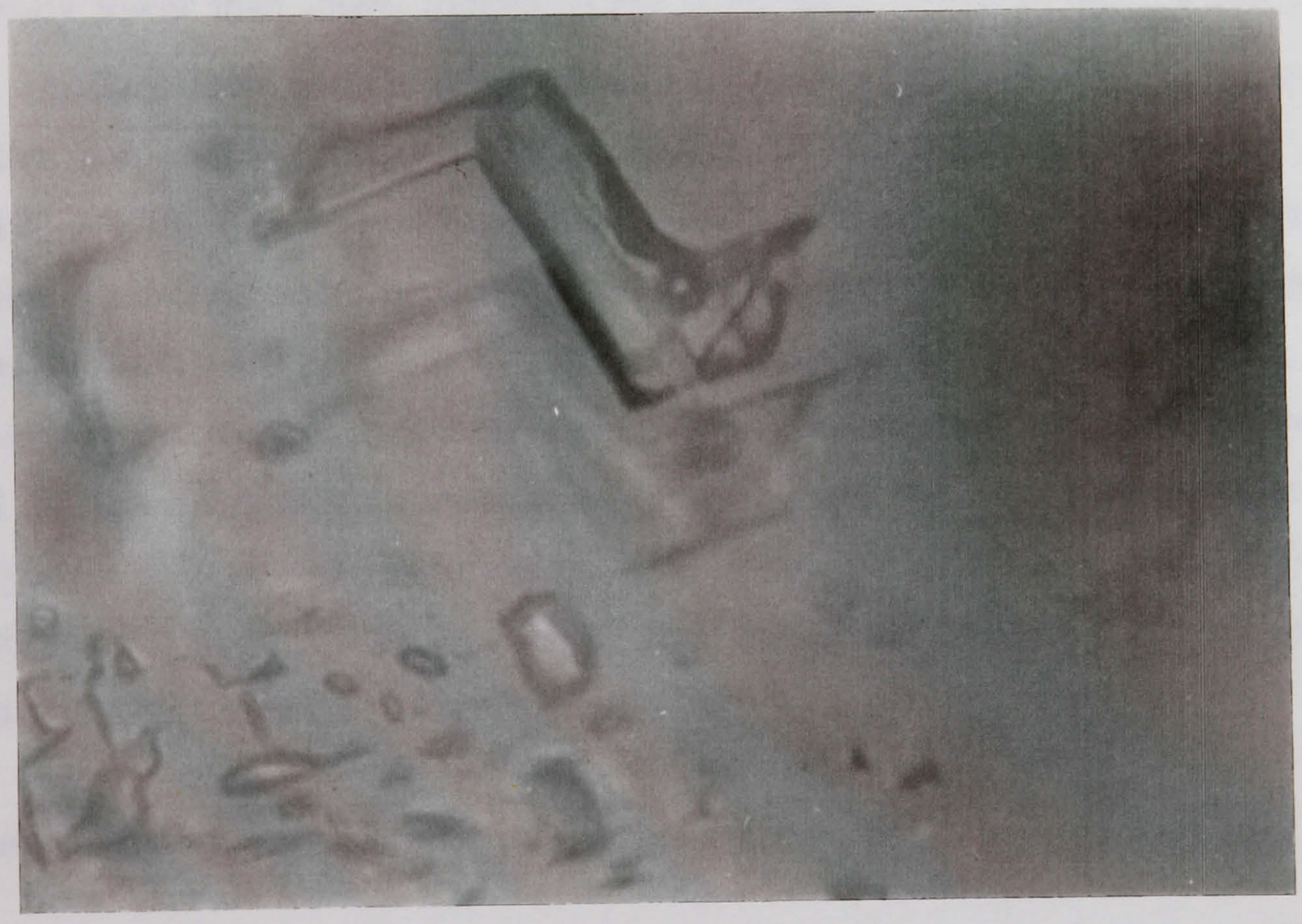


Plate 4.4b



Plates 4.4a and 4.4b. Fluid inclusions in calcite from the Llanharry Mine, S.Wales. (field of view= 60x120μm)

4.4a. Swarms of liquid, monophase, secondary fluid inclusions.

4.4b. Rare two-phase, aqueous liquid-vapour, primary inclusions.

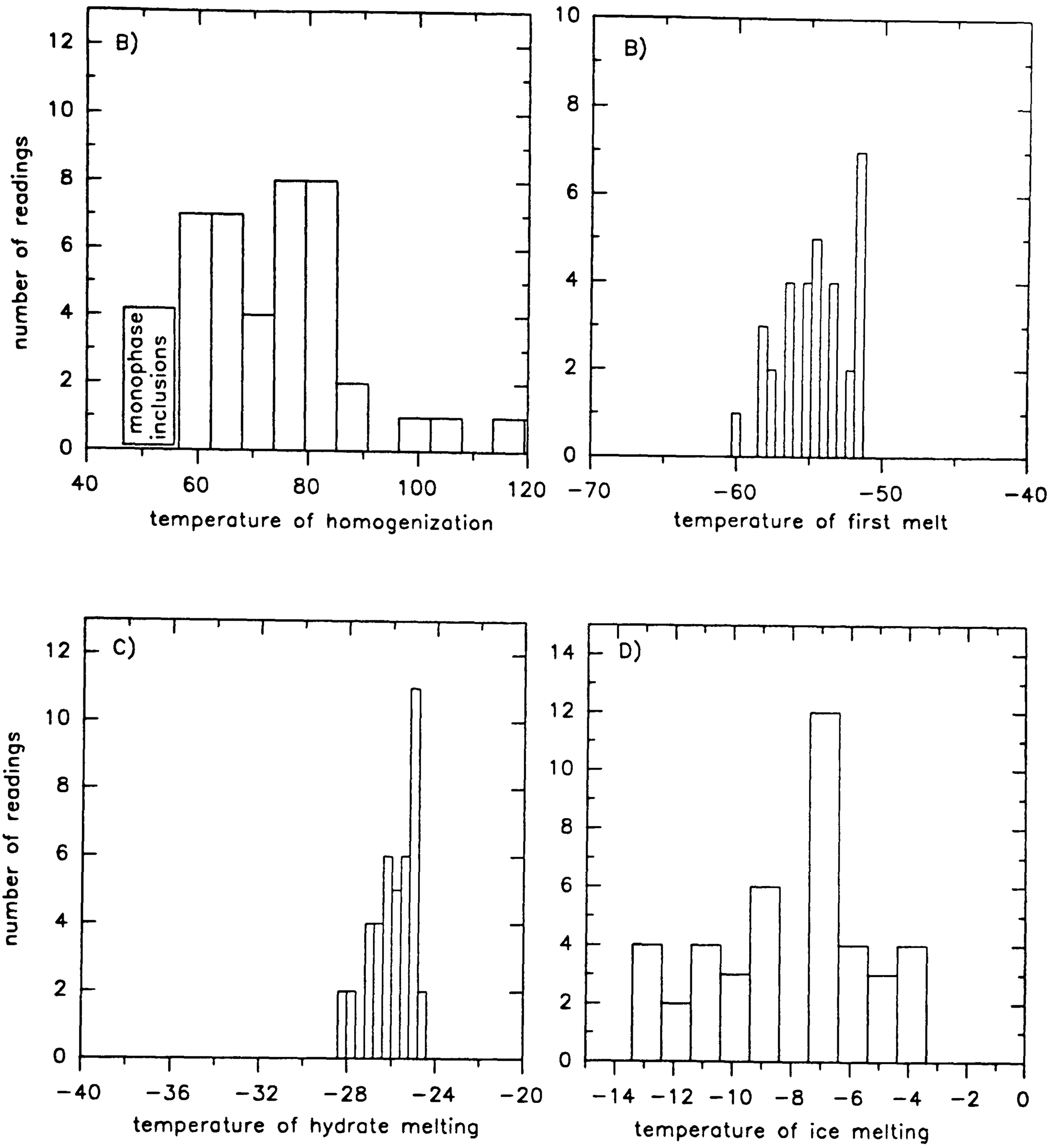
are in agreement with those reported by Rankin & Criddle (1985) The frequency distribution of homogenization temperatures obtained in the present study is shown in Fig.4.12a. Most of the readings fall in the range between 60-90°C. Since the number of readings is restricted, it is difficult to positively assess the form of the distribution. As can be seen from Fig.4.12a, a small number of homogenization temperatures higher than 100°C were also recorded. These are very few and are most probably a result of leakage of the inclusions. No pressure correction is applied to the homogenization temperature data since, as noted by Rankin & Criddle (1985), the present depth of the orebodies (ca 300m), differs only slightly from that at the time of emplacement (Late Triassic). In general, the fluid inclusion homogenization temperatures obtained from both calcite and quartz samples show that the mineralization in Llanharry was formed by low temperature fluids, similar to those encountered in the Derbyshire and Ecton orefields.

Temperatures of first melt were more difficult to record due to the small size of the inclusions (5-15μ). T_{FM} of the Llanharry inclusions are presented in Fig.4.12b. The values are generally lower than -50°C indicating the dominance of NaCl-$CaCl_2$($\pm MgCl_2$) salts in solution. Hydrate melt occurs at temperatures between -24 and -28°C whereas ice is always the last melting phase at temperatures in the range between -13 and -3°C (Figs.4.12c-4.12d). Consequently, the corresponding salinities are not as high as those of the Pennine fluids. As noted previously, the predominance of swarms of small monophase inclusions in both calcite and quartz samples, seriously halted the recording of larger numbers of ice and hydrate melt temperatures. It is therefore possible that the low salinities observed in the Llanharry inclusions may be a result of the predominance of later, secondary over primary fluid inclusions. Furthermore, the number of readings is not large enough to allow a positive identification of the form of the frequency distribution (normal or bimodal) of the ice meting temperatures.

4.5.3. South Crofty, Cornwall

As reviewed in detail in Chapter 2 and in section 4.2.2., hydrothermal mineralization at South Crofty is complex and consists of multiple events with varying affinity to the granitic mass. At South Crofty, fluorite is the dominant gangue mineral and it is present mostly in the late, chlorite stage of mineralization. Fluid inclusions in late fluorite samples were examined in the present study. Three fluorite samples from the early, pegmatite stage were also examined optically for comparison.

The complexity of the fluid system became apparent from the optical observation of fluid



Figs.4.12a-d. Histograms showing the frequency distribution of a) homogenization temperatures (T_H), b) first melting temperatures (T_{FM}), c) hydrate ($T_M h$) and d) ice melting (TLM) temperatures of fluid inclusions in calcite and quartz samples from Llanharry, South Wales.

inclusions. Fluid inclusions of varying size and degrees of fill are abundant in most samples. The great abundance as well as severe overprinting of multiple fluid inclusion generations, not only in a single sample but also in a single field of view (Plates 4.5a, 4.5b), made the distinction between primary and secondary inclusions problematic. The majority of inclusions are two-phase aqueous liquid-vapour systems. High degrees of fill (0.95-0.85) are most common, but vapour-rich inclusions are also present (Plate 4.5c.) Rare, three phase liquid-vapour-solid inclusions were observed in fluorites from the pegmatite stage of the paragenesis. The daughter minerals have the characteristic cubic form of halite crystals (Plate 4.5d).

Previous work by Farmer (1991) defined a broad homogenization temperature range between 120 and 400°C for the chlorite stage of the paragenesis. Homogenization temperatures recorded in the present study are shown in Fig.4.13a. Two generations of fluids are also recognized here. A low temperature stage is constrained between 80 and 150°C whereas, the higher temperature component has a wider spread of values between 200 and 300°C. From the homogenization temperatures alone it is not possible to assess the origin of the fluids. However, the T_H values of the low-temperature component are generally similar to values obtained from the Alston Block fluorites. Further freezing studies were undertaken to estimate the salinity of both the low and high temperature fluid populations.

The frequency distribution of first melt temperatures is shown in Fig.4.13b. The majority of the values lie in the range between -50 and -80°C with only a small number of higher values, between -22 and -30°C. As for the Pennine fluids, the low T_{FM} values are interpreted as characteristic of NaCl-$CaCl_2$-($\pm MgCl_2$)-bearing fluids. These values are in agreement with the previously published values in the area (Farmer 1991). The phenomenon of metastable first melting at temperatures as low as -80°C was also encountered here.

The distribution of both hydrate and ice melt temperatures is far more complicated. As can be seen from Fig.4.13c-d there are three clear, and possibly four, separate modes of ice melt behavior, covering the whole spectrum between 0 and 27°C. Ice melt occurred either prior to or after hydrate melting. Hydrate melt temperatures fall into three main groups, one between +5 and -5°C, a second between -20 and -30°C and a third between -32 and -42°C.

This wide range of T_{LM} and T_Mh illustrates the complexity of the fluids at South Crofty.

Plate 4.5a

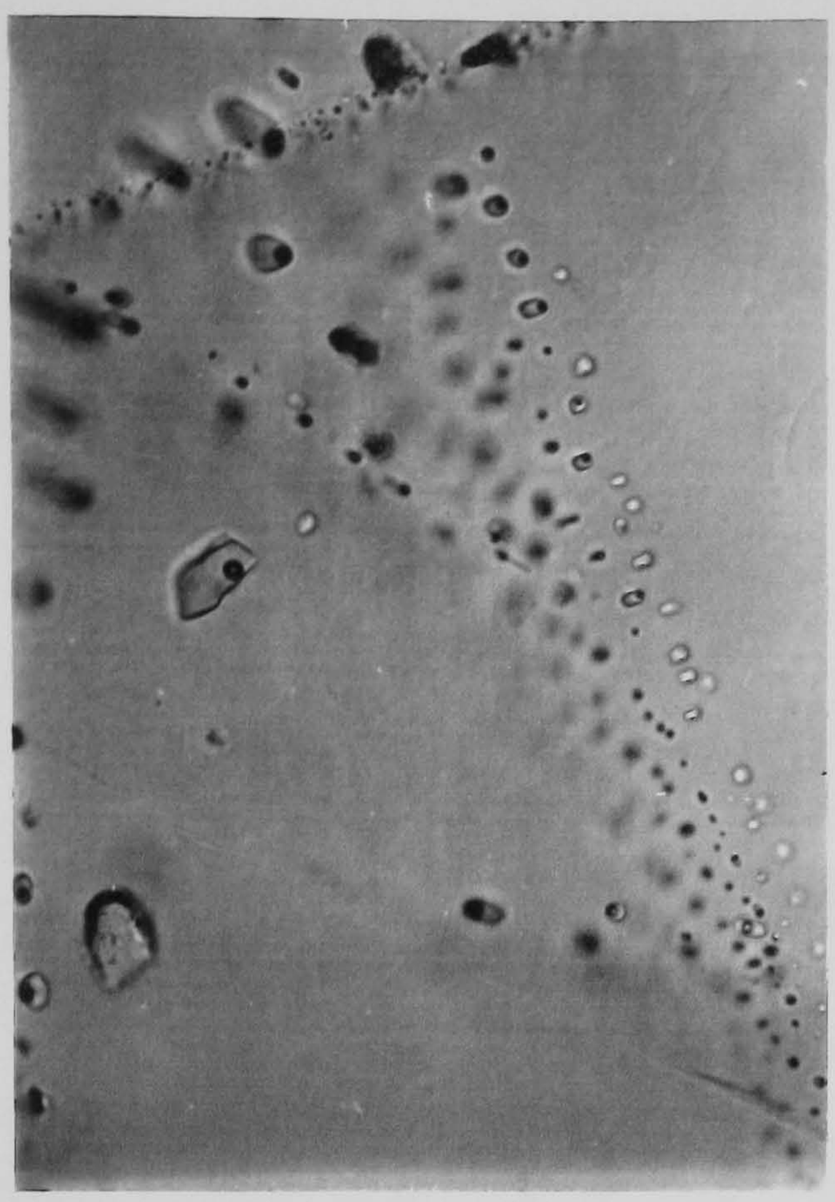


Plate 4.5b

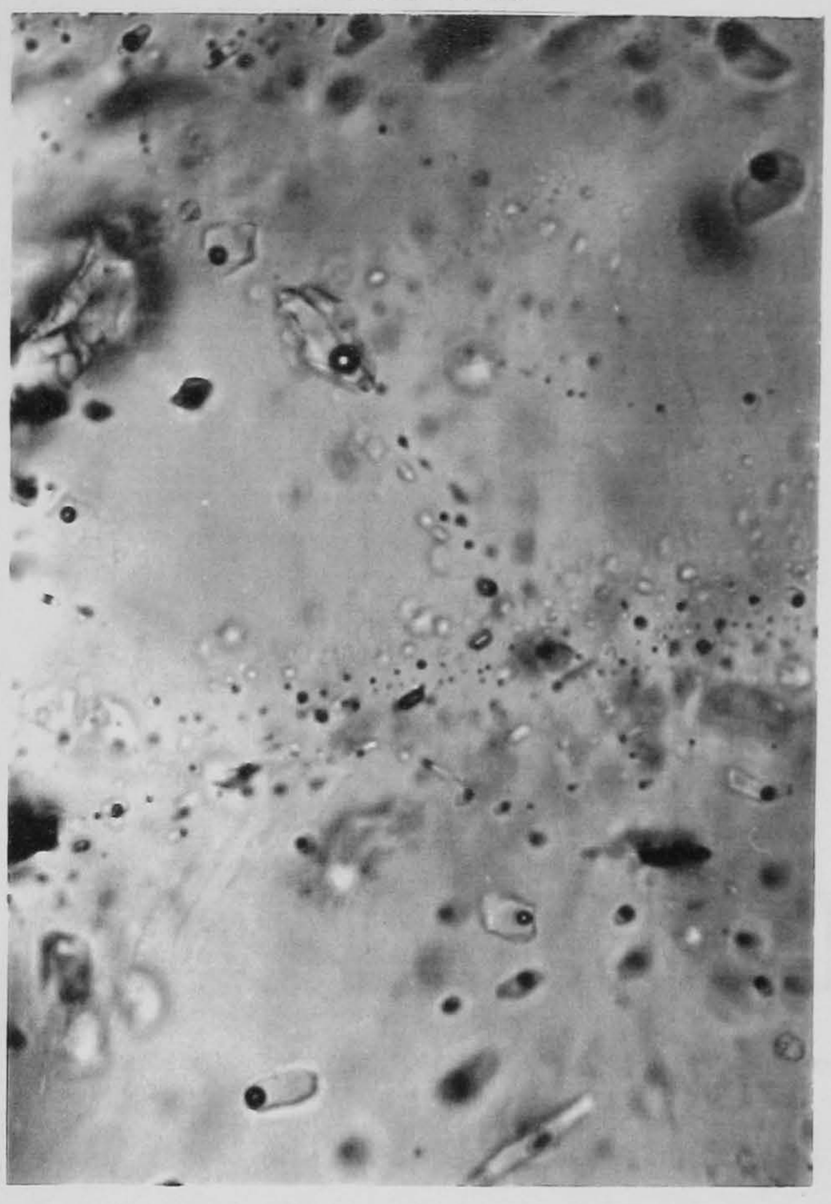


Plate 4.5c

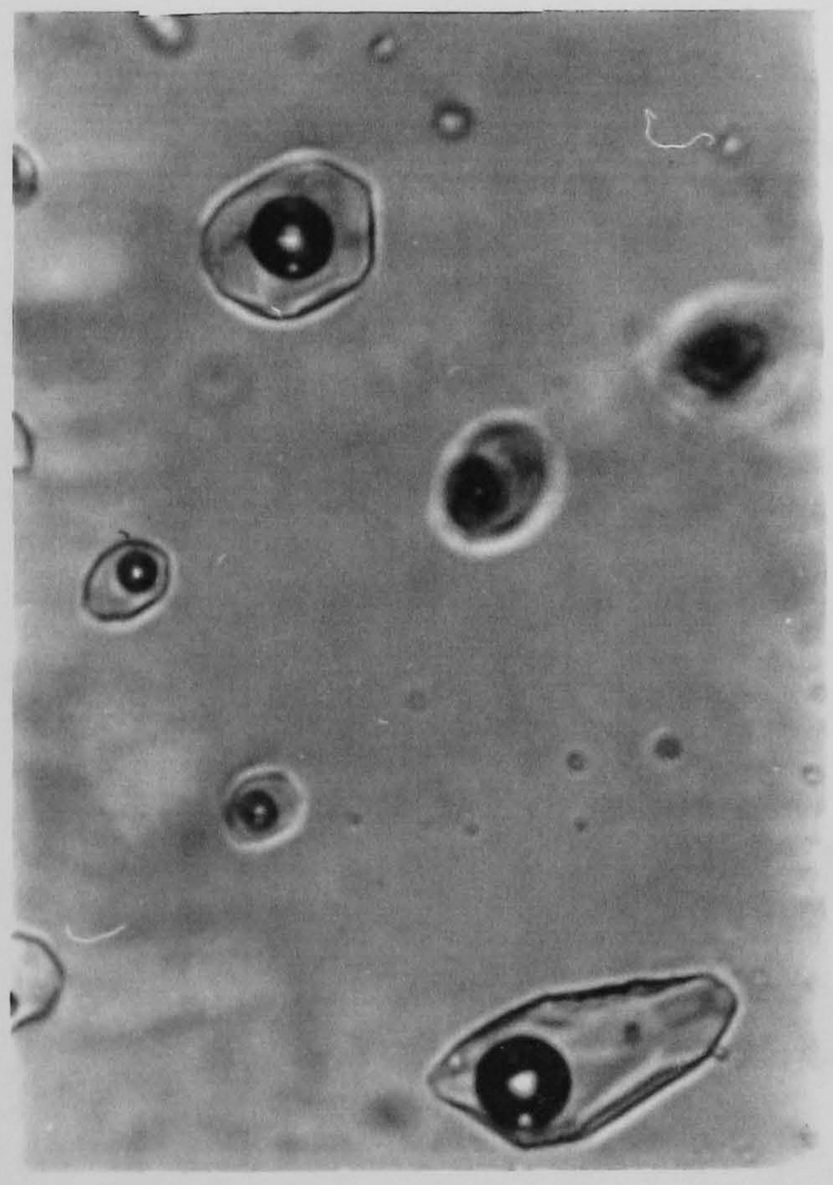
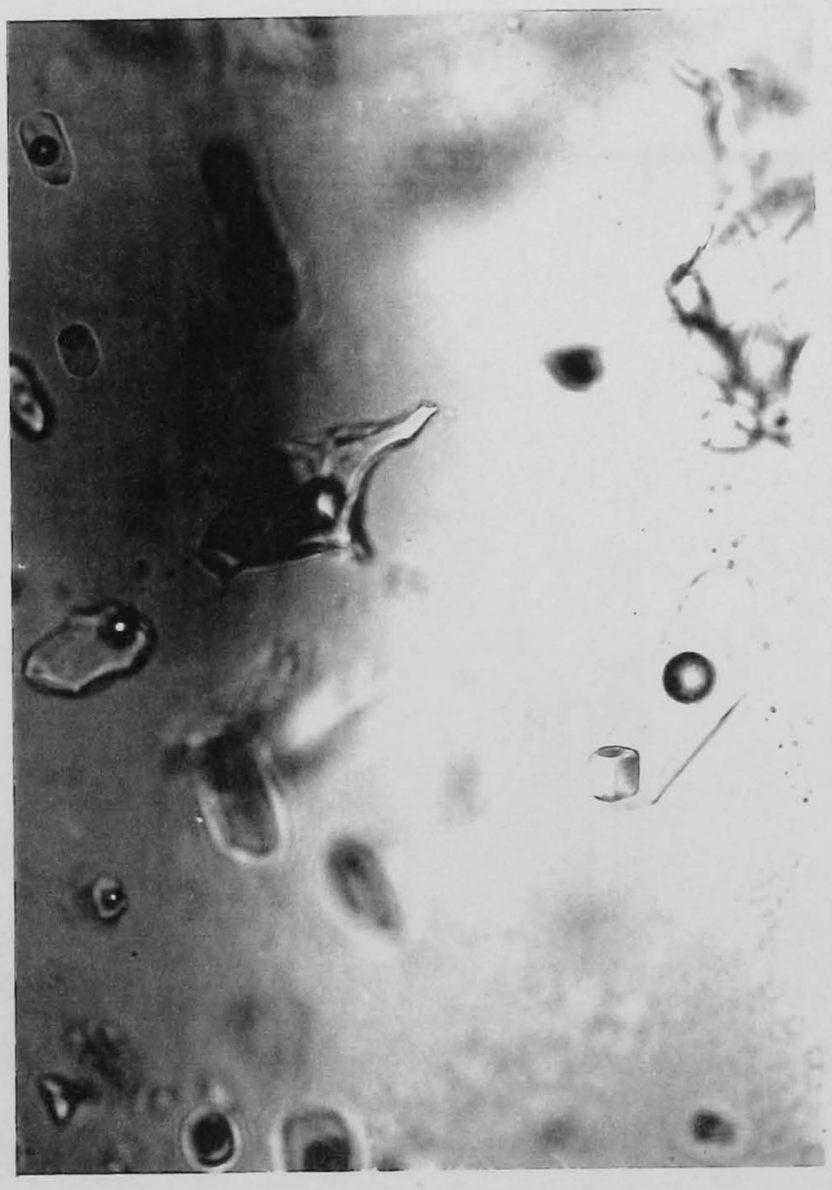
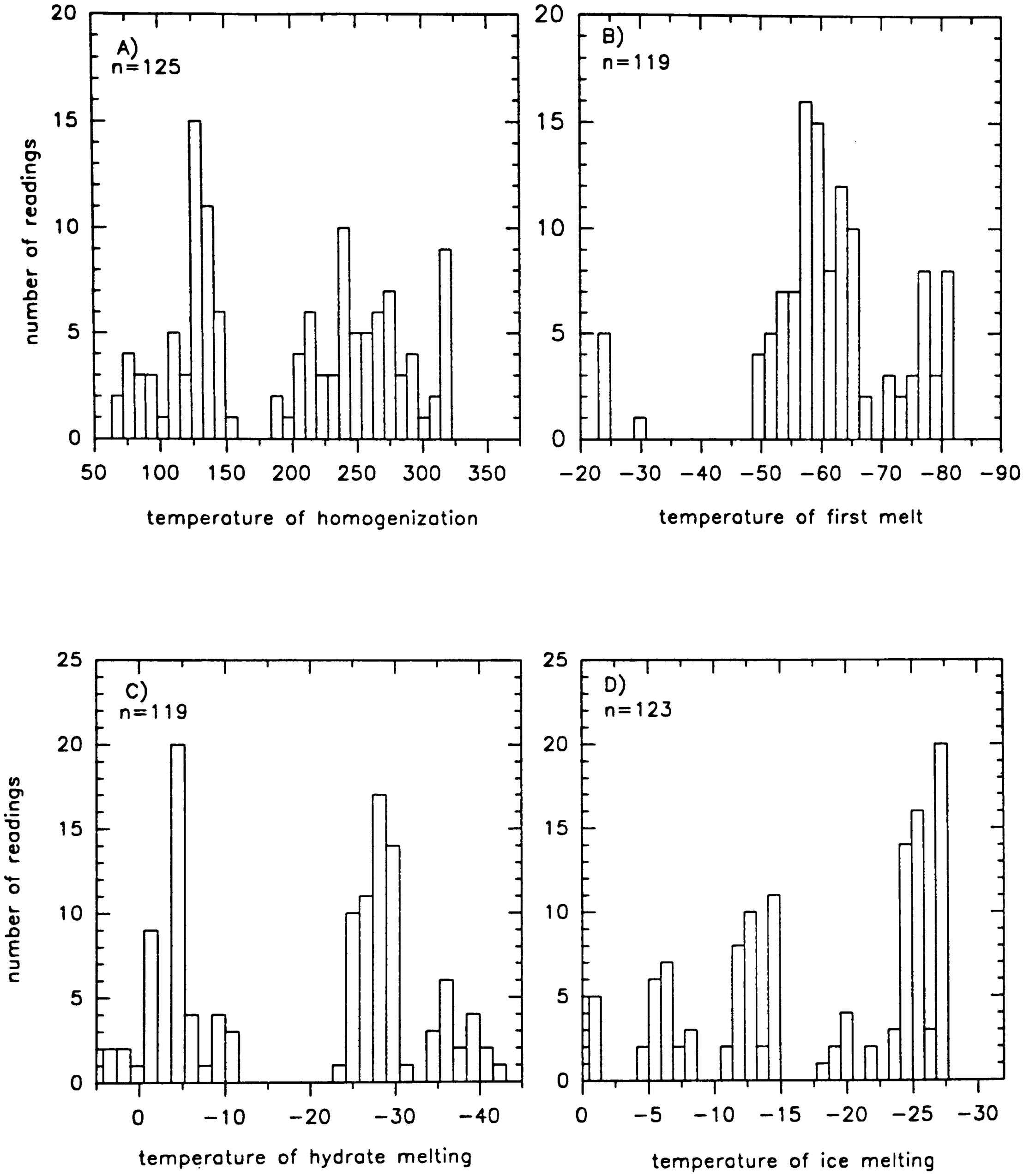


Plate 4.5d



Plates 4.5a-d. Fluid inclusions in fluorite from South Crofty, Cornwall.
4.5a. and 4.5b. Multiple generations of aqueous two-phase, liquid-vapour inclusions in fluorite from the late, chlorite stage of the paragenesis (field of view=360x270μm).
4.5c. Two-phase, aqueous liquid-vapour inclusions with variable degrees of fill, in fluorite from the chlorite stage (field of view=120x90μm).
4.5d. Three-phase, liquid-vapour-solid fluid inclusion in fluorite from the early pegmatite stage (field of view=120x90μm)



Figs.4.13.a-c. Histograms showing the frequency distribution of a) homogenization temperatures (T_H), b) first melting temperatures (T_{FM}), c) hydrate ($T_M h$) and d) ice melting (T_{LM}) temperatures of fluid inclusions in fluorite samples from the late,chlorite stage of mineralization at South Crofty, Cornwall.

The nature of the fluids will be examined in more detail in the following section with the aid of temperature-salinity relationships and $CaCl_2$/NaCl ratios. Of major interest for the purposes of the present study is the low temperature component which shows similarities, in terms of both temperature and salinity, to the Alston block fluids.

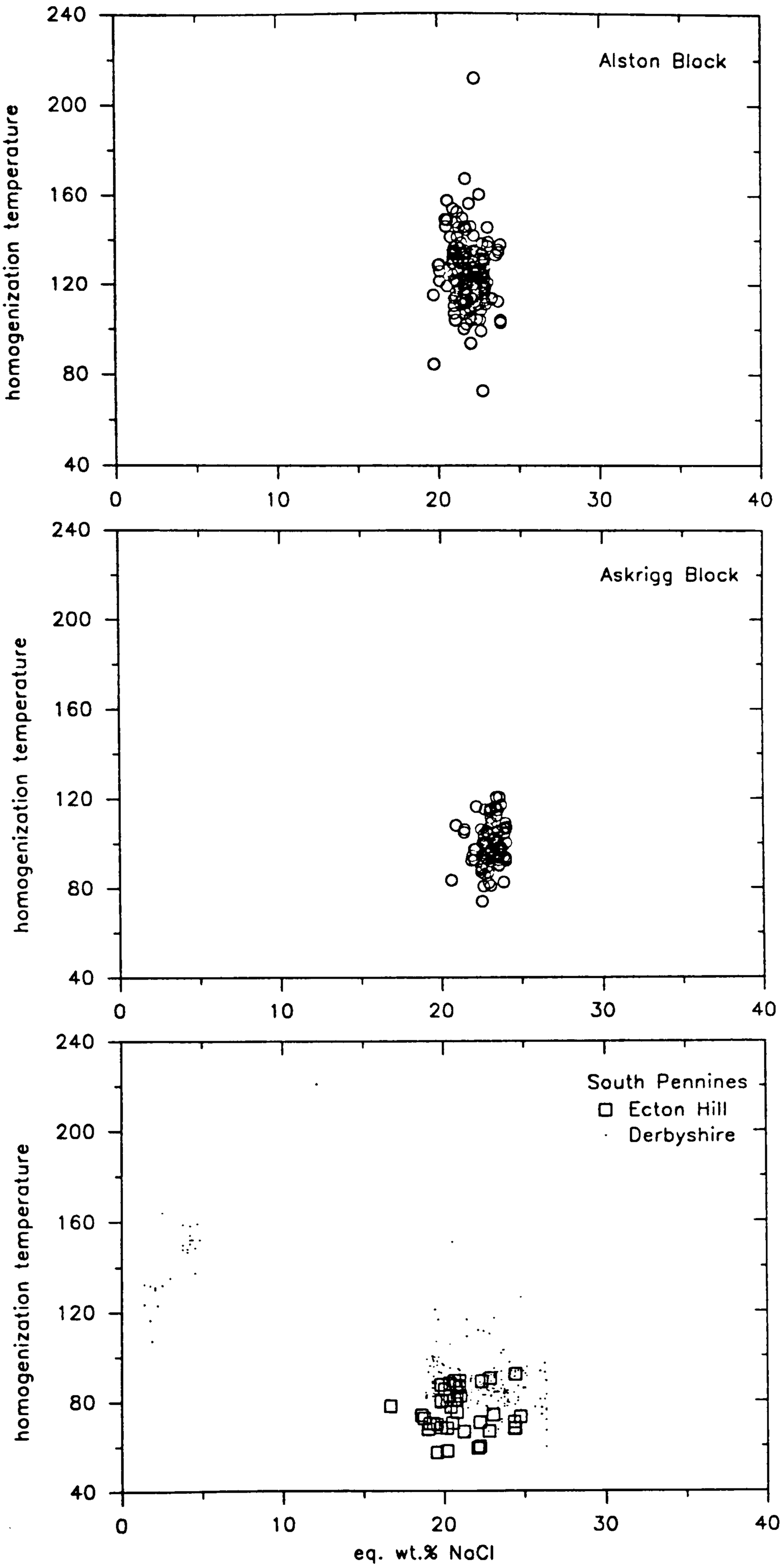
4.5.4. Temperature-Salinity Relationships

Last melt temperatures (ice or hydrate) are converted to total salinity values which are conventionally reported as equivalent weight% NaCl (i.e. the amount of NaCl which produces the corresponding depression of the freezing point). The equation relating the depression of the freezing point with total salinity for the system H_2O-NaCl is given Potter et. al. (1978). Paired homogenization and total salinity values are widely used to construct bivariate temperature-salinity plots as a means of tracing the evolution of the inclusion fluids. Mixing, cooling and boiling can be inferred from trends on these bivariate plots which are derived from T_H and T_{LM} measurements of individual inclusions (Shepherd et. al. 1985a).

i) Pennine samples

Paired homogenization temperature-salinity values for the three Pennine orefields are presented in bivariate plots in Fig.4.14. All fluids (apart from the low salinity component in Derbyshire) are characterized by high salinities, constrained by moderately narrow limits between 18 and 25 eq. wt. %NaCl. The main difference lies in the homogenization temperatures which show a characteristic decreasing trend from the North to the South orefields.

As mentioned in the previous sections, the only diversion from the overall low temperature-high salinity trend is found in a small number of inclusions from two samples from the Northern part of the Derbyshire orefield (Dirtlow Rake and Blue John Cavern). These fluids have relatively high temperatures (between 120-160°C) and very low salinities in the range between 1-5% eq.wt NaCl. Such fluids were found to be in close association with hydrocarbon-bearing inclusions (Moser et. al. 1992). Mixed hydrocarbon-low salinity, aqueous inclusions were also observed (Moser et. al. 1992). However, as shown by the dominance of high salinity fluids throughout the Derbyshire orefield and also, by the exclusive presence of high salinity fluids only, in sphalerite, it can be assumed that the fluids responsible for primary base metal mineralization belong to the low temperature-high salinity group.



Figs.4.14.a-c Bivariate plots showing the homogenization temperature-salinity relationships of fluid inclusions in samples from the three Pennine orefields (Alston, Askrigg, Derbyshire) and Ecton Hill.

Also important is the fact that the T_H-salinity patterns of the Ecton Hill fluids are indistinguishable from the dominant high-salinity, low-temperature fluids of Derbyshire. Thus, from the data presented so far, no distinction can be made between the fluids responsible for the lead-zinc mineralization in the Pennines and the Cu-dominant mineralization at Ecton Hill. A similar evolution might therefore be postulated for both the Pennine and Ecton Hill fluids. However, further comparisons will be made in the following section which is devoted to the determination of the Ca/Na ratios of the fluids.

ii) Llanharry samples

Temperature-salinity relationships of the Llanharry fluids are presented in Fig.4.15 where the T_H-salinity values of the Ecton Hill inclusions are also shown for comparison. No major trends can be distinguished at Llanharry; furthermore as noted previously, the small number of readings does not permit many assumptions. As can be seen from Fig.4.15, a relatively restricted number of inclusions have salinities lower than 10 eq%wt.NaCl, and they may be interpreted as a result of a minor dilution event. The majority of the values lie in the low-temperature, moderate-salinity field similarly to the Derbyshire and Ecton Hill fluids.

iii) South Crofty

Fluid inclusions in samples from the late, chlorite stage of mineralization at South Crofty, exhibit much more complicated character. The temperature-salinity relationships are shown in Fig.4.16. A similar trend to that defined by Farmer (1991) is also seen here. Homogenization temperatures cover the whole spectrum between 70 and 350°C whereas salinities are in the range between 5 and 27 eq.wt%NaCl. One component is characterized by low temperature (<200°C) and moderate to high salinity of 10 to 26 eq wt%NaCl. The second, well defined group is that of higher temperatures (200-350°C) and lower salinities, between 5 and 11eq.wt%NaCl. As can be seen from Fig.4.16, the rest of the high temperature inclusions, cover a wide salinity range, between 11 to 25 eq. wt%NaCl.

As far as the high temperature fluids are concerned two main models were proposed by previous authors to explain the wide variation of salinity values. The earliest model (Jackson et. al. 1989, Shepherd et. al. 1985b) involved mixing of separate fluids (evolved magmatic and heated meteoric water) and required the presence of large scale convection cells to be operating in the area. A second quite different model based on calculations by Bodnar and Cline (1990) has also been proposed. These authors suggested that temperature-salinity relationships, such as those illustrated by the South Crofty samples, can be

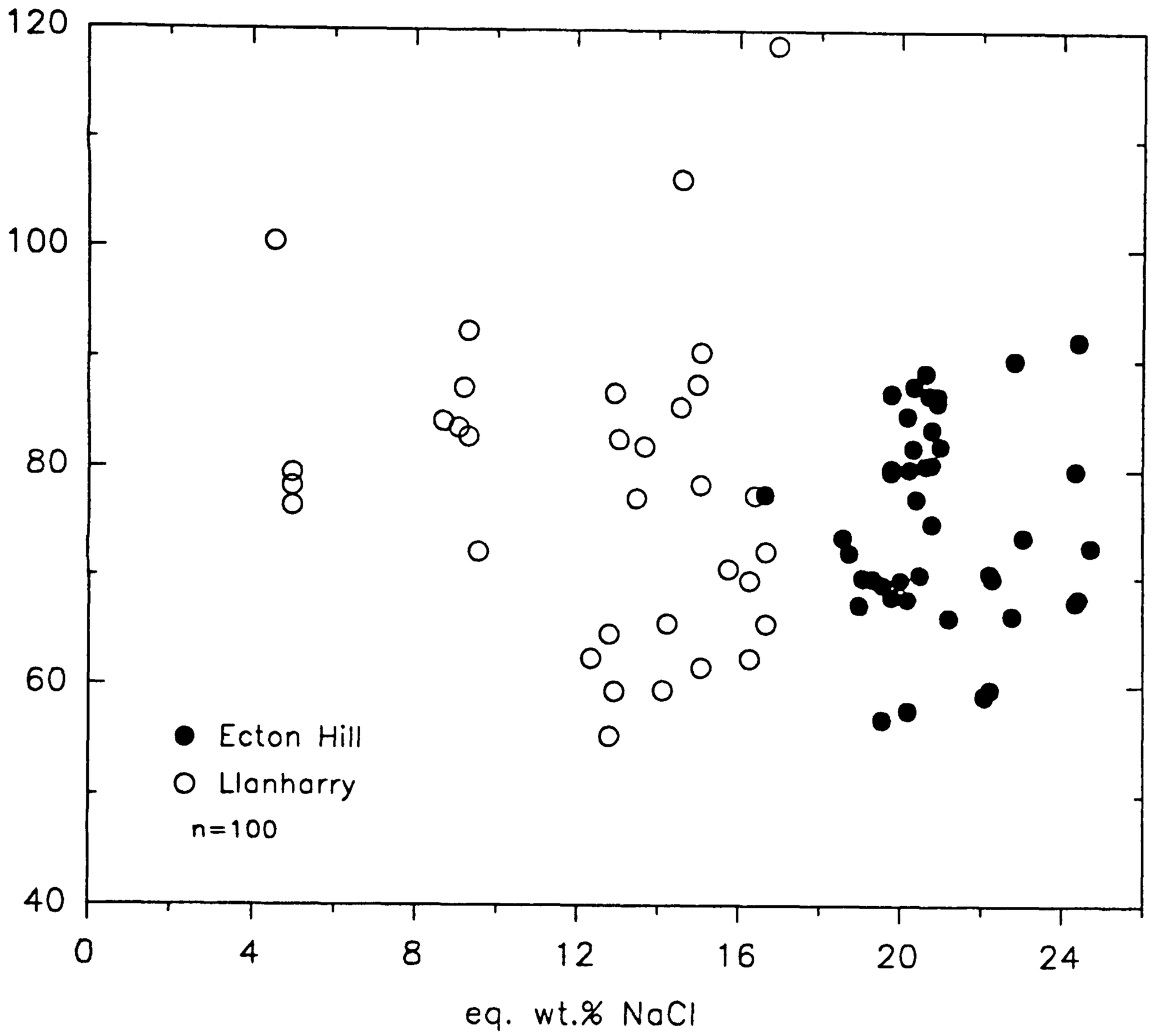


Fig.4.15. Bivariate plot showing the homogenization temperature-salinity relationships of fluid inclusions in samples from Llanharry, South Wales. Data from the Ecton Hill fluid inclusions are also shown for comparison.

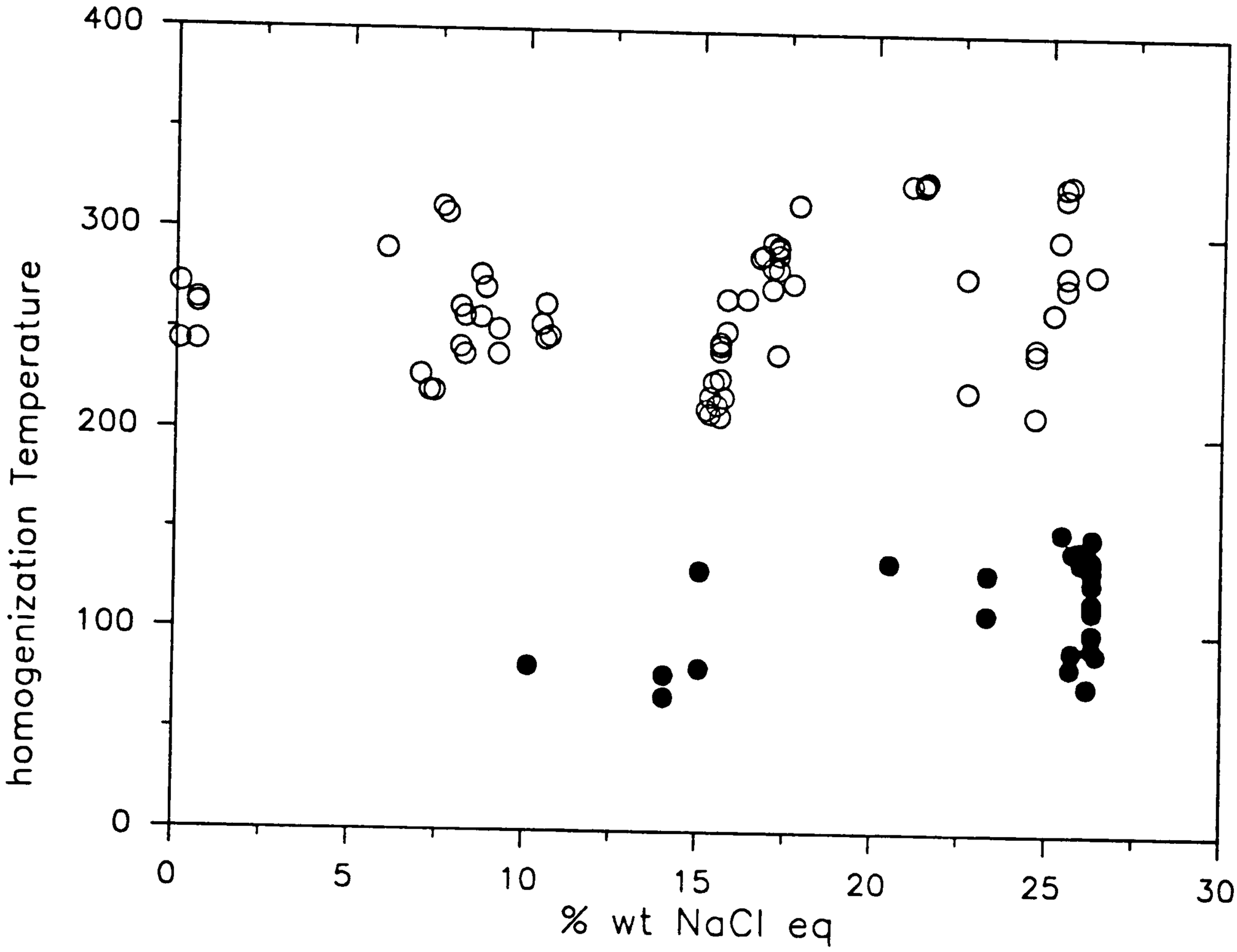


Fig.4.16. Bivariate plot illustrating the relationship between homogenization temperatures and total salinities of fluid inclusions in fluorite from the late, chlorite stage of mineralization at South Crofty, Cornwall.

explained by fluid segregation during the crystallization of a hydrous granitic magma. Their study based on thermodynamic modelling of the albite-H_2O-NaCl system, has shown that in a melt containing 30%mole H_2O crystallizing at 832°C at 2kbar pressure, water saturation could be reached after 57% of the melt had crystallized. If water saturation is reached at pressures under 1.3kbar the first fluids exsolved from the magma will have high salinity (27%NaCl). As crystallization progressed there could be a reduction in salinity to the point that the last fluids exsolved would be almost pure water.

The applicability of the above model to the South Crofty fluids was examined by Farmer (1991). He pointed out that the likely crystallization depth of the Cornish plutons (<5km) could be sufficient to permit initiation of fluid exsolution from a crystalizing melt at lithostatic pressures in excess of 1.3kbar. Thus, the exsolution model of Bodnar & Cline (op. cit.) could provide an alternative explanation of the temperature-salinity relationships in the South Crofty fluids. The model seems to be more applicable for the fluids associated with the early, high temperature stages of mineralization. As far as the late, chlorite stage is concerned, temperatures down to 200°C are not easily accounted for by the exsolution model (Farmer 1991).

In the chlorite stage of the paragenesis temperature-salinity patterns are quite different. As can be seen from Fig.4.16, the dominant trend is one of increasing salinity with decreasing temperature. This trend is more readily explained by the mixing of two fluids, a process that is also supported by the variation in eutectic temperatures. Furthermore, mixing models have been also used in the past to interpret fluid inclusion data from similar vein parageneses elsewhere in Cornwall (Shepherd et al 1985b). Overall, the low-temperature population has in terms of both temperature and salinity many similarities with the Pennine inclusions, as well as, to fluids in quartz-vein samples associated with Pb-Zn-dominant mineralization in SW England, examined by Alderton (1978).

4.5.5. $NaCl/CaCl_2$ ratios

Following the procedure outlined in section 4.4, paired readings of the melting temperatures of both ice and hydrohalite were obtained from a large number of individual inclusions. Phase changes marking the T_{FM}, T_Mh and T_{LM} temperatures are illustrated in a series of photographs in Plates 4.6a-d and 4.7a-c. These paired measurements are plotted in a three phase H_2O-NaCl-$CaCl_2$ (Borisenko 1977, Oakes et.al. 1990) diagram and lead to the estimation of the $NaCl/CaCl_2$+NaCl ratio of the fluid. As mentioned in section 4.4, the more recent phase diagram by Oakes et. al. (1990) is used in the present study.

Plate 4.6a

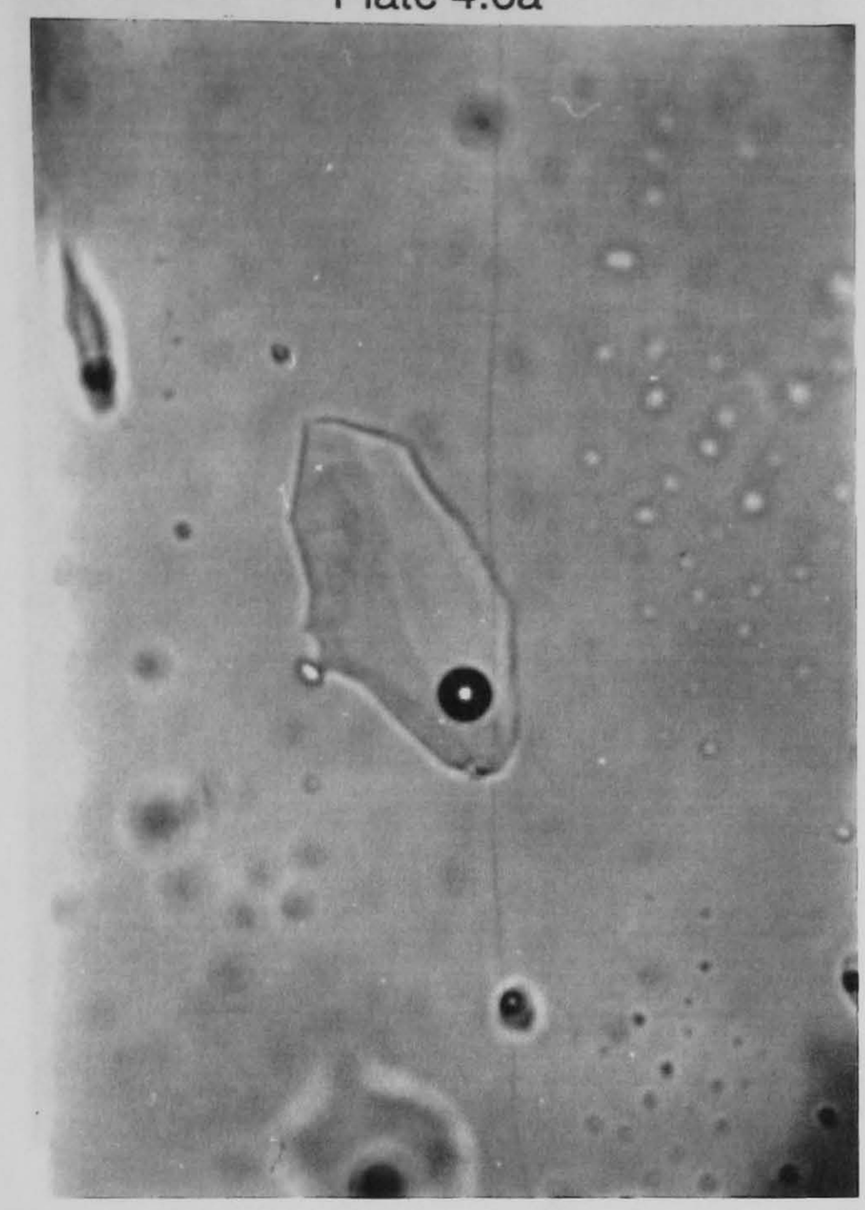


Plate 4.6b

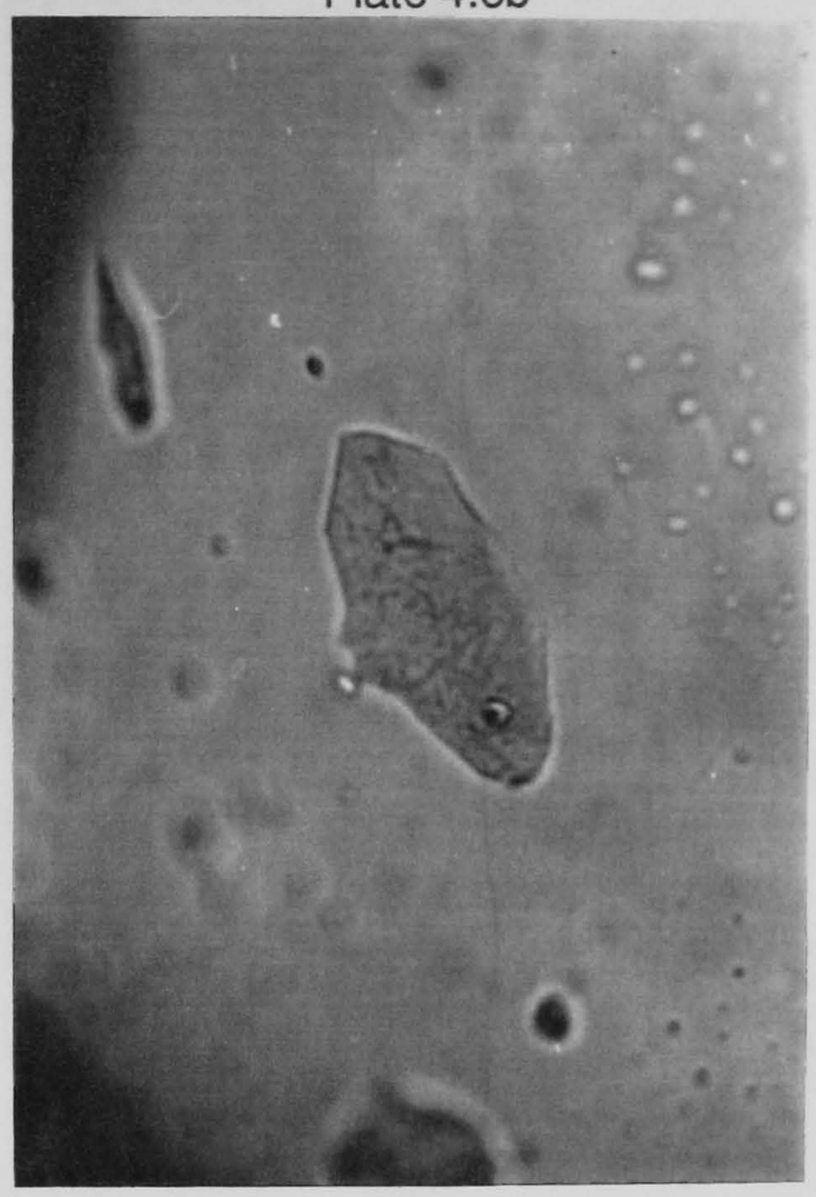


Plate 4.6c

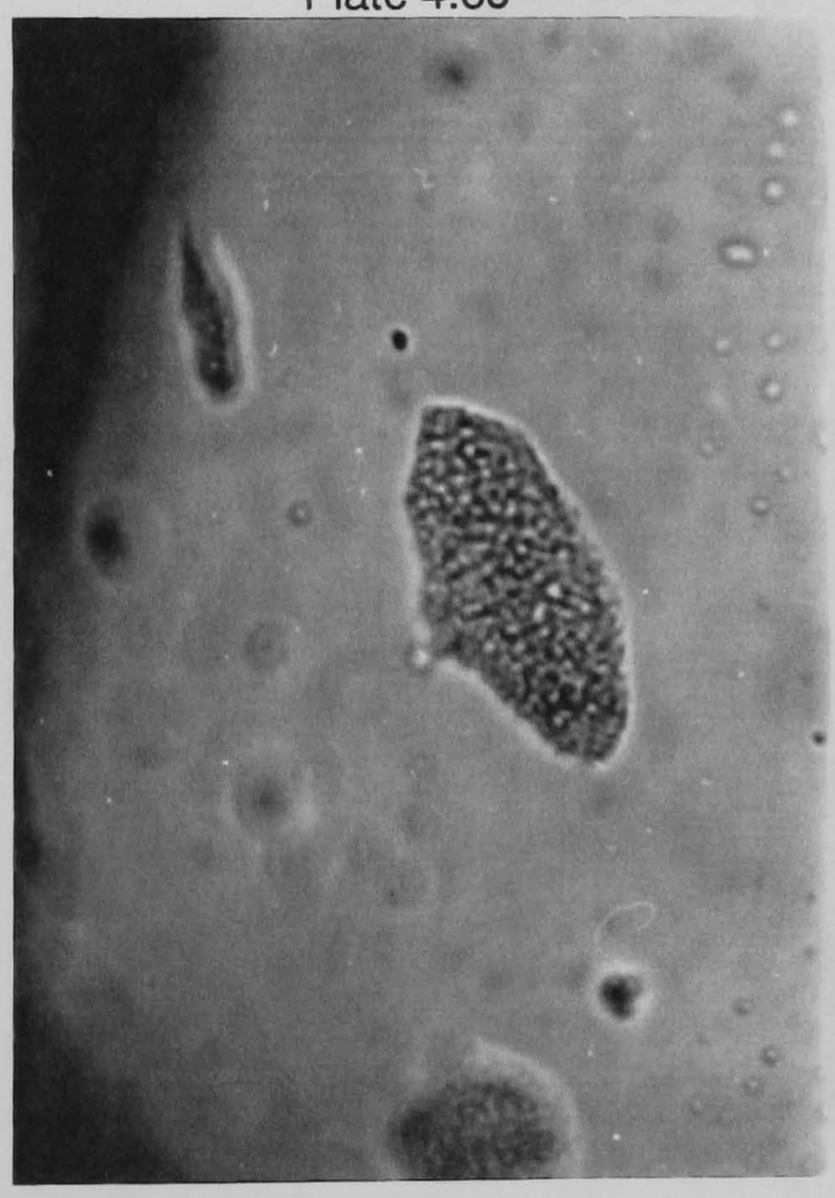
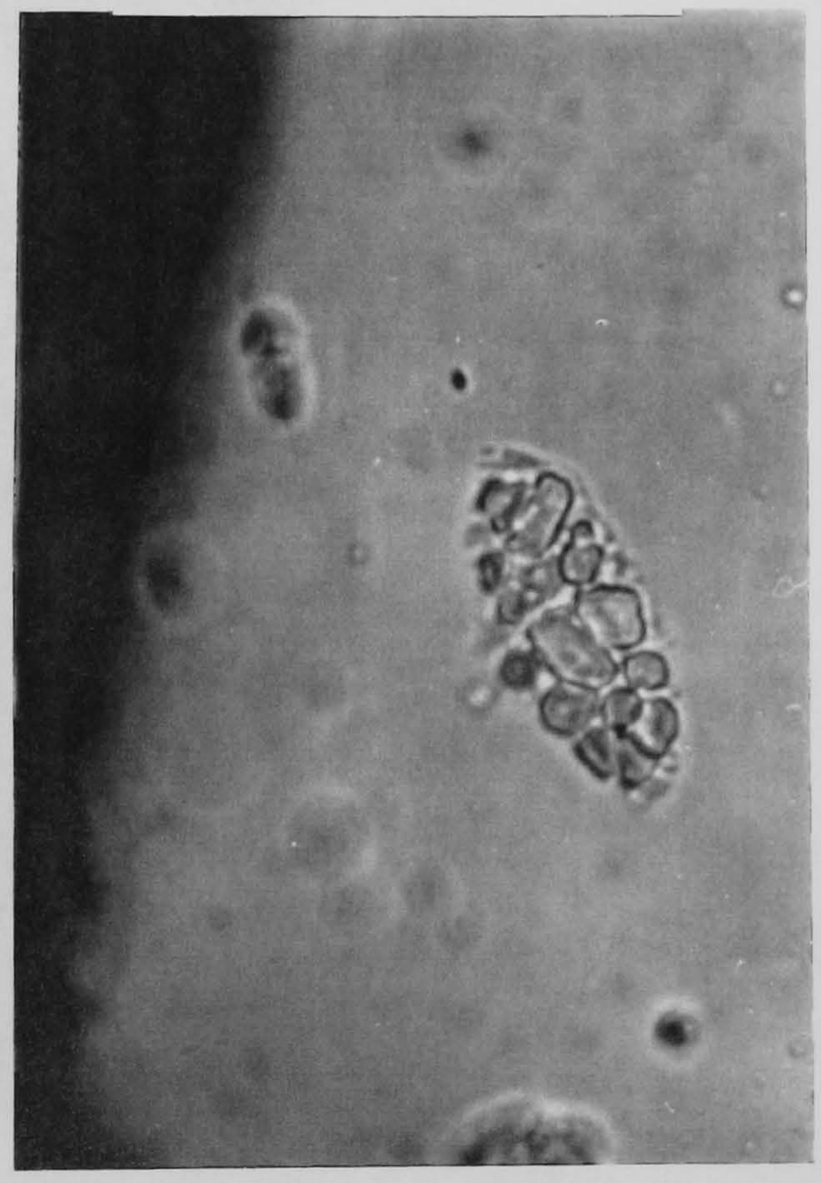


Plate 4.6d



Plates 4.6a-d. Phase changes observed in fluid inclusions during a typical freezing-heating cycle (field of view=120x90μm)
4.6a. T=20°C,(Liquid+vapour)
4.6b. T=-90°C, inclusion completely frozen
4.6c. T=-59°C, a few degrees above T_{FM} (Liquid-vapour+solid)
4.6d. T=-30°C, massive melt (Ice+Hydrohalite+Liquid)

Plate 4.7a

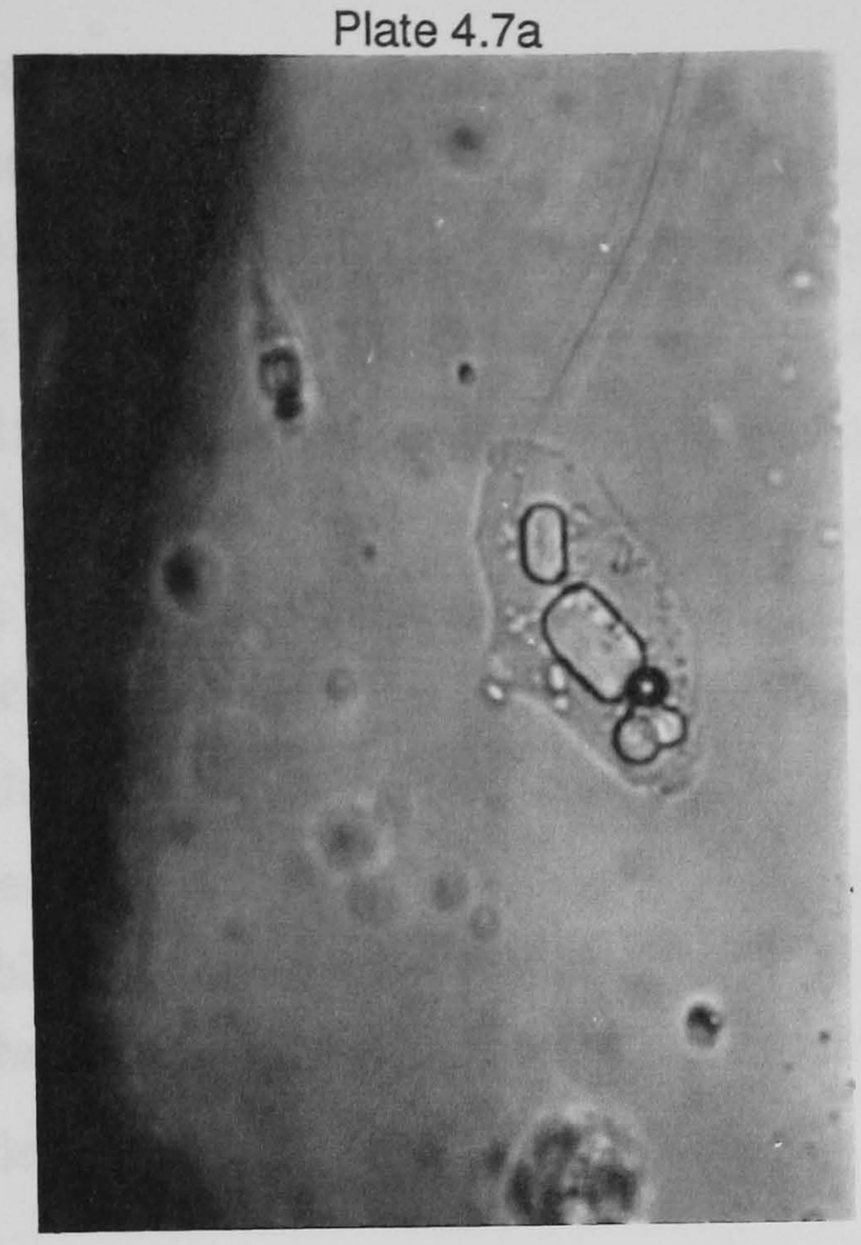


Plate 4.7b

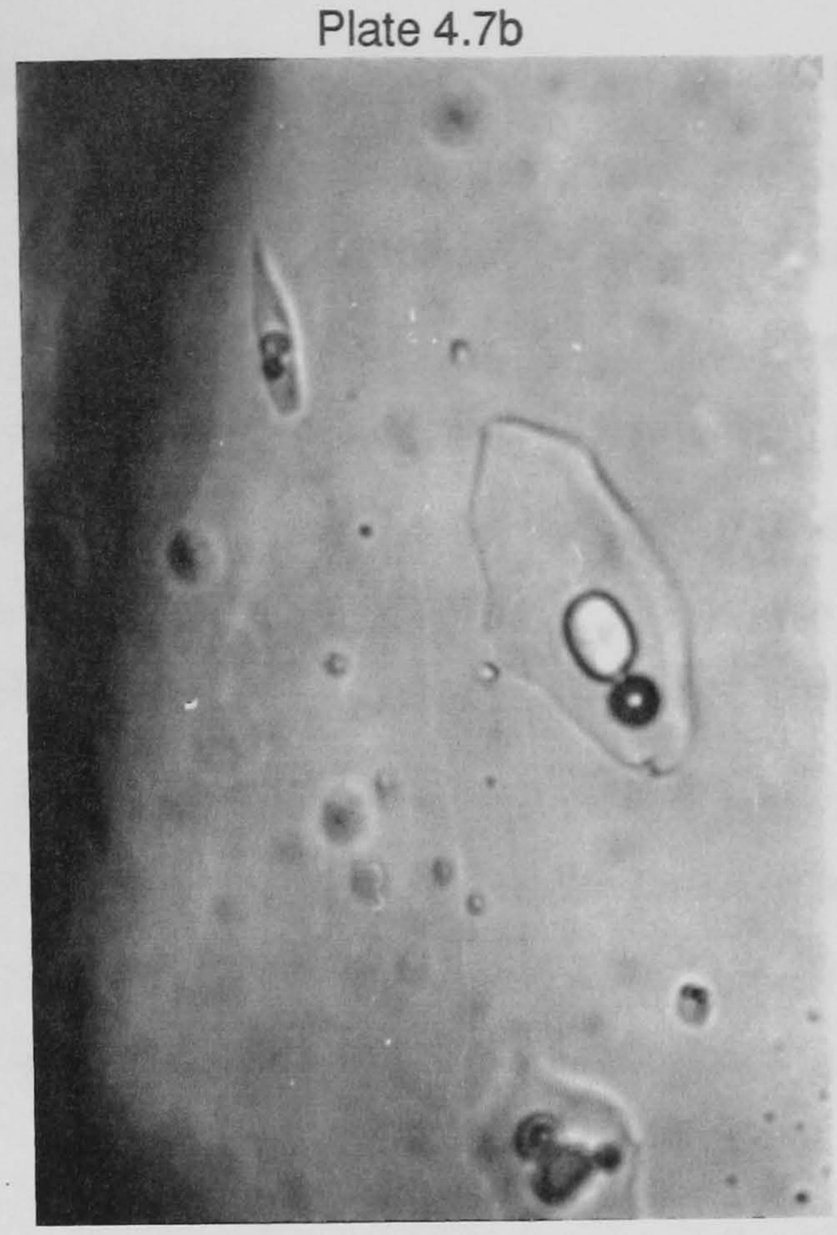
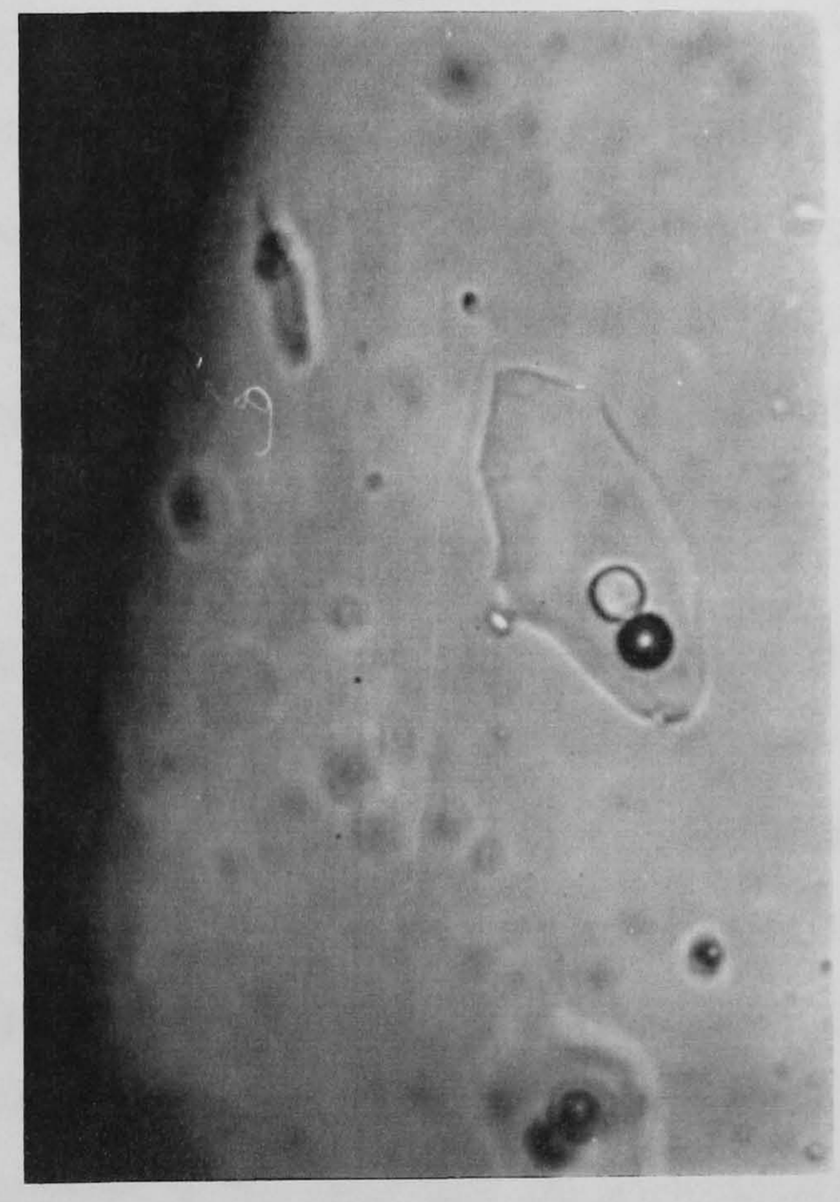


Plate 4.7c



Plates 4.7a-c. Phase changes during heating-freezing cycle (continued)
(field of view=120x90μm)
4.7a. T=-26°C, temperature approaching $T_M h$, (ice+hydrohalite+liquid+vapour)
4.7b. T=-24°C, $T_M h$, (ice+liquid+vapour)
4.7c. T=-20°C, very close to T_{LM} (ice+liquid+vapour)

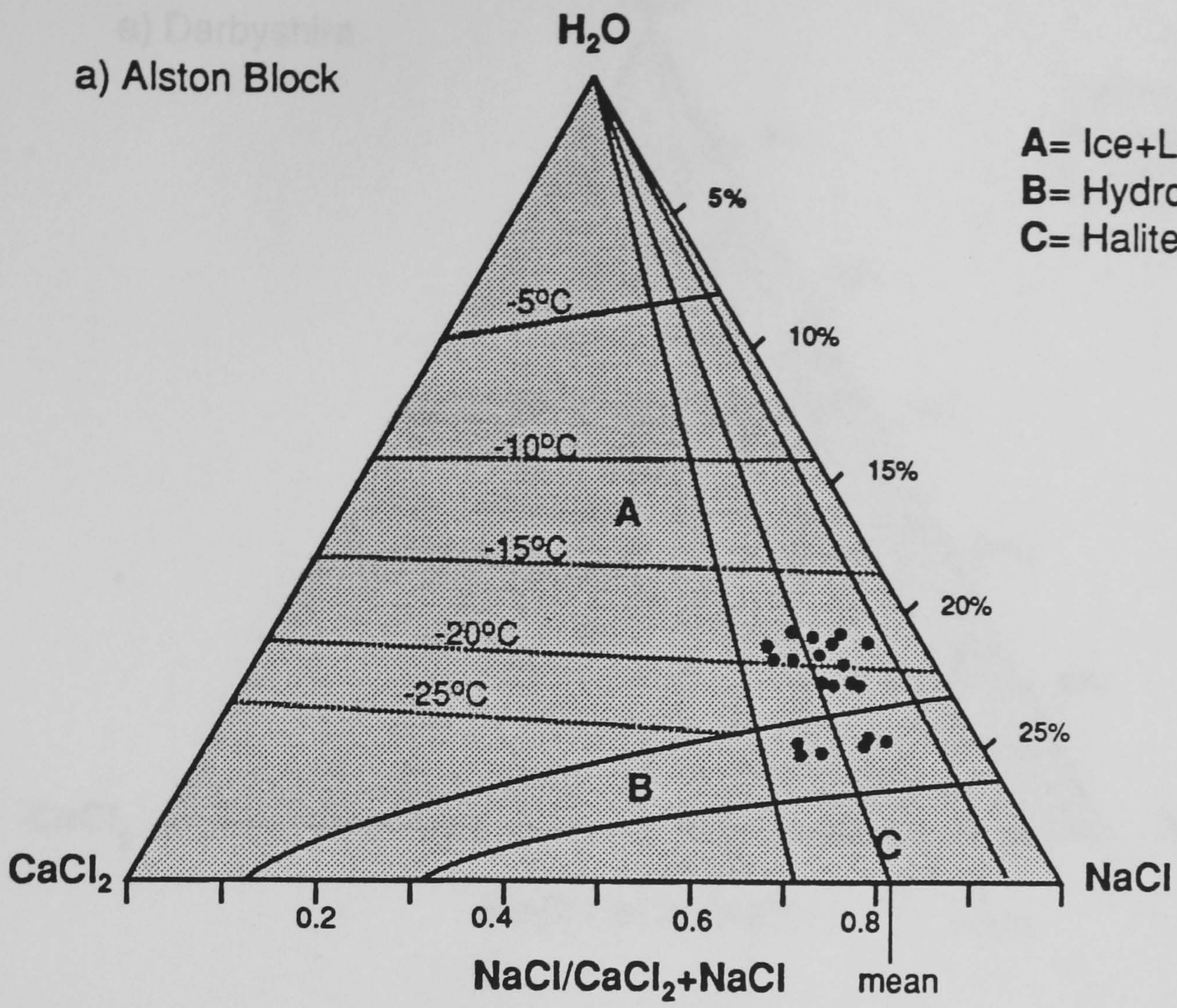
Paired melting temperatures of ice and hydrohalite from samples of the North Pennines (Alston and Askrigg) are shown in Fig.4.17a and 4.17b. Both groups of fluids exhibit similar $NaCl/CaCl_2+NaCl$ weight ratio ranges in between 0.65-0.96 for Alston and 0.75-0.96 for Askrigg. These values are higher than the ones reported previously by Shepherd et al (1982). Underestimation of the temperature of hydrohalite melt temperature is a common problem encountered in most microthermometric studies. As the melting of hydrohalite is very sensitive to even small changes in temperature, high heating rates can cause such an underestimation of the T_Mh reading. This problem was also encountered in the early stages of the present study and resulted in grossly inaccurate estimates of $NaCl/CaCl_2$. Much lower heating rates (down to 0.2°C/min) were then employed in order to overcome this problem. Furthermore, the use of the updated phase diagram by Oakes et al (1990) also led to the estimation of higher $NaCl/CaCl_2$ ratios than the ones obtained from the diagram by Borisenko (1977)

Values from the Derbyshire fluids are also in broad agreement with the North Pennine values. $NaCl/CaCl_2+NaCl$ ratios are in the range between 0.70-0.96, and for Ecton Hill in the range between 0.60-0.95 and a mean of 0.80 (Figs.4.18a, 4.18b). Fluids from the Llanharry Fe-ore are slightly enriched in Ca compared to those of the Pennines. They show a mean value of 0.65 and a range between 0.74-0.50 (Fig.4.19a). The spread of values is relatively large but the majority of the readings fall around 0.60, similar to the Ecton Hill fluids.

The South Crofty fluorites exhibit a much more complicated distribution of Ca/Na ratios. The distribution of $NaCl/CaCl_2+NaCl$ ratios of the low-temperature fluids from the chlorite stage of mineralization is shown in Fig.4.19b. Most of the inclusions from that stage are high salinity fluids (23-26.3 eq wt. %NaCl) and are thus plotted on the hydrohalite + liquid, (C) field of the triangular phase diagram. Paired hydrohalite and ice melting temperature measurements lead to estimated $NaCl/CaCl_2$ ratios in the range between 0.62 and 0.95. Although the salinities are somewhat higher than those reported for the Pennine fluids (some Derbyshire fluids also display such high salinities), the corresponding $NaCl/CaCl_2$ ratios are comparable. This observation provides another line of evidence pointing out similarities of fluids present at the late stage fluorite mineralization at South Crofty with those of the Pennine orefields. As can be seen from Fig.4.19b, only a small number of inclusion fluids from this stage of the paragenesis at South Crofty, have salinities lower than 20%.

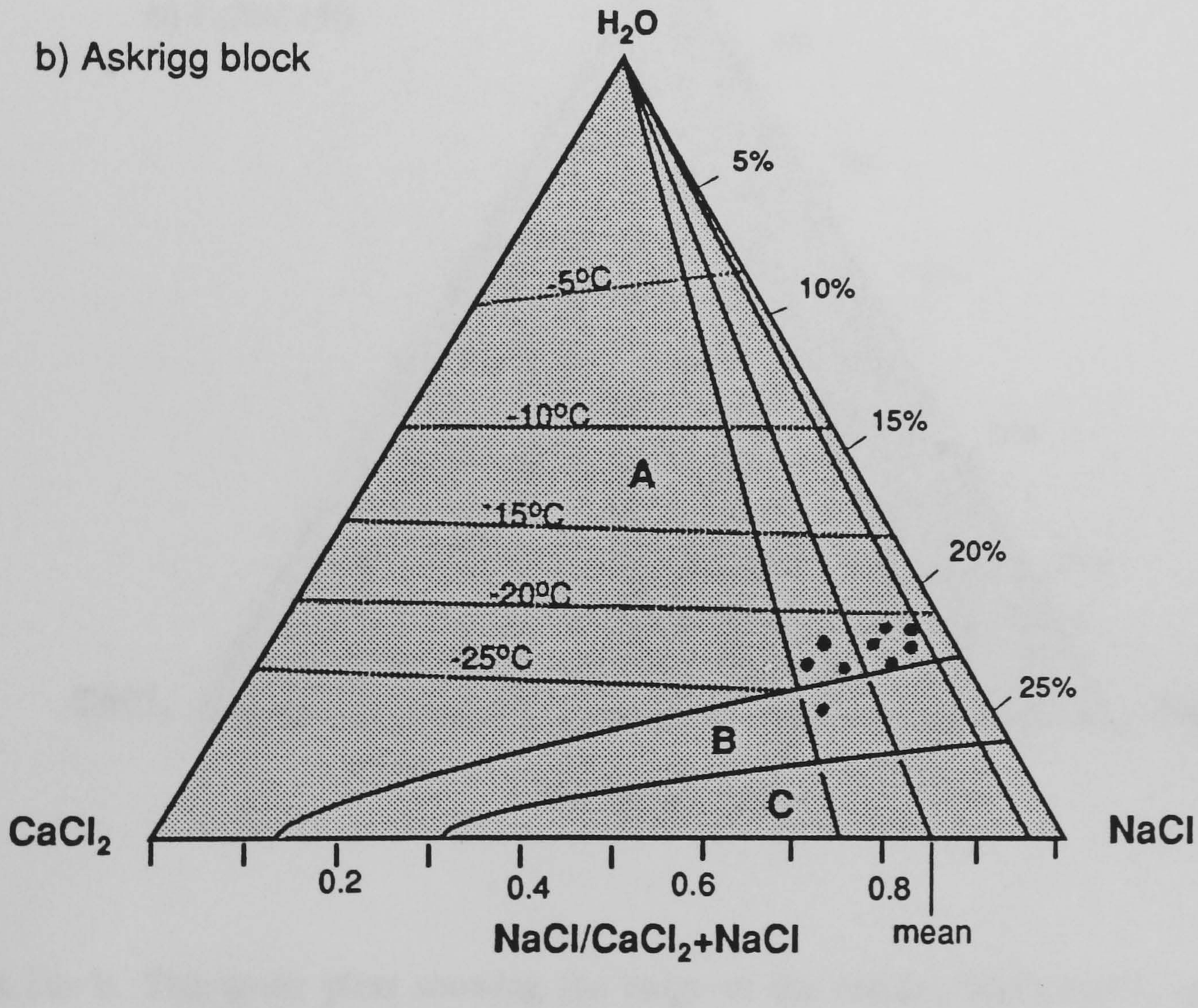
As became evident from the wide range of T_Mh and T_{LM} values, the high-temperature

a) Alston Block



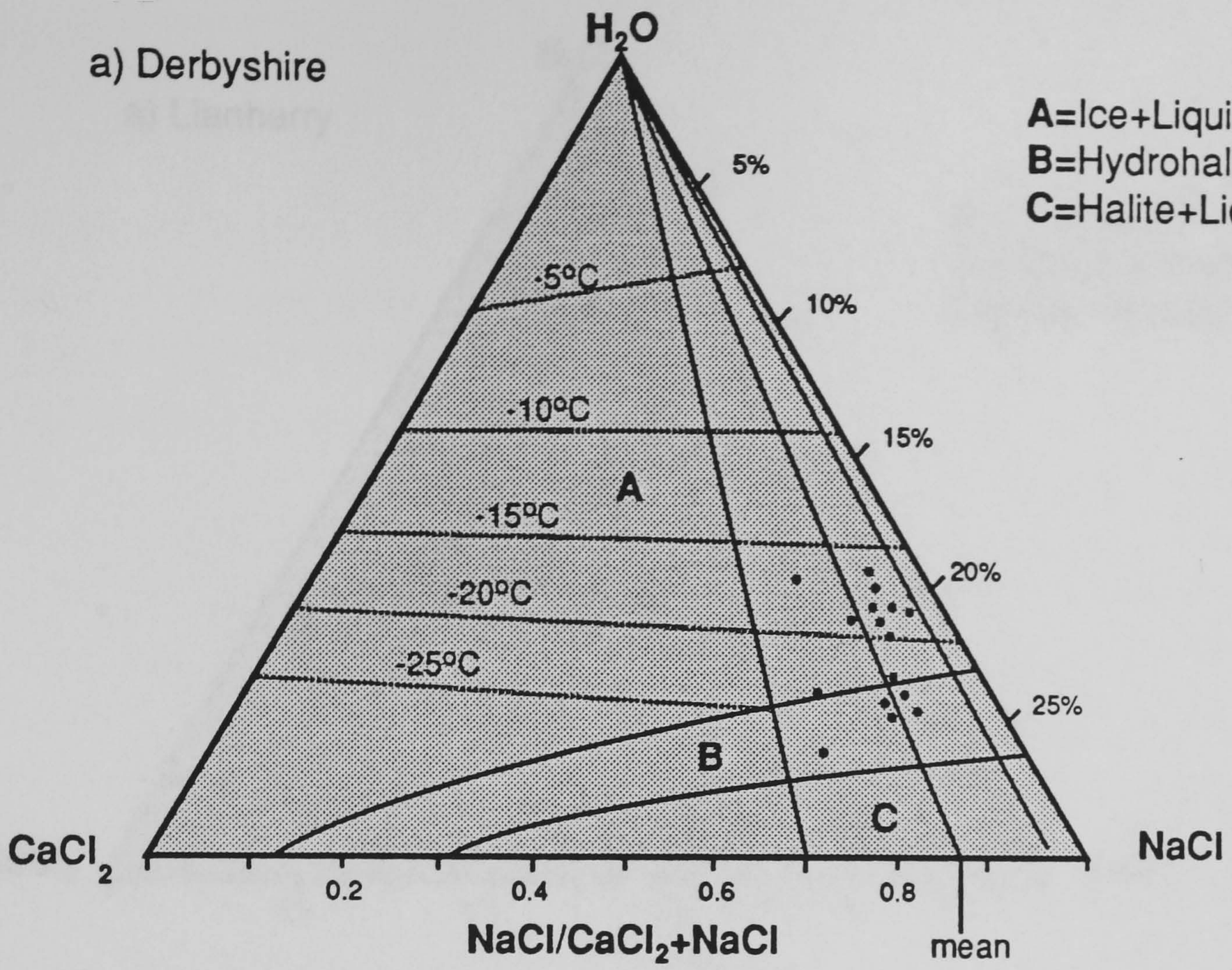
A= Ice+Liquid
B= Hydrohalite+Liquid
C= Halite+Liquid

b) Askrigg block



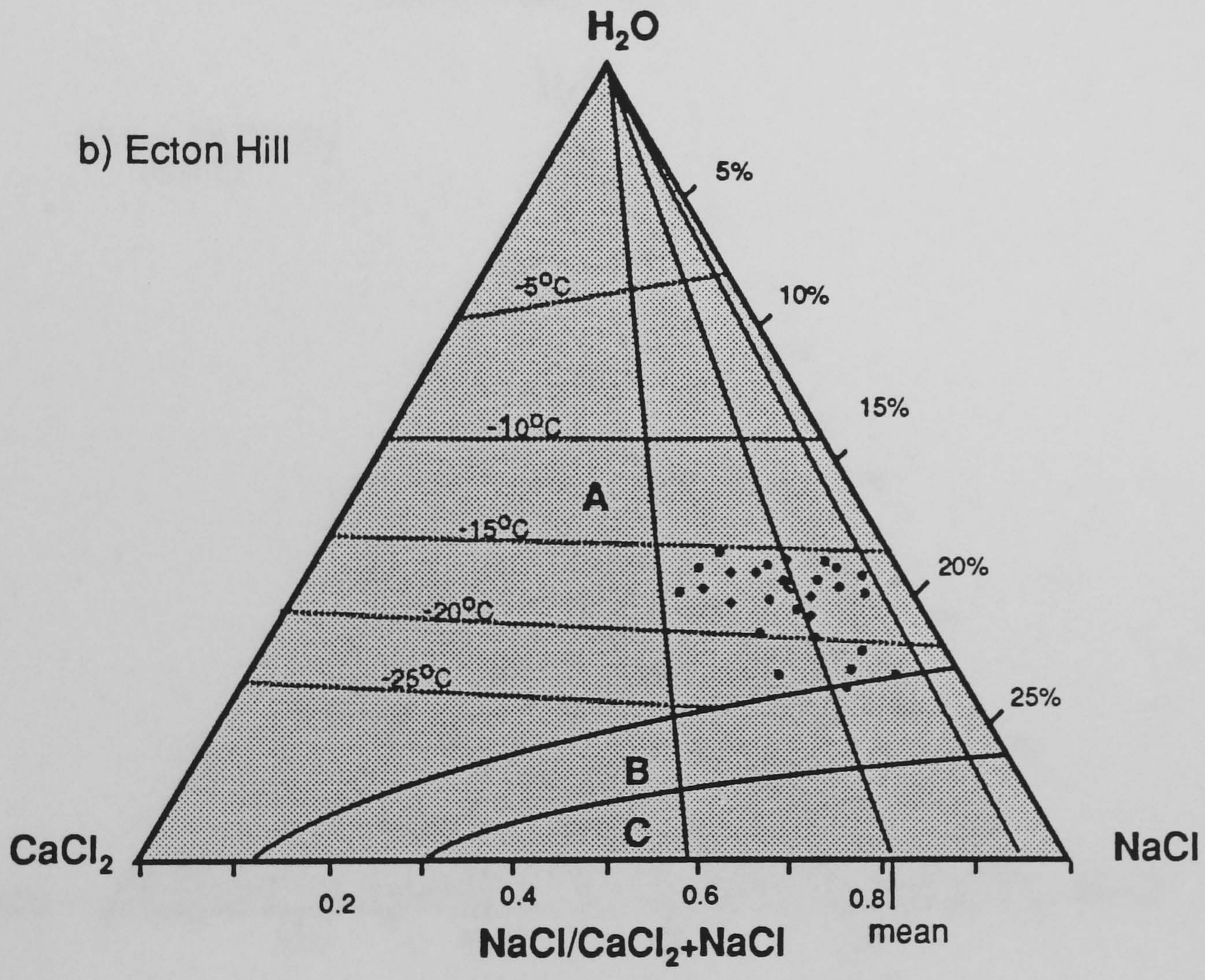
Figs.4.17a-b. Triangular plots showing the range of relative NaCl-$CaCl_2$ contents of fluid inclusions of the North Pennine orefields as estimated from paired $T_M h$-T_{LM} temperatures. Data points represent means of multiple readings on individual samples. (all data are listed in Appendix B). Isotherms for the H_2O-NaCl-$CaCl_2$ system after Oakes et. al. (1990).

a) Derbyshire

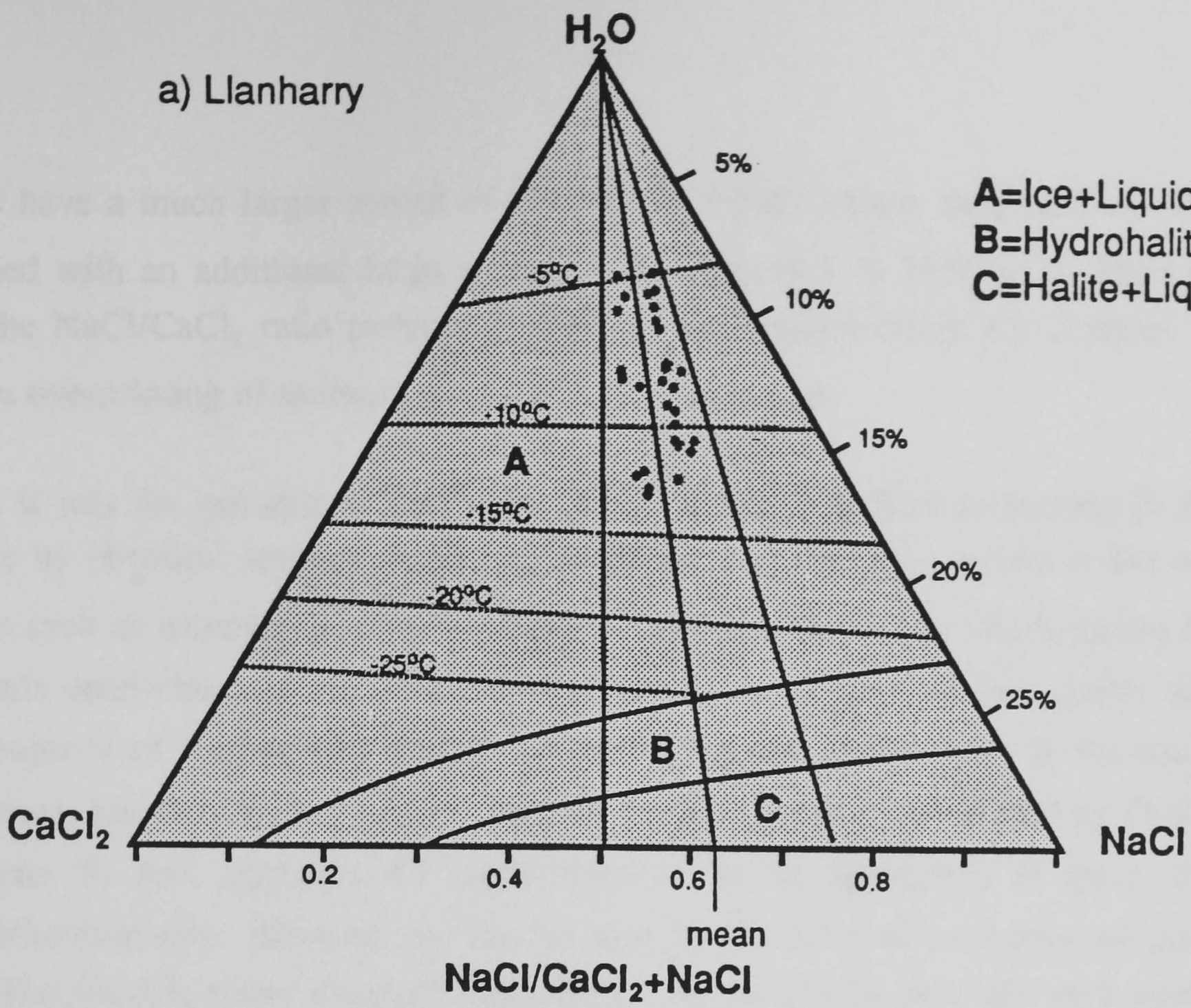


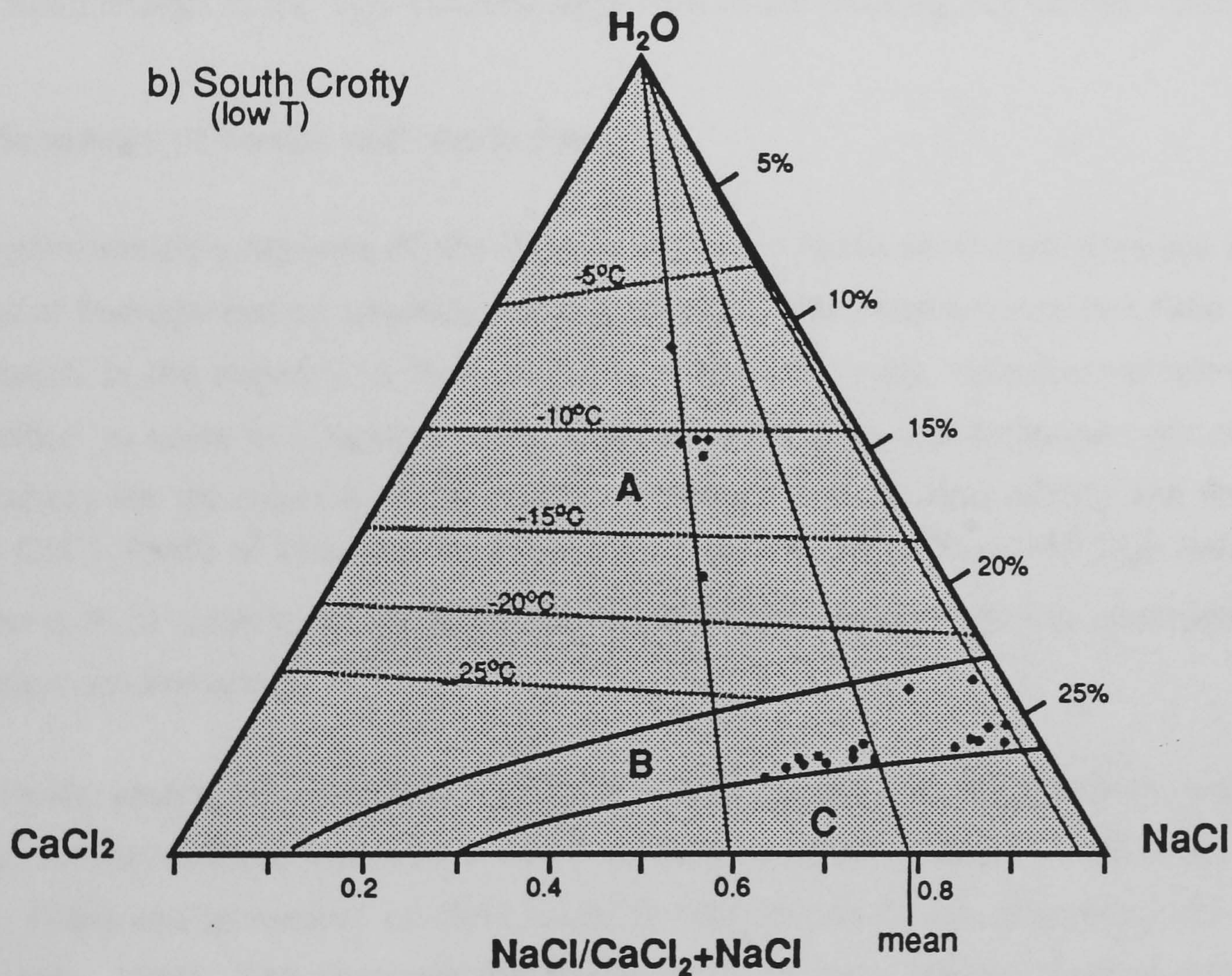
A=Ice+Liquid
B=Hydrohalite+Liquid
C=Halite+Liquid

b) Ecton Hill



Figs.4.18a-b. Triangular plots showing the range of the relative NaCl-$CaCl_2$ contents of fluid inclusions of the Derbyshire and Ecton Hill orefields as estimated from paired T_Mh-T_{LM} temperatures. (for Derbyshire data points represent means of multiple readings on individual samples). Isotherms for the H_2O-NaCl-$CaCl_2$ system after Oakes et. al. (1990).





Figs.4.19a-b. Triangular plots showing the range of the relative NaCl-$CaCl_2$ contents of fluid inclusions from Llanharry and the low temperature group of fluid inclusions in late fluorite from South Crofty, Cornwall. Isotherms for the H_2O-NaCl-$CaCl_2$ system after Oakes et. al. (1990).

fluids have a much larger spread of $NaCl/CaCl_2$+NaCl ratios, ranging from 0.13 to 0.94 coupled with an additional large spread in salinities (0.1 to 26%NaCl). Both the salinity and the $NaCl/CaCl_2$ ratio patterns of the high-temperature fluids are complex and reflect severe overprinting of multiple fluid inclusion generations.

Since it was not possible to determine the Ca contents of fluid inclusions in fluorite and calcite by chemical analysis, recording of paired T_Mh and T_{LM} values is the only way to obtain such an estimate. Rankin & Graham (1988) reported some discrepancies between Ca contents determined by microthermometry and chemical analysis in a quartz sample. For the majority of the samples similar comparisons could not be made in the present study. However, for two Llanharry quartz samples the Na/Ca ratios determined by D-ICP analysis (Chapter 5, and Appendix C) were found to be in agreement to those obtained by microthermometry. However, as can be seen by the form of isotherms of the triangular H_2O-NaCl-$CaCl_2$ phase diagram, the estimate of the Na/Ca ratio are very sensitive, and, even small change in the T_Mh causes a large shift in the resulting Na/Ca ratio estimate.

4.6. Summary of results and conclusions

Microthermometric analysis of the Pennine inclusion fluids confirmed previous published values of homogenization temperatures and salinities. The dominance of one fluid inclusion generation in the majority of the samples is confirmed by the microthermometric results. Therefore as noted in Chapter 3, bulk, fluid inclusion analytical techniques are considered satisfactory for the majority of the samples. Furthermore, the total salinity and the relative NaCl-$CaCl_2$ levels of inclusion fluids obtained from the paired T_{LM} and T_Mh temperatures can be used to convert the semiquantitative chemical analysis results to quantitative fluid-inclusion concentrations.

The fluids associated with base-metal mineralization are low-temperature, high-salinity brines, similar to those observed in MVT deposits of North America (Ohle 1980, Roedder 1976, 1984) and to modern oil-field brines in sedimentary basins (Carpenter et. al. 1974, Sverjensky 1984). The characteristic homogeneity of both homogenization temperatures and salinities of inclusion fluids from MVT districts is also evident in the Pennine samples with the exception of the isolated high-temperature, low-salinity population identified in two fluorite samples from Derbyshire. Differences in homogenization temperatures in the three Pennine orefields can be accounted for by the presence of the Weardale and Wensleydale granites in the North Pennines. A more detailed discussion on the effects of fluid-rock interactions with granitic rocks will be given in the following chapter with the

aid of additional information on the chemical composition of fluid inclusions.

Fluid inclusions in calcite samples from the Ecton Hill Cu-deposit show a slight Ca-enrichment compared to fluids from the rest of the South Pennine orefield. However, the inclusion fluids in samples from these areas are remarkably similar in terms of both homogenization temperature and total salinity. A similar source or evolution path may therefore be postulated for the fluids responsible for both Pb-Zn-dominant and Cu-dominant mineralization in the Pennines. This remarkable overall similarity of the main fluid inclusion characteristics throughout the orefield, in both Pb-Zn-rich and Cu-rich districts, may be envisaged as an indication that low-temperature highly-saline fluids, similar to modern-day basinal brines are involved in the formation of a variety of mineralization types, as initially proposed by Sverjensky (1984, 1986, 1987) for the classical MVT mineralization in general.

The only deviation from the general low temperature-high salinity pattern which characterizes the Pennine orefields is encountered in a restricted number of fluid inclusions in two samples from the northern part of Derbyshire. These fluids have very low salinities and relatively high homogenization temperatures and are commonly found in association with hydrocarbon inclusions. The absence of such fluids in sphalerite shows that they are not associated with the base-metal ore-forming component of the fluid. Inclusions of both groups appear to be primary but, since they were not encountered in the same polished wafers or samples it was not possible to establish their relative timing. This high temperature, low salinity population may be regarded as a separate generation of fluids in close association with hydrocarbons (their homogenization temperatures are within the oil window). Their very low salinity (lower than seawater) is not consistent with a basinal brine signature. The provenance of these fluids will be discussed in more detail in the following chapter with the aid of additional information on their chemical composition.

Fluid inclusions in quartz and calcite samples from the Llanharry Fe-ore deposit in South Wales proved very difficult to examine because of their low abundance in the host minerals and their small size. Their total salinities and relative Na/Ca ratios are lower than those encountered in the Pennine fluids. However taking into account the low homogenization temperatures and the presence of NaCl and $CaCl_2$, as well as the dominance of sedimentary rocks in the area, a sedimentary source seems likely for the ore-fluids at Llanharry. From the restricted number of readings it is not possible to positively identify whether the spread of the salinity values at Llanharry is a result of mixing of two separate fluid populations, or whether it represents a broad continuum.

At South Crofty the patterns of fluid evolution are much more complex. Severe overprinting of several fluid inclusion generations is observed not only in single samples but also in a single field of view. Two main generations of fluids were distinguished in terms of homogenization temperatures and salinities. A distinct low temperature, high salinity (15-26 eq.wt.%NaCl) population was recognized in fluorites from the late, chlorite stage of the paragenesis. Similar low temperature fluids were observed in other parts of the Cornubian orefield related either to Pb-Zn mineralization (Alderton 1978), or to the late stages of Sn-dominant mineralization (Shepherd and Scrivener 1987). Overall, the data from microthermometry provide evidence supporting the involvement of Na-Ca-Cl fluids with a basinal-brine affinity at the late stages of fluorite mineralization in South Crofty. Further consideration of this view will be given in the following chapter in conjunction with further information from the chemical analysis of fluid inclusions.

Chapter 5

Alkali and Halogen Geochemistry of Fluid Inclusions

5.1. Introduction

Results from microthermometry (Chapter 4) have provided some very important constraints regarding the temperature, overall salinity and the relative NaCl-$CaCl_2$ contents of fluid inclusions. In the present chapter results from the chemical analysis of fluid inclusions are used as means to further establish previously reported analogies with modern sedimentary basin brines and fluid inclusions (Shepherd et al 1982, Dunham 1983), as well as to delineate the origin and evolution of the ore forming fluids. The present chapter consists of two parts. The first part is concerned with results on the Na-K-Li concentrations of fluid inclusions whereas, the second part is devoted to their halogen (Cl-Br) signature.

Variations in homogenization temperature and potassium concentrations of inclusion fluids from the three Pennine orefields have been noted and discussed by previous authors (Sawkins 1966a, Rogers 1977, 1978, Small 1978, Rankin & Graham 1988). The impact of these variations on the proposed genetic models for the Pennine mineralization has been the subject of considerable debate (Sawkins 1966a, Dunham 1983, Dunham & Wilson 1985). In this thesis new data on the Na-K-Li concentrations of inclusion fluids from the three Pennine orefields are used in an attempt to examine the regional differences in the nature of mineralizing fluids. Apart from the Pennines, the study extends to samples from the Ecton Hill deposit and the Llanharry Fe-ores of South Wales. Fluid inclusions in fluorite samples from the granite-related mineralization at South Crofty, Cornwall are also examined for comparative purposes.

New data on the Cl and Br concentrations of the inclusion fluids were obtained in the present work. The distribution of these two elements is widely used as a means of tracing the origin of modern-day sedimentary basin brines (Rittenhouse 1967, Carpenter et. al. 1974, Carpenter 1978, Hanor 1987). Despite the common use of Cl/Br ratios in studies of sedimentary brines, there is relatively limited information on the Cl-Br contents of fluid inclusions in samples from MVT deposits. For the areas studied here, apart from preliminary data by Moore (1980) for the Alston block inclusions, there are no published Cl-Br analyses of fluid inclusions. The concentration of these two elements in fluid inclusions was determined in order to highlight the origin of the ore forming fluids and to further examine previously proposed similarities between inclusion fluids and modern-day

basinal oil field brines.

5.2. Summary of previous work

There are no published data on the chemical composition of fluid inclusions in samples from the Llanharry and South Crofty areas. For the Pennines, apart from microthermometry, most of the previous fluid inclusion work consists of determinations of the Na and K contents of the inclusion fluids. The Na/K ratios of inclusion fluids from the Alston block were determined by Sawkins (1966a) and more recently by Rankin & Graham (1988). Results on the Na-K concentration of inclusion fluids from the Askrigg and Derbyshire areas are reported by Rogers (1977, 1978) and Small (1978). Results from all these previous Na-K analyses have shown that the Alston block inclusion fluids are substantially enriched in K compared to Askrigg and Derbyshire. Apart from K, high concentrations of Li in the Alston block fluids are reported by Rankin & Graham (1988). According to their interpretation, temperature-related reactions of the ore forming fluids with the underlying Weardale granite is the cause of the high K and Li concentrations of the Alston block fluids. This aspect is further examined in the present work through new determinations of the Na, K, and most importantly, Li concentration of inclusion fluids from all three Pennine orefields. Furthermore, data from fluid inclusions in fluorites from South Crofty are used in order to evaluate the importance of granitic rocks in modifying the chemistry of the ore-forming fluids.

5.3 Methodology of present work

Neutron Activation Analysis and Decrepitation-ICP were used to determine the Cl-Br and Na-K-Li contents of the inclusion fluids. A detailed description of the methods, experimental procedures as well as the errors involved in chemical analysis was given in Chapter 3. Since the analytical techniques used in the present work are bulk destructive methods, the total volume of analyzed inclusions is not known and the resulting values represent all fluid inclusions present in the sample. The chemical analysis results were combined with the salinity values obtained from microthermometry in order to estimate dilution factors involved in the analysis and to express the values as "true" fluid inclusion concentrations. The calculations used are described in Appendix C. Charge balance ($\Sigma_{cation}/\Sigma_{anion}$) calculations were also performed. Calculated charge balances are within the generally acceptable limit of 0.70 (Shepherd et. al. 1985a). Charge balance calculations showed always an excess of negative charges. This was considered reasonable since, as discussed in Chapter 3, cations such as Ba and Mg were not incorporated in the

calculations.

Microthermometric analysis was also necessary in order to ensure that the analyzed inclusions were members of a single generation. As demonstrated in Chapter 4, fluid inclusions in fluorite and calcite samples from the Pennines, the Ecton Hill and Llanharry ores, are indeed members of a single fluid generation. Therefore, no problems were encountered in their chemical analysis. However, this was not the case in all South Crofty samples. Out of a total number of 12 examined fluorite samples, only five were found to contain a single generation of fluid inclusions. Consequently, bulk chemical analysis had to be restricted to those samples only.

5.4. The Na-K-Li contents of fluid inclusions

Results on the alkali metal concentration of fluid inclusions from 62 samples will be discussed in the present chapter. The obtained ranges of the Na/K and Na/Li atomic ratios in samples from the four different areas of study are shown in Table 5.1. Na/K and Na/Li atomic ratios in samples from the Pennines, Ecton Hill and Llanharry are also presented in the form of bivariate plot in Fig.5.1a. As can be seen from Table 5.1 and Fig.5.1., the Na/K ratios for the Alston block samples are in the range between 5.2 and 24, whereas the Na/Li ratios fall between 40 and 270 The Na/K values are in agreement with previously published ranges by Sawkins (1966a), Rogers (1978) and Rankin & Graham (1988). As can be seen from Fig.5.1, the Alston block fluids are much more enriched in both K and Li compared to the fluids from Askrigg and Derbyshire. Na/K and Na/Li ratios of the Askrigg Block samples fall in the range between 27.5 and 59.5 and 199 to 476 respectively. The Derbyshire fluids have generally lower K and Li concentrations, their Na/K and Na/Li ratios fall between 47.7 to 94.2 and 387 to 911.5 respectively. The only exceptions from this pattern in Derbyshire are the two low salinity-high temperature fluids from Dirtlow Rake and Blue John Cavern (samples DR/1/F, DR/2/F) which are characterized by relatively higher K and Li values.

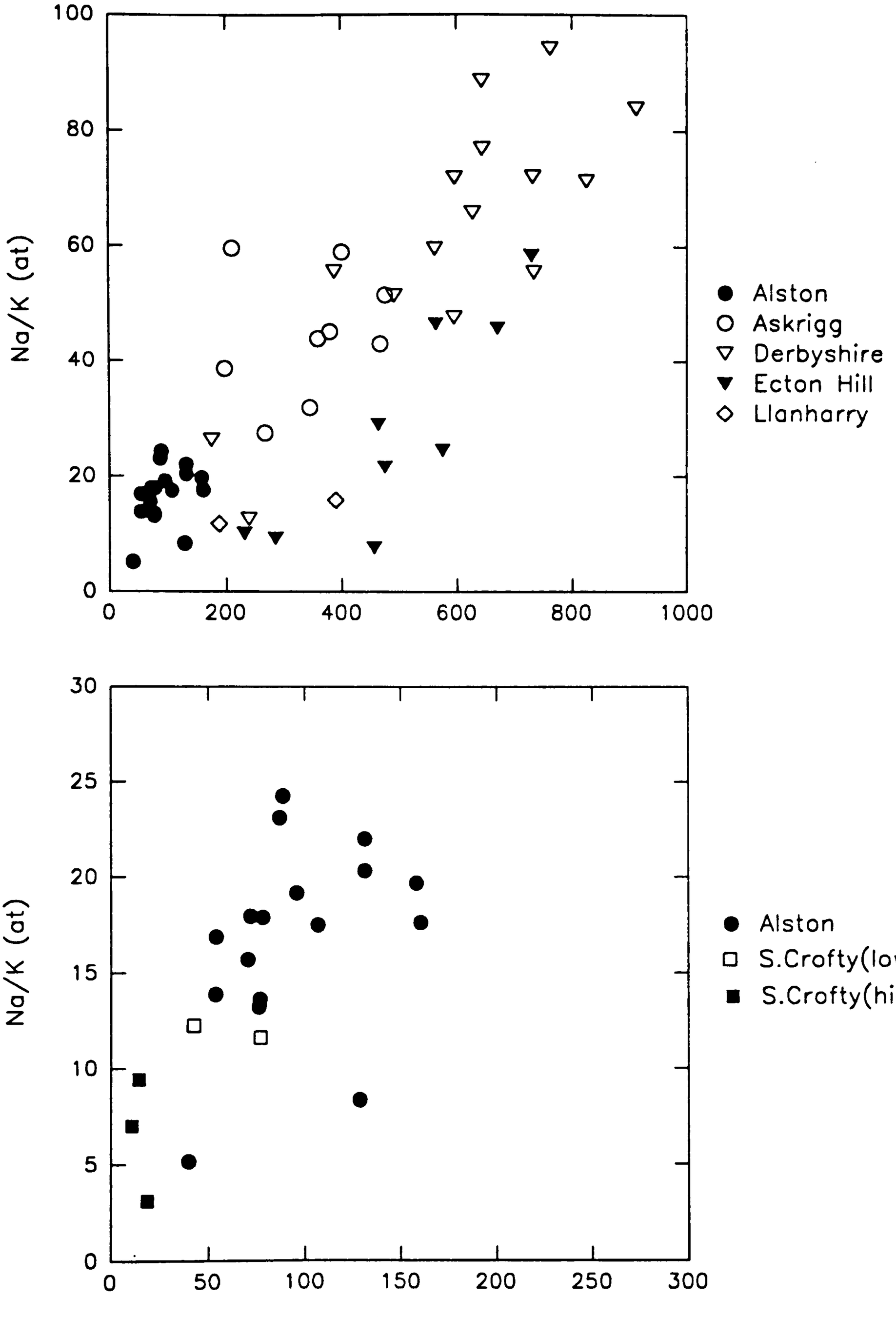
Table 5.1. Ranges of Na/K and Na/Li atomic ratios of fluid inclusions from the four areas of study.

Area	Na/K(at) range	Na/Li(at) range	number of samples (n)
Alston Block	5.2-24	40-270	18
Askrigg Block	27.5-59.5	199-476	9
Derbyshire	48-94	387-911	15
Dirtlow Rake & Blue John Cavern	12.6-26.3	175 -239	2
Ecton Hill	7.7-58.5	231-727	9
Llanharry	8-20.8	188-389	4
S.Crofty (late)	11.6-12.3	42.5-77	2
S.Crofty (early)	3.1-9.4	10.6-18	3

The Na/K ratios of the Ecton Hill fluids obtained in the present work fall within the range of values (6.3-80.7) reported by Masheder & Rankin (1988). No clear pattern is recognized and as can be seen from Table 5.1, the spread of the Na/K ratios from Ecton is wide (7.7 to 58.5) whereas several of the values are higher than those obtained from the rest of Derbyshire (Fig.5.1.). No similar increase is observed in the Li values and, as can be seen from Table 5.1. and Fig.5.1.a, the Na/Li atomic ratios at Ecton lie between 231 and 727.

Problems caused by the small size and low abundance of fluid inclusions in the Llanharry samples seriously impeded their chemical analysis. Consequently, from a total number of ten analyzed samples, paired K and Li data were obtained only for four samples. As shown in Table 5.1, the Na/K ratios of the Llanharry fluids range between 8 and 20.8 coupled with Na/Li ratios between 188 and 389.

Inclusion fluids in fluorite samples from the late chlorite stage of mineralization at South Crofty exhibit a profound K and Li enrichment compared to the Pennine fluids. The Na/K and Na/Li atomic ratios of the South Crofty fluids are presented in Fig.5.1b where the Alston Block values are also shown for comparison. As can be seen from Fig.5.1b, the South Crofty fluids fall into two groups. The early, high temperature group is characterized by very high K and Li concentrations, giving rise to Na/K ratios between 3.1 and 9.4 and Na/Li in the range of 10.6 to 18. The remaining two samples which were also characterized by low homogenization temperatures have Na/K and Na/Li ratios slightly higher, but similar to those of the North Pennines. The Na/K and Na/Li atomic ratios of these samples are 11.6-12.3 and 42.5-77 respectively. As shown in the previous chapter, this low-temperature fluid group has, in terms of both temperature and salinity, many



Figs. 5.1a-b. Bivariate plots showing the variation of the Na/K and Na/Li atomic ratios of inclusion fluids in samples from a) the three Pennine orefields (Alston, Askrigg, Derbyshire), Ecton Hill and Llanharry b) Alston and South Crofty.

aspects in common with the low-temperature, high salinity fluids, typical of the Pennine and MVT mineralization in general. Overall, the observed K and Li enrichment of the South Crofty fluids, coupled with the resemblance of the low-temperature fluid component to the North Pennine fluids can be used as indicators of ore-fluid interaction with lithologies rich in these elements.

5.4.1. Interpretation of Results

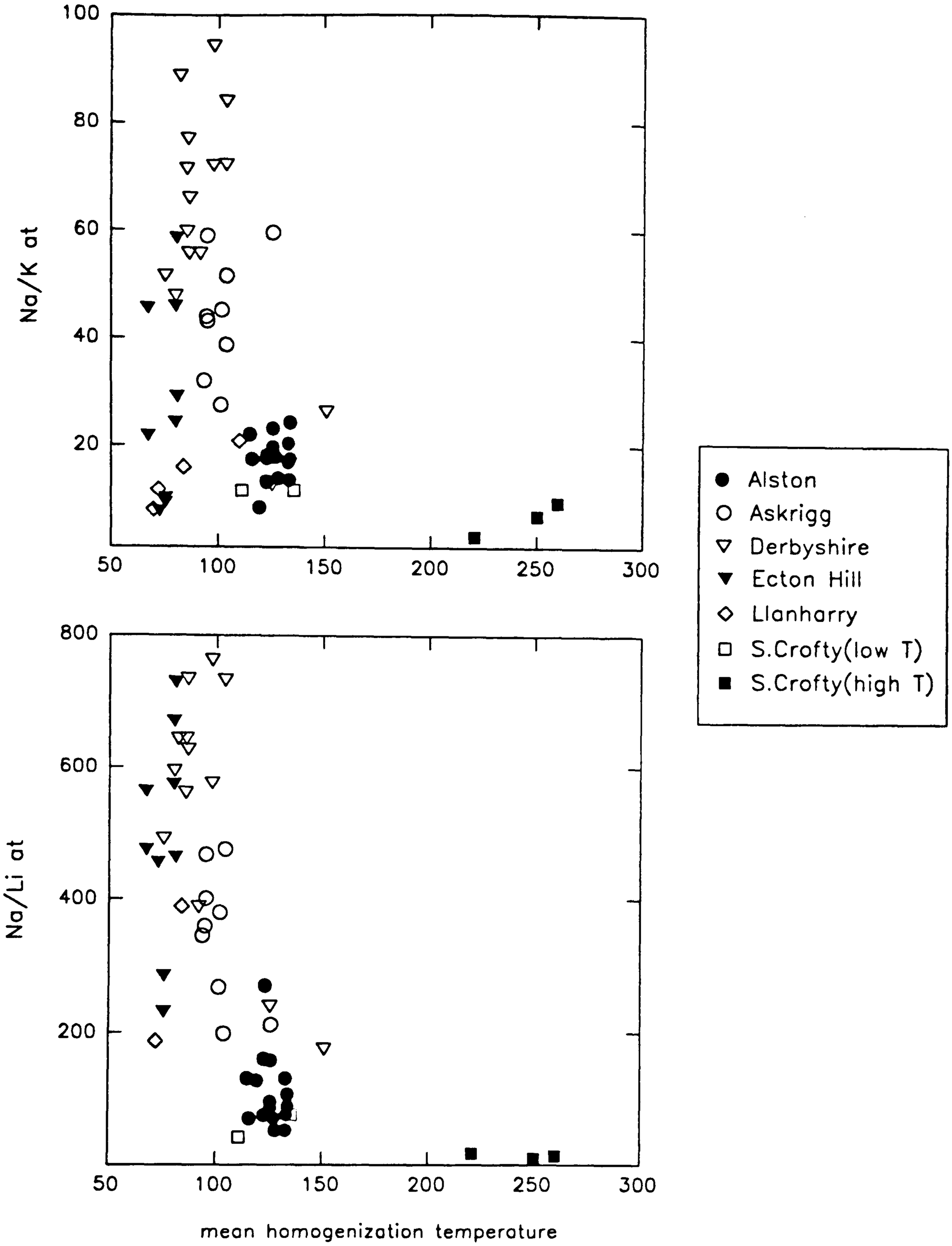
Broad similarities between the chemical composition of basinal, oil field brines and inclusion fluids in MVT deposits have long been discussed in the literature (e.g. Carpenter et. al. 1974, Roedder 1976, 1984). However, as shown in the initial study by Sawkins (1968), the inclusion fluids in samples from MVT deposits are more K-rich than the sedimentary basin brines. This relative K enrichment, which is also evident in the North Pennines, has led to controversy regarding ore genesis in the Pennines, and in most MVT deposits in general. For the North Pennines models involving the contribution from a magmatic component (Sawkins 1966a), juvenile waters (Dunham 1966), or descending brines from Permian or Triassic evaporites (Davidson 1966) were proposed in order to account for the observed potassium enrichment. In a more recent investigation, Sverjensky (1984) examined the thermodynamic consequences of the reactions of a typical oilfield brine at 125°C during flow through and interaction with sandstone and dolostone aquifers containing K-feldspar and muscovite. He suggested that oilfield brines can indeed acquire Na/K ratios similar to those of MVT inclusion fluids through fluid-rock interactions in the sedimentary sequence.

As discussed in more detail in Chapter 2, evidence on the relative timing of mineralization and the emplacement of the Weardale granite, does not support a direct contribution of magmatic fluids to the mineralization in the North Pennines. An alternative explanation for the K-enrichment in the North Pennines was proposed by Rankin & Graham (1988). It involves circulation of brines through the underlying Weardale granite during which they become enriched in K through temperature controlled fluid-rock interaction with potassium-bearing phases such as K-feldspar. This view is also supported by recent chemical, petrographical and mineralogical evidence by Brown et. al. (1987) which indicate that brines were indeed involved in extended fluid-rock interactions in the Weardale granite at the time of mineralization. Therefore, modification of the original composition of the ore forming brine by interaction with the granite is to be expected. This fluid-rock interaction model is further examined here with the aid of new Na-K-Li fluid inclusion data obtained in the present work.

The well defined trend of increasing K and Li from the South to the North Pennine orefields provides another line of evidence on the importance and contribution of the underlying granites in modifying the chemistry of the mineralizing fluids in the North Pennines. The K-enrichment of the Alston block fluids coupled also by higher homogenization temperatures (Fig.5.2a) can be envisaged as a result of interaction with the Weardale granite. As can be seen from Fig.5.1a, the Na/K and Na/Li ratios of inclusion fluids from the Askrigg block occupy an intermediate position between Alston and Derbyshire. Their relative K and Li concentrations also support a granite leaching process since as noted by Brown et. al. (1987), the Wensleydale granite underneath Askrigg is less altered and less fractured than the Weardale granite. Therefore, brine circulation through the granite mass was less extensive and gave rise to the lower K and Li contents of the inclusion fluids in samples from Askrigg. The importance of brine circulation through a granitic mass in modifying the chemistry of the ore fluids is further supported by the high K values found in the South Crofty inclusions. The K concentrations of the low-temperature population are slightly higher but broadly similar with those obtained from Alston block, whereas the high temperature group yielded much higher K values.

For the Derbyshire area there is no conclusive geological or geophysical evidence supporting the presence of a granitic mass in the basement. Therefore, the lower homogenization temperatures and K-concentrations of the inclusion fluids can be envisaged as the result of interaction with lithologies different from the North Pennines. As can be seen in Fig.5.2a and 5.2b there is a broad correlation between homogenization temperature and K and Li concentrations. The higher K and Li values of the North Pennines and South Crofty are also coupled with higher homogenization temperatures. The correlation coefficient between mean Na/K and Na/Li atomic ratios and mean homogenization temperatures in samples from Alston Askrigg Derbyshire and South Crofty is -0.70 and -0.80 respectively. Higher fluid temperatures would indeed enhance the extent of fluid-rock interaction. The influence of temperature is also demonstrated by the two high temperature-low salinity fluids from Dirtlow Rake and Blue John Cavern, which also have higher K, and to a lesser extend Li concentrations, than the rest of the Derbyshire fluids. However, as can be seen from Fig.5.2 the variation of the Na/K and Na/Li ratios is generally more pronounced than the variation in temperature. Regional variations in both fluid temperature and availability of these elements in the surrounding rocks have to be invoked to explain the Na/K and Na/Li distribution patterns in the Pennines and South Crofty samples.

As noted previously the potassium concentrations of the Ecton Hill and Llanharry fluids are higher than those of Derbyshire. However, taking into account the low homogenization



Figs.5.2a-b. Bivariate plots showing the relationship between fluid inclusion homogenization temperatures (T_H °C) an the a) Na/K and b) Na/Li atomic ratios of inclusion fluids in samples from the three Pennine orefields (Alston, Askrigg and Derbyshire), Ecton Hill, Llanharry and South Crofty.

temperatures, the lack of granitic rocks and the dominance of sedimentary rocks in the area, the relative high K content of the inclusion fluids is most possibly a result of ion exchange reactions involving clay mineral alteration (Truesdell 1984, Kharaka et. al. 1985). Interaction with evaporites from the adjacent Cheshire basin has also been proposed for the Ecton Hill fluids (Masheder & Rankin 1988). This previously invoked contribution of fluids from the Cheshire Basin to the Ecton hill mineralization will be further examined using evidence from the Cl-Br concentration of fluid inclusions, as well as from sulphur isotopic investigations (Chapter 6).

The Li distribution patterns of fluid inclusions from the Pennines and South Crofty, are even more pronounced than the ones for potassium. As can be seen in Fig.5.1a, the Alston block fluids are much more Li-rich than those from Derbyshire. The Na/Li ratios of the Askrigg fluids, similarly to Na/K, occupy an intermediate position. A marked Li enrichment is also observed in both the high and low temperature components of the South Crofty fluids (Fig.5.1b). Unlike potassium, the Ecton Hill and Llanharry fluids have relatively low Li concentrations. The trends defined by the Li concentrations of fluid inclusions will be discussed in more detail in conjunction with published Li data from a variety of subsurface waters in both sedimentary and granite-related environments.

5.4.2. Factors controlling the concentration of Li in subsurface waters and inclusion fluids.

The Li distribution in geothermal and sedimentary basin-related waters has been extensively studied by Edmunds et. al. (1984, 1986) and Edmunds (1986). Natural waters from sedimentary basins were found to be enriched in Li relative to seawater. As proposed by Edmunds et. al. (1986). Li because of its low unhydrated and large hydrated ionic radius is readily released from a variety of rock types and has an affinity for ion-exchange on clay minerals whereas it is not easily incorporated in new minerals.

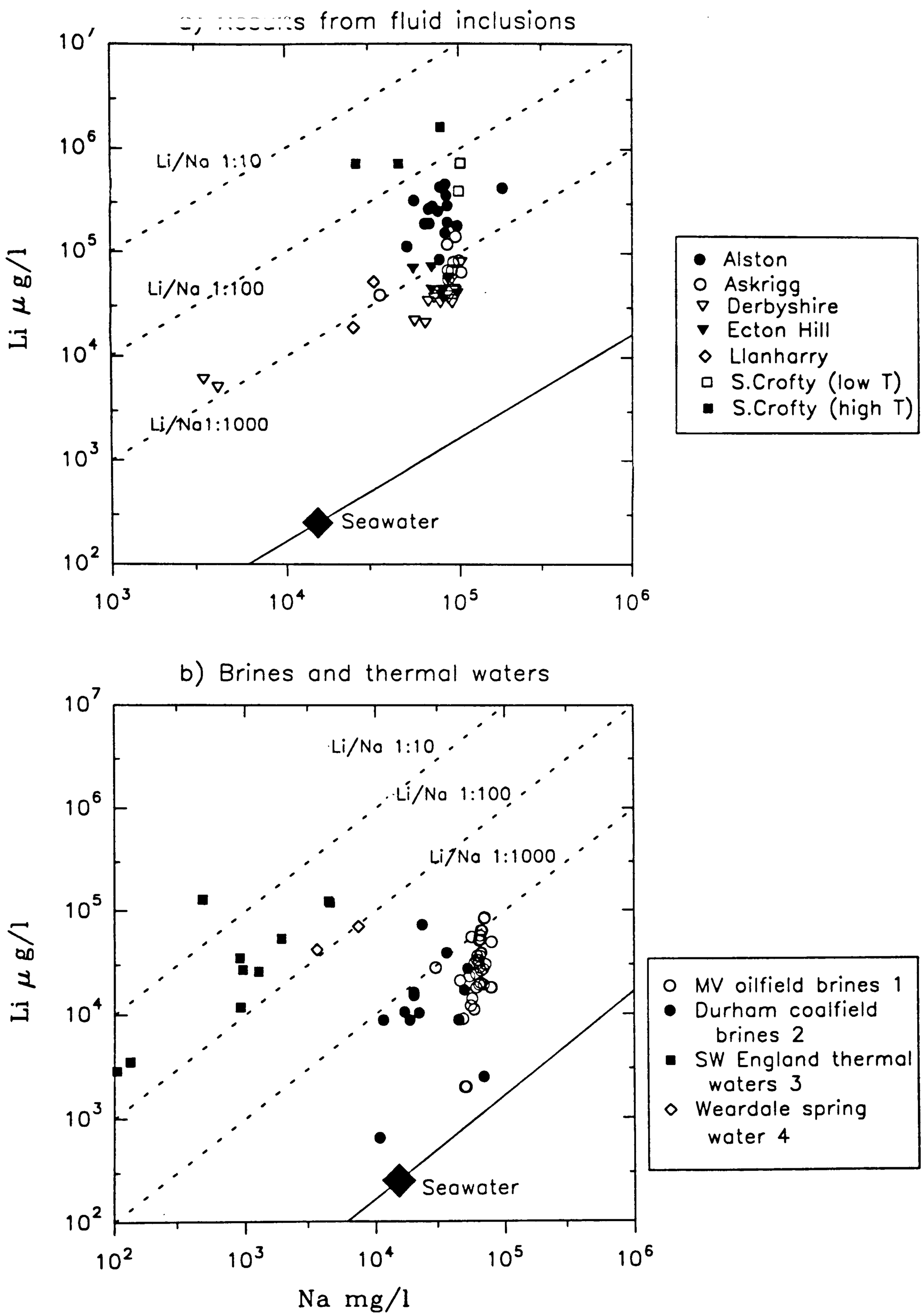
Low to moderate salinity sedimentary basin waters in a variety of aquifers (Triassic sandstone, Cretaceous chalk and Jurassic limestone) have Li/Na weight ratios in between 1:100 to 1:3400 and show an increase in Li values with decreasing salinity (Edmunds et. al. 1986). A number of saline minewaters associated with the Carnmenellis granite were also studied by Edmunds et. al. (1986, 1984). These exhibit a characteristic Li enrichment compared to those from sedimentary environments (op. cit.). The Carnmenellis granite and related biotite adamellites have a mean Li concentration of 278ppm. They contain biotites with reported Li contents in the range of 650-6500ppm. A reasonable average Li value for

the Carnmenellis granite is 1800ppm (Beer et. al. 1978). In contrast, Li is depleted in the hydrothermally-altered granite and in vein minerals. From the Li distribution patterns in geothermal waters associated with granitic rocks it becomes evident that their extreme Li-enrichment is a result of prolonged interaction with Li-rich granites (Edmunds 1986). The higher than seawater Li contents of the sedimentary derived waters mentioned above are likely to be related to equilibria with clay minerals during different stages of diagenesis, with Li partitioning preferentially into the aqueous phase (Edmunds et. al. 1986).

Li and Na concentrations of inclusion fluids obtained in the present study are presented in a bivariate plot in Fig.5.3a. Also shown in Fig.5.3b are Li and Na values of sedimentary brines and geothermal waters discussed above. As can be seen from Fig.5.3a, all inclusion fluids are enriched in Li compared to seawater, but that is also the case for modern oil field brines, as well as, for the sedimentary brines in the U.K shown in Fig5.3b. The Northern Pennine Li/Na weight ratios fall in the range between 1:100 and 1:1000. Compared to the North Pennines, Li decreases in Askrigg, Derbyshire, Ecton and Llanharry fluids and the Li/Na values fall underneath the 1:1000line. Also evident from the Na-Li distribution patterns is the characteristic Li-enrichment of the South Crofty fluids which, as can be seen from Fig.5.3a, have Li/Na weight ratios between 1:10 and 1:100. Of these, the low temperature group is characterized by Li concentrations similar to those encountered in the North Pennines whereas the Li content of the high-temperature inclusions is much higher.

Overall, the Li-enrichment of the North Pennine and South Crofty fluids, coupled with the low Na/Li ratios of thermal minewaters from the Carnmenellis granite, strongly support a fluid-granite interaction process in these areas. The Hercynian granites of SW England are much more enriched in Li than the Caledonian granites of the North of England (Stone and Exley 1985). Nevertheless, the Weardale granite is also relatively enriched in Li due to the presence of Li-rich mica.

The influence of granitic rocks to the inclusion fluid chemistry is also portrayed by the geochemical signature of the granites themselves. As reported by Brown et. al. (1987), the Weardale granite is much more altered and fractured than the Wensleydale granite underneath the Askrigg block. Therefore it provided more fluid channell ways through which the fluids could flow and interact with K-bearing phases such as alkali-feldspar and micas. Fluid flow was more restricted through the Wensleydale granite resulting in the more restricted K and Li enrichment for the Askrigg fluids. Regardless of the ultimate origin of the ore forming fluids the alkali metal distribution patterns provide some insights to the chemical evolution and extend of the fluid-rock interactions. The potassium, and



Figs.5.3a-b. Bivariate logarithmic plots showing the Na-Li concentrations of a) inclusion fluids analyzed in the present work and b) modern-day sedimentary basin brines and thermal and spring waters, sources of data: 1) Carpenter et. al. (1974), Dunham (1975), Dunham et. al. (1987), Manning & Struit (1990).

importantly, the Li-enrichment observed in the North Pennine and South Crofty fluids provide new insights on the importance of the underlying granitic rocks in modifying the chemistry of the ore-forming fluids. Both the Weardale and the Carnmenellis granite are enriched in Li compared to the average granite composition (Rankin & Graham 1988). Circulation of the ore fluids through channell-ways in the granite is the most possible explanation for the Li and K enrichment observed in the North Pennine and South Crofty inclusion fluids.

5.4.3. Alkali Geothermometry

A number of empirical chemical geothermometers based on the alkali concentrations (Na, K, Li) of modern geothermal waters are widely used in geothermal exploration as a means of estimating the temperatures in the fluid source regions. These geothermometers are related to temperature dependent fluid-mineral equilibria involving mainly feldspars, micas and calcite. The theoretical basis of these geothermometers is too elaborate and therefore, it is beyond the scope of the present work to comment on their derivation. A summary of their applications in a variety of geothermal systems is given in a recent review by Truesdell (1984).

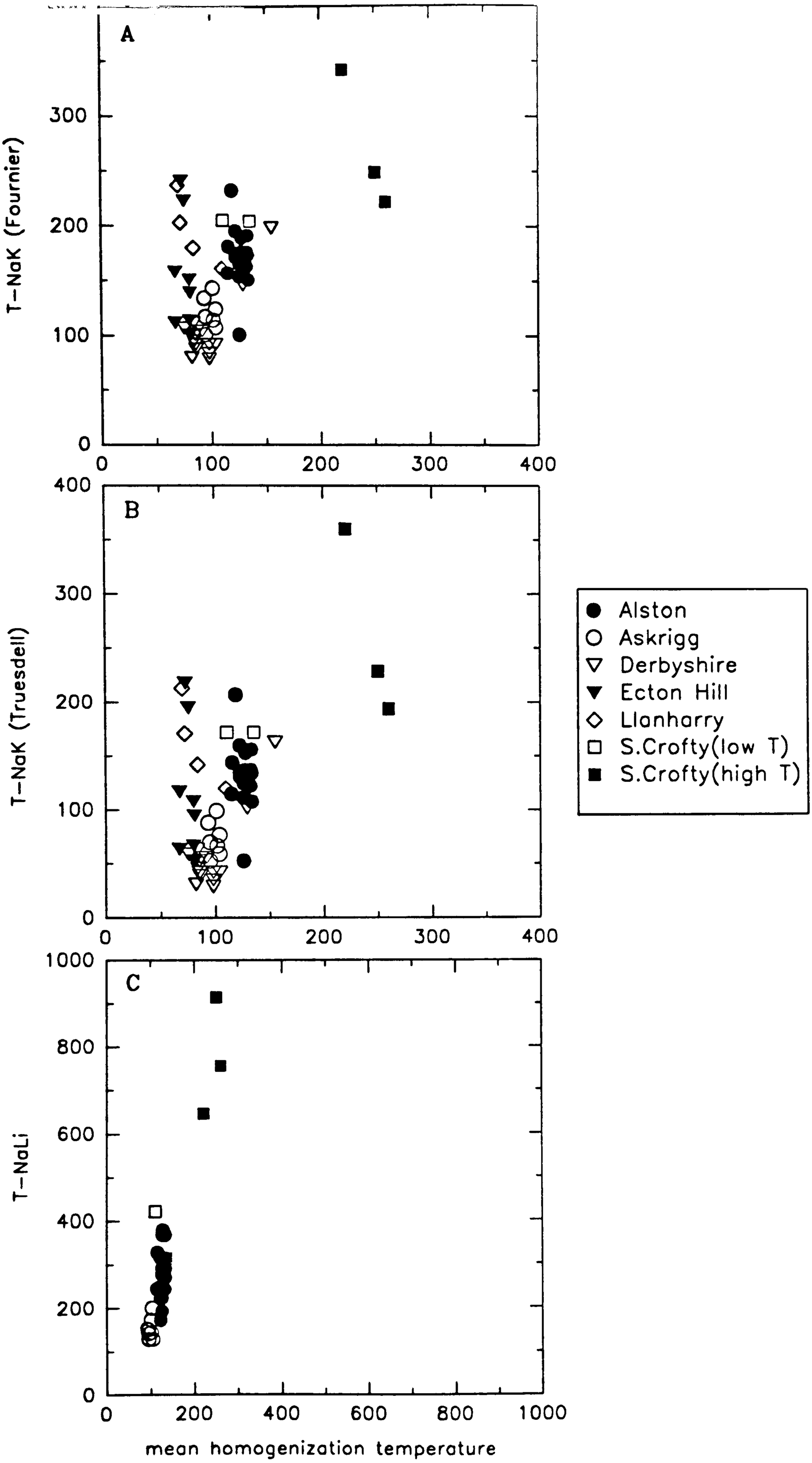
In quartz-mica-feldspar dominated systems, in which the controlling reactions are related to feldspar alteration, geothermometers based on the Na/K ratios of the fluids are the most widely used at temperatures above 180°C. The temperature dependence of the Na/K ratio has been demonstrated by both experimental and theoretical calculations which have also shown that the ratio is essentially independent of pressure. Below 150°C ion-exchange reactions involving clay minerals may become more important leading to the estimation of unreasonably high temperatures (Truesdell 1984). The application of the Na/K geothermometers is based on two assumptions: first, that the fluid has reached chemical equilibrium with the rock, and, second, that other sodium and potassium bearing mineral phases (e.g. albite, muscovite) are of minor importance. As noted by Fournier & Truesdell (1973), the Na/K geothermometer should be applied with caution, since apart from feldspar alteration, it could be affected by several reactions such as the alteration of plagioclase to K-feldspar in which Ca also enters into silicate reactions in competition to Na and K. Also as shown by Hemley (1967) at the same fluid temperature, the Na/K ratios are different in solutions in equilibrium with K-feldspar and albite compared to muscovite and albite. Finally, as mentioned by Fournier & Truesdell (1973) the Na/K geothermometer should only be used for near neutral and alkaline waters.

The NaKCa geothermometer provide an alternative means of estimating temperatures of Ca-rich fluids at depth (Fournier & Truesdell 1973). However, its application to inclusion fluids in the present study was problematic since as discussed in Chapter 3, the absolute Ca concentrations of inclusion fluids in fluorite and calcite could not be determined by chemical analysis. Also lack of knowledge of the pH as well as of the Mg contents of the inclusion fluids seriously inhibits application of this geothermometer. Assumptions on the equilibration state of the inclusion fluids can lead to large errors since, as noted by Fournier & Truesdell (1973) the NaKCa geothermometer cannot be applied in the case that the fluids are depositing calcite.

Fouillac & Michard (1981) introduced a geothermometer based on the relative Na-Li concentration of the fluids. Application of this geothermometer to fluid inclusions from the Alston block by Rankin & Graham (1988) yielded unreasonably high temperatures which are almost twice as high as those determined by the Na/K geothermometers and homogenization temperatures. It is considered unlikely that the NaLi geothermometer provides a realistic estimate of the temperature in the source region of the Alston Block fluids since it is based on experimental data from rocks with background Li values.

Taking into account the general difficulty in accurately determining fluid inclusion chemical compositions, it was only in the last few years that alkali geothermometers have been applied to fluid inclusions (Samson & Russell 1987, Rankin & Graham 1988). Temperatures obtained by Rankin & Graham (1988) for the Alston block fluorites using the Truesdell and Fournier geothermometers were found to be around 40 to 70°C higher than the corresponding homogenization temperatures. The algorithms by Truesdell and Fournier were applied to the samples analyzed in the present work. The relationship between calculated and homogenization temperatures is illustrated in the bivariate plots of Fig.5.4a and 5.4b. The calculations were also extended to the Derbyshire, Ecton Hill and Llanharry fluids but for comparative reasons only since their homogenization temperatures are much too low (generally below 100°C) and as noted previously, the geothermometers are only expected to give valid results for temperatures above 150°C and preferably above 180°C.

However, as can be seen from Fig.5.4a and 5.4b even for the Alston and the late, low temperature South Crofty fluids the Na-K geothermometers yield temperatures higher than homogenization temperatures, in a manner similar to that reported by Rankin & Graham (1988). For the early, high temperature South Crofty fluids the pattern is more complicated. As can be seen from Figs.5.4 in two of the samples the calculated temperature is lower than the homogenization temperature. Similar discrepancies between



Figs.5.4a-c. Bivariate plots showing the relationship between fluid inclusion homogenization temperatures (T_H°C) and the temperatures (T°C) calculated using the a) Fournier Na/K, b) Truesdell Na/K and c) Fouillac & Michard Na/Li geothermometers.

alkali calculated and homogenization temperatures were reported by Bohlke & Irwin (1992) for fluid inclusions in quartz from the St. Austell granite. Overall, application of the empirical geothermometers in fluid inclusions is somewhat more problematic than in geothermal systems since, commonly, important variables of inclusion fluid chemistry, such as pH, are not known. Also, as noted previously, the use of Na/K geothermometers is based on the assumption that alkali feldspars are the dominant rock-forming minerals involved in fluid rock interactions and, most importantly, that chemical equilibria have been attained.

As noted by Rankin & Graham (1988), it is unlikely that the difference between homogenization temperatures and calculated alkali temperatures for the North Pennines represent the positive, depth related, pressure correction which should be applied to homogenization temperatures in order to estimate the true trapping temperature of the fluid. A positive pressure correction of 40 to 70°C for the fluid inclusions from that area would correspond to a pressure correction of 25-75MPa. However, Sawkins (1966a) has produced strong geological arguments supporting the view that the pressure of the North Pennine ore fluids is unlikely to have exceeded 11MPa if the pressure was hydrostatic, and 27.5MPa in the event the pressure was lithostatic. On the basis of these arguments Sawkins (1966a) applied a correction of 20°C to the thermometric data, which is insufficient to account for the discrepancy between the homogenization and calculated temperatures.

As proposed by Rankin & Graham (1988), the Na/K geothermometers more likely reflect inherited fluid equilibration temperatures in a higher temperature, feldspar-rich source region (i.e. the Weardale granite for the Alston block fluids). This hypothesis is in agreement with observations in modern geothermal systems, where the geothermometers are thought to reflect reservoir rather than discharge temperatures (Truesdell 1984). Similar observations can be made for the South Crofty fluid inclusions. The low temperature fluids behave in a similar manner to the North Pennines, whereas, for the early, high temperature group the Na/K geothermometers give a more reasonable temperature estimate. Finally, as can be seen from Fig.5.4c, the Na-Li geothermometer yields too high temperatures for both the north Pennine and South Crofty fluids and is considered unlikely that it provides a realistic estimate of the fluid temperature in the source region. As discussed in the previous section, the high Li concentrations of these fluids are acquired through interaction with Li-rich mineral phases in the granitic rocks. Such a fluid-rock interaction process invalidates the Na-Li geothermometer which should only be applied to fluids associated with background-Li lithologies.

5.5. Cl-Br contents of sedimentary brines and fluid inclusions

One of the most enigmatic aspects of the origin of highly saline sedimentary brines is the process through which they acquire such high salinity. It is a common practice to compare the chemistry of sedimentary basin brines to that of present day seawater since the sediments containing the brines usually have a marine affinity and they contained seawater at some stage of their formation (Carpenter 1978, Hanor 1987). However, this view on the dominance of marine water in sedimentary brines has been challenged by several authors (e.g. Hitchon & Friedman 1969, Knauth & Beunas 1985), who suggested that meteoric waters can also be important constituents of the brines. The concentration of major and trace ions together with the oxygen-hydrogen isotopic signature of the sedimentary brines are used as a means of tracing the origin of the water. However, the original chemical and isotopic signature of a brine can be readily concealed through fluid flow and large-scale interaction with the surrounding rocks. Overall, despite the fact that the ultimate origin of water is in most cases still speculative, the relative concentrations of Cl and Br provide a means of overcoming the masking effect of complicated fluid-rock interactions, since they do not readily participate in diagenetic reactions and do not easily precipitate new minerals.

The importance of Cl/Br ratios as tracers of the origin of sedimentary brines has long been recognized. The initial study linking the Cl/Br ratios of sedimentary brines to their origin (Rittenhouse 1967) was followed by numerous others in a wide variety of sedimentary basin environments (Land & Prezbindowski 1981, Carpenter et. al. 1974, Carpenter 1978, Kharaka et. al. 1987, Connolly et. al. 1990). However, despite the fact that halogen ratios have long been used as tracers of the origin of sedimentary brines, there are relatively few studies involving similar use of halogen ratios in fluid inclusions. (Behr & Gerler 1987, Roedder et. al. 1987, Bein et. al. 1991, Crochetti & Holland 1989, Bohlke & Irwin 1992). In a recent publication by Bohlke & Irwin (1992), in addition to Br/Cl, the I/Cl ratios of inclusion fluids were also determined and used in tracing fluid origin. Fig.5.5 (after Bohlke & Irwin 1992) gives a summary of published halogen ratio values of some surface and subsurface waters. Unfortunately, because of its very low levels in fluid inclusions, iodine could not be determined using the methods available in the present study.

5.5.1. Controls on the Cl/Br ratios of sedimentary brines

The factors governing the distribution of Cl and Br in sedimentary brines and evaporites were initially reviewed by Rittenhouse (1967) and more recently by Carpenter (1978), Sonnenfeld (1984), Hanor (1987) and MacAffrey et. al. (1987). Experimental studies have

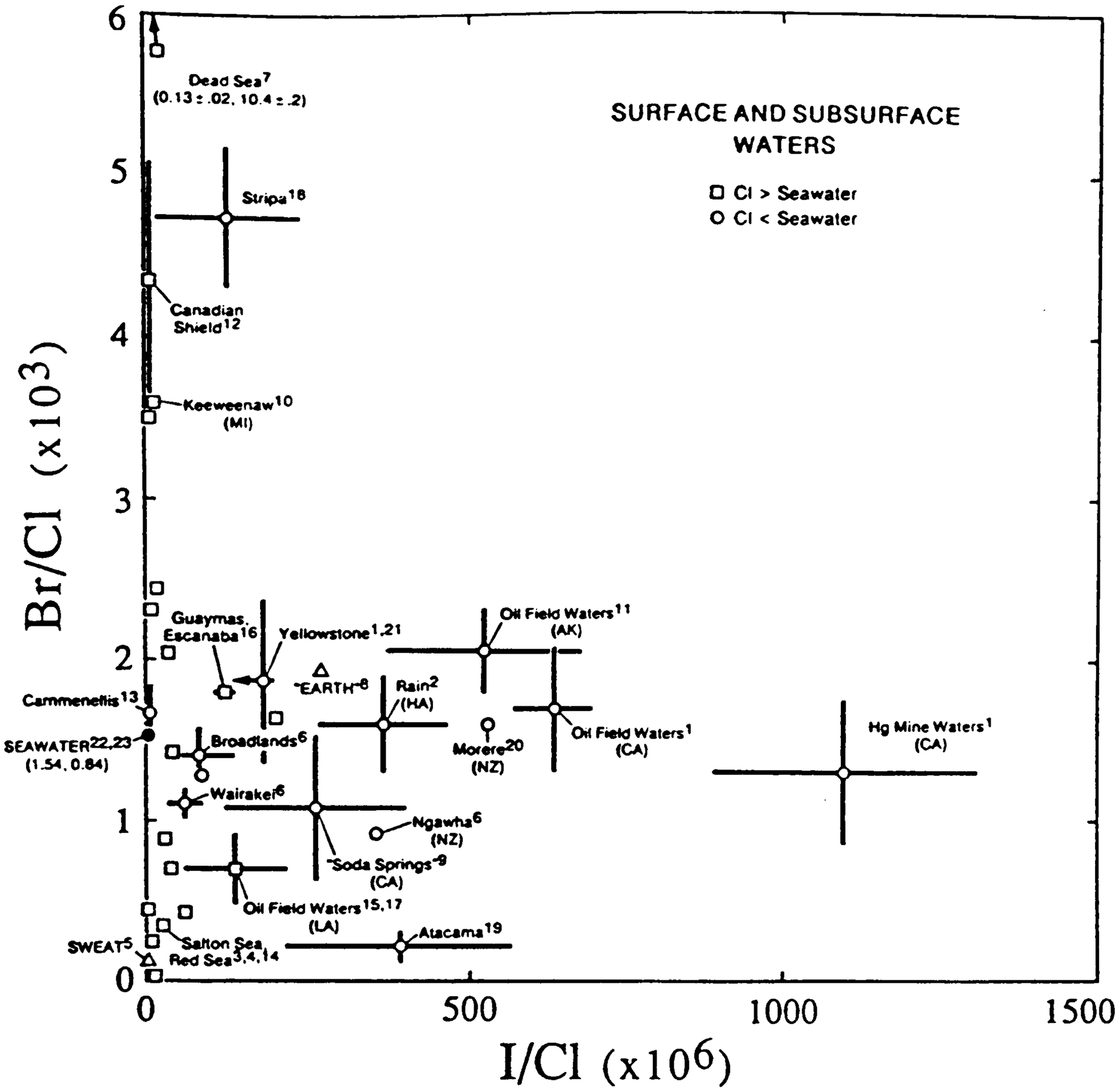


FIG. 1. Halogen ratios in some representative surface waters and ground waters. Br/Cl and I/Cl ratios have ranges of more than two and three orders of magnitude, respectively; saline brines commonly are strongly fractionated in Br/Cl relative to seawater and "Earth" because of evaporative processes; seawater and fluids associated with organic-rich sedimentary rocks have complementary I/Cl ratios, bracketing those of "Earth" and igneous rocks; unlabeled symbols represent waters in sedimentary rocks from various localities reported by WHITE et al. (1963b); symbols with bars represent the means ± 1σ; references: 1 = WHITE et al. (1963b); 2 = DUCE et al. (1963); 3 = WHITE (1968); 4 = BREWER and SPENCER (1969); 5 = ICRP (1975) "model" values; 6 = ELLIS and MAHON (1977) well waters; 7 = NISSENBAUM (1977); 8 = DREIBUS et al. (1979) Cl Chrondrites; 9 = BARNES et al. (1981); 10 = KELLY et al. (1986); 11 = KHARAKA and CAROTHERS (1986); 12 = FRAPE and FRITZ (1987); 13 = EDMUNDS et al. (1987); 14 = CHARLES et al. (1988); 15 = LAND et al. (1988); 16 = CAMPBELL and EDMONDS (1989); 17 = LAND and MACPHERSON (1989); 18 = NORDSTROM et al. (1989); 19 = ALPERS and WHITTEMORE (1990); 20 = W. GIGGENBACH (pers. comm., 1990); 21 = N. C. STURCHIO and J. K. BÖHLKE (unpubl. data): 22 = DREVER (1988); 23 = FUGE and JOHNSON (1986).

Fig.5.5. Halogen (Br/Cl and I/Cl ratios of selected surface and subsurface waters (after Bohlke & Irwin 1992).

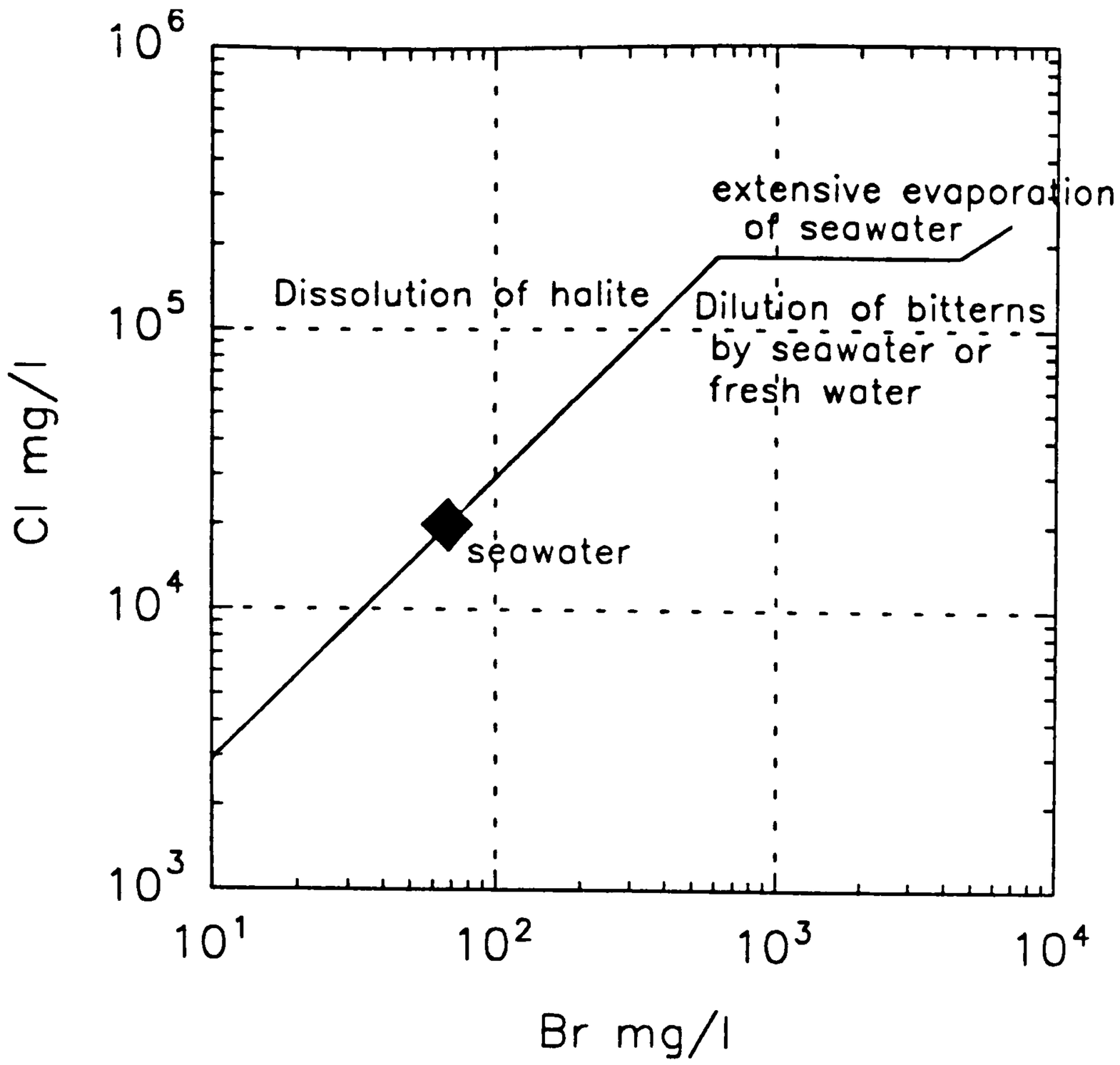
shown that the initial Cl/Br ratio of sedimentary brines is affected by relatively few processes. During the evaporation of seawater both Cl and Br increase conservatively in the hypersaline solution; whereas the Cl/Br ratio remains unaffected (Fig.5.6a). At the point that halite saturation is reached, Cl is preferentially precipitated as NaCl, whereas Br remains in the residual brine, even though the halite lattice can accommodate some Br in solid solution. The degree of this fractionation can be expressed as D.

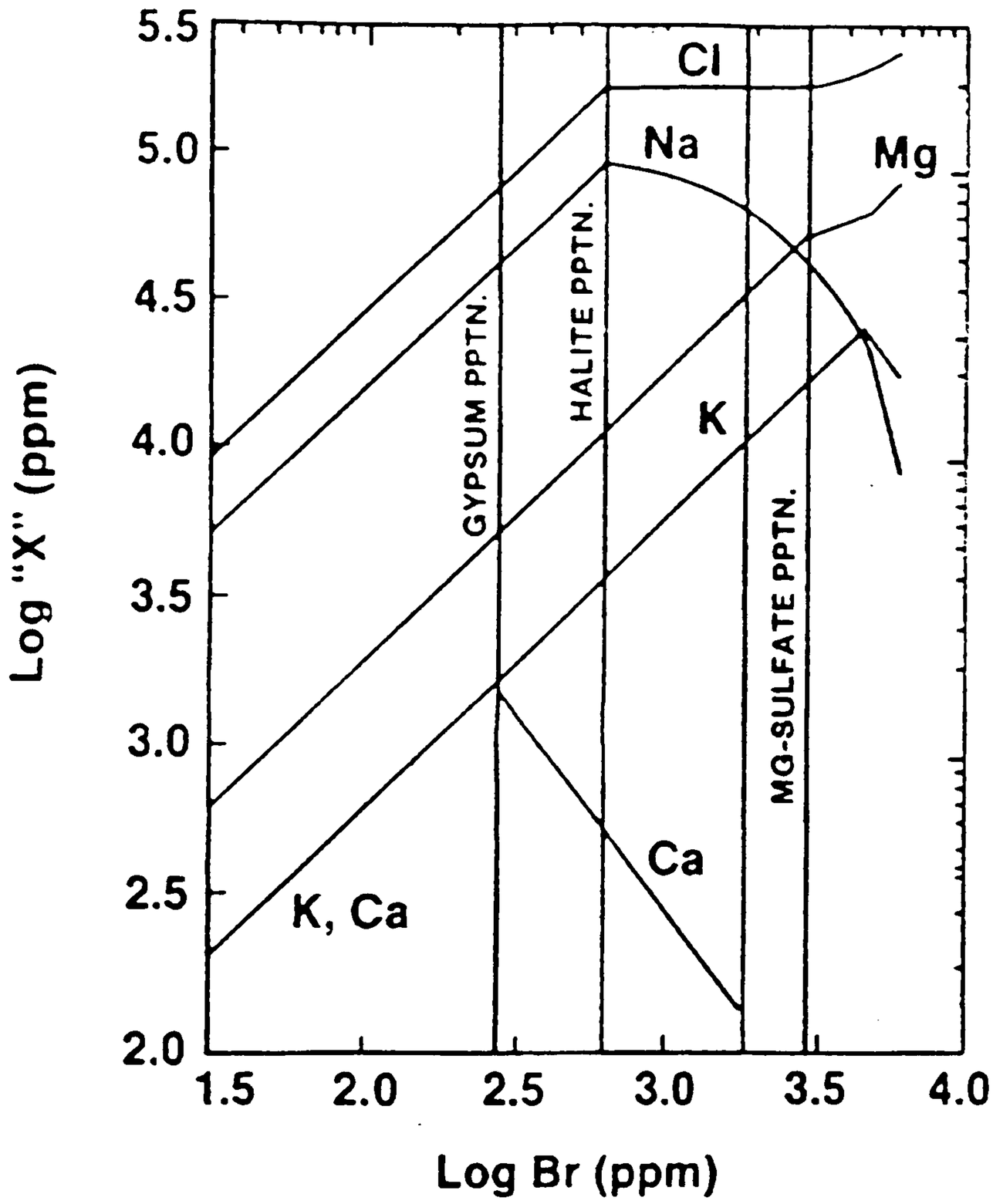
$$(Br/Cl)_{halite} = D \times (Br/Cl)_{brine} \quad (1)$$

If the Cl-Br concentrations are expresses in mass units D has a value of 0.1 at 25°C. Exact values depend on temperature, solid composition and brine composition (Hanor 1987). Three broad types of brines can be distinguished on the basis of their Cl/Br ratios. a) brines with Cl/Br ratio equal to that of seawater (298) which plot directly on the seawater evaporation trajectory (S-E-T), defined by equation (1), are interpreted as ancient evaporite brines that have acquired their high salinity by prolonged subaerial evaporation. b) brines which are enriched in Cl relative to the seawater evaporation line are interpreted as having interacted with evaporite minerals, most commonly halite, acquiring high amounts of Cl but negligible Br. Finally, c) brines that plot on the right and below the seawater evaporation trajectory are interpreted as the result of mixing between highly evaporated brines and fresher water(Fig.5.6a).

Therefore, these three fundamental processes, evaporation, interaction with evaporites and mixing have been recognized as the main mechanisms which influence the Cl/Br ratios of sedimentary basin fluids. Nevertheless, the Cl/Br signature of the brines is hardly ever that well defined indicating that not a single, but usually a combination of the above described processes may be active and influencing the halogen signature of the fluids. Apart from Cl-Br, and as shown in Fig.5.6b, the concentration trends of various ions (K, Ca, Na, Mg) relative to bromide during the evaporation of seawater and precipitation of evaporite minerals are also used as indicators of the origin of sedimentary basin fluids. However, their relationships are much more complicated since, unlike Cl and Br, the concentration of these ions is more readily affected by diagenetic and ion-exchange reactions. Apart from the above described processes (evaporations-leaching of evaporites-mixing), contribution from organic matter has also been proposed as the cause of high Br concentrations in sedimentary brines (Means & Hubbard 1984). However, as noted by Hanor (1987), such a process has yet to be verified by detailed mass balance calculations.

Membrane filtration has also been proposed as an additional process through which





Figs.5.6a-b. Bivariate logarithmic plots showing the concentration trends of a) Cl and b) Ca, K, Mg relative to Br of seawater during evaporation and the precipitation of evaporite minerals (after Carpenter 1978).

subsurface waters can acquire high salinities (Graf 1982). According to that process compacted clays and shales act as semipermeable membranes retarding the flow of dissolved species with respect to water. However, the importance of membrane behavior of rocks is not unequivocally accepted. As suggested by Manheim & Horn (1968), the pressure requirements for significant membrane filtration are too high and are not encountered in geologic environments. Also despite the fact that the mechanism of membrane filtration has been demonstrated by experimental evidence (Kharaka & Berry 1973, Graf 1982), salinities as high as 5 molar NaCl have still, not been achieved experimentally (Egeberg & Aagaard 1989, Hanor 1987). Further consideration on the feasibility of such a mechanism in the areas of study will be given in the following sections.

5.5.2. Cl-Br relationships in Fluid Inclusions

Broad similarities between modern-day sedimentary brines and fluid inclusions from the Pennine ores and also from other MVT deposits, have been noted and discussed by several investigators (Shepherd et. al. 1982, Dunham 1983, Roedder 1976, 1984, Crochetti & Holland 1989, Sverjensky 1984). In the present work results from microthermometry (Chapter 4) have indicated that in terms of both temperature and salinity, inclusion fluids from the Pennines, Ecton Hill, Llanharry, and also from the late stage of mineralization at South Crofty, have aspects in common with the highly saline, sedimentary-basin brines. In order to further establish this indicated affinity to sedimentary brines, it was considered essential to obtain data on the Cl-Br contents of fluid inclusions in samples from these areas. Furthermore, the Cl-Br signature of fluid inclusions can provide an insight to the cause or causes of their high salinity, an aspect that has not been studied extensively so far in MVT districts in general.

The Cl-Br concentrations of the inclusion fluids were calculated using combined data from microthermometry and chemical analysis following the procedure outlined by Shepherd et. al. (1985a). All raw and processed data are listed in Appendix C. The ranges of Cl/Br ratios of fluid inclusions from the four areas of study are presented in Table 5.2. The calculated Cl-Br concentrations of inclusion fluids are presented in a bivariate logCl-logBr plot in Fig.5.7a. Also presented in Fig.5.7b are published Cl-Br values of modern sedimentary brines and thermal waters.

Table 5.2. Ranges of Cl/Br (wt) ratios of inclusion fluids from the Pennines, Ecton Hill, Llanharry and South Crofty, Cornwall.

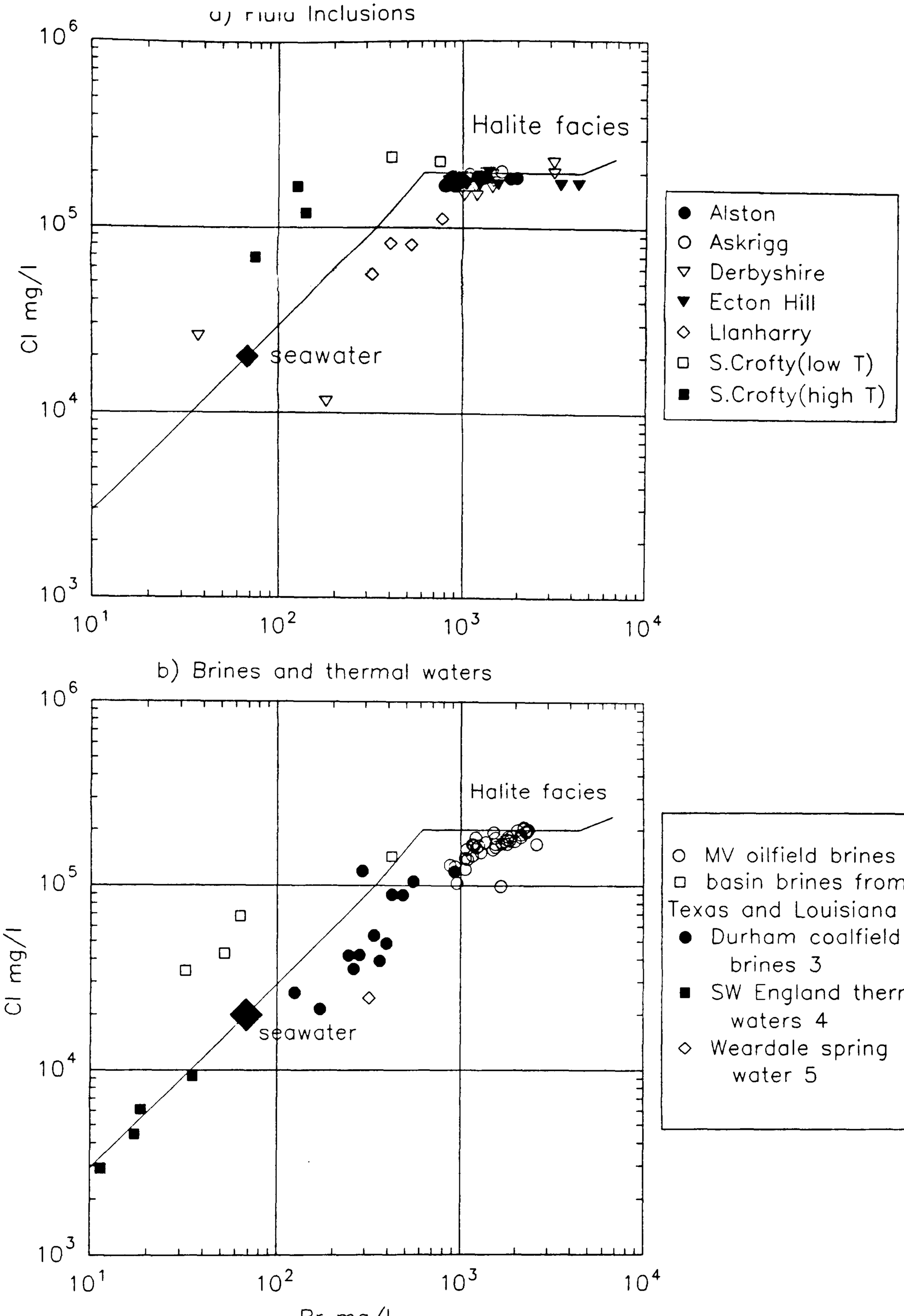
Area	**Cl/Br (weight)**	**number of samples (n)**
Alston Block	95-218	19
Askrigg Block	125-210	9
Derbyshire	63-217	15
Dirtlow Rake and Blue John Cavern	63-696	2
Ecton Hill	40-187	9
Llanharry	153-201	4
S.Crofty (low T)	303-586	2
S.Crofty (high T)	860-1333	3

5.5.2.1. Pennines and South Wales

As can be seen from Table 5.2, the Cl/Br ratios of the Pennine, Ecton Hill and Llanharry fluids are all lower than the seawater value of 298. Also, as can be seen from Fig.5.8a, all Pennine and Ecton Hill fluids plot close to the seawater evaporation trajectory, and are slightly displaced below the field of halite saturation. The same observation can be made for the inclusion fluids from four Llanharry samples which also plot close to the seawater line but have lower salinities than the Pennine fluids.

Two observations can be made on the Cl-Br signature of the Pennine inclusion fluids: a) the Cl-Br relationships in all three Pennine and Ecton Hill inclusion fluids are remarkably similar and b) there is no indication of interaction with evaporites, since the inclusion fluids have higher Br, and not Cl, concentrations relative to the seawater line. As shown in Fig.5.7b, brines for which interaction with evaporites has been proposed have Cl/Br ratios higher than seawater and plot to the left of the seawater evaporation line (data from Kharaka et. al. 1985). As proposed by Hanor (1987), Carpenter (1978) and also by Connolly et. al. (1990), subaerial evaporation of seawater is an important process in enhancing the salinity and the Br contents of sedimentary brines. This is demonstrated also in Fig 5.7b which shows the Cl-Br distribution of metal-rich brines from Central Mississippi (Carpenter et. al. 1974).

As is the case in the inclusion fluids examined in the present study and also in the oil-field

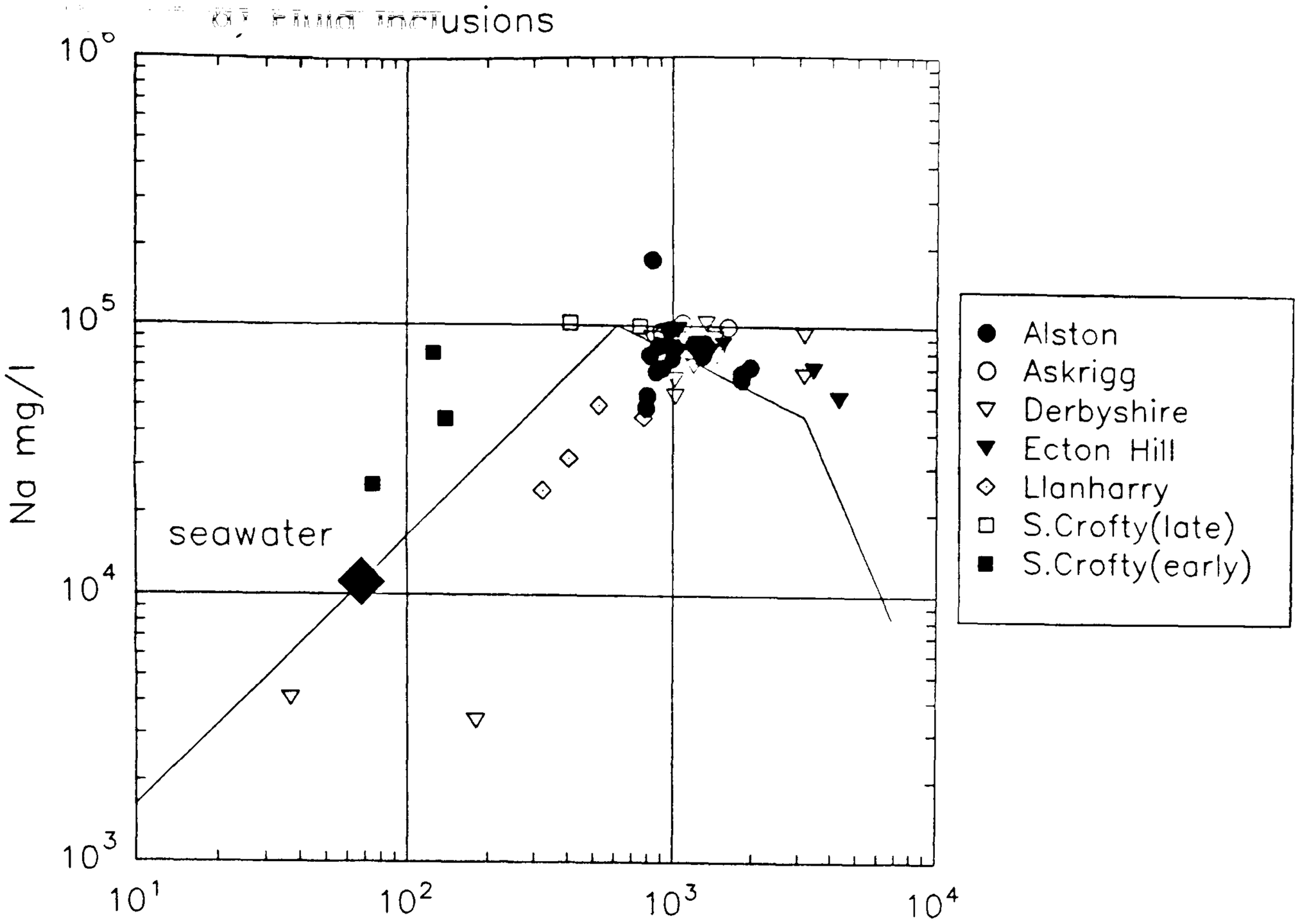


Figs.5.7a-b. Bivariate logarithmic plots showing the Cl-Br concentrations relative to the seawater evaporation trajectory of a) inclusion fluids analyzed in the present work and b) modern-day basinal brines and thermal waters (sources of data: 1) Carpenter et. al. 1974, 2) Kharaka et. al. 1985, 3) Edmunds 1975, 4) Edmunds et. al. 1987 and 5) Manning & Struit 1990).

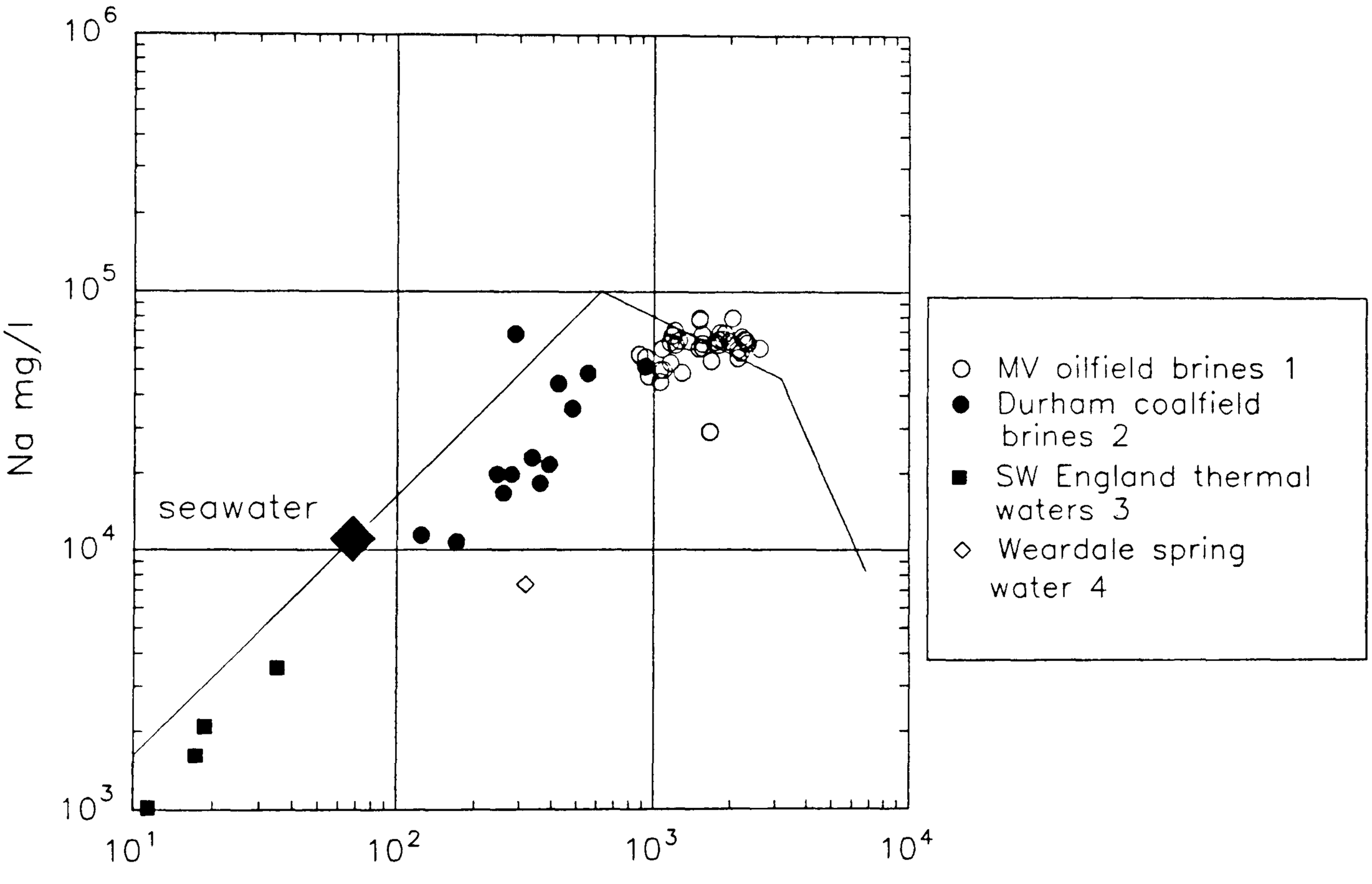
brines of Central Mississippi, few natural subsurface waters plot directly on the seawater evaporation line. It is thus conceivable that additional processes apart from evaporation and leaching of evaporites may have been responsible for their Cl-Br composition. Land & Prezbindowski (1981) suggested that the elevated Br/Cl ratios of some brines in the Gulf Coast, Texas could be produced by incongruent dissolution of halite. Halite dissolution and re-precipitation would preferentially release Br and produce a brine with high Br contents. The theoretical aspects of that process were evaluated by Stoessell & Carpenter (1986). However, there are several problems in applying this model to the Pennine fluids. First as noted by Connolly et. al (1990), unreasonably high water-rock ratios are required in order to generate such high Br concentrations. The recrystallization of halite will produce brines which are also enriched in Na (Fisher & Kreitler 1987). As can be seen from Fig.5.8a, the Na-Br distribution patterns of the Pennine fluids are identical to those of Cl-Br and they do not define any profound Na-enrichment. Consequently, the halite recrystallization process is considered unlikely.

Organic matter has been proposed as a source for I^- in some Iodine-rich brines in the Andarko basin in Oklahoma (Collins 1975). By analogy, an organic source has been invoked for the Br in brines of the Palo Duro basin, Texas (Means and Hubbard 1985). In the UK, organic matter has also been proposed as the source of Br in the coalfield brines of Northern England (Edmunds 1975). A contribution from organic matter cannot be ruled out for the Pennine fluids, particularly in the Derbyshire area where hydrocarbon inclusions are common (Moser et. al. 1992). Nevertheless, contribution from organic matter is not made clear by the Cl/Br data obtained from the two low-salinity fluids from Dirtlow Rake and Blue John Cavern. As can be seen from Fig.5.7a these are the only samples which deviate from the general high salinity pattern in the Pennines. These exceptional fluids are closely associated with organic matter. Mixed low salinity, aqueous-hydrocarbon inclusions are also present in these two samples (Moser et. al. 1992). As can be seen from Table 5.2, the Dirtlow Rake sample (DR/1/F) has a relatively low Cl/Br ratio of 63. On the contrary, fluid inclusions in the Blue John (DR/2/F) sample are depleted in Br and give rise to a very high Cl/Br ratio of 696. Therefore, if organic matter is indeed the source of excess Br in the fluids, it would be expected that both of these low-salinity hydrocarbon-associated fluids would be the most Br-rich. No such pattern is made clear from the above mentioned samples. Overall, the exact role of organic matter in modifying the Cl-Br signature of the inclusion fluids and sedimentary brines is far from clear. As noted by Hanor (1987), despite several speculations, detailed mass balance calculations have yet to be performed to assess this potential source of bromide in both sedimentary brines and inclusion fluids.

a) Fluid inclusions



b) Brines and thermal waters



Figs.5.8a-b. Bivariate logarithmic plots showing the Na-Br concentrations of a) inclusion fluids analyzed in the present work and b) modern-day sedimentary basin brines and thermal waters (sources of data 1) Carpenter et. al. 1974, 2) Edmunds 1975, 3) Edmunds et. al. 1987 and d) Manning & Struit 1990).

5.5.2.2. South Crofty, Cornwall

Most of the studies on the halogen distribution of natural waters and inclusion fluids are oriented towards sedimentary-basin environments. This is partly due to the link between the basin environment and seawater, the chemistry of which is better understood and examined in comparison with current oceans and modern sedimentary brines. So far, there are only limited studies concerning the halogen signature of magmatic waters, as well as, fluid inclusions in minerals from granitic terranes (Bohlke & Irwin 1992). In the present work inclusion fluids in fluorite from the South Crofty Mine were also analyzed for Cl and Br. Results on their Cl-Br-Na systematics are also presented in Fig.5.7a and 5.8a.

The examined South Crofty fluids belong to the late fluorite-chlorite stage of the paragenesis. As shown in Chapter 4, one population of these fluids is characterized by high temperature and wide range of salinities whereas a second, later group, has in terms of both temperature and salinity, many aspects in common with the North Pennine fluids. Previous fluid inclusion investigations at South Crofty (Scrivener et. al. 1986, Farmer 1991), have stressed the possibility that fluids, similar to those associated with the late Pb-Zn mineralization elsewhere in Cornwall (Alderton 1978), were involved at the late stages of mineralization at South Crofty. Data presented in Chapter 4, on the temperature, salinity and relative Na-Ca levels of inclusion fluids in fluorite from the late stage of mineralization at South Crofty, have provided evidence supporting this view. This possibility is further examined in the present section with the aid of Cl-Br fluid inclusion data.

As can be seen from Table 5.2 and Figs.5.7a and 5.8a, the two low temperature South Crofty fluids are slightly depleted in Br but quite similar to inclusion fluids from the Pennine orefields. In addition to homogenization temperature, salinity and alkali metal ratios, their halogen signature provides another line of evidence supporting their general resemblance to the Northern Pennine fluids and to evolved sedimentary brines in general. The rest of the South Crofty samples however, show a quite different Cl-Br distribution. These high temperature fluids are severely depleted in Br relatively to Cl. It is probably not appropriate to compare these fluids with modified seawater or with sedimentary basin brines since both their temperature and chemical composition do not indicate a sedimentary signature. Their Cl/Br ratios are very similar to those reported by (Bohlke & Irwin 1992) for inclusion fluids in quartz from a quartz-tourmaline-topaz (greisen) assemblage in the St Austell granite (Br/Cl range between 1124 and 1234). Their Cl/Br ratios are also significantly higher than seawater but, as noted by Bohlke & Irwin (1992), they are also lower than those of hydrothermal fluids dissolving evaporites (e.g. the Salton Sea and Red

Sea brines). (Fig.5.9)

Due to the scarcity of published Cl-Br data of inclusion fluids from granitic terranes, the halogen signature of hot springs and saline minewaters could highlight some not sufficiently understood aspects. In the UK, studies of the Cl/Br ratios of mine waters in the Carnmenellis granite have been undertaken extensively by Edmunds et al (1984, 1986, 1987). The Cl, Br and Na values of these waters are also plotted in Figs.5.7b and 5.8b. These saline minewaters have an halogen signature distinctly different from the inclusion fluids from South Crofty and St. Austell. As proposed by Edmunds et. al. (1984, 1987), the Carnmenellis minewaters acquired the halogens through interaction with the granitic rocks, and most probably biotite, which has a Cl/Br ratio very similar to that of seawater (Fuge 1974). Despite that the Cl-Br ratio of the Carnmenellis waters is identical to that of seawater, a seawater source for the fluids was considered unlikely by Edmunds (op. cit.) on the basis of oxygen-hydrogen isotopic data which are more consistent with a meteoric origin. Congruent and incongruent reactions with biotite and, to a lesser extend, muscovite were proposed by Edmunds (op. cit.), as the main processes leading to the build up of Cl, Br, Li, B and possibly K in the fluids. The following reaction was proposed by Edmunds et. al. (1987).

$$K_2(Mg,Fe)_4\,(Fe,Al,Li)_2\,[Si_6Al_2O_{20}]\,(OH)_2\,(F,Cl)_2 + 3H_2O + 12H^+ =$$

[biotite]

$$= Al_2Si_2O_5(OH)_4 + 4H_4SiO_4 + 2K^+ + 4(Mg^{+2},Fe^{+2}) + 2(Fe^{+3},Al^{+3},Li^+) + 2(F^-,Cl^-)$$

[kaolinite]

Overall, from the case studies described above and from data obtained in the present work, it becomes evident that there is no clear "magmatic" halogen fluid signature for granite-derived or granite-associated fluids. In both the St. Austell and South Crofty inclusion fluids, as well as, in the thermal minewaters, there is considerable overlap between the invoked magmatic and sedimentary halogen characteristics. The processes influencing the halogen distribution of magmatic and related waters are not clearly understood. As proposed by Bohlke & Irwin (1992) several processes could lead to the lower Br/Cl ratios found in high temperature fluids. The Br/Cl ratios of the inclusion fluids could represent either the halogen composition of magmas possibly modified significantly by crustal contamination such as assimilation of evaporite-bearing sediments with low Br/Cl, or, fractionation of Br and Cl during magma crystallization, fluid phase separation or high

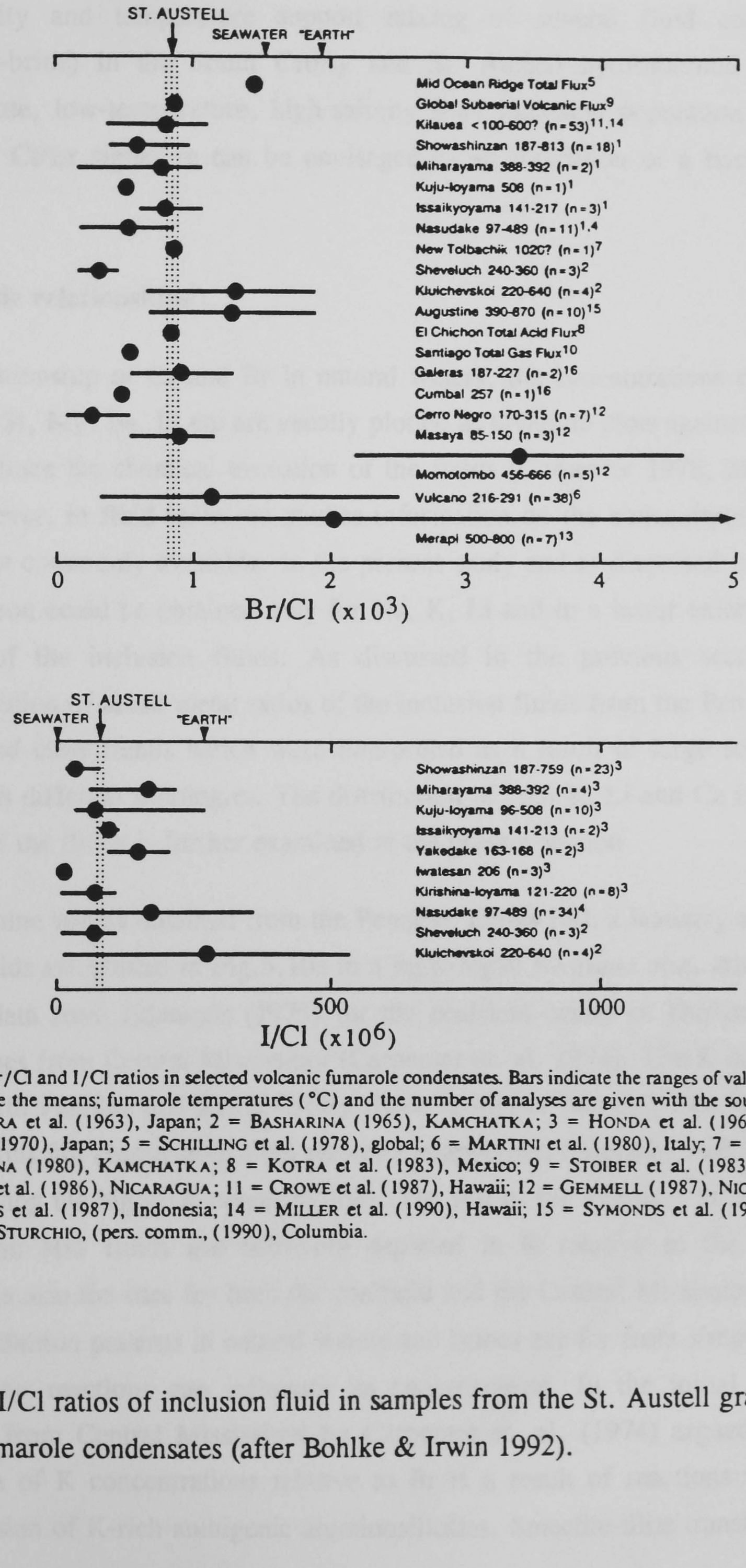


FIG. 7. Br/Cl and I/Cl ratios in selected volcanic fumarole condensates. Bars indicate the ranges of values reported; dots indicate the means; fumarole temperatures (°C) and the number of analyses are given with the sources of data: 1 = SUGIURA et al. (1963), Japan; 2 = BASHARINA (1965), KAMCHATKA; 3 = HONDA et al. (1966), Japan; 4 = HONDA (1970), Japan; 5 = SCHILLING et al. (1978), global; 6 = MARTINI et al. (1980), Italy; 7 = MENYAILOV and NIKITINA (1980), KAMCHATKA; 8 = KOTRA et al. (1983), Mexico; 9 = STOIBER et al. (1983), global; 10 = STOIBER et al. (1986), NICARAGUA; 11 = CROWE et al. (1987), Hawaii; 12 = GEMMELL (1987), NICARAGUA; 13 = SYMONDS et al. (1987), Indonesia; 14 = MILLER et al. (1990), Hawaii; 15 = SYMONDS et al. (1990), Alaska; 16 = N. C. STURCHIO, (pers. comm., (1990), Columbia.

Fig.5.9. Br/Ca and I/Cl ratios of inclusion fluid in samples from the St. Austell granite and selected volcanic fumarole condensates (after Bohlke & Irwin 1992).

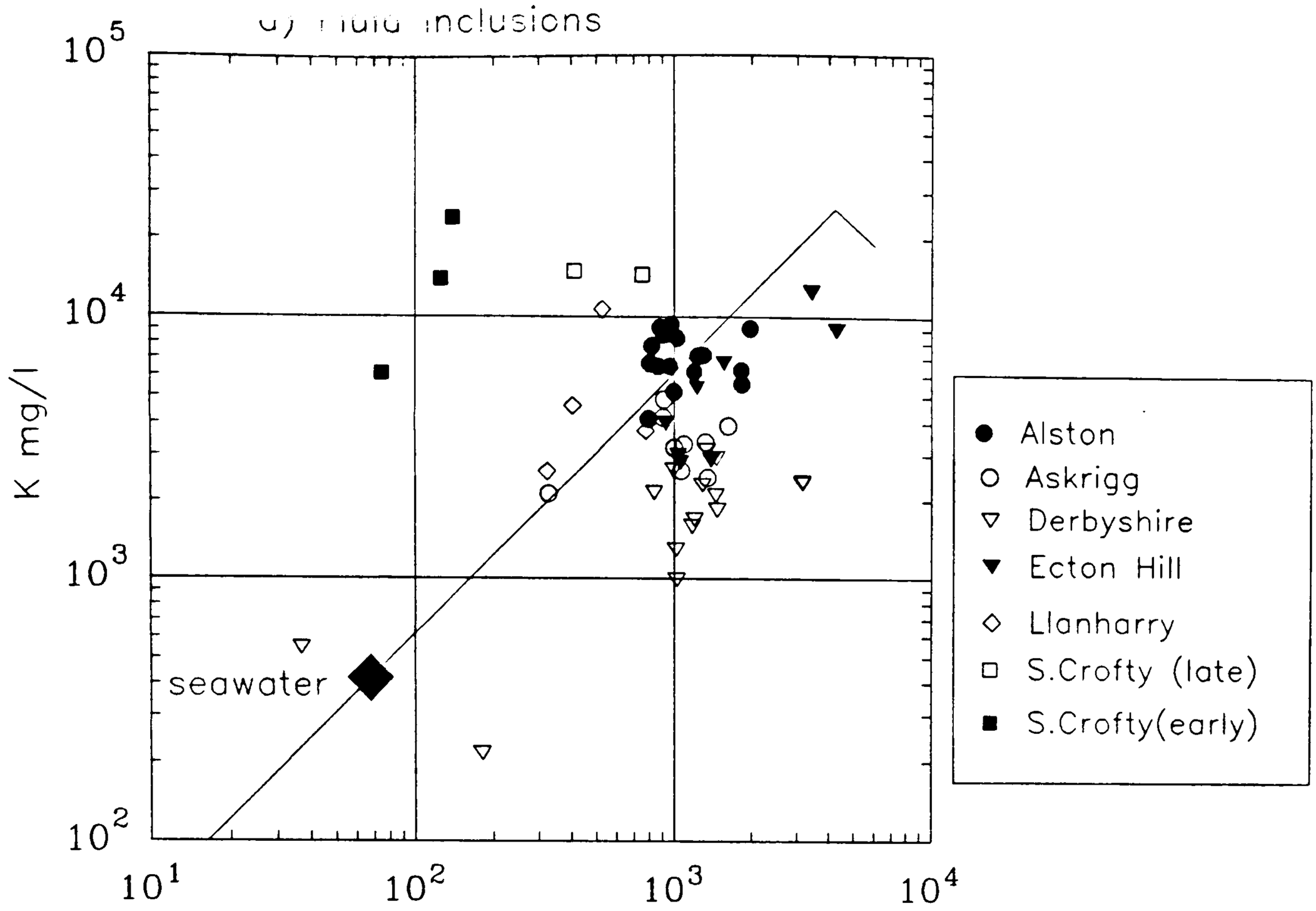
temperature fluid-rock interactions. More information is needed for the Cl-Br distribution in igneous biotites in order to clearly evaluate their potential as sources of Cl and Br and overall salinity in general. The observed overlap in Cl/Br patterns coupled with large variations in salinity and temperature support mixing of several fluid components (magmatic-meteoric-brine) in the South Crofty and St. Austell hydrothermal systems. However, for the late, low-temperature, high-salinity fluid inclusion population at South Crofty, the "brine" Cl/Br signature can be envisaged as an indication of a basinal-brine affinity.

5.6. Cation-Bromide relationships

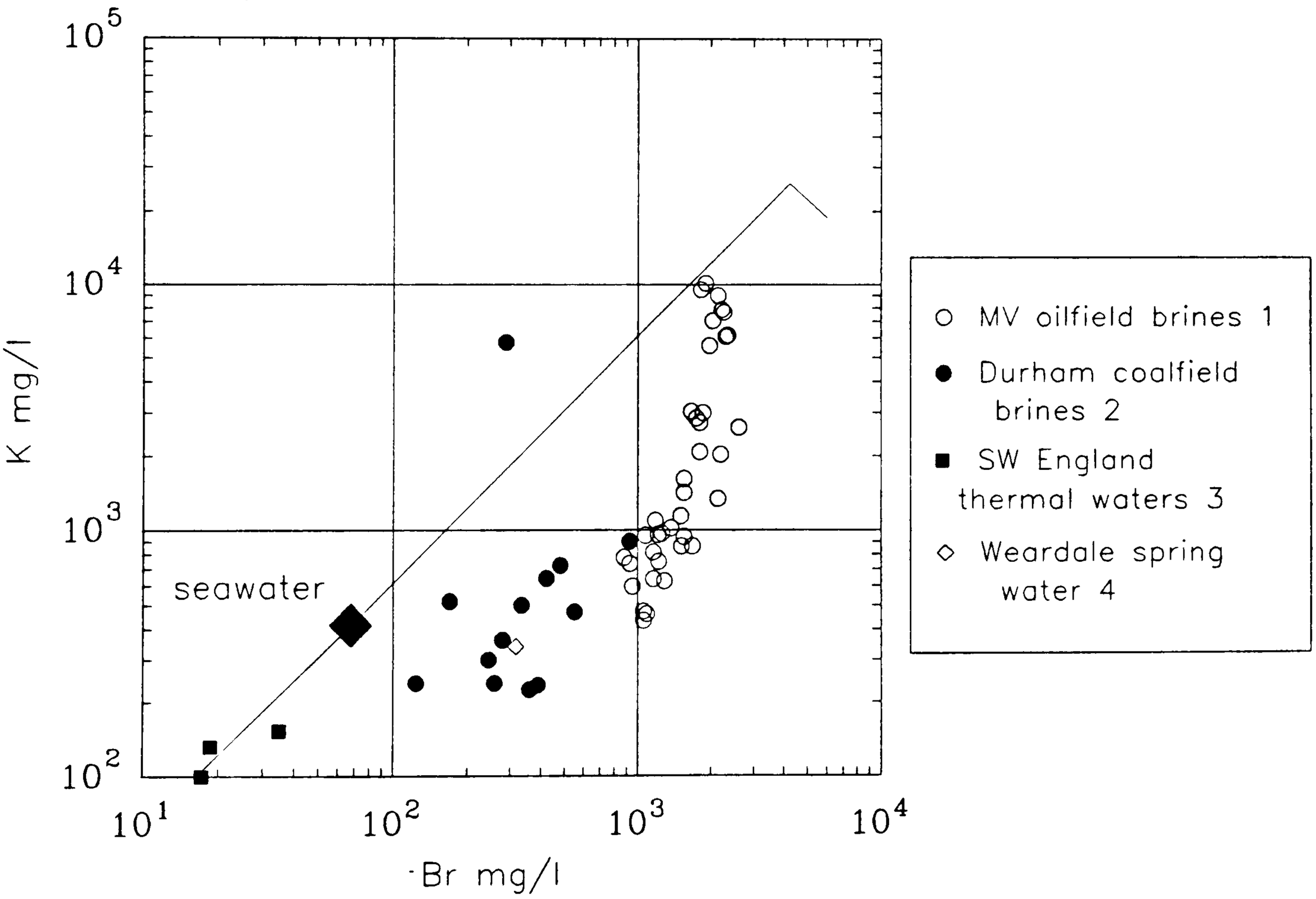
Apart from the relationship of Cl and Br in natural waters, the concentrations of cations such as K, Ca, Na, Sr, Mg, Ba, Li etc are usually plotted as bivariate plots against Cl or Br in order to further trace the chemical evolution of the fluids (Carpenter 1978, MacAffrey et. al. 1987). However, in fluid inclusion studies information on the concentrations of all these elements is not commonly available. In the present study and as discussed in Chapter 3, reliable information could be obtained only for Na, K, Li and to a lesser extend for the Ca concentration of the inclusion fluids. As discussed in the previous sections, the geographical distribution of alkali metal ratios of the inclusion fluids from the Pennines and South Crofty defined clear trends which were interpreted as a result of large scale fluid-rock interaction with different lithologies. The distribution of both K, Li and Ca in relation to the Br contents of the fluids is further examined in the present section

Potassium and bromine values obtained from the Pennine, Ecton Hill, Llanharry and South Crofty inclusion fluids are plotted in Fig.5.10a in a logK-logBr bivariate plot. Also plotted in Fig.5.10b, are data from Edmunds (1975) for the coalfield brines of Durham and of modern oilfield brines from Central Mississippi (Carpenter et. al. 1974). The K-enrichment observed in the North Pennine and South Crofty fluids is further demonstrated here. Data from these two regions fall clearly above the seawater evaporation trajectory with the South Crofty fluids exhibiting the higher K concentrations. The rest of the Pennines as well as the Llanharry and Ecton Hill fluids are relatively depleted in K relative to the seawater evaporation line as is also the case for both the coalfield and the Central Mississippi brines. The potassium distribution patterns in natural waters and brines are far from simple since a number of diagenetic reactions can influence its concentration. In the initial study of sedimentary brines from Central Mississippi by Carpenter et. al. (1974) argued that the substantial variation of K concentrations relative to Br is a result of reactions with clay minerals and formation of K-rich authigenic aluminosilicates. Smectite-illite transformation

a) Fluid inclusions



b) Brines and thermal waters

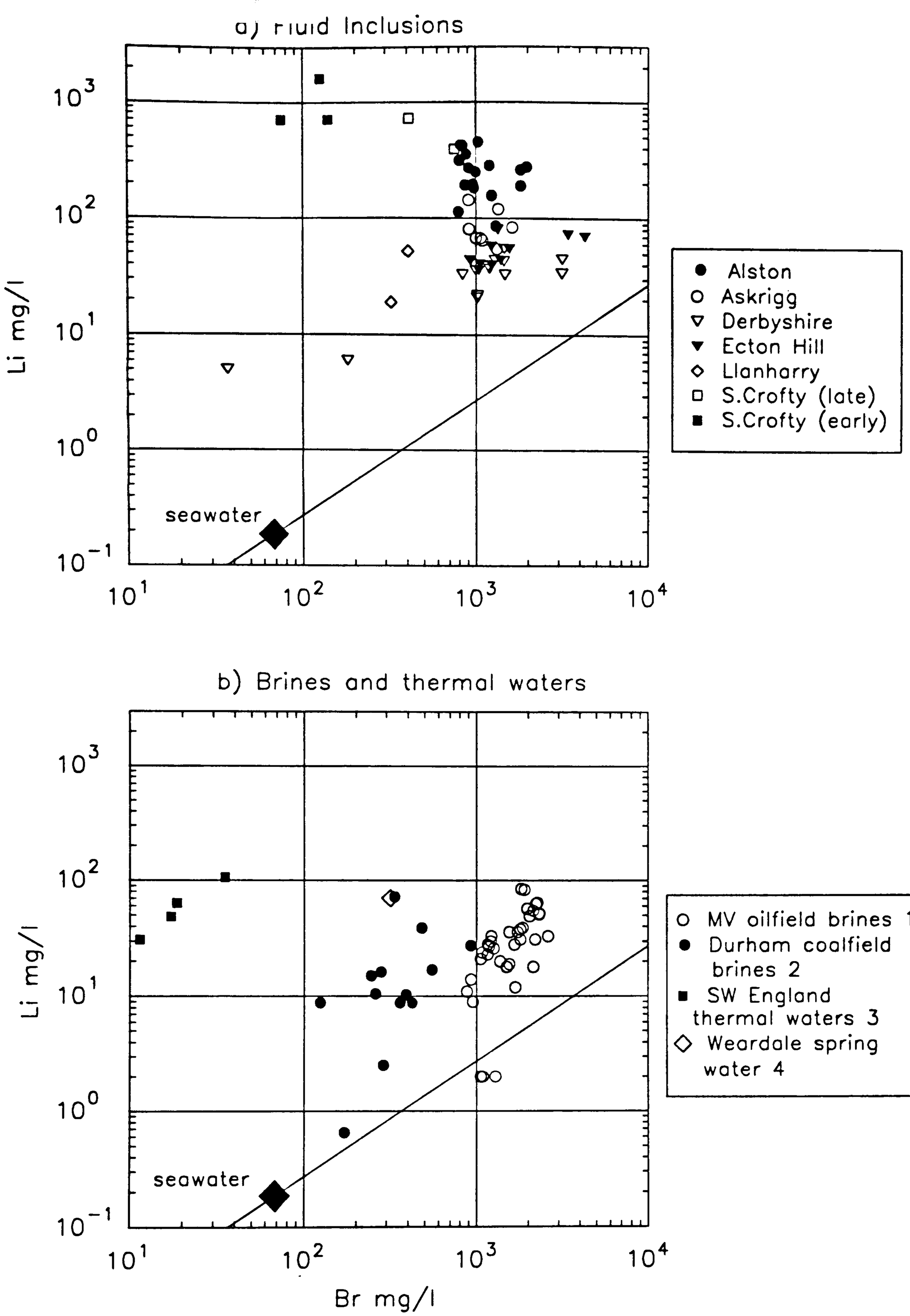


Figs.5.10a-b. bivariate logarithmic plots showing the K-Br concentrations of a) fluid inclusions studied in the present work and b) modern-day sedimentary basin brines and thermal waters (sources of data as in Fig.5.8.).

reactions have also been proposed as the cause of K depletion of saline formation waters (Sanders 1991). As can be seen from Fig.5.10b, the coalfield brines of North England are similarly depleted in K relative to the seawater line. Ion-exchange reactions favouring the fixation of K^+ during early diagenesis were similarly proposed by Edmunds (1975).

For the North Pennine fluids it is clear that an additional process than seawater evaporation influenced the K contents off the fluids. As discused in the previous section and taking into account the presence of granitic rocks in the Alston Block and South Crofty areas, it is evident that the granites provided a more than adequate source of K in the fluids. Similar high K concentrations were encountered in fluid inclusions from the St Austell granite (Rankin & Alderton 1985, Bohlke & Irwin 1992). As suggested by Bottrell & Yardley (1988), these high K contents of the inclusion fluids may not be entirely inconsistent with a magmatic origin of the fluids in those areas, since Cl-solutions in granitic systems at the suggested temperatures of trapping (500-600°C), could have K/Cl ratios in the order of 0.18-0.23 (Lagache & Weisbrod 1977). However, as it was shown in the alkali geothermometry section, the high K contents of the South Crofty inclusion fluids are not entirely consistent with equilibration temperatures indicated by the alkali geothermometers. Similar discrepancies were also encountered by Bohlke & Irwin (1992), and could indicate that either the mineral buffers were significantly different than the ones assumed in using the geothermometers or that the fluids were heated or most probably cooled out of equilibrium with the silicate minerals. Severe overprinting of multiple fluid inclusion generations in late fluorite from South Crofty was recognized by microthermometric studies. Mixing of end member fluid components could result in the observed discrepancy between the alkali geothermometers and homogenization temperatures.

The Li-Br distribution patterns of inclusion fluids, brines and thermal waters are shown in Fig.5.11a and 5.11b. As discussed in detail in section 5.4.2, the North Pennine and South Crofty fluids are characterized by distinctly high Li/Na ratios. An analogous Li-enrichment is also observed in relation to Br. However, apart from the Alston and South Crofty areas, inclusion fluids from the South Pennines, Ecton and Llanharry are also enriched in Li compared to the seawater evaporation line. A similar pattern is also observed in subsurface waters from both sedimentary and granitic environments (Fig.5.11b). In a recent study by MacAffrey et al (1987) it was demonstrated that during the evaporation of seawater Li continues to increase in the fluid during until the resulting brine becomes approximately 70-110 times more concentrated than the initial seawater. However, as can be seen in Fig.5.11, the Li-Br systematics observed in all studied inclusion fluids indicate that apart from seawater evaporation another cause of Li-increase has to be sought.

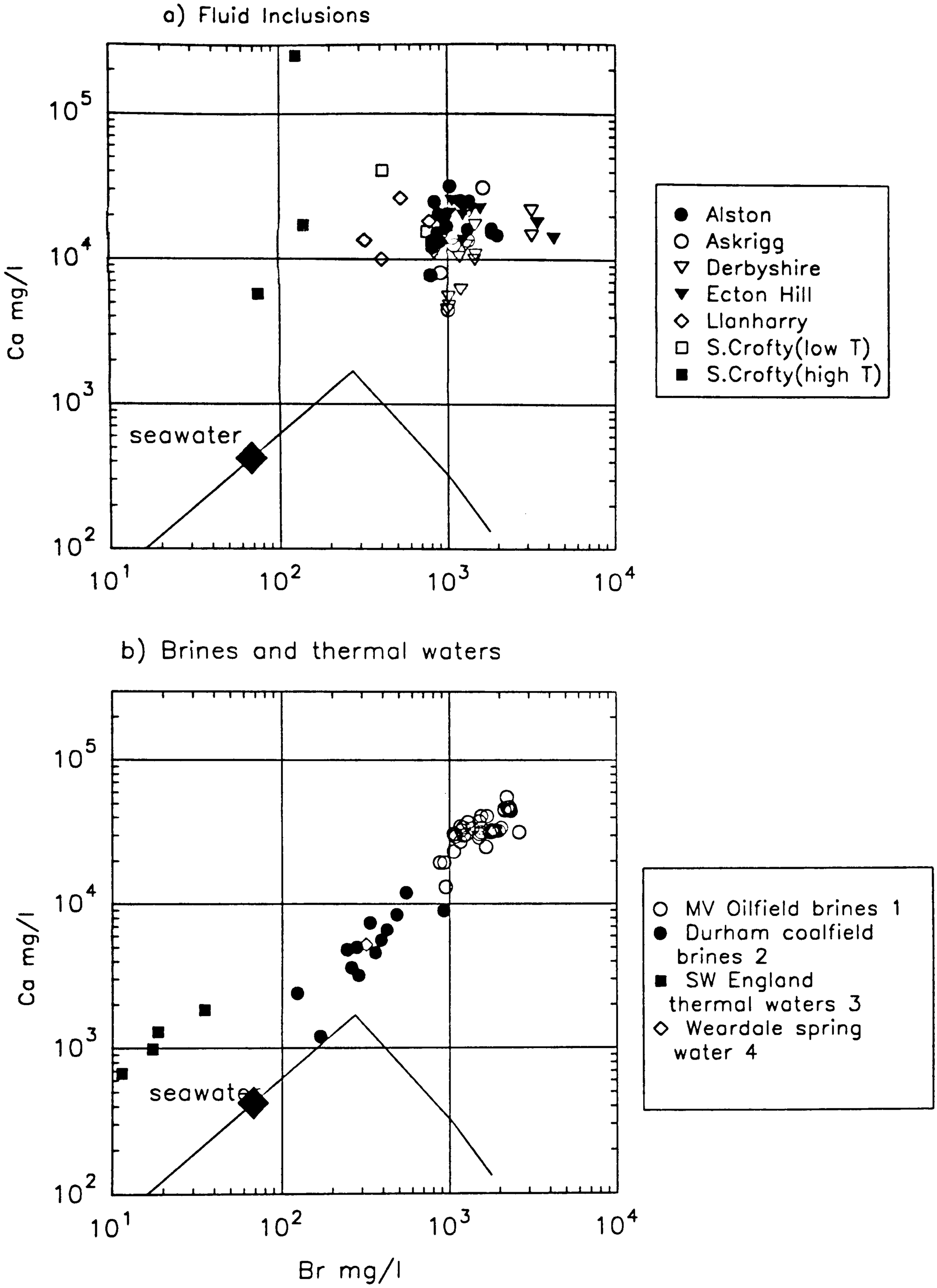


Figs.5.11a-b. Bivariate logarithmic plots showing the Li-Br concentrations of a) inclusion fluids studied in the present work and b) modern-day sedimentary basin brines and thermal waters (sources of data as in Fig.5.8).

For the South Crofty, Alston and to a lesser extend Askrigg fluids, a process involving brine interaction with granitic rocks is considered as the dominant Li-enrichment process. For the rest of the inclusion fluids and sedimentary brines, both the regional host rock geology, as well as, their lower temperatures and lower Li contents relative to the North Pennines and South Crofty, are not consistent with a granite-leaching process. Their higher than seawater Li/Br ratios have to be attributed to ion-exchange reactions. Li is generally more mobile than Na and K and therefore, can become enriched in the fluid phase by exchange with Na and K on clay minerals (Collins 1975, Edmunds et. al. 1986).

After sodium, calcium is the second most abundant cation in the inclusion fluids studied in the present work. That is also the case for the majority of modern-day sedimentary brines (i.e. Carpenter et. al. 1974, Kharaka et. al. 1987). As mentioned in Chapters 3 and 4, the calcium contents of fluid inclusions in fluorite andcalcite could not be determined by chemical analysis; consequently, the relative Na-Ca levels of inclusion fluids were estimated by microthermometric analysis alone. The uncertainties and errors involved in those estimates were discussed in Chapter 4. Calcium and bromine data obtained in the present study are plotted in a bivariate, logCa-logBr plot in Fig,5.12a. All inclusion fluids are Ca-rich compared to the seawater evaporation line. The same pattern is also observed in the brines from Central Mississippi and also in the coalfield brines of Durham (Fig.5.12b). A common cause of the higher than seawater Ca concentrations encountered in modern-day basinal brines is dolomitization of calcite resulting in Ca-enrichment and Mg-depletion of the fluid phase (Edmunds 1975, Connolly et. al. 1990, Spenser 1987). Reliable Mg values could not be obtained for the inclusion fluids, as Mg in most of the samples was found to be below detection limits. In general, it is conceivable that Mg values of the inclusion fluids are low.

As can be seen from Fig.5.12b, the SW England thermal waters are also enriched in Ca relative to seawater; however, their overall salinities are much lower than the ones encountered in fluid inclusions and sedimentary brines. Edmunds et al (1984, 1986) proposed that these waters, of invoked meteoric origin, acquired both their Na and Ca contents from feldspars. Their molar Na/Ca ratios fall in the range between 1.3 and 4, and are lower than those predicted from the stoichiometry of the reaction of oligoclase to kaolinite suggesting either a degree of preferential dissolution of more anorthitic feldspar or an incongruent process (Edmunds et. al. 1984). Both the SW England thermal waters and the high temperature inclusion fluids from South Crofty exhibit a quite separate Ca-Br distribution pattern from the rest of the inclusion fluids and modern-day sedimentary brines in general. They are clearly Br-depleted and Ca-rich. Despite the fact that a number of the



Figs.5.12a-b. Bivariate logarithmic plots showing the Ca-Br concentrations of a) fluid inclusions studied in the present work and b) modern-day sedimentary basin brines and thermal waters (sources of data as in Fig.5.8).

high temperature fluids at South Crofty are also characterized by high salinities, their high temperature and chemical composition do not indicate a basinal-brine affinity. They most possibly represent the result of varying degrees of mixing between magmatic-meteoric and possibly brine end members. A similar process was also favoured by Farmer (1991) who examined these early, high temperature fluids in greater detail. The severe overprinting of several fluid populations masks the original features of these fluids and seriously restrains the identification of their ultimate origin. The low temperature component of the South Crofty fluids has a similar Ca-Br signature to the Pennine samples and to the sedimentary basin brines in general. Both the Cl-Br ratios and the K-Na-Li-Ca systematics of these fluids strongly supports a sedimentary brine origin.

5.7. Summary of results and general discussion

For the majority of the fluid inclusions examined in the present study both the alkali metal ratios, as well as, their halogen signature are consistent with a basinal-brine origin. Large scale fluid-rock interactions with different lithologies are envisaged as the cause of the geographical trends defined by the distribution of the alkali metal ratios. The influence of the underlying granites in modifying the chemistry of the ore-forming fluids is demonstrated by the high K and, more profoundly Li, concentrations of the North Pennines inclusion fluids. The granite-leaching model is further supported by the elevated Li concentrations of the South Crofty fluids. Furthermore, the low temperature, high salinity fluid inclusion population at South Crofty can also be interpreted as a modified basinal brine since, in terms of both temperature, salinity and overall chemical composition has many aspects in common with the North Pennine fluids.

The similarity between modern-day sedimentary basin brines and fluid inclusions becomes more evident in view of their halogen signature. The Cl/Br ratios of inclusion fluids from all three Pennine orefields, and also of Ecton Hill and Llanharry were found to be constrained by relatively narrow limits and remarkably similar to those of modern oil field brines. Their high Br contents relative to seawater are not consistent with processes involving interaction with evaporite sequences. Overall, the Cl/Br fluid inclusion data indicate that subaerial seawater evaporation and small scale dilution by fresher waters may be the cause of their high Br contents and high salinities. The striking homogeneity of both temperature and chemical composition of inclusion fluids encountered in the classical MVT deposits is also evident in the Pennines. No significant difference was recognized in the Ecton Hill and Llanharry fluids. Their Cl/Br ratios fall in the range defined by the Pennine samples. Therefore, a similar evolution can be postulated for the fluids responsible for both

the Pb-Zn-dominant and the Cu-rich mineralization in the Pennines and Ecton Hill respectively. In the Pennines, the only deviation from the general high salinity, high Br pattern is encountered in two Derbyshire fluids in fluorite from Dirtlow Rake and Blue John Cavern. These fluids are characterized by very low salinities (lower than seawater) and are commonly associated with hydrocarbons. The very restricted occurrence of these fluids in Derbyshire argues against their direct participation to the base-metal mineralization in the region.

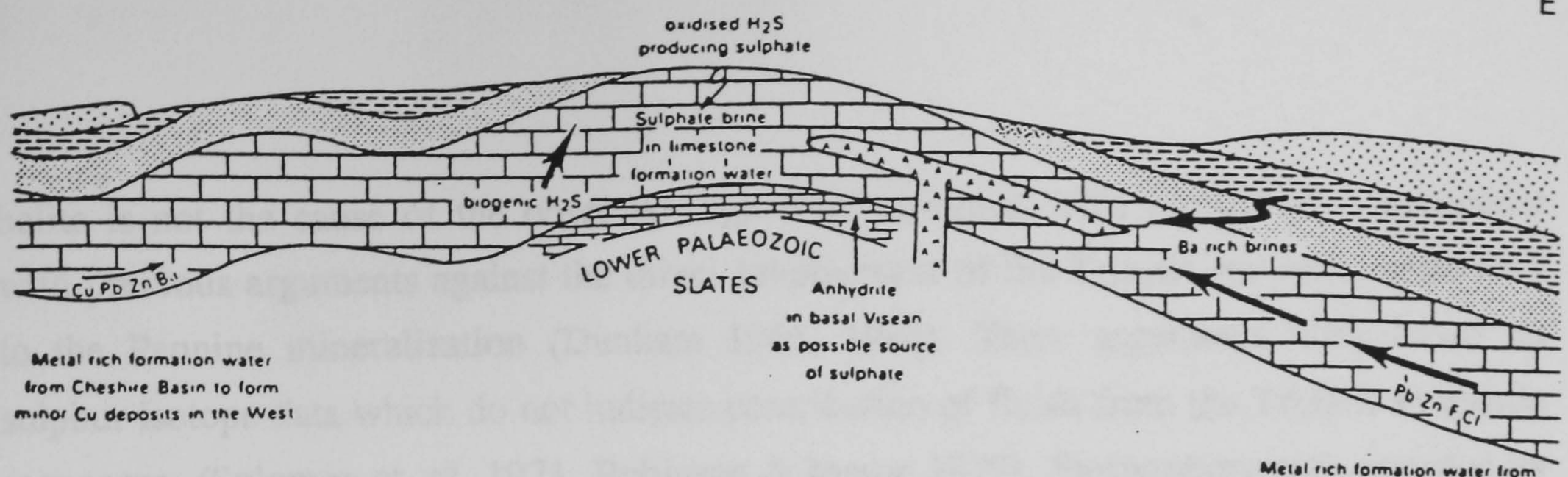
A sedimentary brine component was also recognized in the late stage of mineralization at South Crofty. Cl/Br ratios in these low temperature fluids strongly resemble those of the Pennines and of sedimentary brines in general. The Cl-Br signature of the early, high-temperature fluids, although significantly different, does not provide conclusive evidence regarding their origin.

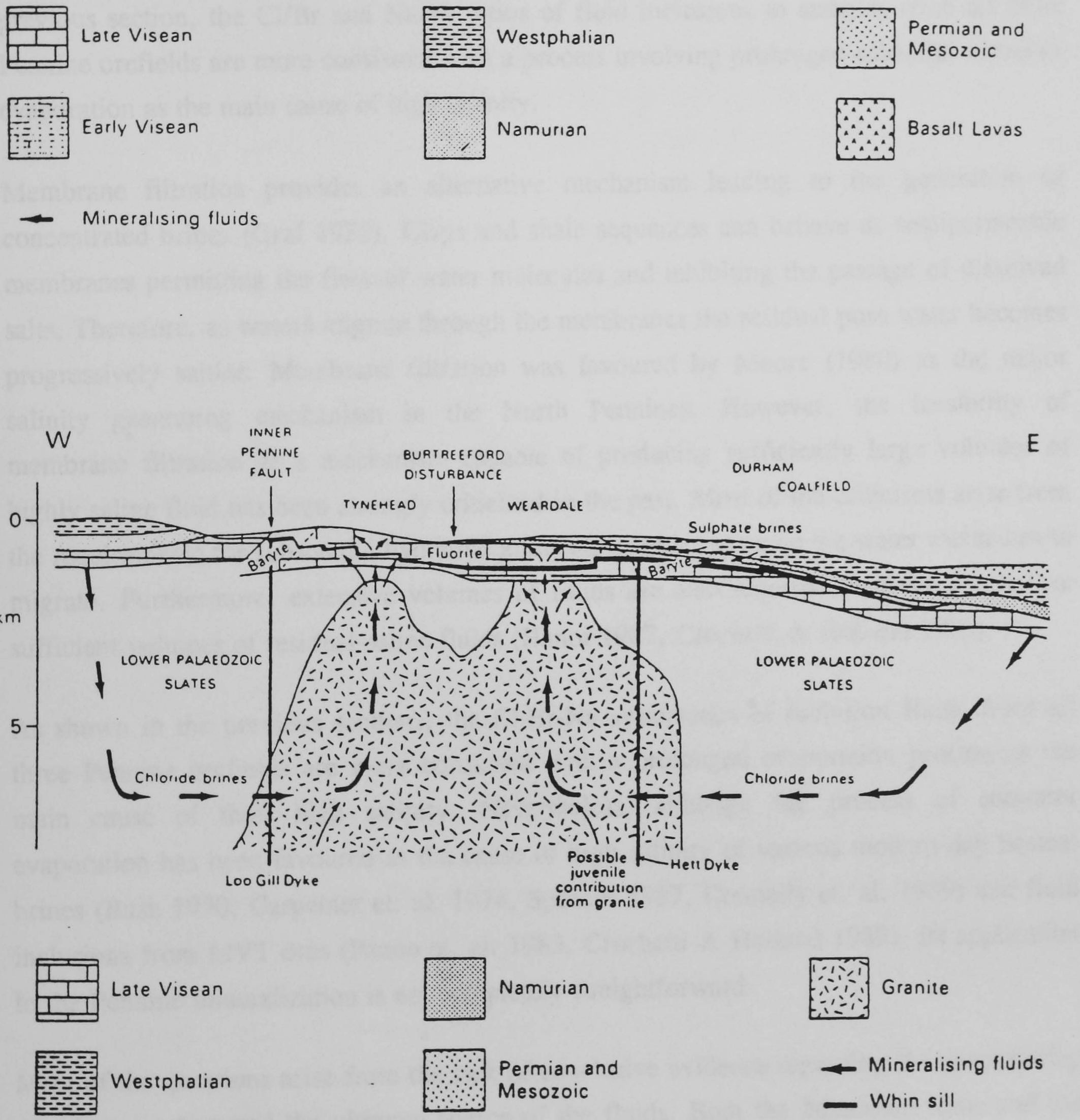
5.8. Implications for the source and evolution of mineralizing fluids in the Pennine orefields

As noted in the previous section the combined results from microthermometry and chemical analysis of fluid inclusions support the general sedimentary basin evolution models for ore genesis in the Pennines. Such models, involving expulsion of saline brines from sedimentary sequences have been proposed by many previous authors (Colman et. al. 1989b, Worley & Ford 1977, Dunham 1983, Solomon et. al. 1971, Mostaghel & Ford 1986). Schematic representations of these models for the North and South Pennines are shown in Figs.5.13a and 5.13b.

Nevertheless, despite the general agreement regarding the ore-forming potential of sedimentary brines in the Pennines and in MVT ores in general, there are still aspects not fully understood. As discussed in Chapter 2, the ultimate origin of the water component and the source of metals and sulphur have been subjects of considerable debate. Furthermore, the processes leading to the generation of highly saline, ore-forming brines (as indicated from fluid inclusions), have not been investigated thoroughly. This aspect is further examined here in view of data on the Cl-Na-Br contents of fluid inclusions.

As discussed in greater detail in the previous section, there are three basic mechanisms through which sedimentary brines can acquire high salinities. These are: a) Leaching of evaporites b) Prolonged seawater evaporation c) Membrane filtration. The Cl/Br and Na/Br data of fluid inclusions in samples from all three Pennine orefields indicate that leaching of





Figs.5.13a-b. Schematic representations of previously proposed genetic models for mineralization in the a) South Pennine and b) North Pennine Orefields (after Worley & Ford 1977, and Solomon et. al. 1971).

halite is not the cause of the observed high fluid salinities. This suggestion is consistent with previous arguments against the direct involvement of the Triassic evaporite sequences to the Pennine mineralization (Dunham 1966, 1983). These arguments were based on sulphur isotope data which do not indicate contribution of fluids from the Triassic evaporite sequences. (Solomon et. al. 1971, Robinson & Ineson 1979). Furthermore and as noted by Dunham (1983), leaching of these evaporite sequences would require percolation of the ore forming fluids through the impermeable Namurian shale cover. Overall, as shown in the previous section, the Cl/Br and Na/Br ratios of fluid inclusions in samples from all three Pennine orefields are more consistent with a process involving prolonged subaerial seawater evaporation as the main cause of high salinity.

Membrane filtration provides an alternative mechanism leading to the generation of concentrated brines (Graf 1982). Clays and shale sequences can behave as semipermeable membranes permitting the flow of water molecules and inhibiting the passage of dissolved salts. Therefore, as waters migrate through the membranes the residual pore water becomes progressively saltier. Membrane filtration was favoured by Moore (1980) as the major salinity generating mechanism in the North Pennines. However, the feasibility of membrane filtration as a mechanism capable of producing sufficiently large volumes of highly saline fluid has been strongly criticized in the past. Most of the criticisms arise from the requirements for substantial hydraulic gradients in order to cause the water molecules to migrate. Furthermore, extensive volumes of fluids are also required in order to produce sufficient volumes of residual-saline fluids (Hanor 1987, Crochetti & Holland 1989).

As shown in the previous sections, the Cl-Br-Na systematics of inclusion fluids from all three Pennine orefields are more consistent with a prolonged evaporation process as the main cause of their high salinity. Nevertheless, although the process of seawater evaporation has been favoured as the cause of high salinity of various modern-day basinal brines (Bush 1970, Carpenter et. al. 1974, Spencer 1987, Connolly et. al. 1989) and fluid inclusions from MVT ores (Panno et. al. 1983, Crochetti & Holland 1989), its application to the Pennine mineralization is not completely straightforward.

Most of the questions arise from the lack of conclusive evidence regarding the exact timing of mineralization and the ultimate source of the fluids. Both the Namurian shale and the Dinantian limestone sequences have been proposed as possible sources of ore-fluids in the Pennines (Solomon et. al. 1971, Robinson & Ineson 1979, Dunham 1983, Colman et. al. 1989b). The Namurian shales were particularly favoured as sources of ore-fluids on the basis that they can provide both ore-metals and heat (Jones & Plant 1989). On the basis of

Sr isotope data from fluorites and a calculated fluid inclusion age of 206My (based on the Rb/Sr isochron), Shepherd et. al. (1982) also favoured a shale source for the fluids in North Pennines. However, and as emphasized by Dunham (1983), because the age of mineralization is not unequivocally confirmed, such a model needs further consideration before being conclusively accepted. Taking into account these general uncertainties, the applicability of the seawater evaporation process will be discussed separately for shale and limestone fluid sources.

In general, the subaerial evaporation process is difficult to reconcile in the dominantly humid conditions indicated by the Namurian shale sequences. Recent geochemical and sedimentological evidence from the Namurian shales indicates formation of deltas at the edge of the basins giving rise to turbiditic sediments that were followed by marine transgressions. Periods of higher salinity are indicated by the presence of goniatite phases in the pelagic interbeds (Jones & Plant 1989). However, taking into account the criticism surrounding the membrane filtration process, it is not clear, how salinities as high as those indicated by the fluid inclusions can be produced by the shale sequences alone.

If the shales are accepted as the source of fluids, additional processes have to be invoked to explain the high salinity and the Cl/Br systematics of the fluids. The following sequence of events can be suggested. i) initial membrane filtration and expulsion of the residual pore fluids from the shales. ii) down-dip movement of the dense fluids into the limestone sequences. iii) Further increase in salinity through subaerial evaporation. iv) further compaction and migration of fluids up-dip through the limestones coupled with minor dilution with fresh water. More information on the texture, mineralogical and chemical composition of the shales would be of great value in order to further assess their potential as sources of highly saline ore-forming fluids.

The subaerial evaporation process is more easily reconciled if the Dinantian limestones are considered as the sources of ore-fluids. Connate water could originate from the deep parts of the Dinantian sequence (Fig.5.14b) where there is evidence of hypersalinity. In the South Pennine region, the Hathern I borehole at the margin of Widmerpool gulf has revealed regressive sabkha evaporites at the base of the Dinantian with nodular anhydrite (Llellwellyn & Stabbins 1968). Also a previously unsuspected extension of the Edale gulf has recently been proven by the Eyam borehole which penetrated nearly 2000m of limestones. Nodular anhydrites and dolomites of sabkha affinity were also encountered in the basal carbonate units (Anderton et. al. 1983). In the Northern Pennine region no such evaporite sequences have been encountered. Evidence of hypersalinity in the form of

stromatolite bearing limestones is seen in the Northumberland gulf during periods of delta absence (Anderton et. al. 1983), whereas, anhydrites have been encountered in Visean limestones in west Cumberland (Llewellyn et. al. 1968). In the case of fluids originating from the deep Carboniferous limestone sequences, the metals, fluorine and possibly barium could be provided by transformation of unstable aragonite to calcite during early diagenesis and dolomitization of calcite (Ferguson et. al. 1975, Worley & Ford 1977).

As far as the low salinity component of the Derbyshire fluids is concerned, a process proposed by Mostaghel & Ford (1986) and Price (1976) may be considered. They suggest that hydrocarbons and connate waters can coexist initially as a single phase at high temperatures. But on increasing salinity and/or decreasing temperature hydrocarbons will exsolve from the solution. Therefore, as connate waters increase in salinity and decrease in temperature moving upwards in the sedimentary sequence, petroleum will be separated and pooled in front of the advancing brines. This model provides an explanation on the origin of these low salinity high temperature fluids of Derbyshire since they are commonly associated with hydrocarbon inclusions or are present in the form of mixed low salinity aqueous and oil inclusions. However, since no such fluids were encountered in any other part of the Derbyshire orefield, a process involving restricted percolation of meteoric waters along fractures in those areas is also possible.

In general, although the data presented here favour a sedimentary, marine origin for the ore fluids and indicate a process of subaerial evaporation as the source of salinity, the exact mechanism through which this is achieved is not clear. Shale membrane filtration cannot be ruled out as a possible mechanism of enhancing the salinity of the ore-fluids. Also, as noted by Hanor (1987) membrane filtration could also cause some increase of the Br content of the fluids; however, experimental evidence to confirm such a process is not available. Furthermore, as emphasized by the numerous critics of membrane filtration (e.g. Crochetti & Holland 1989, Egeberg & Aagaard 1989), more experimental evidence on the feasibility of the membrane-filtration mechanism is needed since, the generation of salinities reaching up to 5 molal Cl by membrane filtration of dilute waters have yet not been achieved experimentally. Similarly to membrane filtration, the generation of large volumes of high salinity fluids by extensive evaporation is not free from criticisms. Land & Prezbindowski (1981) argued against such a process because of the lack of sufficient volumes of brines in evaporites to account for the large volumes of resulting saline waters. Means & Hubbard (1987) have also alleged that the Cl-Br ratios of sedimentary brines might not represent a simple record of seawater concentration or halite dissolution and argued that they might be influenced by other parameters such as organic matter. However, as discussed in the

previous section, increase of the Br content of fluid inclusions due to contribution from organic matter in the South Pennines did not become evident from the data obtained in the present study. Information on the iodine content of fluid inclusions would be of great value to further evaluate the importance of organic matter in modifying the chemistry of the ore-fluids.

Overall, the data presented here are consistent with a sedimentary basin fluid expulsion process of ore formation. The homogeneity of fluid chemistry in all three Pennine orefields indicates a common evolution of the ore forming fluids in the Pennines. The Cl/Br data indicate a marine origin for the saline component and, by implication, for the ore-fluid. The data further support previously invoked similarities between modern oil-field, basinal brines and ore-forming fluids. Despite the fact that published Cl/Br data from fluid inclusions in MVT deposits are not abundant, similar Cl-Br systematics consistent with subaerial seawater evaporation, have also been encountered in fluid inclusions from the Viburnum Trend (Crochetti & Holland 1989, Panno et. al. 1983). For the Pennine mineralization further information on the Br contents of the possible source rocks (shales or Carboniferous limestones) is needed in order to resolve questions surrounding the feasibility of both membrane filtration and subaerial evaporation processes. Evidence on the isotopic composition of trace ore-metal contents of both the shales and limestones, as well as, on the oxygen-hydrogen isotopic composition of fluid inclusions will be of great value in further delineating the source of the ore-fluids.

As discussed in the previous sections, the observed variation of the alkali metal ratios in the three Pennine orefields indicates modification of the initial brine through fluid-rock interaction with different lithologies. The higher K and Li contents of the inclusion fluids in the Northern Pennine orefield can be accounted for by temperature-related reactions with granitic basement rocks (Fig.5.13b. Therefore, previous interpretations involving direct contribution of granite derived fluids to the mineralization (Sawkins 1966a) are not considered necessary to explain the high K and Li contents of the inclusion fluids from the North Pennine orefields.

Also important is the fact that inclusion fluids in calcite samples from the Cu-rich mineralization of Ecton Hill are virtually undistinguishable from those in samples from the rest of the Derbyshire orefield. Therefore from the data presented so far a similar fluid evolution for both sets of fluids seems likely. This aspect will be discussed in more detail in the following Chapter in the view of new sulphur isotope data.

Chapter 6

A Sulphur Isotope Study on the Ecton Hill Cu Deposit

6.1. Introduction

The sulphide mineralization of Ecton Hill is of special interest in the context of the present study because, unlike the rest of the Derbyshire deposits, the ore paragenesis is dominated by copper instead of lead and zinc. The dominance of Cu in the paragenesis and also the location of the orebodies (at the south-western edge of the Derbyshire Dome) has led previous authors to suggest a separate source for the ore-forming fluids compared to those for the rest of the orefield, and to invoke genetic links between the Ecton mineralization and the red-bed copper deposits in the Cheshire Basin (Aitkenhead et. al. 1985, Masheder & Rankin 1988). However, as shown in Chapters 4 and 5, the Ecton Hill inclusion fluids are remarkably similar to those throughout the Derbyshire orefield (Fig.4.13). Homogenization temperatures are narrowly constrained between 60-90°C, whereas, total salinities fall in the range between 18-24% NaCl. Therefore, a sulphur isotope study was carried out on both sulphate and sulphide minerals from Ecton in an attempt to resolve aspects of the origin of sulphur species and to further delineate the nature and chemical evolution of the mineralizing fluids. The geology of the Ecton Hill deposit was briefly reviewed in Chapter 2. A more detailed description of the local stratigraphy, structural controls and paragenesis is given in the following section.

6.2. Geological Background

The Ecton Hill copper mines are situated to the west of the Peak District mining field within the Staffordshire border in the valley of the river Manifold. The geology of the area has been described by Critchley (1979), Aitkenhead & Chisholm (1982), Aitkenhead et. al. (1985) and, Astrop (1987). The following description is based on the above mentioned publications. The mineralization is restricted to the central parts of two major structures, the Ecton and Mixon-Morridge anticlines, where Lower Carboniferous (Dinantian) limestones are flanked by younger mudstones (Fig.6.1). A generalized representation showing the lateral and vertical relationships between Dinantian formations in the Ecton Hill and adjacent areas is shown in Fig.6.2.

Pre-Carboniferous rocks do not crop-out in the area. However, extrapolation from the Caldon Low borehole, 10Km south of Ecton Hill, stresses the possibility that the lowest

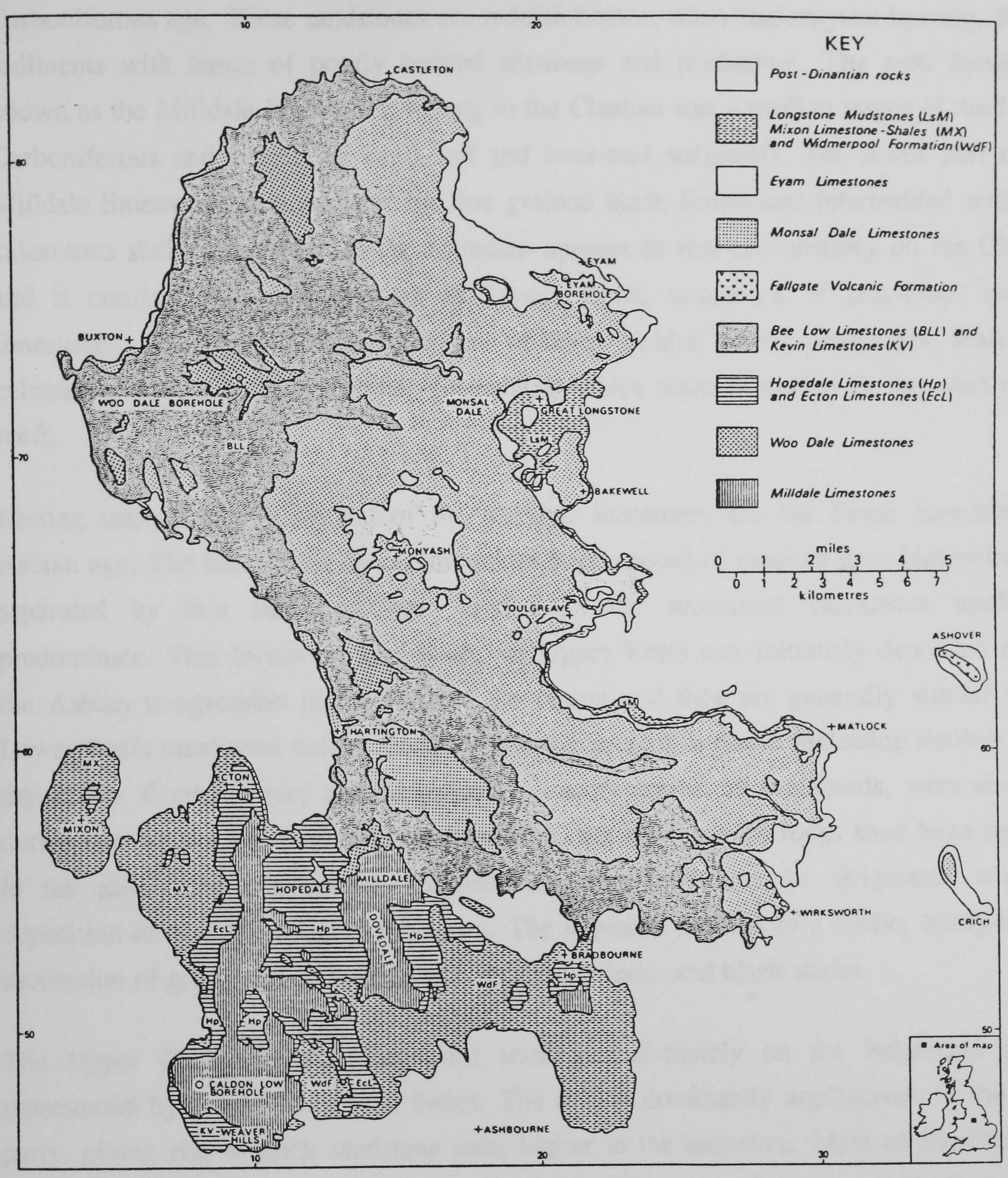


Fig.6.1. Sketch-map showing the Dinantian formations of the Peak District (South Pennines), (after Aitkenhead et. al. 1985).

rocks underlying the area belong to the Redhouse sandstone formation of Devonian or Carboniferous age. These sandstones are reddish-brown, often chalcopyrite-bearing, pebbly sediments with bands of poorly bedded siltstones and mudstones. The next formation, known as the Milldale limestones, belong to the Chadian and Arundian stages of the Lower Carboniferous and consist of knoll-reef and inter-reef sediments. The lower part of the Milldale limestones is dominated by fine grained black limestones interbedded with thin calcareous shales. The base of the Arundian appears to rest conformably on the Chadian and it consists of a unit, known as Lower Reefs, composed of pale-grey, micritic limestones. The Upper Arundian consists of thinly bedded muddy limestones, shales and calcareous shales. (Upper Milldale limestones) which were deposited to the west of the reefs.

Resting unconformably on top of the Milldale limestones are the Ecton limestones of Asbian age. The base of the Ecton limestones is composed of medium grey biosparite beds separated by thin shale partings. Higher in the succession calcareous mudstones predominate. This formation known also as Upper Reefs was initiatialy deposited during the Asbian trangression in the East of the region and they are generally similar to the Lower Reefs mentioned before. Stromatolites are present in places indicating shallow water deposition. Contemporary altered volcanics, locally known as wayboards, were abundant during the Asbian and Arundian sedimentation, but no extrusive rocks have been reported in the area. The argillaceous sedimentation continued into the Brigantian with the deposition of the Mixon limestone-shales. The sequence consists of a cyclic, thinly-bedded succession of grey, muddy limestones, calcareous shales and black shales.

The Upper Carboniferous (Namurian) rests unconformably on the Brigantian and is represented by the Millstone Grit facies. The unit is dominantly argillaceous in the lower parts, giving rise to thick sandstone units higher in the sequence. Most of the Namurian succession has been eroded away in the Ecton Hill area. However, indications of its presence are encountered in more western parts in the country around Leek (Aitkenhead et.al.1985)

The Hercynian orogeny is the main structural event in the region. It produced an east-west compression causing the more mobile sediments of the West to form a series of strongly linear folds with near vertical axes and roughly N-S trends (the Ecton anticline). These movements also created extensive faulting and jointing which subsequently became mineralized (Critchley 1979). The age of mineralization has been estimated on the basis of Pb radiometric dating at 180$\pm$ 40Ma (Moorbath 1962). However, because of the

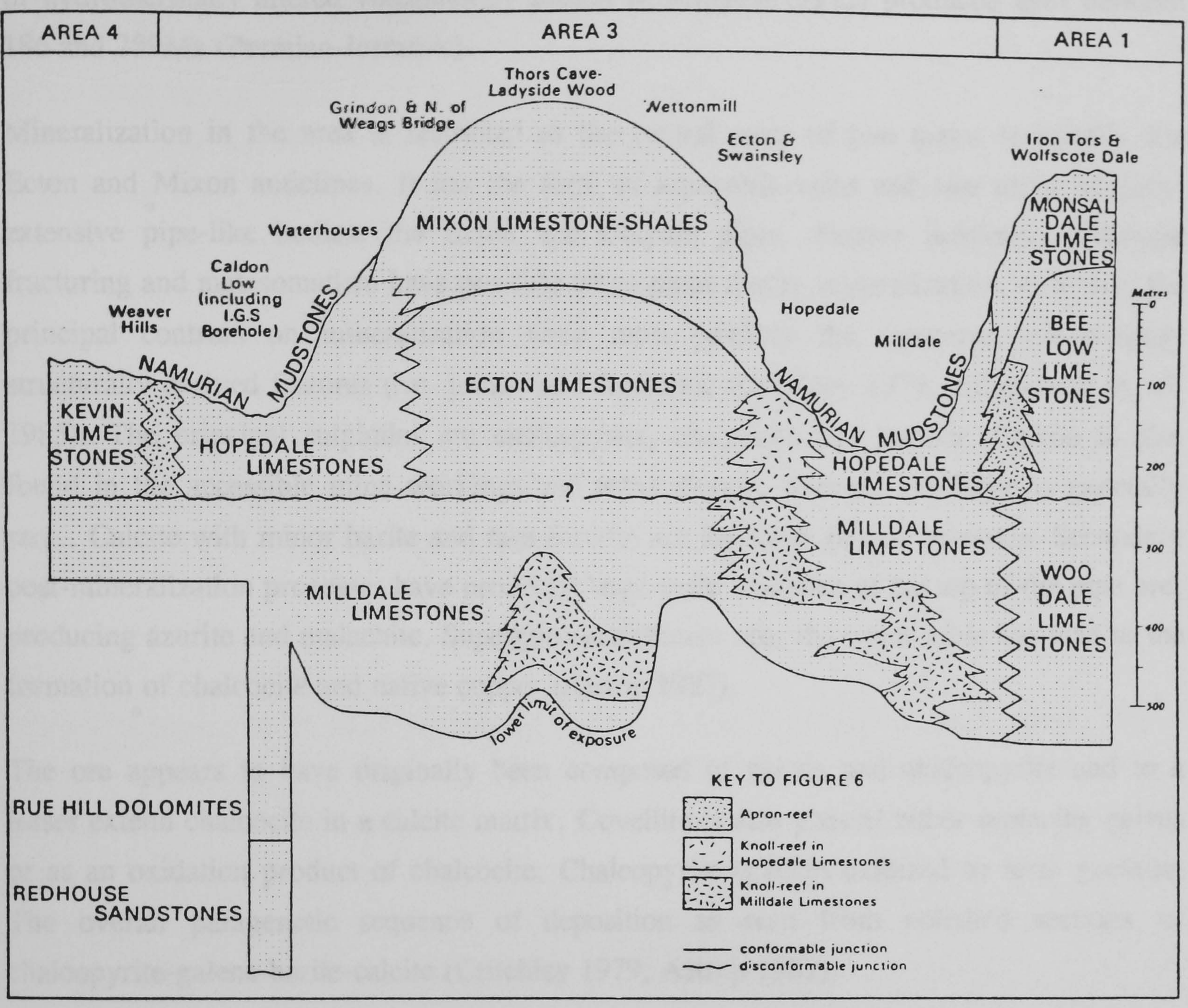


Fig.6.2. Schematic representation of the lateral and vertical relationships of Carboniferous formations in the Ecton Hill and adjacent areas (after Aitkenhead & Chisholm 1982).

radiogenic nature of lead, the reliability of this method of dating has been questioned by many authors (e.g. Dunham 1983). More recent age estimates based on radiometric dating of hydrothermally altered volcanics by Ineson & Mitchell (1972) produced ages between 186 and 289*Ma (Permian-Jurrassic)*.

Mineralization in the area is restricted to the central parts of two major structures, the Ecton and Mixon anticlines. It has the form of numerous veins and two large laterally-extensive pipe-like bodies, the Ecton and Clayton pipes. Passive infilling,, hydraulic fracturing and metasomatism have possibly taken place during mineralization, however, the principal controls on mineralization were most possibly the numerous pre-existing, structurally derived features (i.e. joints, and fractures) (Critchley 1979, Aitkenhead et. al. 1985). The principal sulphides are chalcopyrite, chalcocite and bornite. Galena is also found in the accessible mine workings and mine dumps, whereas sphalerite is generally rare.. Calcite with minor barite and rare fluorite are the main gangue minerals. Secondary post-mineralization processes have produced large scale oxidation at the top of the pipe ore, producing azurite and malachite. Supergene enrichment near the water table has lead to the formation of chalcocite and native copper (Astrop 1987).

The ore appears to have originally been composed of galena and chalcopyrite and to a lesser extend chalcocite in a calcite matrix. Covellite is also present either replacing galena or as an oxidation product of chalcocite. Chalcopyrite is often oxidized to form goethite. The overall paragenetic sequence of deposition as seen from polished sections is: chalcopyrite-galena-barite-calcite (Critchley 1979, Astrop 1987).

6.3. Previous work

Published $\delta^{34}S$ data from previous sulphur isotope studies in the Pennines and related sediment-hosted base metal deposits in the UK, are presented in Table 6.1. Also shown for comparison are values obtained in more recent studies for the red bed copper mineralization in the Triassic of the Cheshire basin. As can be seen from the data in Table 6.1, the $\delta^{34}S$ systematics vary considerably in each deposit. Such variations are also typical in MVT ores and, as noted by Heyl et. al. (1974), may indicate the complexity of the processes of ore deposition.

6.3.1 North Pennines

An extensive sulphur-carbon-oxygen isotope study was undertaken by Solomon et. al. (1971) on barite, calcite and sulphide samples from the Alston orefield in the North

Pennines. The uniformity of the isotopic composition of the barite sulphur was interpreted as an indication of a homogeneous source for sulphate. The average $\delta^{34}S$ value (+19‰) is in agreement with a Mississippian (Lower Carboniferous) seawater source for the sulphate (Thode & Monster 1965, Claypool et. al. 1980). The discrepancy between the isotopic composition of the North Pennine barites and Permian evaporites ($\delta^{34}S$ 10‰) which are similar to coeval seawater sulphate, was interpreted as an indication that Permian evaporites were not the source of sulphate in the mineralizing fluids. Solomon et. al. (1971) suggested that the barite sulphate was derived from connate water, residual from Lower Carboniferous seawater, which was present in the Carboniferous rocks when mineralization occurred. The wide range of sulphide sulphur $\delta^{34}S$ values strongly argues against a magmatic origin. A connate water source from the deeper levels of the sedimentary sequence was seen by Solomon et.al (1971) as the most possible source of sulphide sulphur and the mineralizing fluids in general. Barite was thought to be deposited as a result of mixing of reducing Ba-rich with $SO_4^=$ bearing brines.

6.3.2. South Pennines

Compared to the North Pennines, a quite different trend in sulphur isotope distribution is reported by Robinson & Ineson (1979) in the Derbyshire orefield. Both sulphate and sulphide $\delta^{34}S$ values are widespread, with values in barite ranging from +4 to +23‰ and -23 to +7‰ in the sulphides. Fractionation factors between barite and galena are too low and yield temperatures in excess of 200°C (op. cit), much higher than the fluid inclusion homogenization temperatures, interpreted by these authors as an indication of isotopic disequilibrium between barite and galena. The large spread of both sulphide and sulphate isotopic values are in agreement with ratios obtained from a variety of MVT ores elsewhere in the world (Heyl et al 1974). Isotopic disequilibrium is also a common feature of MVT ores in general. As proposed by Robinson and Ineson (1979), it is not possible to explain the isotopic trends of the South Pennine orefield by simple modification of a common sulphur source. According to these authors, the trends are better explained by mixing of different sulphur sources. Thermal sulphate reduction by hydrocarbons, was proposed as the dominant mechanism of sulphide deposition. The model favoured by Robinson & Ineson (1979) for the precipitation of sulphides involves mixing of Permian connate or sabkha brines that were derived in the east of the orefield with reducing fluids in the limestones.

Contributions from separate sources of sulphate and sulphide sulphur were also invoked for individual Pb-Zn sulphide vein deposits in Lower Carboniferous rocks of Central Wales,

West Shropshire, Tyndrum Scotland, Leadhills and Greenside (Pattrick & Russell 1989). They proposed that the underlying country rocks are the source of sulphide sulphur, whereas sulphate sulphur was derived from sulphate-rich groundwaters. However, as noted by the authors themselves, detailed information on the $\delta^{34}S$ values of the source rocks is required in order to assess the validity of the model.

Overall, the constraints on the various sulphate reduction and sulphide deposition mechanisms are far from clear. Particularly controversial are the temperature limits over which sulphate reduction (bacterial or thermochemical) takes place. A more detailed discussion on the various sulphate reduction mechanisms and the possible sulphur sources will be given in the following section, in conjunction with the data obtained in the present work.

6.3.3. Red Bed Cu-mineralization in the Cheshire Basin

The sulphur isotopic distribution in sulphate and sulphide minerals from the red-bed copper mineralization in the Triassic of the Cheshire basin were examined in a recent study by Naylor et.al (1989). A summary of the results by Naylor et. al. (1989) is also shown in table 6.1. A basinal brine expulsion model is favoured for ore genesis in the area whereas, a magmatic origin for the sulphur species is refuted by both isotopic and fluid inclusion data (op. cit.)1989). The narrow range of barite sulphur isotopic values (mean +17‰) was interpreted as an indication that the bulk of the barite sulphur was derived from the Upper Triassic evaporites (mean +19‰). The distribution of $\delta^{34}S$ values for the sulphides was interpreted as a result of a closed system reduction of a sulphate bearing brine. A thermochemical sulphate reduction mechanism is favoured by Naylor et. al. (1989). The basinal fluid expulsion model is consistent with the host rock geology of the area which involves evaporite and sandstone successions which are envisaged as the sources of sulphur and metals in the ore forming chloride brines, and also, as oxidizing agents needed for the copper mineralization. However, the feasibility of the non-bacterial sulphate reduction at temperatures below 200°C has been questioned by several authors (Anderson 1983, Ohmoto & Rye 1979). A more detailed discussion on the various sulphide precipitation mechanisms will be given in the following section in conjunction with the data obtained in the present work.

Table 6.1. Sulphur isotopic composition of sulphide and sulphate minerals from the Pennines and related sulphide deposits.

Orefield	Mineral	$\delta^{34}S$ range ‰	Reference
Alston Block	Barite ($BaSO_4$)	+17.1 to +20.9	Solomon et. al. (1971)
	Galena (PbS)	+15 to -5.9	"
Askrigg Block	Galena (PbS)	-0.6 to -3.8	Ineson & Mitchell (1975)
Derbyshire and N. Midlands	Galena (PbS)	-8.4 to +3.2	Coomer & Ford (1975)
South Pennines	Barite (BaSO4)	+4 to +23	Robinson & Ineson (1979)
South Pennines	Galena (PbS)	-23 to +7	"
Lower Carboniferous PbS-ZnS veins*	Barite ($BaSO_4$)	+12 to +24	Pattrick & Russell (1989)
	Sulphides	-10 to +18.6	
Cheshire Basin Cu-deposits	Barite ($BaSO_4$)	+13.8 to +19.3	Naylor et.al. (1989)
	Gypsum-Anhydrite	+18.4 to +20.8	
	Galena (PbS)	+1.3 to +15.7	"
	Chalcopyrite ($CuFeS_2$)	+10.7 to +16.2	"
	Bornite-tenantite	-1.8	"

* refers to the following areas: Tyndrum, Castletown, Leadhills, Force Crag, Greenside, W.Shropshire, and Central Wales (after Pattrick & Russell 1989).

6.4. Sulphur isotope distribution in the Ecton Hill deposit.

The sulphur isotope composition of barite, galena and chalcopyrite samples was determined in the present study. Most of the samples were collected from the mine dumps due to the restricted access to the underground workings. However, three sulphide (chalcopyrite-galena) samples were collected from mineralized veins in the underground workings. All sample numbers, and localities are presented in Appendix A. The analyses were carried out in the Stable Isotope Laboratories of the NERC Isotope Geosciences Laboratory, Keyworth.

6.4.1. Experimental procedure

Prior to analysis the hand specimens were crushed in a porcelain pestle and mortar and then the sulphate (barite) and sulphide (galena and chalcopyrite) mineral grains were hand picked under a binocular microscope. No further separation was needed since both the sulphate and sulphides were adequately coarse grained and hand picking, although time

consuming, was efficient. Samples and standards were prepared by mixing cuprous oxide (Cu_2O) with the materials to be analyzed. Following a procedure by Robinson & Kusakabe (1975), the sulphides were converted to SO_2 by combustion of the sulphide mixture at 1080°C. The sulphates were ground with 200mg Cu_2O plus 600mg of SiO_2 to assist burning in the sulphur line. They were combusted at a higher temperature (1120°C); the SO_3 was reduced to SO_2 whereas, CO_2 impurities were removed by cryogenic separation techniques following the procedure of Coleman and Moore (1978). The resulting SO_2 gas samples were analyzed in a V6 SIRA 10 mass spectrometer. Results are reported in the δ notation as permil (‰) deviation from the Canon Diablo Troilite standard,, CDT. The overall analytical reproducibility is better than $\pm$0.1‰.

6.4.2. Results and Discussion.

The results obtained in the present study are presented in Table 6.2 and Fig.6.3. All sulphate sulphur $\delta^{34}S$ values are high and group within a narrow range between +21.1 and +24.9‰, with a mean value of +22.5‰. In contrast, all the sulphide $\delta^{34}S$ values are negative. Chalcopyrite samples have $\delta^{34}S$ values ranging from -15.1 to -7.1‰ with a mean of -10.7‰, whereas the two galena samples yielded values of -11.2 and -7.3‰. In general, the distribution of sulphide and sulphate sulphur isotopic values, although not as widespread, is similar to the values obtained by Robinson and Ineson (1979) in samples from the Derbyshire orefield.

The $\delta^{34}S$ values of the coexisting, although not necessarily co-precipitated, chalcopyrite-galena-barite in sample ECT/1/S can be used to estimate temperatures of deposition and to examine whether these minerals have achieved isotopic equilibrium. However, the $\Delta_{BaSO4-PbS}$ fractionation factors are too low and yield temperatures in excess of 200°C. The application of the barite-chalcopyrite sulphur isotope geothermometer by Ohmoto & Rye (1979) yields a temperature of 207°C. These temperatures are much higher than the fluid inclusion homogenization temperatures (60-90°C) and are considered to represent isotopic disequilibrium between sulphate and sulphide minerals. As noted by Ohmoto (1986), sulphur isotopic disequilibrium is a common phenomenon for sulphide mineral pairs involving pyrite and chalcopyrite. According to Ohmoto (1986), this phenomenon may simply reflect the fact that pyrite and chalcopyrite did not coprecipitate with simple sulphides, since precipitation of pyrite and chalcopyrite from H_2S bearing fluids requires some mechanism of oxidation. Isotopic disequilibrium between sulphate and sulphide minerals is also common at low temperature ore-forming environments, particularly at temperatures below 200°C (Ohmoto 1986).

Table 6.2. Sulphur Isotopic data from the Ecton Hill Cu-deposit

Sample I.D.	Mineral	$\delta^{34}S‰$
ECT/1 (ECT/1/S)	chalcopyrite+(PbS+ $BASO_4$)	-7.1
ECT/4	chalcopyrite+ (calcite)	-14.8
ECT/6	chalcopyrite+(calcite)	-15.0
ECT/6	chalcopyrite+(calcite)	-15.1
ECT/7	chalcopyrite+(calcite)	-11.4
ECT/2 (ECT/1/S)	galena+($CuFeS_2$+ $BaSO_4$)	-11.2
ECT/9	galena+(calcite)	-7.3
ECT/3 (ECT/1/S)	barite+($CuFeS_2$+ PbS)	+21.4
ECT/10	barite	+23.8
ECT/11	barite+(calcite)	+24.9
ECT/12	barite+(calcite)	+21.1
ECT/12	barite+(calcite)	+21.3

In order to further examine the proposed genetic links between the Ecton Hill mineralization and the Red Bed copper deposits of the Cheshire basin it is necessary to compare the sulphur isotope distribution in the two areas. However, the two sets of data have little in common. The sulphide sulphur isotopic values of Ecton Hill are all negative whereas, the Cheshire basin sulphides have positive values, reaching up to +16.2‰. Furthermore, the $\delta^{34}S$ values obtained from the Ecton Hill barites fall in the narrow range between 21.3 and 24.9‰ (mean 21.5‰), and are heavier than the ones of the Cheshire basin mineralization (mean 17‰). The hypothesis that barite in the Cheshire basin was derived directly from solutions passing through or derived from the Triassic gypsum and anhydrite horizons within the Mercia Mudstone group ($\delta^{34}S=+19‰$), was proposed by Naylor et.al. (1989). Such a model cannot be applied to the Ecton Hill barites since the $\delta^{34}S_{BaSO4}$ values are substantially higher than the ones of the Cheshire Basin and the Triassic evaporites.

The Ecton Hill sulphate $\delta^{34}S$ values are more readily explained by the means of a connate water source. As noted by Solomon et.al. (1971), Robinson & Ineson (1979) and Pattrick & Russell (1989), high positive values of barite sulphur can be explained if Carboniferous seawater is invoked as the main source of sulphate. As shown by Claypool et. al. (1980) values of Carboniferous seawater can reach values up to +25‰ (Fig.6.4.). Ohmoto & Rye (1979) suggested that clay membrane filtration processes could modify of the isotopic composition of trapped seawater. The resulting fluid will have heavier sulphate sulphur

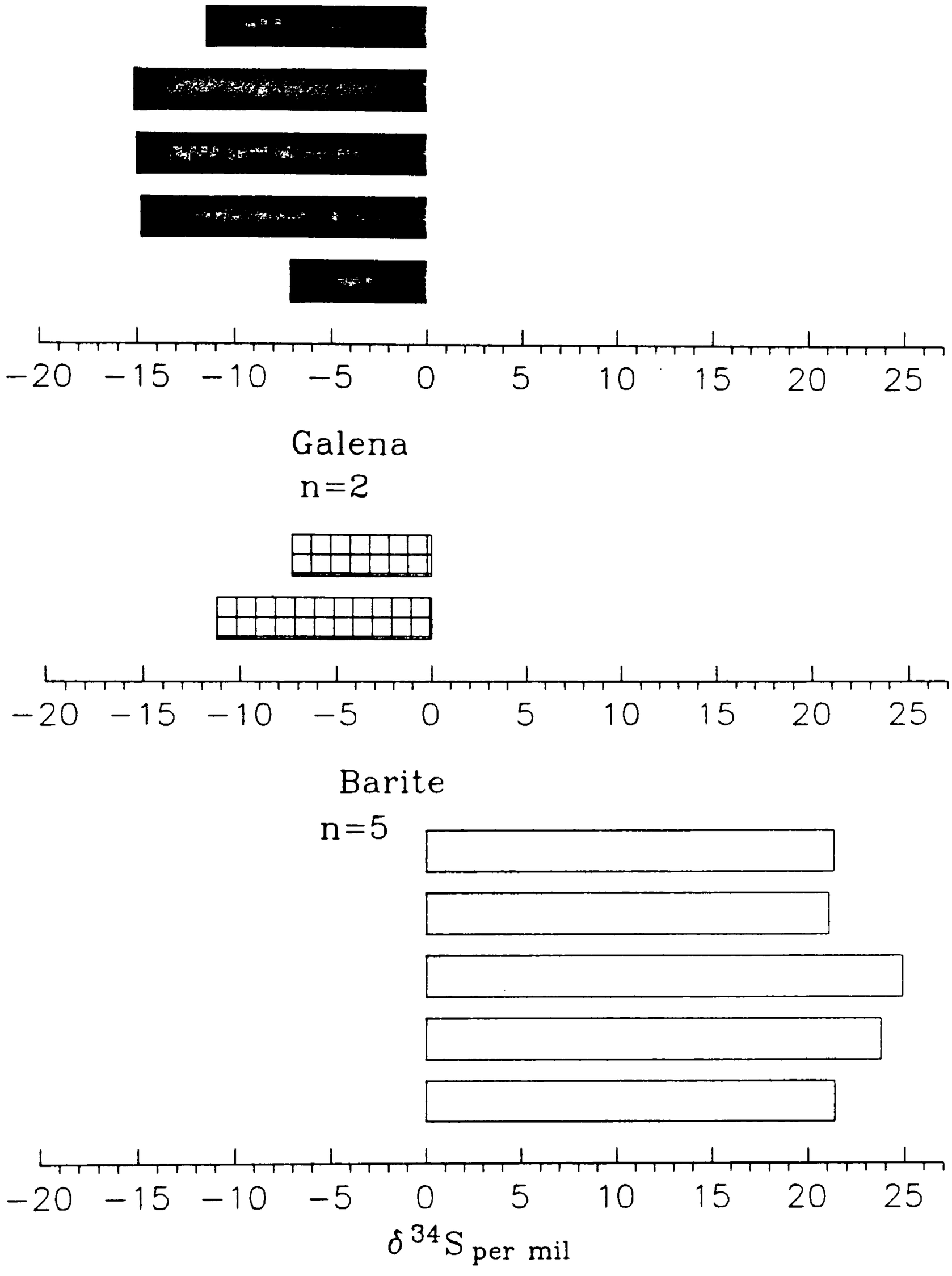


Fig.6.3. The sulphur isotopic composition of chalcopyrite, galena and barite samples from the Ecton Hill Cu-rich mineralization.

values since the lighter isotopic compounds are preferentially absorbed in the clay matrix. Minor isotopic fractionation leading to an increase of $\delta^{34}S$ values in the late stage of evaporation is also reported by Raab & Spiro (1991).

The negative and relatively wide spread $\delta^{34}S$ values of the Ecton Hill sulphides imply a more complicated process of sulphide generation. Two main mechanisms leading to metal sulphide precipitation are recognized. a) sulphate reduction b) sulphide sulphur supplied from a separate source. Bacterial sulphate reduction has been considered as a major mechanism for sulphide formation in a variety of sediment hosted deposits. The observed isotopic differences between sulphate and sulphide ($\Delta so_4\text{-}H_2s$= 20-30‰) at Ecton Hill are consistent with bacteriogenic sulphate reduction where Δ falls in the range of 40 ± 20‰ (Ohmoto & Rye 1979). Bacterial sulphate reduction is indeed recognized as an important mechanism through which sulphide is deposited in a number of sediment-hosted deposits (Trudinger et. al. 1985). Furthermore, in the case of the Ecton Hill organic mater (pyrobitumens and methane) is encountered in the limestones (Astrop 1987) and therefore, can provide the nutrient supply to the sulphur reducing bacteria. The only limiting factor in fully accepting the bacterial reduction as the main cause of sulphide deposition is the temperature range (60-90°C) indicated by the fluid inclusion homogenization temperatures. The generally accepted upper temperature limit within which sulphur reducing bacteria operate is around 50°C (Trudinger et. al. 1985). However, there are reports indicating that certain thermophyllic species can exist at temperatures up to 80°C (Pfennig & Widdell 1982). The homogenization temperatures were recorded from fluid inclusions in calcite samples. The possibility that the measurements are erroneous due to necking-down and leakage cannot be ruled out. However, large scale necking-down does not seem viable since similar readings were obtained in fluorite by Masheder & Rankin (1988). Furthermore, despite the fact that the exact position of calcite in the paragenetic sequence is not readily established, some of the calcite must have been precipitated with the sulphides since chalcopyrite inclusions are common in the calcite crystals.

Thermochemical sulphate reduction by hydrocarbons has also been proposed as a significant mechanism for hydrogen sulphide formation and the precipitation of base metal sulphides in some MVT ores (Powell & MacQueen 1984). However, reduction of sulphate in the absence of bacteria is known to be a very slow process at temperatures below 300°C and has often been ruled out as a viable mechanism in the low temperature environment (100-200°C) of MVT ores (Anderson 1983). Also, as noted by Ohmoto & Rye (1979), the mechanisms of non-bacterial sulphate reduction by organic compounds and the role of H_2S or other forms of reduced sulphur, especially at temperatures below 200°C, are still not

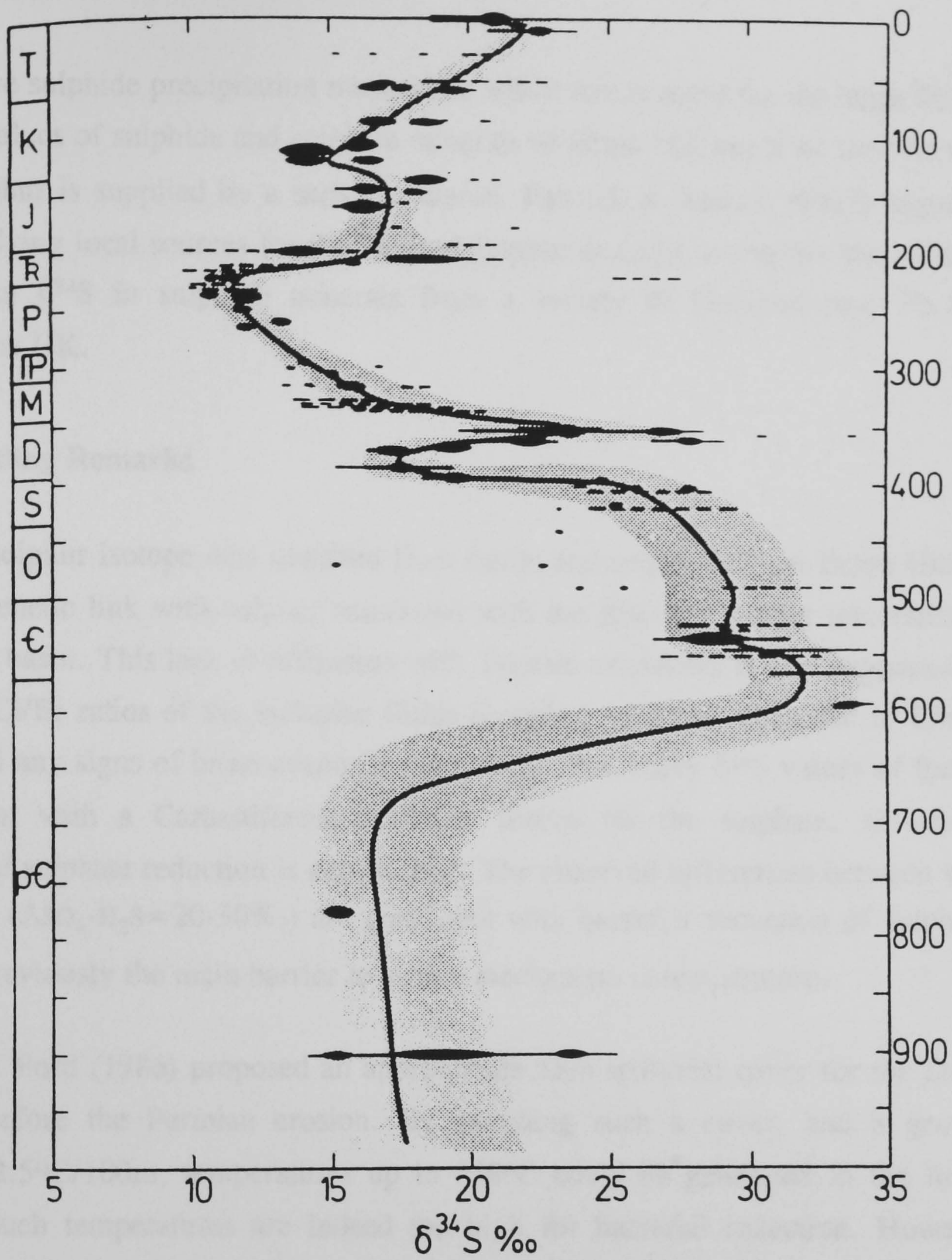


Fig. 9. Summary sulfur isotope age curve for sulfate. All data from our work, and most of those published elsewhere (for references see Figs. 4—8) are shown as *solid areas* or *lines* that qualitatively indicate the number of analyses, plotted at their most probable age. Horizontal *dashed lines* signify the range of relatively few analyses. The *heavy line* is our best estimate (see text) for $\delta^{34}S$ of sulfate mineral in equilibrium with the world ocean surface sulfate of that date. The *shaded area* is our estimate of the uncertainty of this curve.

Fig.6.4. Summary of the sulphur isotope age curve for sulphate (after Claypool et. al. 1980).

well understood.

An alternative sulphide precipitation mechanism which can account for the large differences in the $\delta^{34}S$ values of sulphide and sulphate minerals of Ecton Hill could be the one whereby reduced sulphur is supplied by a separate source. Pattrick & Russell (1989) argued for a process involving local sources for the reduced sulphur in order to explain the considerable differences in $\delta^{34}S$ in sulphide minerals from a variety of Carboniferous Pb-Zn vein deposits in the UK.

6.5. Concluding Remarks

Overall the sulphur isotope data obtained from barite and sulphides from Ecton Hill do not reveal any genetic link with sulphur associated with the Red Bed copper mineralization in the Cheshire basin. This lack of affiliation with Triassic evaporites is also supported by the data on the Cl/Br ratios of the inclusion fluids described which as discussed in Chapter 5, do not reveal any signs of brine-evaporite interaction. The heavy $\delta^{34}S$ values of the barites are consistent with a Carboniferous seawater source for the sulphate. However, the mechanism of sulphate reduction is not as clear. The observed differences between sulphide and sulphate ($\Delta SO_4\text{-}H_2S$=20-30‰) are consistent with bacterial reduction of sulphate. As mentioned previously the main barrier to such a mechanism is temperature.

Mostaghel & Ford (1986) proposed an approximate 5km sediment cover for the Dinantian limestones before the Permian erosion. By assuming such a cover, and a geothermal gradient of 2.5°C/100m, temperatures up to 150°C could be generated in the limestone sequences. Such temperatures are indeed too high for bacterial reduction. However, as noted by Anderson (1983), it is not clear whether the brine escape route represents a thermal anomaly in cool country rocks or, the whole region was raised to ore-deposition temperatures. This question is of fundamental importance to the general pattern of fluid flow and has a direct bearing to the viability of bacterial sulphate reduction near the site of deposition. If it is assumed that the ore fluids were warmer than the enclosing rocks, bacterial reduction at some distance from the hydrothermal system is possible (Anderson 1983).

In the case of Ecton Hill the fluid inclusion temperatures are too low for thermochemical sulphate reduction at the site of deposition and slightly higher than the generally accepted limit of bacterial reduction (80°C) (Trudinger et. al. 1985). Overall the sulphur isotope data favour a bacterial reduction model. However, more information is needed regarding

both the temperature limits of each reduction mechanism, as well as, the time-temperature trajectory of basin development in order to dismiss or wholly accept any of the above models. The source of copper in the fluids is also not clear. Contribution from Cu-bearing fluids from the Cheshire basin cannot be ruled out. Also, information on the sulphur isotopic composition of chalcopyrite from the basement Redhouse sandstones will be of great value in evaluating the potential of a more local source of copper in the Ecton Hill mineralization.

Chapter 7

Conclusions and recommendations for further work

7.1 Concluding Remarks

The broad similarities between the classical Mississippi Valley-Type (MVT) and the Pennine mineralization of the British Isles have been noted and discussed in the literature (e.g. Dunham, 1983). The broadly common geological setting and the remarkable uniformity of the temperature-salinity patterns of the ore forming fluids (as confirmed by the present fluid inclusion study in Chapter 4), provided most of the evidence supporting the links between the MVT and Pennine mineralization. Similarly to the MVT mineralization, models involving the expulsion of fluids from sedimentary basins, have also been favoured for ore-genesis in the Pennines (Dunham 1983, Atkinson et. al. 1982, Shepherd et. al. 1982). However, as discussed in detail in the previous chapters, there are still issues that remain unresolved. Particularly controversial is the exact timing of mineralization, the ultimate origin and evolution of ore-forming fluids of the ore-forming constituents, as well as the mechanisms of ore-transport and precipitation. The present study has concentrated on the origin and evolution of ore-forming fluids associated with mineralization in the Pennines, Ecton Hill, Llanharry and South Crofty areas using evidence from extensive fluid inclusion investigations.

Previously encountered problems in fluid inclusion analysis, caused mainly by the small size of fluid inclusions, have largely been overcome by modern experimental methods such as the Decrepitation-ICP and Neutron Activation Analysis used in the present study. These two methods, described in Chapter 3, have been further developed for the chemical analysis of single generation fluid inclusions in fluorite and calcite samples. The use of these two methods enabled determination of both major (Cl, Na) and trace (K, Li, Br) elements in fluid inclusions. Cross-examination of the results with those obtained by independent methods, such as crush-leach ICP and ion chromatography, proved the validity of the methods and the reliability of the data. Furthermore, statistical evaluation of the results provided an estimate of the extent and the sources of error inherent in the chemical analysis of fluid inclusions. Small sample size requirements and relatively simple sample preparation procedures enabled the routine analysis of large numbers of samples. Attempts to determine the Pb-Zn-Cu contents of fluid inclusions were largely unsuccessful because of contamination problems. Results from time-resolved ICP analysis of electrolytically-

cleaned samples showed that contamination from adherent sub-microscopic sulphide grains rather than fluid inclusions, was the major source of Pb-Zn-Cu in the analyses reported here and elsewhere in the literature.

Microthermometric analysis was carried out in the present work mainly in order to identify the fluid inclusion populations in the studied samples and to estimate the relative Ca-Na levels of the inclusion fluids. Homogenization temperature and total salinity data are in general agreement with previously published results for the Pennine, Ecton Hill, Llanharry and South Crofty areas. Despite the fact that microthermometry occupied an "auxiliary" role in the present study, paired homogenization, T_{LM} and T_{Mh} data are reported here for the first time. The data enable the estimation of the Ca/Na ratios of the fluids and also the quantification of the semiquantitative chemical analysis results.

For the English Pennines, Ca/Na ratios determined here, do not define any regional geographical trends and provide another line of evidence on the uniformity of the key features of MVT fluids. The data are comparable with previously published results from several MVT deposits showing that the fluids are mainly Na-Ca-Cl high-salinity brines with Na and Cl as dominant ionic species. The only regional variation of microthermometric results in the three Pennine orefields is defined by the distribution of fluid inclusion homogenization temperatures. The fluid-temperatures exhibit a well-defined increasing trend from the South to the North Pennines. This trend is interpreted as the result of interaction of the ore-fluids with the underlying Weardale and, to a lesser extend, the Wensleydale granites in the North Pennines.

The relative Ca-Na levels of the Ecton Hill inclusion fluids are equally well constrained showing only a minor Ca-enrichment compared to the rest of the Pennines. This lack of regional variation of major dissolved ionic species in fluids associated with both Pb and Cu-dominant mineralization may be interpreted as an indication of a common fluid source environment or as the result of extensive buffering by the host carbonate sequences. The only deviation from this low-temperature high salinity pattern of the Pennine fluids is observed in two fluorite samples from the Derbyshire orefield. These isolated low salinity-high temperature fluids are closely associated with hydrocarbons and do not appear to be directly related to the main stage Pb-Zn mineralization.

Detailed microthermometric analysis of fluid inclusions in calcite and quartz samples from the Llanharry Fe-deposit was seriously impeded by the low abundance and small size of the inclusions. The restricted number of readings show that, in terms of homogenization

temperature and Ca/Na ratios, the fluids are similar to those of Ecton Hill, whereas, total salinities are lower. From the limited data obtained here, it is not possible to positively identify whether variations in salinity are caused by the presence of separate fluid inclusion populations with varying salinities or whether they are part of a broad continuum.

Homogenization temperature-salinity data from the late, chlorite stage fluorite from South Crofty are in agreement with previous microthermometric work by Farmer (1991). Apart from the high temperature-variable salinity fluids, a distinct low temperature-high salinity population was also identified. Paired T_{LM}-T_{Mh} measurements obtained in the present work reveal that both the total salinities and Ca/Na ratios of this late, low temperature population are similar to those of the Pennine fluids. Therefore previous hypotheses (e.g. Alderton 1978, Shepherd et. al. 1985b, Farmer 1991) on the involvement of low-temperature, high-salinity fluids at South Crofty are further supported by the new data obtained during the present study.

The influence of fluid-rock interactions in modifying the chemistry of the ore-forming fluids was investigated with the aid of the observed regional variations of the alkali metal contents of fluid inclusions in the separate areas of study. Previously reported variations of the potassium content of fluid inclusions in the Pennines (e.g. Rankin & Graham 1988) were confirmed by results from all three Pennine orefields obtained in the present study. Furthermore, data on the variation of Li contents of inclusion fluids in the Pennines showed that apart from K, lithium also defines a clear increasing trend from the South to the North Pennine orefields. These regional trends defined by the K and Li contents of the inclusion fluids in the three Pennine orefields are interpreted as a result of higher fluid temperatures and extensive interaction with granitic rocks in the North Pennines compared to the lower temperatures and lack of underlying granitic rocks in the South Pennines. The high K and Li concentrations of the inclusion fluids in fluorite samples from the granite-related mineralization at South Crofty provide further evidence supporting this fluid-granite interaction hypothesis.

The Cl-Br concentrations of inclusion fluids were determined as a means of identifying the source(s) of high salinity of the inclusion fluids. The Cl/Br ratios of the inclusion fluids from all three Pennine orefields (Alston, Askrigg and Derbyshire) are well constrained and provide new evidence indicating the remarkable uniformity of the ore-fluids in the region. The Cl-Br-Na data indicate that interaction of the fluids with halite is not the cause of their high salinity. They are more consistent with a prolonged subaerial seawater evaporation process. Previously proposed models invoking large scale filtration by semipermeable

shale-clay membranes (Moore 1980, Plant et. al. 1989) cannot be ruled out by the data presented here. However, it is still not clear whether the membrane filtration process alone can produce adequate volumes of high salinity ore-forming fluids. As noted by several authors (e.g. Hanor 1987, Kharaka et. al. 1985), more experimental data are needed in order to establish the feasibility and the effects of membrane filtration on the chemistry of basinal brines.

The Cl-Br data from Ecton Hill fall in the range defined by the rest of the Pennine fluids. Similarly, the results are not consistent with leaching of evaporites and therefore, they do not support previous speculations (Masheder & Rankin 1989) involving migration of fluids from the adjacent Cheshire Basin which are considered (Naylor et. al. 1989) as having interacted with evaporites. At Llanharry, the fluids are not as saline as in the Pennines. However, as with the Pennine samples, the Cl-Br data are also consistent with a marine origin for the fluids. At South Crofty the Cl-Br fluid signature is more complex. The Cl/Br ratios of the low temperature group are similar to the Pennines and therefore, indicate contribution from fluids of basinal brine affinity during the late stage of mineralization. For the early, high temperature inclusions, data from microthermometry indicated large scale overprinting caused by the presence of several fluid populations of possible magmatic, meteoric, and seawater origin. Therefore, their Cl-Br systematics should not be compared to the relative simple seawater patterns. Although a clear "magmatic" halogen signature cannot be defined, the data are similar to those most recently obtained by Bohlke & Irwin (1992) from inclusion fluids with magmatic affinity, in quartz samples from the St. Austell granite.

Sulphur isotope analyses were undertaken in sulphide and sulphate samples from the Ecton Hill Cu-deposits in order to further trace the origin of sulphur at this unique locality and to compare the results with those reported by previous investigators (Robinson & Ineson 1979, Solomon et. al. 1971) for the rest of the Pennine region. The sulphate data obtained in the present work indicate that seawater of Carboniferous age is the main source of sulphate. The sulphate-sulphur isotope results are consistent with the patterns defined by the Cl-Br fluid inclusion data. They provide additional evidence indicating that the ore-forming fluids are not associated with the Triassic evaporites of the Cheshire basin. The sulphide-sulphur data are more complex and open to interpretation. The sulphide-sulphur isotope systematics are generally consistent with a bacterial sulphate reduction process for the precipitation of sulphides. Problems may arise by the fact that the homogenization temperatures may be higher than the generally accepted temperature limits of bacterial reduction. On the other hand the temperatures of homogenization are too low for a non-

bacterial reduction process to be active. Such problems are not restricted to the Ecton Hill deposit. They are commonly encountered in the studies of most MVT deposits worldwide, and they are closely related to the general lack of knowledge of the exact timing of mineralization and the time-temperature relationships of the host sedimentary basins.

Overall the fluid inclusion data obtained in the present work support a basinal brine origin for the ore-forming fluids in the Pennines, Ecton Hill, Llanharry and also at the late stage of the South Crofty mineralization. Still, the ultimate origin and source rocks of the water component remain speculative. However, the paired temperature-salinity and Cl/Br data are more consistent with a process involving evolution of an original seawater source, whereas, comparison of the relative Na-K-Li levels in the separate areas of study indicate large-scale modification of the original brine composition through interaction with different lithologies.

7.2. Recommendations for further work.

Since the majority of the samples studied in the present work contained one dominant fluid inclusion generation, bulk analytical techniques were initially considered and proved to be satisfactory. However, the methods could not be used for the majority of the South Crofty samples in which multiple fluid inclusion generations were present. Therefore, development and use of point analytical techniques is necessary in order to provide an insight to the complicated hydrothermal mineralization events in this area. Analysis of individual fluid inclusions in fluorite by Laser-ablation ICP-MS is promising since it provides lower detection limits and will enable the determination of elements such as sulphur, free from large-scale Ca interferences.

As repeatedly emphasized by many previous investigators, probably the major barrier in unequivocally establishing the genesis of MVT ore deposits, is the lack of knowledge regarding the exact timing of mineralization. These problems are also encountered in the ore deposits studied here but were not addressed in the present work because methods for reliable, direct dating of the mineralization are still not widely available. Future investigations towards that scope would be of great value in resolving problems such as the possible source rocks of the fluids and the time-temperature framework of the sedimentary basin evolution.

Oxygen-hydrogen isotopic studies are commonly carried out as a means of tracing the origin of modern-day sedimentary basin brines. Similar investigations in fluid inclusions are still not routine and were not possible during the present study. Although oxygen-

hydrogen isotopes alone cannot provide unequivocal answers regarding the origin of the fluids, combination of the isotopic and chemical composition fluid inclusion data would be of great value.

Further information on the origin of ore-metals might be obtained through detailed comparative Pb-S isotope studies of the ore-sulphides and of the possible source rocks such as the shales and limestones. Such information could also resolve some of the problems arising from the complexity and ambiguous interpretations of the sulphur isotope data. More detailed mineralogical an textural investigations of the possible fluid-source rocks, and most importantly the Namurian shale sequences are also needed in order to further examine their potential as orefluid sources, as well as, the feasibility of the fluid evolution mechanisms such as membrane filtration and subaerial evaporation.

The effects of fluid-rock interaction were investigated in the present study through determinations of the Na-Ca-K-Li contents of the inclusion fluids. Elements such as Mg and Ba may provide an additional insight into these interactions but data obtained from the present techniques were not considered reliable. It is possible that ICP-MS can be used to detect a greater range of elements in the future. As noted previously, Laser-ablation ICP-MS is particularly promising and may offer the opportunity of a direct measurement of these elements and also the Cl-Br and metal levels of individual fluid inclusions.

Determination of iodine in the fluid inclusions could provide further evidence regarding the evolution of the ore-forming fluids mainly in terms of their association with organic matter. Although contribution from organic matter in enhancing the Br contents of inclusion fluids is not evident from the data obtained in the present work, knowledge of the iodine contents of the inclusion fluids could provide further constraints on that subject. Furthermore, additional hydrocarbon associated inclusion fluids need to be examined in order to further highlight this possibility.

Finally, extension of the present work, to other deposits in the UK, such as the Mendip Hills, Shropshire, the Lake District orefields, and to other similar deposits worldwide, would provide a very interesting field for future research. Recent investigations by Bethke & Marshak (1990) emphasized the importance of large-scale tectonic deformation to long-distance brine migrations in North America. Therefore, apart from research oriented to aspects of ore-genesis of individual deposits, more regional investigations may have great potential towards an understanding of the intriguing ore-formation phenomena associated with sedimentary basins worldwide.

References

Aitkenhead, N., Chisholm, J. I. and Stevenson, I. P.,1985. Geology of the country around Buxton, Leek, and Bakewell. *Memoirs of the British Geological Survey*, sheet 111, 168p.

Aitkenhead, N., and Chisholm, J. I., 1982. A standard nomenclature for the Dinantian formations of the Peak District of Derbyshire and Staffordshire. *Institute of Geological Sciences Report* 82/8, 18p.

Alderton, D. H. M. and Rankin A. H., 1983. The character and evolution of hydrothermal fluids associated with the kaolinized St Austell granite, southwest England. *Journal of the Geological Society, London*, v.140, p.297-309.

Alderton, D H M. , Thompson, M., Rankin, A H., and Chryssoulis, S L. 1982. Developments of the ICP-linked decrepitation technique for the analysis of fluid inclusions in quartz: *Chemical Geology*, v.37, p.203-213.

Alderton, D. H. M., 1975. Fluid inclusion studies in SW England. *Proceedings of the Ussher Society*, v.3, p.214-217.

Alderton, D. H. M., 1978. Fluid inclusion data for the lead-zinc ores from SW England. *Transactions of the Institution of Mining and Metallurgy,* (section B), v.87, p.132-135.

Anderson, G. M., 1973. The hydrothermal transport and deposition of galena and sphalerite near 100°C. *Economic. Geology*, v.68, p.480-492.

Anderson, G. M., 1975. Precipitation of Mississippi Valley-Type ores. *Economic. Geology*, v.70, p937-942.

Anderson, G. M., 1978. Basinal brines and Mississippi Valley-Type ore deposits. *Episodes*, no.2, p.15-19.

Anderson, G. M., 1983. Some geochemical aspects of sulfide precipitation in carbonate rocks. (in) Kirsvarsanyi, G., Grant, S.K., Pratt, W. P., and Koenig, J. W., (eds), *International Conference on Mississippi Valley-Type lead-zinc deposits.* Proceedings volume: Rolla, University of Missouri, Rolla. p.61-76.

Anderson, G. M., & Macqueen, R. W., 1982. Ore Deposit Models-6. Mississippi Valley-Type lead-zinc deposits. *Geoscience Canada*, v.9, p.108-117.

Anderton, R., Bridges, P. H., Leeder, M. R., and B. W. Sellwood, 1983. *A dynamic stratigraphy of the British Isles, a study in crustal evolution.* George Allen & Unwin, London, Boston, Sydney, 301 pages.

Astrop, P., 1987. Relationships between structure, mineralization and hydrocarbon distribution at Ecton copper Mine, Staffordshire. *B.Sc thesis, Mining Geology, Imperial College,* 148p.

Atkinson, P., McMoore, J., and Evans, A. M., 1982. The Pennine orefields of England with special reference to recent structural and fluid inclusion investigations. *Bulletin du B.R.G.M., section II*, no.2, p.149-156.

Banks, D. A. and Yardley, B. W. D., 1992. Crush-leach analysis of fluid inclusions in small natural and synthetic samples. *Geochimica et Cosmochimica Acta*, v.56, p.245-248.

Barnes, H. L., 1983. Ore-depositing reactions in Mississippi Valley-Type deposits, (in) Kirsvarsanyi, G., Grant, S.K., Pratt, W. P. and Koenig, J. W., (eds), *International Conference on Mississippi Valley-Type lead-zinc deposits.* Proceedings volume: Rolla, University of Missouri, Rolla. p.7-19.

Barrett, T. J., and Anderson, G. M., 1982. The solubility of sphalerite and galena in NaCl brines. *Economic. Geology,* v.77, p.1923-1933.

Bastin, E. S. (ed.), 1939. Contributions to the knowledge of the lead and zinc deposits of the Mississippi Valley region. *Geological Society of America*, Special Paper no.24, 156p.

Beer, K. E., Edmunds, W. M., and Hawkes, J. R., 1978. A preliminary look at Lithium in the United Kingdom, *Energy*, v.3, p.281-292.

Behr, H. J., and Gerler, J., 1987. Inclusions of sedimentary brines in Post-Variscan mineralizations in the Federal Republic Of Germany,- A study by Neutron Activation Analysis. *Chemical Geology*, v.61, p.65-77.

Bein, A., Hovorka, S. D., Fisher, R. S., and Roedder, E., 1991. Fluid inclusions in bedded Permian halite, Palo Duro basin, Texas: Evidence for modification of seawater in evaporite brine pools and subsequent early diagenesis. *Journal of Sedimentary Petrology*, v.61, No.1, p.1-14.

Bennett, B A, Parry, S J., and Christoula, M., 1992. Determination of chlorine, bromine and sodium in fluid inclusions by neutron activation analysis. *Analyst* (in press).

Bethke, C. M. and Marshak, S., 1990. Brine migrations across North America - the plate tectonics of groundwater. *Annual Review of Earth and Planetary Science*, v.18, p.287-315

Bjorlykke, A. & Sangster, D. F., 1981. An overview of sandstone lead deposits and their relationship to red-bed copper and carbonate hosted lead-zinc deposits. (in) Skinner, B.J.(ed.) *Economic.Geology, 75th Anniversary volume,* p.179-213.

Bodnar, R. J., and Cline, J., 1990. Microthermometric and phase behavior of magmatic-hydrothermal fluids. *PACROFI III, Abstracts, Toronto*, p.17.

Bohlke, J. K., and Irwin, J. J., 1992. Laser microprobe analyses of Cl, Br, I, and K in fluid inclusions: Implications for sources of salinity in some ancient hydrothermal fluids. *Geochimica et. Cosmochimica Acta*, v.56, p.203-225.

Borisenko, A. S., 1977. Study of the salt compositions of gas-liquid inclusions in minerals by the cryometric method. *Geologiya i Geofizika,* v.18, no.8, p.16-27.

Bottrell, S. H., and Yardley, B. W. D., 1988. The composition of granite derived ore fluid from SW England determined by fluid inclusion analysis. *Geochimica et Cosmochimica Acta,* v.52, p.585-588.

Bromley, A. V., and Hall, J., 1987. Tin mineralization in SW England, *Proc. NATO Miner. Process. Conf., Falmouth,* p.95-262.

Brown, G. C, Ixer, R. A., Plant, J., and Webb, P.C. 1987. Geochemistry of granites beneath the North Pennines and their role in ore formation. *Transactions of the Institution of Mining and Metallurgy,* (section B). v.96, p.55-66.

Bush, P. R, 1970. Chloride-rich brines from sabkha sediments and their possible role in ore formation. *Transactions of the Institution of Mining and Metallurgy* (section B), v.79, p.137-144.

Carpenter, A. B., Trout, M. L., and Picket, E.E., 1974. Preliminary report on the origin and chemical evolution of Lead-Zinc rich brines in Central Mississippi. *Economic. Geology*, v.69, p.1191-1206.

Carpenter, A. B., 1978. Origin and chemical evolution of brines in sedimentary basins. *Oklahoma Geological Survey Circular*, 79, p.60-77.

Cathles, L. M., & Smith, A. T., 1983. Thermal constraints on the formation of Mississippi Valley-type lead zinc deposits and their implications for episodic basin dewatering and deposit genesis. *Economic. Geology*, v.78, p.983-1002.

Chen, Y., 1991. $^{40}Ar/^{39}Ar$ geochronology of granitic intrusion and Sn-Cu(-W) mineralization, Carn Brea-Carn Marth-Carnmenellis area, Cornwall, U.K. (Abstract), Abstracts-Programs of the *Geological Society of America*, 1991 Annual Meeting, San Diego, California October 21-24, 1991.

Chesley, J. T., Halliday, A. N. and Scrivener, R. C., 1991. Samarium-Neodymium direct dating of fluorite mineralization. *Science*, v.252, p.949-951.

Chryssoulis, S L., 1983. *Ph.D Thesis, University of London, Imperial College*, two volumes, 271 pages.

Chryssoulis, S. L. and Rankin, A. H., 1988. Decrepitometry of fluid inclusions in quartz from the Guadalkazar granite of Mexico: Principles and application to mineral exploration. *Mineralium Deposita*, v.23, p.42-49.

Claypool, G., E., Holser, W. T., Kaplan, I. R., Sakai, H., and Zak, I., 1980. The age curves of sulphur and oxygen isotopes and their mutual interpretation. *Chemical Geology*, v.28, p.199-260.

Coleman, M. L. & Moore, M. P., 1978. Direct reduction of sulphates to sulphur dioxide for isotopic analysis. *Analytical Chemistry*, v.50, p.1594-1595.

Collins, A. G., 1975. *Geochemistry of oil field waters*. New York, Elsevier Scientific Publications Company, 496p.

Colman, T. B., Ford, T. B., and Laffdey, N., 1989a. Metallogeny of the Pennine orefields. (in) *Metallogenic models and exploration criteria for buried carbonate hosted deposits, a multidisciplinary study in Eastern England*, BGS, The Institution of Mining and Metallurgy, Plant,J.& Jones, R. G. (eds) p.13-23.

Colman, T. B., Jones, R.G., Plant, J.A., and Smith, K. 1989b, Metallogenic Models (in) as above, p.123-133.

Connolly, C., Walter, L. M., Baadsgaard, H., and Longstaffe, F. S., 1990. Origin and evolution of formation waters, Alberta Basin, Western Canada sedimentary basin, part I, chemistry. *Applied Geochemistry,* v.5, p.397-413.

Coomer, P., & Ford, T.D., 1975. Lead and sulfur isotope ratios of some galena specimens from the South Pennines and North Midlands. *Mercian Geologist*, v.5, no.4, p.291-304.

Crawford, M. L., 1981. Phase equilibria in aqueous fluid inclusions. (in), Hollister, L. S., and Crawford, M. L. (eds), *Short Course in fluid inclusions, Applications to petrology, Mineralogical Association of Canada*, p.75-100.

Critchley, M. F., 1979. A geological outline of the Ecton copper mines, Staffordshire. *Bulletin of the Peak District Mines Historical Society*, v.7, p.177-191.

Crochetti, C. A., and Holland, H. D., 1989. Sulphur-lead isotope systematics and the composition of fluid inclusions in galena from the Viburnum Trend, Missouri. *Economic Geology*, v.84, p.2196-2216.

Czamanske, C K., Roedder, E., and Burns, F C. 1963. Neutron Activation Analysis of fluid inclusions for copper, manganese and zinc. *Science*, v.140, p.401-403.

Darbyshire, D. P. F., and Shepherd, T. J. 1985. Chronology of granite magmatism and associated mineralization. *Journal of the Geological Society Of London*, v.142, p.1159-1177.

Davidson, C. F., 1966. Some genetic relationships between ore deposits and evaporites. *Transactions of the Institution of Mining and Metallurgy, (section B)*, v.75, p.B215-225.

Davis, D. W., Lowenstein, T. K., and Spencer, R. J., 1990. Melting behavior of fluid inclusions in laboratory grown halite crystals in the systems NaCl-H_2O, NaCl-KCl-H_2O, NaCl-$MgCl_2$-H_2O and NaCl-$CaCl_2$-H_2O. *Geochimica et Cosmochimica Acta,* v.54, p.591-601.

Deer, W. A., Howie, R. A. and Zussman, J. 1962. *Rock forming minerals*. London, Longman, Green & Co., 5vols.

Dozy, J.J., 1970. A geological model for the genesis of lead-zinc ores of the Mississippi Valley, U.S.A. *Transactions of the Institution of Mining and Metallurgy*, (section B), v.79, p.163-170.

Dunham, K.C., 1934, Genesis of the Northern Pennine ore deposits. *Quarterly Journal of the Geological Society of London*, v.90, p.689-720.

Dunham, K. C., 1948. Geology of the Northern Pennine orefield, v.1, Tyne to Stainmore. *Memoirs of the Geological Survey Great Britain*. 357p.

Dunham, K. C., 1966. The role of juvenile solutions, connate waters, and evaporite brines in the genesis of lead-zinc-fluorine-barium deposits. *Transactions of the Institution of Mining and Metallurgy,* (section B), v.75, p.B226-229.

Dunham, K. C., Fitch, F.J., Ineson, P. R., Miller, J. A..,and Mitchell, J.G., 1968. The geochronological significance of argon 40- argon 39 determinations on White Whin from the Northern Pennine orefield. *Proceedings of the Royal Society of London, A*, v.307, p.251-266.

Dunham, K. C., 1983. Ore genesis in the English Pennines, a fluoritic subtype. (in) Kirsvarsanyi, G., Grant, S.K., Pratt, W. P., and Koenig, J. W., eds. *International Conference on Mississippi Valley-Type lead-zinc deposits. Proceedings volume*: Rolla, University of Missouri, Rolla. p.86-111.

Dunham, K. C., & Wilson, K., 1985. Geology of the Northern Pennine orefield, v.2., Stainmore to Craven . *Economic Memoirs British Geological Survey*. 247p.

Edmunds, W. M., 1975. Geochemistry of brines in the Coal Measures of North East England. *Transactions of the Institution of Mining and Metallurgy,* (section B), v.84, p.39-52.

Edmunds, W. M., Andrews, J.N., Burgess, W. G., Kay, R. L. F., and Lee, D. J., 1984. The evolution of saline and thermal groundwaters in the Carnmenellis granite. *Mineralogical Magazine*, v.48, p.407-424.

Edmunds, W. M., 1986. Geochemistry of geothermal waters in the UK, (in) Downing, R. A., and Gray, D. A. (ed), *Geothermal Energy- the potential in the United Kingdom: Her Majesty's Stationery Office, London*, chapter 6, p.111-122.

Edmunds, W. M., Cook, J. M., and Miles, D. L., 1986. Lithium mobility and cycling in dilute continental waters. *Extended abstracts of water-rock interaction, Reykjavic, Iceland, Orkustofnun,* p.183-187.

Edmunds, W. M., Kay, R. L. F., Miles, D.L., and Cook, J.M., 1987. The origin of saline groundwaters in the Carnmenellis granite, Cornwall (UK): Further Evidence from minor and trace elements. (in) Fritz, P., and Frape, S. K., (eds) *Geological Association of Canada Special Paper, 33,* p.127-144.

Egeberg, K. P., and Aagaard, P., 1989. Origin of formation waters from oil fields on the Norwegian shelf. *Applied Geochemistry*, v.4, p.131-142.

Farmer, C. B., and Halls, C., 1992. Paragenetic evolution of cassiterite-bearing loads at South Crofty Mine, Cornwall, United Kingdom. *Proceedings of the 8th IAGOD symposium, Ottawa, Ontario*, E. Schweizerbart'sche, Verlalgbuchhandlung, Stutgart (in press).

Farmer, C. B., 1991. Paragenetic evolution of composite lodes at South Crofty Mine, Cornwall, UK., *PhD thesis,Imperial College, University of London 1991.*

Ferguson, J., Bubela, B., and Davis, P. J., 1975. Simulation of sedimentary ore-forming processes: concentration of Pb and Zn from brines into organic and Fe-carbonate sediments. *Geol. Rundschau,* bd, 64, (3), pp.767-782.

Fisher, S. R., and Kreitler, C. W., 1987. Geochemistry and hydrodynamics of deep-basin brines, Palo Duro Basin, Texas, USA. *Applied Geochemistry*, v.2, p.459-476.

Ford, T.D., 1976. The ores of South Pennines and Mendip Hills, England. A comparative study. (in) W.H. Wolf (ed.), *Handbook of stratiform and stratabound ore deposits*, v.5, p.161-195.

Fouillac, C., and Michard, G., 1981. Sodium-Lithium ratio in water applied to geothermometry of geothermal waters. *Geothermics,* v.10, p.55-70.

Fournier, R. O., and Truesdell, A. H., 1973. An empirical Na-K-Ca geothermometer for natural waters. *Geochimica et Cosmochimica Acta*, v.37, p.1255-1275.

Fowler, A. D., and Anderson, T., 1991. Geopressure zones as proximal sources of hydrothermal fluids in sedimentary basins and the origin of Mississippi Valley-type deposits in shale-rich sequences. *Transactions of the Institution of Mining and Metallurgy*,(section B), v.100, p.14-18.

Fuge, R., 1974. Chlorine, (in) Wedepohl, K. H., (ed), *Handbook of Geochemistry: Springer Verlag, New York,* chapter 17.

Garven, G., 1985. The role of regional fluid flow in the genesis of the Pine Point deposit, Western Canada sedimentary basin. *Economic Geology*, v.80, p.307-324.

Garven, G., and Freeze, R. A. 1984a.. Theoretical analysis of the role of groundwater flow in the genesis of stratabound ore deposits: 1, Mathematical and numerical model. *American Journal of Science*, v.284, p.1085-1124.

Garven, G., and Freeze, R. A., 1984b. Theoretical analysis of the role of groundwater flow in the genesis of stratabound ore deposits: 1, Mathematical and numerical model. *American Journal of Science*, v.284, p.1125-1174.

Gayer, R. A., and Criddle, A. J., 1970. Mineralogy and genesis of the Llanharry iron ore deposits, Glamorgan. *Proceedings of the Ninth Commonwealth Mining Metallurgy Congress*, London,1969, v.2, p.605-626.

Giordano, T. H. and Barnes, H. L., 1981. Lead transport in Mississippi Valley-type ore solutions. *Economic Geology*, v.76, p.2200-2211.

Graf, D. L., 1982. Chemical osmosis, reverse chemical osmosis, and the origin of subsurface brines. *Geochimica et. Cosmochimica Acta,* v.46, p.1431-1448.

Grappin, C., Saliot, P., Sabouraud, C., and Touray, J-C., 1979. Les variations des rapports Cl/Br Na/Br et K/Br dans les inclusions fluides des quartz de la cicatrice evaporitique de Bramans-Termignon (Vanoise, Alpes Francaises). *Chemical Geology*, v.25, p.41-52.

Gustafson, L. B. and Williams, N. 1981. Sediment-hosted stratiform deposits of copper, lead and zinc. (in) Skinner B. J. (ed) *Economic Geology, 75th Anniversary volume*, p.139-178.

Hall, W., and, Friedman, I., 1963. Composition of fluid inclusions, Cave-in -Rock fluorite district, Illinois and Upper Mississippi Valley zinc lead district. *Economic Geology,* v.58, pp.886-911.

Hall, W., and, Friedman, I, 1969. Oxygen and Carbon isotopic composition of ore and host rock of selected MVT ores. *U.S. Geological Survey Professional Paper*, 650-C, p.C140-148.

Hall, D. L., Sterner, M. S. and Bodnar, R. J. 1988. Freezing point depression of NaCl-KCl-H_2O solutions. *Economic Geology*, v.83, p.197-202.

Halliday, A. N., Shepherd, T. J., and Dickin, A. P., 1990. Sm-Nd evidence for the age and origin of a Mississippi Valley Type deposit. *Nature*, v.344, p.54-57.

Halls, C., 1992 personal communication.

Hanor, J.S., 1979a, The sedimentary genesis of hydrothermal fluids. (in) *Geochemistry of hydrothermal ore deposits*. Barnes, H.L.,(ed) New York: John Wiley & Sons, p.137-172.

Hanor, J. S. 1979b, Dissolved methane in sedimentary brines: Potential effect on the PVT properties of fluid inclusions. *Economic Geology.*, v.75., p.603-617.

Hanor, J. S., 1987. Origin and Migration of Subsurface Sedimentary Brines. *Society of Economic Paleontologists and Mineralogists Short Course No.21.*

Hemley, J. J., 1967. Aqueous Na/K ratios in the systems K_2O-Na_2O-Al_2O_3-SiO_2-H_2O. (abstract). *Program,1967, Annual meeting, Geological Society of America, New Orleans, Louisiana,* p.94-95.

Heyl, A. V., Landis, G. P., and Zartman, R. E., 1974. Isotopic evidence for the origin of Mississippi Valley-Type mineral deposits, a review. *Economic Geology*, v.69, p.992-1006.

Hitchon, B. and Friedman, I., 1969. Geochemistry and origin of formation waters in the western Canada sedimentary basin I. Stable isotopes of hydrogen and oxygen. *Geochimica et. Cosmochimica Acta*, v.33, p.1321-1349.

Ineson, P.R., 1976. Ores of the Northern Pennines,the Lake District and North Wales. (in) W.H. Wolf (ed.), *Handbook of stratiform and stratabound ore deposits*, v.5, p.197-230.

Ineson, P. R., and Mitchell, J. G., 1972. Isotopic age determination on clay minerals from lavas and tuffs of the Derbyshire orefield. *Geological Magazine*, v.109, p.501-512.

Ineson, P. R. , and Ford, T.D., 1982. The South Pennine orefield, its genetic theories and eastward extension. *Mercian Geologist*, v.8, p.285-303.

Ixer, R. A., and Townley, R. 1979. The sulphide mineralogy and paragenesis of the South Pennine orefield, England. *Mercian Geologist*, v.7, p.51-63.

Jackson, S. A., and Beales,F. W., 1967. An aspect of sedimentary basin evolution : the concentration of Mississippi Valley Type ores during the late stages of diagenesis. *Bulletin of the Canadian Petroleum Geologists*, v.15, p.393-433.

Jackson, N. J., Willis-Richards, J., Manning, D. A. C., and Sams, M., 1989. Evolution of the Cornubian orefield, SW England, Part 1, Mineral deposits and ore forming processes. *Economic Geology,* v.84 p.1101-1133.

Jackson, N. J., Halliday, A. N., Sheppard, S. M. F. and Mitchell, J. G., 1982. Hydrothermal activity in the St. Just Mining district, Cornwall, England. (in) A.M. Evans (ed) *Mineralization associated with acid magmatism*, Wiley, Chichester, p.137-179.

Jackson, N. J., Moore, J. McM, and Rankin, A. H., 1977. Fluid inclusions and mineralization at Cligga Head, Cornwall, England. *Journal of the Geological Society, London.* v.134, p.343-349.

Jones, D. G., and Plant, J. A., 1989. geochemistry of shales. (in) *Metallogenic models and exploration criteria for buried carbonate hosted deposits, a multidisciplinary study in Eastern England, BGS, The Institution of Mining and Metallurgy*, Plant, J. & Jones, R. G. (eds), p.65-94.

Kharaka, Y. K., Hull, R. W. and Carothers, W. W., 1985. Water-rock interactions in sedimentary basins, (in) *Relationship of organic matter and mineral diagenesis, SEPM short course No.17*, p.79-174.

Kharaka, Y. K., Maest, W. W., Carothers, L. M., Law, P.J., Lamothe, P. J., and Fries, T. L., 1987. Geochemistry of metal-rich brines from Central Mississippi Salt Dome basin, USA. *Applied Geochemistry,* v.2, p.543-561.

Kharaka, Y. K. and Berry, F. A. F., 1973. Simultaneous flow of water and solutes through geological membranes I, experimental investigation. *Geochimica et. Cosmochimica Acta*, v.37, p.2577-2603.

Knauth, L. P., and Beunas, M. A., 1986. Isotope geochemistry of fluid inclusions in Permian halite with implications for the isotopic history of ocean water and the origin of subsurface waters. *Geochimica et Cosmochimica Acta* v.50, p.419-433.

Koslowski, A., 1984. Calcium-rich inclusion solutions in fluorite from the Strzegom pegmatites, Lower Silesia. *Acta Geologica Polonica,* v.34, no.1-2, p.131-137.

Lagache, M., and Weisbrod, A., 1977. The system: Two alkali feldspars-KCl-NaCl-H_2O at moderate to low temperatures and low pressures. *Contributions to Mineralogy and Petrology,* v.62, p.77-101.

Land, L. S., and Prezbindowski, D. R., 1981. The origin and evolution of saline formation water, Lower Cretaceous carbonates, south-central Texas, USA. *Journal of Hydrology*, v.54, p.51-74.

Leveridge, B. E., Holder, M. T, and Goode, A. J. J., 1990. Geology of the country around Falmouth. *Memoirs of the British Geological Survey*, sheet 352, London HMSO 1990.

Lindblom, S., Rankin, A H., and Thomson, M., 1989. Fluid inclusion composition of Baltic Shield quartz associated with mineralization, Sweden. *Applied Geochemistry*, v.4, p.473-481.

Llewellyn, P. G., and Stabbins, R., 1968. Lower Carboniferous evaporites and mineralization in the eastern and central Midlands of Britain. *Transactions of the Institution of Mining and Metallurgy* (section B), v.77, p.170-173.

Llewellyn, P. G., and Stabbins, R., 1970. The Hathern Anhydrite series, Lower Carboniferous, Leicestershire, England. *Transactions of the Institution of Mining and Metallurgy,* (section B), v.79, p.1-15.

Llewellyn, P. G., Mahmood, S. A., and Stabbins, R., 1968. Nodular anhydrite in Carboniferous Limestone, west Cumberland. *Transactions of the Institution of Mining and Metallurgy* (section B), v.77, p.18-25.

Luckscheiter, B., and Parekh, P P., 1979. A new method for the determination of dissolved elements in fluid inclusions. *N. Jahrb. Mineral. Monats*. v.3, p.135-144.

Lydon, J. W, 1986. Models for the generation of metalliferous hydrothermal systems within sedimentary rocks and their applicability to the Irish Carboniferous Zn-Pb deposits. (in) Geology and genesis of mineral deposits in Ireland, *Irish Association for Economic Geology*. p.555-577.

MacCaffrey, M. A., Lazar, B., and Holland, H.D., 1987. The evaporation path of seawater and the coprecipitation of Br and K with halite. *Journal of Sedimentology,* v.57, No.5, p.928-937.

MacDonald, R., Gass, K.N., Thorpe, R.S., and Gass, I. G., 1984. Geochemistry and petrogenesis of the Derbyshire Carboniferous basalts. *Journal of the Geological Society London*, v.141, p.147-159.

Manheim, F., T. and Horn, M. K., 1968. Composition of deeper subsurface waters along the Atlantic Continental Margin. *Southeastern Geology*, v.9, p.215-231.

Manning, D. A. C., and Struitt, D. W., 1990. Metallogenetic significance of a North Pennine springwater. *Mineralogical Magazine,* v.54, p.629-636.

Masheder, R., and Rankin, A. H., 1988. Fluid inclusion studies on the Ecton Hill Copper deposits, North Staffordshire. *Mineralogical Magazine,* v.52, p.473-482.

McLimans, R. K., 1987. The application of fluid inclusions to migration of oil and diagenesis in petroleum reservoirs. *Applied Geochemistry*, v.2. p.585-603.

Means, J. L. and Hubbard, N., 1987. Short-chain aliphatic acid anions in deep subsurface brines: A review of their origin, occurrence, properties, and importance new data on their distribution and geochemical implications in the Palo Duro Basin, Texas. *Organic Geochemistry*, v.11, No.3, p.177-191.

Miller, J. C. and Miller, J. N., 1988. *Statistics for analytical chemistry*, 2nd edition, John Willey & Sons, New York, Chichester, Brisbane, Toronto, 227p.

Mitchell, R. H., and Krouse, H. R., 1971. Isotopic composition of sulphur and lead from the Greenhow-Skyreholme area, Yorkshire, England. *Economic Geology*, v.66, p.243-251.

Moorbath, S., 1962. Lead isotope abundance studies on mineral occurrences in the British Isles and their geological significance. *Philosophical Transactions of the Royal Society,* v.254a, p.295-360.

Moore, G. R., (1980). A chemical and isotopic study of fluid inclusions from the Northern Pennine orefield. *Ph.D thesis, University of Durham.*

Moser, M. R., Rankin, A. H., and Milledge, H. J., 1992. Hydrocarbon-bearing fluid inclusions in fluorite associated with the Windy Knoll Bitumen deposit, UK. *Geochimica et Cosmochimica Acta,* v.56, p.155-168.

Mostaghel, M.A., and Ford, T. D., 1986. A sedimentary basin evolution model for ore genesis in the South Pennine orefield. *Mercian Geologist*, v.10, p.209-224.

Naylor, H., Turner, P., Vaughan, D. J., Boyce, A. J., and Fallick, A. E., 1989. genetic studies of red bed mineralization in the Triassic of the Cheshire Basin, northwest England. *Journal of the Geological Society, London*, v.146, p.685-699.

Noble, E. A., 1963. Formation of ore deposits by water of compaction. *Economic Geology.*, v.58, p.1145-1156.

Norman, D I., Kyle, P. R., Baron, C., 1989. Analysis of trace elements including rare earths in fluid inclusion liquids. *Economic Geology*, v.84.,P.162-166.

Oakes, C. S., Bodnar, R. J., and Simonson, J. M., 1990. The system NaCl-$CaCl_2$-H_2O: 1. The ice liquidus at 1at total pressure. *Geochimica et Cosmochimica Acta*, v.54, p.603-610.

Ohle, E. L., 1980. Some considerations in determining the origin of ore deposits of the MVT type, part 2. *Economic Geology,* v.75, p.161-172.

Ohmoto, H., 1986. Stable Isotope Geochemistry of Ore Deposits. (in): Valley, J. W., Taylor, H. P., and O'Neil, J. R., (eds) *Stable isotopes and High Temperature Geological Processes.* Reviews in Mineralogy, 16, Mineralogical Society Of America, p.460-491.

Ohmoto, H., and Rye, R. O., 1979. Isotopes of Sulphur and Carbon. (in): Barnes, H. L. (ed) *Geochemistry of Hydrothermal Ore deposits,* 2nd edition, Wiley & Sons, New York, N.Y. p.509-567.

Orr, W. L., 1977. Geologic and geochemical controls on the distribution of hydrogen sulphide in natural gas. (in): Campos, R., and Goni, J. (eds). *Advances in Organic Geochemistry,* 1975. Enadisma, Madrid, p.571-597.

Panno, S. V., Harbottle, G., Sayre, E. V. and Hood, W. C., 1983. Genetic implications of halide enrichment near a Mississippi Valley-Type ore deposit. *Economic Geology*, v.78, p.150-156.

Pattrick, R. A. D., and Russell, M. J., 1989. Sulphur isotopic investigation of Lower Carboniferous vein deposits of the British Isles. *Mineralium Deposita*, v.24, p.148-153.

Pfennig, N., and Widdell, F. 1982. The bacteria of the sulphur cycle. *Philosophical Transactions of the Royal Society of London*, v.298B, p.433-441.

Pinkney, D.M., & Rye, R.O., 1972, Variation of $^{18}O/^{16}O$, $^{13}C/^{12}C$, texture and mineralogy in altered limestone in the Hill Mine Cave-in-Rock district, Illinois. *Economic Geology,* v.67, p.1-18.

Plant, J. A., Jones, D. G., Brown, G. C., Colman, T. B., Cornwell, J. D., Smith, K., Smith, N. P. J., Walker, A. S. D., and Webb, P. C., 1988. Metallogenic Models and Exploration criteria for buried Carbonate-hosted ore deposits: results of a multidisciplinary study in Eastern England. (in) *Mineral Deposits within the European Community*, Springer-Verlag Berlin Heidelberg, p.322-352.

Potter, R. W., Clynne, M. A. and Brown, D. L., 1978. Freezing point depression of aqueous sodium chloride solutions. *Economic Geology*, v.73, p.284-285.

Powell, T. G., and MacQueen, R. W., 1984. Precipitation of sulphide ores and organic matter: sulphate reductions at Pine Point, Canada. *Science,* v.224, p.63-66.

Price, L. C., 1976. Aqueous solubility of petroleum as applied on its origin and primary migration. *American Association of Petroleum Geologists Bulletin,* v.60, p.313-344.

Puchner, H F., and Holland, H D., 1966. Neutron Activation Analysis of fluid inclusions in Quartz. *Economic Geology*, v.61, p.1390-1398.

Raab, M., and Spiro, B., 1991. Sulphur isotope variations during seawater evaporation with fractional crystallization. *Chemical Geology,* (isotope Geoscience Section), v.86, p.323-333.

Ramsey, M H., and Thomson, M., 1985. Correlated Variance in simultaneous Inductively Coupled Plasma Atomic-emission Spectrometry: Its causes and correction by a parameter-related Internal standard method. *Analyst*, v.110, p. 519-530.

Ramsey, M. H., Thomson, M. and Hale, M., 1992. Objective evaluation of precision requirements for geochemical analysis using robust analysis of variance. *Journal of Geochemical Exploration*, v.44, p.29-44.

Rankin, A. H., 1989. Fluid Inclusions. *Geology Today,* January-February 1989, p.21-24.

Rankin, A. H., and Graham, M. J., 1988. Na, K, Li contents of mineralizing fluids in the North Pennine orefield, England and their genetic significance. *Transactions of the Institution of Mining and Metallurgy,* (section B), v.97, p.97-107.

Rankin, A. H and Criddle, A. J., 1985. Mineralizing fluids and metastable low temperature inclusion brines at Llanharry iron deposit, South Wales. *Transactions of the Institution of Mining and Metallurgy,* (section B), v.94, p.126-133.

Rankin, A. H, and Alderton, D. H. M., 1983. Fluid inclusion petrography of SW England granites and its potential to mineral exploration. *Mineralium Deposita,* v.18, p.335-347.

Rankin, A H., Miller, M F., and Carter, J S., 1987. The release of trace elements and volatiles from crinoidal limestone during thermal decrepitation: *Mineralogical Magazine*, v.51, p.517-525.

Rankin, A. H., Herrington, R., Ramsey, M. H., Coles, B., Christoula, M. and Jones, E., 1991. Current developments and applications of ICP-AES techniques for the geochemical analysis of fluid inclusions in minerals. Proceedings of the 8th IAGOD symposium, Ottawa, Ontario (in press).

Rankin A. H. and Alderton, D. H. M., 1985. Fluids in granites from southwest England. (in) *High Heat Production (HHP) Granites, Hydrothermal Circulation and Ore Genesis.* Halls, C., (ed) Institution Of Mining and Metallurgy (London) Special Publication., p.287-299.

Rittenhouse, G., 1967. Bromine in oilfield waters and its use in determining the possibilities of origin of these waters. *American Association Of Petroleum Geologists Bulletin*, v.51, no12, p.2430-2440.

Robinson, B. W., and Kusakabe, M., 1975. Quantitative preparation of sulphur dioxide for 34S/32S analyses from sulphides by combustion with cuprous oxide. *Analytical Chemistry,* v.47, p.1179-1181.

Robinson, B.W., & Ineson, P. R., 1979. Sulfur, Oxygen and Carbon isotope investigations of lead-zinc-barite-fluorite-calcite mineralization,, Derbyshire, England. *Transactions of the Institution of Mining and Metallurgy* (section B), v.89, p.107-117.

Roedder, E., 1958. Technique for the extraction and partial chemical analysis of fluid filled inclusions in minerals: *Economic Geology*, v.53, p.235-269.

Roedder, E., 1976, Fluid inclusion evidence on the genesis of ores in sedimentary and volcanic rocks, (in) Wolf K. H. (ed), *Handbook of stratiform and stratabound ore deposits,* v.2, p.67-110.

Roedder, E., 1979. Fluid Inclusions as samples of ore fluids. (in) Barnes, H.L. (ed) *Geochemistry of hydrothermal ore deposits* 2nd edition, p.684-737. New York: John Wiley & Sons.

Roedder, E., 1960. Fluid inclusions as samples of ore-forming fluids. *XXI Int. Geol. Congr. Proc.* section 16, p.218-229.

Roedder, E., 1984. Fluid Inclusions. *Mineralogical Society of America, Reviews in Mineralogy,* v.12, 644p.

Roedder, E., 1990. Fluid inclusion analysis - prologue and epilogue: *Geochimica et Cosmochimica Acta,* v.54, p.495-507.

Rogers, P. J., 1977. Fluid inclusion studies in fluorite from the Derbyshire orefield. *Transactions of the Institution of Mining and Metallurgy,* (section B), v.86, p.128-132.

Rogers, P. J., 1978. Fluid inclusion studies in fluorite from the Askrigg block. *Transactions of the Institution of Mining and Metallurgy,* (section B), v.87, p.125-131.

Russell, M. J. and Smith, F. W., 1979. Plate separation, alkali-magmatism and fluorite mineralization in northern and central England. (Abstract): *Transactions of the Institution of Mining and Metallurgy,* (section B), v.88, p.30.

Russell, M.J.,& Skauli, H., 1991, A history of theoretical developments in carbonate hosted base metal deposits and a new Tri-level enthalpy classification. *Economic Geology Monograph 8*, p.96-116.

Sabouraud, C-R., 1974. determination par activation neutronique des rapports Cl/Br des inclusions fluides de divers gypses. Correlation avec les donnes de la microcryoscopie et interpretation genetiques : *Sedimentology*, v.21, p.415-431.

Samson, I. M. and Russell, M. J., 1987. Genesis of the Silvermines Zinc-Lead-Barite deposit, Ireland: Fluid Inclusion and stable isotope evidence. *Economic Geology*, v.82, p.371-394.

Sanders, L. L., 1991. Geochemistry of formation waters from the Lower Silurian Clinton Formation (Albion Sandstone), Eastern Ohio. *American Association of Petroleum Geologists Bulletin,* v.75, p.1593-1608.

Sangster, D.F., 1983. Mississippi Valley Type deposits: a geological melange. (in) Kirsvarsanyi, G., Grant, S.K., Pratt, W. P., and Koenig, J. W. (eds.) *International Conference on Mississippi Valley-Type lead-zinc deposits*. Proceedings volume: Rolla, University of Missouri, Rolla. p.7-19.

Sangster, D.F., 1986. Age of mineralization in Mississippi Valley Type (MVT) deposits: a critical requirement for genetic modelling. (in) Geology and genesis of mineral deposits in Ireland, *Irish Association for Economic Geology*. p.625-633.

Sangster, D.F, 1990, Mississippi Valley Type and Sedex Lead-Zinc deposits, a comparative review. *Transactions of the Institution of Mining and Metallurgy*, (section B), v.99, p.B21-42.

Sasaki, A., and Krouse,H. R., 1969. Sulfur isotopes and the Pine Point lead-zinc mineralization. *Economic Geology,*. v.64, p.718-730.

Sawkins, F. J. 1966a. Ore genesis in the North Pennine orefield in the light of fluid inclusion studies. *Economic Geology*, v.61, p.385-401.

Sawkins, F. J., 1966b. Preliminary fluid inclusion studies of the mineralization associated with the Hercynian granites of SW England. *Transactions of the Institution of Mining and Metallurgy* (Section B), v.75, p.109-112.

Sawkins, F. J., 1968. The significance of Na/K and Cl/SO_4 ratios in fluid inclusions and subsurface waters, with respect to the genesis of Mississippi Valley-type ore deposits. *Economic Geology*, v.63, p.935-942.

Scrivener, R.C., Shepherd, T. J., and Garrioch, N., 1986. Ore genesis at Wheal Pendarves and South Crofty mine, Cornwall- a preliminary fluid inclusion study. *Proceedings of the Ussher Society*, v.6, p.412-416.

Sharp, J. J. Jr.,1978. Energy and momentum transport model of the Quachita basin and its possible impact on the formation of economic mineral deposits. *Economic Geology,* v.73, p.1057-1068.

Shepherd, T., Rankin, A H., and Alderton, D H M., 1985a. *A practical guide to fluid inclusion studies*: Blackie (Glasgow and London) 237p.

Shepherd, T.J., and Scrivener, R. C., 1987. Role of basinal brines in the formation of polymetallic vein deposits Kit-Hill-Gunnislake area: SW England. *Proceedings of the Ussher Society*, v.6, p.491-497.

Shepherd, T. J., and Darbyshire, D. P. F., 1986. Fluid inclusion Rb-Sr geochronology of mineral deposits. (in) Nesbitt, R. W., and Nicholl, I. (eds.), *Geology in the real world, Institution of Mining and Metallurgy*, p.403-412.

Shepherd, T. J., Miller, M. F., Scrivener, R. C., and Darbyshire, D. P. F., 1985b. Hydrothermal fluid evolution in relation to mineralization in SW England with special reference to the Dartmoor-Bodmin area. (in) C. Halls (ed), *High Heat production granites, hydrothermal circulation and ore genesis, the Institution of Mining and Metallurgy,* p.345-364.

Shepherd, T. J., Darbyshire, D. P. F., Moore, G. R., and Greenwood, D. A., 1982. Rare earth element and isotopic geochemistry of the North Pennine ore deposits. *Bull. BRGM (2), section II,* no.4, 1982, p.371-377.

Sibson, R.H., Moore, J.McM., and Rankin, A. H., 1975. Seismic pumping - a hydrothermal fluid transport mechanism. *Journal of the Geological Society*, v.131, p.653-659.

Small, A. T. 1978. Zonation of Pb-Zn-Cu-F-Ba mineralization in part of the North Yorkshire Pennines. *Transactions of the Institution of Mining and Metallurgy,* (section B), v.87, p.9-14.

Smith, F. W., 1973. Fluid Inclusion studies on fluorite from the North Wales orefield. *Transactions of the Institution of Mining and Metallurgy,* (section B), v.82, p.174-176.

Smith, F. W.,1974, Factors governing the development of fluospar orebodies in the North Pennine orefield. *Ph.D thesis, University of Dunham*

Solomon, M., Rafter, T. A., and Dunham, K. C., 1971. Sulphur, and oxygen isotope studies in the Northern Pennines in relation to ore genesis. *Transactions of the Institution of Mining and Metallurgy,* (section B), v.80, p.259-275.

Sonnenfeld, P., 1984. *Brines and Evaporites*. Academic Press, Inc., 581p.

Spencer, R. J., 1987. Origin of Ca-Cl brines in Devonian formations, Western Canada Sedimentary Basin. *Applied Geochemistry*, v.2, p.373-384.

Stoessell, R. K., and Carpenter, A. B., 1986. Stoichiometric saturation tests of $NaCl_{1-x}Br_x$ and $KCl_{1-x}Br_x$. *Geochimica et Cosmochimica Acta,* v.50, p.1465-1474.

Stone, M., and Exley, C. S., 1985. High Heat Production granites of southwest England and their associated mineralization: a review. (in) *High Heat Production (HHP) granites, hydrothermal circulation and ore genesis,* Halls C., (ed), Institution of Mining and Metallurgy Special Publication, p.571-593.

Sverjensky, D. A., 1987. The role of migrating oil-field brines in the formation of sediment hosted Cu-rich deposits. *Economic Geology*, v.82, p.1130-1141.

Sverjensky, D. A., 1986. Genesis of Mississippi Valley-Type lead-zinc deposits. *Annual Review of Earth and Planetary Science*, v.14, p.177-199.

Sverjensky, D. A., 1984. Oil-Field brines as ore forming solutions. *Economic Geology*, v.69, p.843-863.

Sverjensky, D. A., 1981. The origin of a Mississippi Valley-Type deposit in the Viburnum Trend, Southwest Missouri. *Economic Geology*, v.76, p.1848-1872.

Taylor, H. P., 1974. The application of oxygen and hydrogen isotope studies to problems of hydrothermal alteration and deposition. Economic. Geology., v.69, p.843-883.

Thode, H. G., and Monster, J., 1965. Sulphur isotope geochemistry of petroleum, evaporites and ancient seas. *American Association of Petroleum Geologists, Memoir 4*, p.367-377.

Thomson, M., and Walsh, J N., 1988. A handbook of inductively couple plasma spectrometry, 2nd edition. Blackie and sons (Glasgow), 280p.

Thomson, M., Rankin, A. H., Walton, S. J., Halls, C., and Foo, B N. 1980. The analysis of fluid inclusion decrepitates by inductively coupled plasma atomic emission spectroscopy: an exploratory study: *Chemical Geology*, v.30, p.121-133.

Thomson, M., Hale, M. and Coles, B., 1992. Geochemical reconnaissance using stream-sediment pebble coatings and laser ablation ICP-AES. *Transactions of the Institution of Mining and Metallurgy*, (section B), v.101, p.9-13.

Trudinger, P. A., Chambers, L. A., Smith, J. W., 1985. Low temperature sulphate reduction: biological versus abiological. *Canadian Journal of Earth Sciences*, v.22, p.1910-1918.

Truesdell, A. H., 1984. Chemical Geothermometers for Geothermal exploration. (in) *Fluid Mineral Equilibria in Hydrothermal Systems,* Henley, R. W., Truesdell, A. H. and Barton, P. B.,(eds), Society of Economic Geology Publication, El Paso, Texas, Chapter 3, 31-44.

Vaughan, D. J., and Ixer, R. A., 1980. Studies of sulfide mineralogy of north Pennine ores and its contribution to genetic models. *Transactions of the Institution of Mining and Metallurgy*, (section B), v.89, p.99-110.

White, D. E., 1974. Diverse origins of hydrothermal ore fluids. *Economic Geology*, v.69, p.954-973.

Wickman,, F E., and Khattab,K., 1972. Non-destructive activation analysis for fluid inclusions in fluorite: *Economic Geology*, v.67, p.236-239.

Williams, M.,1958. Geology and mineralization of the Llanharry hematite deposits, South Wales. *Ph.D thesis University of London*

Worley, N.E. and Ford, T.D., 1977. Mississippi Valley Type orefields in Britain. *Bulletin of the Peak District Mines Historical Society*, v.6, p.201-208.

Dunham, K. C., 1992, Geology of the Northern Pennine Orefields, v.1, Tyne to Stainmore (2nd edition), *Economic Memoir of the British Geological Survey*, 299p.

APPENDICES

Appendix A

Sample localities and description

A) North Pennines, Alston Block

Sample I.D.	Mineral Association	Colour-Texture	Locality	NGR
AL/1/F	fluorite	colourless brecciated	Blackdene Mine	NY868389
AL/2/F	fluorite +(quartz)	green vuggy crystal	Blackdene Mine	NY868389
AL/3/F	fluorite + (ZnS)	massive colourless	Blackdene Mine	NY868389
AL/4/F	fluorite	colourless brecciated	Blackdene Mine	NY868389
AL/5/F	fluorite cutting Whin Sill	colourless massive	Blackdene Mine (Whin decline)	NY880397
AL/6/F	fluorite	green-colourless-massive-banded	Whiteheaps Mine	NY950470
AL/7/F	fluorite	colourless-massive	Whitehope Mine	NY956464
AL/8/F	fluorite	colourless massive	Cambokeals Mine	
AL/9/F	fluorite + (ZnS)	colourless-massive	Cambokeals Mine 240' level	NY932381
AL/10/F	fluorite + (ZnS)	colourless-massive	Cambokeals Mine	NY932381
AL/11/F	fluorite + (PbS)	purple-vuggy crystal	Boltsburn Mine	NY956442
AL/12/F	fluorite	green-vuggy crystal	Redburn Mine	NY928434
AL/13/F	fluorite	massive colourless	Redburn Mine	NY928434
AL/14/F	fluorite + (PbS)	green-vuggy crystal	N.Heights Vein	NY925389
AL/15/F	fluorite	green-vuggy crystal	N.Heights Vein	NY925389
AL/16/F	fluorite + (PbS-ZnS)	colourless-vuggy crystal	Flushimere	NY914313

AL/17/F	fluorite	yellow-vuggy crystal	Scordale Mine	NY761227
AL/1/C	calcite	massive	Blackdene Mine	NY868389
AL/2/C	calcite	massive-brecciated	Redburn Mine	NY928434
ST/1/B	barite	colourless-crystal	Settlingstones	NY851690
SLB/1/B	barite	colourless-crystal	Silverband Mine	NY702320
NRT/1/B	barite + (PbS)	colourless-crystal	Langley Barony Mines	NY837638
NRT/2/B	barite	colourless-crystal	Langley Barony Mines	NY837638
NRT/1/W	Witherite	colourless-crystal	Langley Barony Mines	NY837638

B) North Pennines, Askrigg Block

Sample I.D.	Mineral Association	Colour-Texture	Locality	NGR
AS/1/F	fluorite crystal + ($CuFeS_2$)	colourless-crystal	Gielfields Mine	SE118650
AS/2/F	fluorite	colourless-crystal	Gill Head Mine	SE066625
AS/3/F	fluorite + (calcite)	colourless-crystal	Duckstreet Quarry	SE092642
AS/4/F	fluorite + (barite-PbS)	colourless-crystal	Coldstones Quarry	SE123639
AS/5/F	fluorite	colourless-crystal	Coldstones Quarry	SE123639
AS/6/F	fluorite	colourless-crystal	Hartley Birkett, Kirkby Stephen	NY802082
AS/7/F	fluorite	purple-crystal	Appletreewhick	SE058605
AS/8/F	fluorite + (PbS)	colourless-crystal	Lolly Scar Mine	SE073725
AS/9/F	fluorite	purple-crystal	Swinden Lime Quarry	SD981615
AS/10/F	fluorite + (calcite)	colourless-crystal	Raygill Skipton	SD902899

C) South Pennines, Derbyshire

Sample I.D.	Mineral Association	Colour-Texture	Locality	NGR
DR/1/F	fluorite	purple-colourless banded	Dirtlow Rake	SK152823
DR/2/F	fluorite	purple-vuggy crystal	Blue John Cavern	SK137832
DR/4/F	fluorite +(barite)	purple vuggy -crystal	Odin Mine	SK135835
DR/5/F	fluorite + (barite-PbS)	colourless crystal	Hazard Mine	SK155920
DR/6/F	fluorite	colourless crystal	Riben Mine	SK301589
DR/7/F	fluorite	colourless massive	Sallet Hole II	SK219741
DR/8/F	fluorite +(barite-PbS)	colourless massive	Sallet Hole II	SK219741
DR/9/F	fluorite +(barite)	colourless massive	Sallet Hole I	SK220742
DR/10/F	fluorite +(PbS)	colourless massive	Sallet Hole I underground	SK220742
DR/11/F	fluorite +(PbS)	light yellow crystal	Fall Hill Mines Ashover	SK358623
DR/12/F	fluorite +(ZnS)	colourless crystal	Milltown Quarry nr.Ashover	SK356363
DR/13/F	fluorite +(calcite)	colourless crystal	Milltown Quarry nr.Ashover	SK356363
DR/14/F	fluorite +(PbS)	colourless crystal	Gregory load Ashover	SK349362
DR/15/F	fluorite +(PbS)	colourless crystal	Church Rake, Crich Hill	SK342555
DR/16/F	fluorite	colourless crystal	Crich Open cut	SK343555
DR/17/F	fluorite +(PbS)	colourless crystal	Mill Close Mine	SK259626
DR/18/F	fluorite +(PbS-ZnS)	colourless crystal	Mill Close Mine	SK259626
DR/19/F	fluorite + (PbS)	colourless crystal	Ladywash Mine	SK219776
DR/1/C	calcite+(fluorite)	crystal	Milltown Quarry	SK356363
DR/2/C	calcite+ (fluorite)	massive	Sallet Hole II	SK219741

D) Ecton Hill

Sample I.D.	Mineral Association and Texture	Locality
ECT/1/ (ECT/1/S)	massive chalcopyrite	Deep Ecton Mine dumps
ECT/2/ (ECT/1/S)	massive galena	Deep Ecton Mine dumps
ECT/3/ (ECT/1/S)	massive light pink barite	Deep Ecton Mine dumps
ECT/1/C	calcite crystal	Deep Ecton Mine dumps
ECT/2/C	smokey calcite crystal	Deep Ecton Mine dumps
ECT/3/C	calcite crystal	Deep Ecton Mine dumps
ECT/4/	calcite crystal + chalcopyrite inclusions	Deep Ecton Mine dumps
ECT/5/C	massive calcite + (barite)	Waterbank dumps
ECT/6/	massive calcite + chalcopyrite inclusions	Waterbank dumps
ECT/7/	mineralized calcite veinlet + chalcopyrite	Salt's Level A
ECT/8/C	vuggy calcite crystal	Salt's Level A
ECT/9/	mineralized calcite veinlet + galena	Salt's Level A
ECT/10/B	colourless massive barite	Waterbank dumps
ECT/11/B	light pink massive barite+(calcite)	Waterbank dumps
ECT/12/B	colourless massive barite +(calcite)	Waterbank dumps

E) Llanharry Mine, South Wales

Sample I.D.	Mineral Association and Texture	Locality
LL/1/C	calcite crystal	Level 925'
LL/2/C	calcite crystal	Level 780
LL/3/C	calcite crystal	Level 780
LL/4/C	calcite crystal +stalactitic goethite	Level 216'
Ll/5/C	calcite crystal +goethite	Level 925'
LL/1/Q	calcite crystal +haematite	Level 925'
LL/2/Q	quartz crystal +banded haematite-goethite	Level 925'
LL/3/Q	quartz crystal + goethite	Level 216'
LL/4/Q	quartz crystal + stalactitic goethite	Level 925'

F) South Crofty, Mine Cornwall

Sample I.D.	Mineral Association	Locality
SC/1/F-CH	fluorite-chlorite stage	Providence Lode 420 level
SC/2/F-CH	fluorite-chlorite stage	Reeves Lode
SC/3/F-CH	fluorite-chlorite stage	Reeves Lode
SC/4/F-CH	fluorite-chlorite stage	Roskear "E" Lode 360 level
SC/5/F-CH	fluorite-chlorite stage	Roskear "E" Lode
SC/6/F-CH	fluorite-chlorite stage	North Pool Zone 360 level
SC/7/F-CH	fluorite-chlorite stage	North Pool Zone 360 level
SC/1/F-PG	fluorite-pegmatite stage	Dolcoath Lode 290 level
SC/2/F-PG	fluorite-pegmatite stage	Dolcoath Lode 315 level
SC/3/F-PG	fluorite-pegmatite stage	Dolcoath Lode 340 level

Appendix B

Data from Microthermometry

Table I Stage calibration standards

Substance	melting point(°C)
octane	-56.8
decane	-29.7
tridecane	-5.5
tetradecane	+5.9
benzil	+95
$AgNO_3$	212
$NaNO_3$	306
KNO_3	334
H_2O	-0
CO_2-H_2O synthetic inclusion	-56.6

Table II. Data from microthermometry (°C)

XNaCl refers to the NaCl/$CaCl_2$+NaCl ratio calculated from the paired T_{LM} and T_Mh readings and the NaCl-H_2O-$CaCl_2$ phase diagram by Oakes et. al. (1990)

Sample AL/2/F

T_H	T_{FM}	T_{Mh}	T_{LM}	%NaCl	XNaCl
157.8	-48	-22.5	-17.1	20.56	0.89
129.6	-53	-22.6	-17.5	20.86	0.88
121.9	-50	-23	-17.8	21.08	0.84
131.8	-50	-22.9	-17.7	21.00	0.85
114.0	-58	-23.2	-17.7	21.00	0.82
133.5		-23.2	-17.7	21.00	0.82
136.9	-60	-23.2	-17.7	21.00	0.82
134.5	-61	-22.7	-17.6	20.93	0.87
136.6	-58	-21.5	-18.2	21.37	0.97
133.4	-58	-22.7	-17.6	20.93	0.87
122.8	-56	-23.1	-18.4	21.55	0.83
129.8	-58	-23.5	-18.3	21.48	0.79
120.0	-58	-23.5	-18.3	21.48	0.79
129.7		-22.5	-18.0	21.27	0.89
133.5		-23.3	-18.3	21.48	0.81

130.7		-23.1	-18.3	21.48	0.83
125.5	-56	-23.1	-18.3	21.48	0.83
149.3	-54	-22.7	-17.0	20.46	0.87
141.5	-54	-22.7	-17.4	20.76	0.87
145.8		-23.2	-18.0	21.27	0.82
x=132.9	-55.3	-22.9	-17.9	21.12	0.85
std=10.3	3.71	0.45	0.43	0.33	0.04

AL/5/F

T_H	T_{FM}	$T_M{}^h$	T_{LM}	%NaCl	XNaCl
131.9	-61	-23.6	-20.1	22.8	0.78
130.1	-62	-23.9	-18.6	21.7	0.75
108.8	-60	-23.6	-18.6	21.7	0.78
120.3	-60	-23.2	-18.7	21.7	0.82
126.8	-61	-23.8	-19.7	22.5	0.76
135.0	-60	-23.2	-19.1	22.1	0.82
121.3	-61	-23.4	-18.8	21.8	0.80
112.6	-59	-23.7	-21.5	23.7	0.77
135.1		-23.7	-18.8	21.8	0.77
145.8		-23.5	-20.5	21.0	0.79
99.3	-67	-24.0	-19.9	22.6	0.74
130.2	-57	-24.6	-20.0	22.7	0.72
122.7	-61	-24.5	-20.0	22.7	0.72
133.7	-63	-25.1	-20.1	22.8	0.69
133.5	-63	-25.1	-19.9	22.6	0.96
x=125.8	-61.1	-23.9	-19.6	22.4	0.76
std=11.9	2.4	-0.64	0.84	0.6	0.04

AL/6/F

T_H	T_{FM}	$T_M{}^h$	T_{LM}	%NaCl	XNaCl
131.9	-56	-23.9	-18.9	21.9	0.74
109.2	-56	-23.9	-19	21.9	0.74
160.4	-51	-23.8	-19.8	22.6	0.76
130.7	-60	-23.8	-20.3	22.9	0.76
146.3	-56	-23.4	-19.0	22.0	0.80
129.6	-56	-23.4	-18.5	21.6	0.80
145.8	-58	-23.4	-18.5	21.6	0.80
135.6	-53	-23.2	-17.8	21.1	0.82
122.0	-56	-23.9	-19.0	22.0	0.75
135.0		-24.1	-19.5	22.4	0.74
126.4		-23.9	-19.7	22.5	0.74
113.6	-58	-23.1	-18.6	22.7	0.83
125.9		-23.6	-18.6	22.7	0.78
167.4	-54	-23.8	-18.6	22.7	0.76
125.7	-54	-22.8	-19.0	22.0	0.86
144.7	-56	-23.6	-18.7	21.8	0.78
152.7	-54	-22.6	-18.0	21.2	0.88
141.5	-54	-22.7	-18.0	21.2	0.87
133.7	-54	-22.9	-18.4	21.5	0.85
148.1	-54	-22.2	-17.9	21.1	0.92
x=136.3	-55.2	-23.4	-18.8	21.8	0.80
std=14.7	2.14	0.5	0.67	0.5	0.05

AL/7/F

T_H	T_{FM}	$T_M{}^h$	T_{LM}	%NaCl	XNaCl

	-53	-22.4	-17.6	20.9	0.9
	-53	-23.4	-18.6	21.7	0.80
	-56	-23.0	-18.9	21.2	0.85
	-56	-23.1	-18.5	21.6	0.83
	-53	-24.1			0.74
	-53	-24.3	-19.5	22.4	0.73
	-56	-22.9	-18.7	21.7	0.85
	-54	-23.0	-18.1	21.3	0.74
173.9	-58	-23.9	-19.3	22.2	0.85
72.8	-59	-23.9	-20.0	22.7	0.85
146.1	-58	-24.1	-18.6	21.7	0.74
113.9	-58	-22.4	-17.7	21.0	0.9
122.4	-58	-22.5	-17.7	21.0	0.89
84.6	-54	-22.7	--16.1	19.7	0.87
131.4	-58	-23.1	-18.0	21.2	0.83
142.1	-60	-23.5	-19.3	22.2	0.79
211.9	-60	-23.5	-19.4	22.2	0.79
x=133.4	-56.2	-23.2	-17.8	20.9	0.83
std=42	2.37	0.6	2.8	2.6	0.05

AL/10/F

T_H	T_{FM}	T_{Mh}	T_{LM}	%NaCl	XNaCl
124.4	-63	-23.4	-18.8	21.8	0.8
124.9	-60	-24.0	-19.5	22.4	0.74
128.0	-60	-23.4	-19.5	22.4	0.80
126.2	-60	-23.9	-18.8	21.8	0.75
115.4	-63	-23.4	-18.8	21.8	0.80
122.4	-64	-23.4	-18.9	21.9	0.80
123.5	-60	-24.33	-19.0	22.0	0.73
126.4	-60	-23.4	-18.8	21.8	0.80
114.2		-23.8	-20.3	22.9	0.76
127.2	-63	-24.1	-20.3	22.9	0.74
139.1	-58	-23.5	-20.6	23.1	0.79
131.8	-63	-23.5	-19.8	22.6	0.79
137.3	-63		-20.5	23.0	
132.3	-58	-23.2	-18.9	21.9	0.81
150.0	-58	-23.0	-18.4	21.5	0.84
126.4	-63	-23.9	-19.5	22.4	0.75
123.4	-63	-23.9	-19.5	22.4	0.75
125.7	-63	-23.9	-20.2	22.8	0.75
126.2	-63	-23.4	-19.5	22.4	0.80
125.9	-58	-23.4	-19.5	22.4	0.80
93.8		-22.4	-19.0	22.0	0.9
125.9	-61	-23.5	-19.4	22.3	0.79
10.6	2.1	0.43	0.66	0.47	0.04

AL/12/F

T_H	T_{FM}	T_{Mh}	T_{LM}	%NaCl	XNaCl
117.9	-53	-23.0	-19.7	22.5	0.84
119.0	-54	-23.5	-20.4	23.0	0.79
123.2	-54	-23.5	-20.4	23.0	0.79
124.4	-53	-22.8	-20.0	22.7	0.86
125.6	-53	-22.8	-20.0	22.7	0.86
130.7	-53	-23.2	-20.0	22.7	0.82
131.7	-53	-23.2	-20.3	22.9	0.83
126.2	-53	-23.1	-19.2	22.1	0.79

135.5	-53	-23.5	-19.2	22.1	0.79
134.0	-54	-23.5	-19.0	22.0	0.82
123.6	-54	-23.2	-19.2	22.1	0.74
114.3	-51	-24.0	-19.0	22.0	0.82
126.7	-53	-23.2	-19.9	22.6	0.82
108.7	-53	-23.2	-19.9	22.6	0.85
108.7	-53	-22.9	-19.0	22.0	0.84
116.9	-53	-23.0	-19.9	22.6	0.80
123.4	-52	-23.4	-19.9	22.6	0.84
x=122.7	-53.1	-23.2	-19.7	22.5	0.82
std=7.8	0.5	0.3	0.46	0.33	0.03

AL/11F

T_H	T_{FM}	T_{Mh}	T_{LM}	%NaCl	XNaCl
104.6	-57	-23.5	-19.6	22.4	0.79
111.4	-57	-23.5	-19.6	22.4	0.79
112.2	-56	-23.1	-18.1	21.3	0.83
	-58	-23.9	-18.9	21.9	0.75
	-63	-22.9	-18.4	21.5	0.85
	-67	-22.9	-18.5	21.6	0.85
117.5	-67	-22.9	-18.8	21.8	0.85
115.6	-58	-22.9	-18.8	21.8	0.85
	-66	-23.7	-17.6	20.9	0.77
	-66	-23.7	-19.0	22.0	0.77
114.6	-55	-22.4	-17.9	21.1	0.9
121.5	-57	-23.2	-18.0	21.2	0.81
110.5	-55	-22.8	-17.7	21.0	0.86
125.4	-65	-23.8	-18.0	21.2	0.76
125.9	-57	-22.3	-18.0	21.3	0.91
117.0	-57	-22.7	-17.9	21.1	0.87
113.2	-60	-23.3	-18.4	21.5	0.81
113.1	-59	-22.9	-18.7	21.8	0.85
111.2	-55	-23.2	-18.4	21.5	0.82
112.2	-57	-23.2	-18.7	21.8	0.82
x=115.1	-60	-23.1	-18.4	21.6	0.83
std=5.7	4.4	-0.43	0.6	0.42	0.04

AL/14/F

T_H	T_{FM}	T_{Mh}	T_{LM}	%NaCl	XNaCl
121.9	-58	-24.3	-19.0	22.0	0.73
116.0	-56	-24.5	-18.6	21.7	0.72
129.7	-58	-24.3	-18.9	21.9	0.73
129.5	-58	-24.0	-18.7	21.7	0.74
120.1	-58	-24.0	-18.7	21.7	0.75
122.1	-58	-24.0	-18.8	21.8	0.75
132.7	-58	-24.0	-18.7	21.7	0.75
135.4	-58	-24.0	-18.7	21.7	0.75
127.3	-63	-23.7	-18.6	21.7	0.77
121.1	-59	-23.7	-18.6	21.7	0.77
131.8		-23.8	-18.1	21.3	0.76
138.8			-18.3	21.4	
146.3	-58	-23.4	-17.0	20.5	0.80
149.0	-58	-23.9	-17.1	20.6	0.75
129.2	-53	-22.7	-16.5	20.1	0.87
128.8	-54	-23.8	-16.4	20.0	0.76
115.3	-55	-22.7	-16.1	19.7	0.87

126.0	-53	-22.4	-16.5	20.1	0.9
121.7	-53	-22.4	-16.5	20.1	0.9
119.4	-59	-22.8	-17.1	20.5	0.86
x=128.1	-57	-23.6	-17.8	21.1	0.79
std=9.2	-3.0	0.7	1.03	0.8	0.06

AL/15/F

T_H	T_{FM}	$T_M{}^h$	T_{LM}	%NaCl	XNaCl
135.0	-65	-24.0	-17.6	20.9	0.74
136.5	-63	-24.0	-18.1	21.3	0.74
131.8	-65	-24.3	-17.5	20.9	0.73
129.8	-61	-25.3	-17.6	20.9	0.68
130.7	-61	-27.8	-17.6	20.9	0.52
115.7		-22.4	-18.0	21.2	0.9
115.7		-22.4	-17.0	20.5	0.9
116.3		-22.4	-17.0	20.5	0.9
154.1	-63	-25.3	-17.6	20.9	0.68
137.6	-67		-17.9	21.1	
107.1					
120.2					
127.2					
130.7					
124.6					
x=127.5	-64	24.2	17.6	20.9	0.75
std=11.6	2.1	2.2	0.8		

AL/16/F

T_H	T_{FM}	$T_M{}^h$	T_{LM}	%NaCl	XNaCl
117.1	-58	-23.4	-18.1	21.3	0.8
113.0	-58	-22.8	-18.7	21.7	0.86
124.1	-58	-22.9	-18.7	21.7	0.85
133.5	-55	-23.0	-18.5	21.6	0.84
111.7	-55	-22.6	-18.5	21.6	0.88
116.0	-57	-22.4	-18.5	21.6	0.98
104.1	-53	-22.4	-17.8	21.0	0.9
114.1	-55	-22.0	-19.2	22.1	0.94
118.0	-53	-22.1	-19.6	22.4	0.93
115.7	-54	-22.1	-19.6	22.4	0.93
113.8	-56	-22.2	-19.2	22.1	0.92
102.5	-55	-22.4	-18.7	21.8	0.92
105.0	-55	-22.1	-19.0	22.0	0.93
107.1	-54	-22.1	-18.6	21.7	0.93
138.1	-56	-16.5	-23.1	24.0	0.85
104.2	-54	-17.0	-23.0	23.9	0.85
103.0	-54	-16.5	-23.1	24.0	0.85
135.8	-60	-17.8	-24.0	23.7	0.75
134.7	-60	-18.6	-23.9	23.6	0.75
133.3	-60	-18.8	-24.0	23.6	0.74
x=117.2	-56.0	-21.0	-23.2	22.4	0.87
std=12.0	2.2	2.4	2.3	1.0	0.07

AL/17/F

T_H	T_{FM}	$T_M{}^h$	T_{LM}	%NaCl	XNaCl
100.4					
100.4		-24.3	-18.5	21.6	0.73

114.3	-62	-24.3	-20.9	23.3	0.73
113.4	-62	-24.1	-20.9	23.3	0.74
116.3	-63	-22.9	-18.7	21.7	0.85
120.9	-62	-23.9	-20.5	23.0	0.76
121.2	-62	-23.6	-20.2	22.8	0.78
124.7	-62	-23.8	-20.1	22.8	0.76
119.9	-62	-23.6	-20.1	22.8	0.78
119.2	-62	-23.5	-20.2	22.8	0.79
118.4	-63	-23.5	-20.2	22.8	0.79
112.8	-63	-23.4	-20.2	22.8	0.80
119.2	-62	-23.5	-20.3	22.9	0.79
104.2	-61	-23.4	-19.1	22.1	0.80
124.7	-61	-23.6	-20.2	22.8	0.78
125.2	-60	-24.3	-19.3	22.2	0.73
120.3	-60	-22.9	-19.3	22.2	0.85
121.3	-61	-23.3	-20.2	22.8	0.81
111.2	-61	-23.1	-19.8	22.6	0.83
x=116.2	-62	-23.6	-19.9	22.6	0.79
std=7.6	1.0	0.5	0.5	0.5	0.04

AS/1/F

T_H	T_{FM}	T_Mh	T_{LM}	%NaCl	XNaCl
100.4	-53	-23.2	-21.9	24.0	0.82
94.2	-52	-22.4	-21.7	23.9	0.9
104.4	-52	-22.7	-21.7	23.9	0.87
1128.3					
105.6	-54	-22.3	-21.2	23.5	0.91
117.1	-53	-22.4	-21.5	23.7	0.9
98.3	-59	-21.6	-21.2	23.5	0.96
87.0	-53	-21.6	-20.3	22.9	0.96
106.1	-60	-22.5	-21.6	23.8	0.89
107.4	-61	-22.4	-22.0	24.0	0.9
106.6	-62	-22.5	-22.0	24.0	0.89
104.4	-62	-23.2	-21.8	23.9	0.82
106.8	-60	-22.7	-21.9	24.0	0.87
109.0	-62	-22.6	-21.9	24.0	0.88
105.0	-60	-22.7	-21.8	23.9	0.87
105.0	-56	-22.1	-21.2	23.5	0.93
92.1	-56	-22.9	-20.6	23.1	0.85.
102.3		-22.7	-20.8	23.3	0.87
99.2		-22.7	-20.9	23.3	0.87
101.5		-22.2	-21.2	23.5	0.92
x=104.3	-57	-22.5	-21.4	23.7	0.89
st=8.7	3.9	0.4	0.5	0.3	0.04

AS/2/F

T_H	T_{FM}	T_Mh	T_{LM}	%NaCl	XNaCl
93.0	-54	-16.5	-21.8	23.9	0.94
93.9	-54	-16.2	-21.3	23.6	0.94
93.4	-54	-16.2	-21.3	23.6	0.94
92.3	-54	-16.2	-21.3	23.6	0.94
99.5	-57	-20.8	-21.9	24.0	0.94
102.1	-57	-20.6	-21.9	24.0	0.94
94.9	-54				
100.6	-56	-18.7	-22.0	24.1	0.94
120.6	-56	-19.6	-22.1	24.2	0.94

112.4	-56	-19.8	-22.1	24.2	0.94
116.3	-54		-21.5	23.8	
115.3	-54		-20.4	23.0	
114.4	-57		-20.2	22.8	
99.7	-57	-22.7	-20.0	22.7	0.87
99.5	-58	-22.7	-20.0	22.7	0.87
97.6	-56	-22.4	-19.0	22.0	0.92
97.2	-55	-22.2	-19.2	22.1	0.92
x=103.7	-55	-19.6	-21.0	23.4	0.93
std=10.3	1.5	2.5	1.1	0.74	0.03

AS/3/F

T_H	T_{FM}	T_{Mh}	T_{LM}	%NaCl	XNaCl
101.7	-62	-19.9	-22.3	23.4	0.94
101.5	-56	-19.9	-22.1	23.4	0.94
98.4	-59	-18.6	-22.5	23.6	0.94
97.1	-59	-19.0	-22.5	23.6	0.94
100.7	-59	-19.9	-22.3	23.4	0.94
101.7	-60	-20.2	-22.0	23.4	0.94
100.7	-60	-19.9	-22.3	23.4	0.94
101.5	-63	-20.2	-22.2	23.3	0.94
99.3	-60	-19.9	-22.2	23.4	0.94
101.0	-57	-21.8	-20.0	22.7	0.95
100.6	-57	-21.5	-20.1	22.8	0.97
102.4	-55	-21.8	-19.9	22.6	0.95
103.7	-54	-21.8	-19.9	22.6	0.95
104.2	-56	-21.3	-19.9	22.6	0.98
105.2	-53	-21.7	-20.1	22.8	0.96
104.0	-53	-21.6	-20.2	22.9	0.96
104.4	-52	-21.1	-20.3	22.9	0.99
102.2	-54	-21.8	-19.9	22.6	0.95
98.6	-56	-21.7	-20.1	22.8	0.96
106.0	-56	-21.6	-20.1	22.8	0.96
				x=22.7	0.96
				std=0.12	0.01

AS/4/F

T_H	T_{FM}	T_{Mh}	T_{LM}	%NaCl	XNaCl
115.6	-50	-23.8	-20.6	23.1	0.76
111.6	-50	-23.4	-20.5	23.0	0.80
81.0	-54	-23.3	-20.5	23.0	0.80
93.8	-54	-23.7	-20.5	23.0	0.77
93.7	-54	-23.7	-20.5	23.0	0.77
100.8	-50	-23.7	-20.0	22.7	0.77
95.2	-50	-23.8	-20.8	23.2	0.76
91.4	-50	-23.0	-20.8	23.2	0.84
98.5	-50	-23.8	-20.8	23.2	0.76
100.8	-50	-23.8	-20.0	22.7	0.76
91.0	-56	-22.4	-19.9	22.6	0.9
93.8	-58	-22.2	-19.9	22.7	0.92
95.4		-22.1	-20.1	22.8	0.93
94.5		-22.4	-19.8	22.5	0.9
86.4		-22.9	-20.0	22.7	0.85
87.3		-22.3	-19.7	22.4	0.91
88.6		-22.0	-19.8	22.5	0.94
89.4		-22.0	-20.1	22.8	0.94

96.7		-22.2	-20.0	22.7	0.92
93.6		-22.4	-20.7	22.2	0.90
x=95.0	-52	-22.9	-20.2	22.9	0.85
std=8.0	2.9	0.7	0.4	0.3	0.07

AS/6/F

T_H	T_{FM}	$T_M{}^h$	T_{LM}	%NaCl	XNaCl
94.1	-59	-22.8	-20.0	22.7	0.86
93.3	-60	-21.6	-20.1	22.8	0.96
92.9	-60	-22.3	-20.2	22.8	0.91
94.0	-58	-22.5	-20.1	22.8	0.89
103.0					
116.6	-59	-21.9	-19.2	22.1	0.95
115.3	-63	-22.6	-20.0	22.7	0.88
115.0	-60	-23.0	-21.2	22.5	0.84
106.8	-55	-23.3	-20.3	22.9	0.81
109.3	-61	-23.4	-20.6	23.1	0.80
101.6	-60	-23.3	-20.8	23.2	0.81
102.6	-61	-23.4	-20.8	23.2	0.80
102.8	-61	-23.4	-20.9	23.3	0.80
104.9	-62	-23.3	-20.8	23.2	0.81
116.1	-61	-23.2	-20.9	23.3	0.82
x=104.5	-60	-22.8	-20.4	23.0	0.85
std=8.6	1.9	0.6	0.5	0.4	0.05

AS/8/F

T_H	T_{FM}	$T_M{}^h$	T_{LM}	%NaCl	XNaCl
94.5	-53	-22.5	-18.9	21.9	0.89
92.4	-57	-22.4	-18.8	21.8	0.9
108.2		-21.7	-17.6	20.9	0.96
92.6	-59	-22.4	-19.1	22.0	0.9
92.7	-59	-22.4	-19.1	22.0	0.9
105.0		-21.8	-18.2	21.4	0.95
96.2	-57	-22.2	-20.3	22.9	0.92
83.6	-56	-21.9	-17.2	20.6	0.95
82.3	-57	-21.8	-20.3	22.9	0.95
106.4	-60	-22.3	-19.7	22.4	0.91
88.4	-53	-22.3	-19.8	22.5	0.91
74.1	-53	-22.2	-19.8	22.5	0.92
89.6	-55	-22.0	-19.7	22.4	0.94
96.9	-55	-21.8	-20.6	23.1	0.95
95.3	-58	-23.2	-21.4	23.6	0.82
95.6	-55	-22.4	-20.6	23.1	0.9
100.1	-51	-22.4	-19.8	22.5	0.9
100.1	-51	-23.1	-19.9	22.6	0.83
80.8	-52	-22.6	-19.9	22.6	0.88
95.0	-51	-22.9	-19.8	22.5	0.85
x=93.5	-55	-22.3	-19.5	22.3	0.91
std=8.7	2.8	0.4	1.0	0.74	0.04

AS/10/F

T_H	T_{FM}	$T_M{}^h$	T_{LM}	%NaCl	XNaCl
96.4	-56	-18.4	-23.5	23.7	0.74
98.6	-59	-18.1	-23.6	23.7	0.74
97.9	-59	-18.5	-23.6	23.7	0.74

96.8	-60	-17.5	-21.5	23.9	0.75
90.6	-61	-19.3	-23.9	23.6	0.74
91.4	-61				
90.0	-60	-18.8	-23.2	23.6	0.75
95.1	-59	-19.0	-23.5	23.6	0.74
93.8	-59	-18.6	-23.0	23.6	0.75
94.3	-59	-19.1	-23.1	23.6	0.74
82.7	-57	-17.5	-22.9	23.9	0.75
94.1	-58	-16.7	-23.4	23.9	0.75
92.4	-60	-18.9	-22.9	23.6	0.74
107.0	-59	-16.8	-22.6	23.9	0.75
96.8	-58	-18.0	-22.7	23.7	0.75
106.4	-59	-23.4	-18.3	21.4	0.80
x=95.3	-59	-18.6	-22.8	23.5	0.75
std=5.9	1.1	1.5	1.4	0.6	0.01

DR/1/F

T_H	T_{FM}	$T_M{}^h$	T_{LM}	%NaCl	XNaCl
107.2	-22		-1.1	1.9	
131.9	-22		-1.4	2.5	
130.1	-21		-1.2	2.0	
132.3	-23		-0.8	1.4	
116.4			-1.0	1.7	
123.1			-1.2	2.2	
131.1			-1.2	2.0	
131.7			-1.0	1.7	
123.5			-0.8	1.4	
x=125.3	-22.2		-1.1	1.9	
std=8.7	0.7		0.2	0.4	

DR/2/F

T_H	T_{FM}	$T_M{}^h$	T_{LM}	%NaCl	XNaCl
135.0	-26		-1.7	3.0	
149.8	-27		-2.2	3.7	
158.7	-27		-2.2	3.7	
147.8	-27		-2.2	3.7	
164.0	-23		-1.4	2.5	
146.6	-29		-2.4	4.0	
148.1	-26		-2.4	4.0	
154.1	-26		-2.5	4.2	
152.2	-26		-2.6	4.4	
152.0			-2.5	4.2	
150.2			-2.5	4.2	
159.1			-2.8	4.6	
148.4	-26		-2.7	4.5	
152.0	-26		-2.9	4.8	
137.5	-26		-2.7	4.5	
158.1	-28		-2.5	4.2	
x=150.9	-26		-2.4	4.0	
std=7.5	1.4		0.4	0.6	

DR/4/F

T_H	T_{FM}	$T_M{}^h$	T_{LM}	%NaCl	XNaCl
88.8	-57	-22.5	-17.5	20.9	0.89
89.0	-61	-23.0	-18.5	21.6	0.84

89.8	-62	-23.2	-18.5	21.6	0.82
89.8	-63	-23.3	-18.6	21.7	0.81
87.7					
88.9	-58	-23.3	-18.5	21.6	0.81
88.5	-60	-22.8	-18.5	21.6	0.86
87.4	-59	-22.7	-17.4	20.8	0.87
87.9	-58	-22.5	-17.5	20.9	0.89
90.6	-55	-21.8	-16.3	19.9	0.95
81.3	-55	-21.8	-17.0	20.5	0.95
87.6	-55	-22.1	-17.0	20.5	0.93
83.9	-55	-14.3	-22.7	24.3	0.86
76.0	-63	-11.0	-22.8	24.7	0.86
93.4	-61	-2.7	-22.6	25.9	0.87
96.7	-61	-0.8	-23.4	26.2	0.88
74.1	-66	-2.3	-23.1	26.0	0.88
77.2	-65	-2.3	-23.6	26.0	0.88
74.1	-59	-7.6	-23.1	25.1	0.87
77.4	-62	-5.1	-23.5	25.6	0.87
88.9	-63	-1.8	-24.4	26.0	0.79
82.9	-64	-1.7	-24.7	26.0	0.74
x=85.5	-60			23.3	0.86

DR/5/F

T_H	T_{FM}	T_Mh	T_{LM}	%NaCl	XNaCl
75.7	-55	-22.5	-20.1	22.8	0.89
88.4	-61	-22.8	-19.2	22.1	0.86
111.1	-61	-23.4	-19.6	22.4	0.80
90.9	-55	-22.5	-20.5	23.0	0.89
86.7	-52	-22.8	-19.6	22.4	0.86
117.0	-53	-22.4	-20.5	23.0	0.90
111.4	-55	-22.4	-19.1	22.1	0.90
109.9	-52	-24.0	-20.1	22.8	0.74
92.6	-55	-23.5	-20.0	22.7	0.79
87.2	-55	-23.5	-19.3	22.2	0.79
76.9	-57	-22.9	-15.9	19.6	0.85
78.0	-53	-22.9	-17.6	20.9	0.85
68.5	-54	-23.0	-16.4	19.9	0.84
68.5	-54	-21.9	-16..6	20.2	0.95
67.9	-54	-23.0	-17.6	20.9	0.84
78.9	-56	-22.9	-16.6	20.2	0.85
87.2	-57	-22.4	-17.6	20.9	0.90
84.8	-55	-23.0	-19.1	22.1	0.84
76.9	-54	-22.4	-18.3	21.4	0.90
80.1	-55	-23.1	-16.7	20.3	0.83
x=86.9	-55	-22.9	-18.5	21.6	0.85
std=14.9	2.3	0.5	1.5	1.1	0.05

DR/6/F

T_H	T_{FM}	T_Mh	T_{LM}	%NaCl	XNaCl
82.6	-59	-22.3	-19.5	22.4	0.91
85.4	-59	-22.5	-20.5	23.0	0.89
85.4	-56	-22.1	-19.3	22.2	0.93
86.7	-55	-22.3	-20.5	23.0	0.91
84.0	-60	-22.4	-20.7	23.2	0.90
93.4	-60	-22.8	-17.6	20.9	0.86
91.7	-60	-23.0	-17.6	20.9	0.84

80.5	-59	-22.3	-17.8	21.1	0.91
91.4					
91.5		-22.5	-20.5	23.0	0.89
82.3	-56	-22.3	-18.3	21.4	0.91
80.3	-56	-23.1	-18.5	21.6	0.83
83.8	-62	-22.2	-18.6	21.7	0.92
85.9	-56	-22.5	-19.8	22.5	0.89
82.7	-59	-22.7	-19.8	22.5	0.87
90.4	-55	-22.5	-20.5	23.1	0.89
89.7	-55	-22.4	-20.0	22.7	0.90
70.0	-58	-22.2	-19.9	22.6	0.92
84.0	-58	-22.7	-20.5	23.1	0.87
85.5	-59	-22.0	-20.3	22.9	0.94
86.2	-59	-22.4	-19.9	22.6	0.90
x=85.4	-58	-22.5	-19.5	22.3	0.89
std=5.2	1.9	0.3	1.1	0.8	0.03

DR/7/F

T_H	T_{FM}	T_Mh	T_{LM}	%NaCl	XNaCl
	-53	-21.6	-16.5	20.0	0.96
	-53	-21.9	-15.9	19.6	0.95
		-21.6	-16.5	20.0	0.96
		-21.8	-15.4	19.2	0.95
		-21.8	-15.0	18.8	0.95
	-53	-21.6	-16.6	20.2	0.96
	-53	-21.5	-14.7	18.6	0.98
	-53	-22.0	-16.1	19.7	0.94
	-53	-22.0	-16.1	19.7	0.94
	-53	-21.4	-15.0	18.8	0.98
99.4	-55	-22.2	-15.7	19.4	0.92
100.0	-54	-22.0	-15.5	19.2	0.94
97.7	-56	-21.9	-15.6	19.3	0.95
97.7	-54	-22.2	-15.9	19.5	0.92
98.6	-54	-22.4	-15.5	19.2	0.90
99.7	-54	-22.7	-15.5	19.2	0.87
95.1	-52	-23.6	-15.6	19.3	0.78
106.4	-53	-22.7	-15.8	19.5	0.87
97.3	-53	-21.9	-15.9	19.5	0.94
96.4	-51	-21.9	-16.2	19.8	0.94
95.7	-51	-22.1	-15.9	19.5	0.93
99.5	-53	-22.2	-16.0	19.6	0.92
92.9	-51	-23.7	-16.0	19.6	0.77
92.9	-51	-22.2	-15.2	19.0	0.82
98.6	-53	-22.2	-15.1	18.9	0.82
x=97.9	-53	-22.1	-15.7	19.4	0.91
std=3.3	1	0.5	0.5	0.4	0.06

DR/8/F

T_H	T_{FM}	T_Mh	T_{LM}	%NaCl	XNaCl
80.1	-57	-22.7	-22.7	24.5	0.87
85.7	-63	-23.9	-23.5	24.9	0.75
85.7	-63	-23.4	-23.2	24.8	0.80
105.0		-19.5	-16.8	20.3	0.94
94.5	-56	-22.7	-16.8	20.3	0.87
126.2	-57	-23.6	-23.0	24.7	0.78
108.8	-56	-22.4	-18.2	21.4	0.90

150.7	-55	-22.3	-17.0	20.5	0.91
120.9	-56	-22.7	-15.7	19.4	0.87
81.4	-55	-20.5	-16.2	19.8	0.98
x=103.9	-57	-22.4	-19.3	22.1	0.87
std=23.2	3	1.4	3.3	2.4	0.07

DR/11/F

T_H	T_{FM}	$T_M{}^h$	T_{LM}	%NaCl	XNaCl
75.7	-61	5.5	-26.3	26.3	0.68
	-45		-9.5		
87.8	-66	4.3	-24.8	26.3	0.74
80.8	-66	-3.6	-23.3	25.9	0.87
92.7	-71	-1.2	-23.6	26.2	0.79
76.6	-68	5.3	-25.8	26.3	0.68
80.8	-68	-0.9	-26.0	26.2	0.68
71.8		3.8	-26.3	26.3	0.68
59.8		3.5	-27.2	26.3	0.63
116.3		-21.8	-16.0	19.6	0.95
x=80.2	-63.8	-0.6	-22.9	25.5	0.74
std=16.4	8.7	8.61	5.7	2.2	0.11

DR/12/F

T_H	T_{FM}	$T_M{}^h$	T_{LM}	%NaCl	XNaCl
84.5	-62	-17.8	-23.2	23.7	0.85
82.3	-62	-17.4	-23.3	23.9	0.85
83.1	-62	-17.8	-23.2	23.7	0.85
83.3	-62				0.85
79.4	-62				0.94
84.1	-62	-17.8	-23.3	23.7	0.94
81.1	-56	-20.5	-22.5	23.4	0.94
77.5	-66	-17.8	-21.7	23.7	0.85
84.4	-65	-17.8	-21.6	23.7	0.85
97.2		-16.4	-22.6	24.0	0.85
81.7	-59	-18.0	-22.8	23.7	0.85
84.8	-58	-17.2	-23.1	23.9	0.85
85.4	-60	-17.6	-22.9	23.7	0.85
84.8	-60	-17.2	-23.1	23.9	0.84
80.7	-60	-17.2	-23.1	23.9	0.85
85.5	-51	-22.0	-21.2	23.5	0.94
x=83.8	-60	-18.0	-22.7	23.7	0.88
std=4.2	3.6	1.5	0.7	0.15	0.04

DR/13/F

T_H	T_{FM}	$T_M{}^h$	T_{LM}	%NaCl	XNaCl
94.5	-55	-23.1	-23.0	24.7	0.83
84.5	-55	-23.1	-21.6	23.8	0.83
83.7	-66	-23.0	-21.6	23.8	0.84
86.6	-60	-23.2	-22.7	24.5	0.82
95.0	-61	-23.7	-23.6	25.1	0.87
91.1	-61	-23.7	-23.6	25.1	0.87
81.5	-61	-23.0	-22.7	24.5	0.84
93.5					
93.3	-60	-23.0	-22.1	24.1	0.84
90.5	-61	-22.9	-22.3	24.3	0.85
101.3	-60	-23.2	-21.2	23.5	0.82

102.6	-58	-23.2	-21.4	23.6	0.82
92.8	-56	-23.3	-20.8	23.2	0.81
70.7	-55	-22.7	-21.2	23.5	0.87
72.0	-56	-22.7	-21.2	23.5	0.87
84.5	-59	-22.7	-20.0	22.7	0.84
82.5	-56	-23.0	-20.2	22.9	0.84
79.9	-65	-20.0	-22.7	23.4	0.94
67.5	-55	-20.0	-21.8	23.4	0.84
87.0		-19.0	-22.8	23.6	0.85
83.6	-59	-17.6	-23.3	23.9	0.85
x=86.6	-59	-22.3	-22.0	23.9	0.85

DR/15/F

T_H	T_{FM}	T_{Mh}	T_{LM}	%NaCl	XNaCl
81.8	-54	-20.9	-15.5	19.2	0.98
82.0	-54	-21.8	-15.0	18.8	0.95
81.3	-53	-20.8	-15.0	18.8	0.98
91.5	-60	-21.9	-20.2	22.9	0.95
83.3	-53	-22.2	-15.6	19.3	0.92
82.7	-53	-21.9	-17.0	20.5	0.95
80.7	-53	-23.7	-16.2	19.8	0.77
95.8	-52	-21.7	-16.3	19.9	0.96
95.6	-53	-21.7	-15.3	19.1	0.96
92.4	-52	-21.9	-16.1	19.8	0.95
90.8	-52	-22.2	-15.6	19.3	0.92
73.1	-52	-22.1	-19.6	22.4	0.93
91.9	-53	-21.8	-20.6	23.1	0.95
77.2	-56	-21.9	-20.8	23.3	0.95
84.2	-56	-22.5	-20.8	23.3	0.89
94.2	-53	-21.9	-17.5	20.8	0.95
82.0	-55	-21.9	-20.2	22.9	0.95
87.7	-55	-22.1	-18.0	21.2	0.93
91.1	-52	-21.9	-20.0	22.7	0.95
87.7	-52	-21.9	-18.9	21.9	0.95
88.8	-55	-21.9	-20.2	22.9	0.95
x=86.5	-54	-21.9	-17.8	21.1	0.94
std=6.3	2	0.5	2.2	1.7	0.04

DR/16/F

T_H	T_{FM}	T_{Mh}	T_{LM}	%NaCl	XNaCl
93.3	-77	-23.3	-22.4	24.3	0.81
91.1	-76	-23.4	-22.4	24.3	0.80
93.1	-76	-22.9	-21.2	23.5	0.85
88.3					
88.7					
92.6	-76	-24.2	-22.4	24.3	0.74
92.1	-74	-24.0	-23.4	25.0	0.74
93.3	-74	-24.0	-22.7	24.5	0.74
93.3	-74	-23.9	-23.0	24.7	0.75
93.2	-74	-24.1	-23.2	24.8	0.74
83.9	-53	-22.5	-21.0	23.4	0.89
71.7	-63	-22.5	-21.0	23.4	0.89
83.2	-53	-22.4	-21.4	23.6	0.90
78.6	-63	-23.9	-22.4	24.3	0.75
91.9	-63	-24.0	-22.0	24.1	0.74
89.5	-72	-22.4	-22.0	24.1	0.90

91.1	-63	-23.4	-21.8	24.0	0.80
91.9	-71		-19.5	22.4	
116.3		-22.4	-18.2	21.4	0.90
116.3		-22.4	-18.2	21.4	0.90
x=91.7	-69	-23.3	-21.6	23.7	0.82
std=10.2	8.0	0.7	1.5	1.1	0.07

DR/18/F

T_H	T_{FM}	T_Mh	T_{LM}	%NaCl	XNaCl
77.9	-63	-23.6	-21.7	23.9	0.78
77.2	-58	-22.4	-19.9	22.6	0.90
78.8	-63	-23.3	-21.5	23.7	0.81
79.5	-63	-23.7	-21.9	24.0	0.77
86.0	-63	-22.4	-15.7	19.4	0.90
86.0	-63	-22.4	-16.8	20.3	0.90
81.0	-63	-22.4	-17.7	21.0	0.90
84.8	-63	-22.4	-18.6	21.7	0.90
79.7	-63	-22.9	-21.7	23.9	0.85
	-65	-22.2	-19.1	22.1	0.92
81.4	-51	-21.8	-15.1	18.9	0.95
83.9	-61	-22.3	-15.0	18.8	0.91
82.7	-52	-21.8	-15.1	18.9	0.95
75.5	-60	-22.0	-16.7	20.2	0.94
85.1	-60	-22.0	-16.7	20.2	0.94
82.9	-59	-22.8	-16.6	20.2	0.86
76.9	-57	-22.2	-16.1	19.7	0.92
90.4	-56	-22.1	-16.6	20.2	0.93
87.6	-56	-22.1	-16.1	19.7	0.93
x=82.1	-60	-22.5	-17.8	21.0	0.89
std=4.1	4	0.5	2.4	1.8	0.05

DR/19/F

T_H	T_{FM}	T_Mh	T_{LM}	%NaCl	XNaCl
88.4	-53	-22.0	-15.5	19.2	0.94
87.1		-22.4	-16.5	20.1	0.90
89.6		-22.2	-16.5	20.1	0.92
87.9	-56	-22.2	-15.5	19.2	0.92
85.8		-22.4	-15.5	19.2	0.90
87.9	-56	-22.7	-15.8	19.5	0.87
89.6	-56	-22.2	-16.5	20.1	0.92
78.7	-60	-22.7	-19.0	22.0	0.87
78.7	-55	-22.3	-16.1	19.7	0.81
83.8	-61	-22.7	-20.5	23.0	0.87
87.0	-60	-23.2	-19.0	22.0	0.82
89.8		-22.6	-20.0	22.7	0.88
90.9	-60	-22.9	-18.6	21.7	0.85
87.5	-60	-23.2	-19.5	22.4	0.82
84.9	-55	-21.9	-19.9	22.6	0.94
87.5	-51	-21.8	-20.3	22.9	0.95
89.8	-57	-22.0	-17.0	20.5	0.94
78.3	-57	-22.0	-16.9	20.4	0.94
82.0	-59	-22.1	-17.0	20.5	0.93
81.6	-62	-21.6	-16.1	19.7	0.96
94.4	-55	-22.7	-20.5	23.1	0.87
77.9	-61	-21.9	-19.9	22.6	0.94
x=85.9	-57	-22.4	-17.8	21.0	0.90

	std=4.6	3	0.4	1.9	1.4	0.05

DR/1/C

T_H	T_{FM}	T_{Mh}	T_{LM}	%NaCl	XNaCl
72.9	-62	-13.1	-23.4	24.4	0.86
75.8	-58	-22.9	-20.2	22.8	0.85
77.8	-59	-23.4	-19.8	22.6	0.80
89.2	-57		-22.5		
89.9	-62				
73.3	-61	-13.1	-23.4	24.4	0.86
75.3	-63				
	-60	-12.9	-23.6	24.4	0.76
73.6	-57				
69.4	-59	-13.3	-23.1	24.4	0.86
66.5	-61	-22.9	-20.0	22.7	0.85
64.6	-57	-23.4	-18.3	21.4	0.80
x=75.3	-59	-18.1	-21.6	23.4	0.83
std=8.1	2	5.3	2	1.2	0.04

ECT/3/C

T_H	T_{FM}	T_{Mh}	T_{LM}	%NaCl	XNaCl
80.5	-60	-26.3	-17.2	20.6	0.61
77.3	-58	-23.7	-16.9	20.4	0.77
79.9	-56	-25..8	-16.2	19.8	0.7
80.2	-56	-25.8	-16.2	19.8	0.64
75.1	-59	-25.1	-17.4	20.8	0.69
80.6	-58	-23.4	-17.4	20.8	0.80
82.0	-58	-25.6	-16.8	20.3	0.65
86.6	-57	-226.4	-17.6	20.9	0.60
	-67	-23.0	-16.6	20.2	0.84
87.0	-57	-23.4	-16.2	19.8	0.80
70.3	-56	-24.5	-17.0	20.5	0.72
73.7	-60	-25.2	-14.7	18.6	0.68
87.7	-55	-24.2	-16.8	20.3	0.84
x=80	-58	-24.8	-16.7	20.2	0.71

ECT/4/

T_H	T_{FM}	T_{Mh}	T_{LM}	%NaCl	XNaCl
57	-59	-23.7	-15.9	19.6	0.77
86.2	-59	-23.2	-17.6	20.9	0.82
82.2	-64	-23.4	-17.7	21.0	0.80
88.8	-61	-23.8	-17.6	20.9	0.76
88.9	-52	-23.1	-17.2	20.6	0.83
86.9	-57	-23.4	-17.3	20.7	0.80
83.8	-59	-23.9	-17.4	20.8	0.75
x=80.8	-59	-23.5	-17.2	20.6	0.79

ECT/8/C

T_H	T_{FM}	T_{Mh}	T_{LM}	%NaCl	XNaCl
57.8	-58	-22.7	-16.6	20.2	0.87
69.9	-57	-22.8	-15.6	19.3	0.86
73.8	-59	-22.8	-20.5	23.0	0.86
68.1	-57	-22.5	-16.6	20.2	0.89

66.5	-63	-23.2	-20.1	22.8	0.82
67.5	-57	-23.4	-15.1	19.0	0.80
x=67.3	-58	-22.9	-17.4	20.7	0.85

ECT/7/

T_H	T_{FM}	T_M^h	T_{LM}	%NaCl	XNaCl
69.3	-53	-22.4	-16.2	19.8	0.9
70.0	-52	-22.6	-15.3	19.1	0.88
70.4	-52	-23.4	-19.3	22.2	0.80
77.7	-53	-21.7	-12.6	16.7	0.96
66.3	-52	-26.3	-18.0	21.2	0.61
72.9	-51	-23.1	-23.0	24.7	0.83
68.1	-52	-22.5	-22.5	24.4	0.89
91.8	-50	-23.1	-22.5	24.4	0.83
72.4	-51	-22.4	-14.9	18.7	0.90
69.4	-52	-22.4	-15.9	19.6	0.90
	-52	--24.3	-19.4	22.3	0.73
x=72.7	-52	-22.2	-16.5	20.0	0.92

ECT/9/

T_H	T_{FM}	T_M^h	T_{LM}	%NaCl	XNaCl
67.8	-53	-26.7	-22.4	24.3	0.59
59.7	-53	-23.4	-19.3	22.2	0.80
	-53	-24.3	-22.4	24.3	0.73
90.0		-19.5	-20.2	22.8	0.94
59.1	-55	-23.4	-19.1	22.1	0.80
67.2			-17.7	20.9	0.79
x=69	-54	-23.5	-20.7	23.1	0.77

Llanharry samples

LL/4/C (L216 calcite)

T_H	T_{FM}	T_M^h	T_{LM}	%NaCl	XNaCl
78.3	-52	-24.6	-3.0	5.0	0.72
76.5	-52	-24.6	-3.0	5.0	0.72
79.5	-52	-26.6	-3.0	5.0	0.65
87.3	-56	-26.0	-6.0	9.2	0.62
83.7	-51	-28.2	-5.9	9.0	0.50
82.9		-25.3	-6.0	9.3	0.68
92.5	-52	-25.5	-6.0	9.3	0.66
100.5	-51	-28.2	-2.7	4.5	0.50
128.6	-54	-26.0	-6.0	9.2	0.63
144.6	-54	-26.0	-6.0	9.2	0.63
145.2	-55	-27.0	-5.7	8.8	0.57
x=100	-53	-26.1	-4.8	7.6	0.62

LL/5/C

T_H	T_{FM}	T_M^h	T_{LM}	%NaCl	XNaCl
61.7	-53	-25.6	-6.5	9.9	0.65
68.4	-55	-25.6	-8.0	11.7	0.65
66.0	-52	-24.6	-8.3	12.1	0.72
76.8	-51	-26.5	-8.4	12.3	0.60
77.2	-54	-27.5	-8.4	12.3	0.54
78.1	-55	-24.6	-8.1	11.9	0.72

66.5	-53	-24.6	-8.4	12.3	0.72
69.4	-52	-25.6	-6.2	9.5	0.65
74.2	-52	-26.5	-4.6	7.3	0.60
90.8	-55	-27.5	-4.6	7.3	0.54
x=72.9	-53	-25.8	-7.2	10.7	0.64

LL/3/Q

T_H	T_{FM}	$T_M{}^h$	T_{LM}	%NaCl	XNaCl
87.8		-25.1	-10.9	15.0	0.69
72.4		-26.9	-12.6	16.7	0.57
118.6	-54	-26.8	-12.9	16.9	0.58
70.8	-56	-26.0	-11.7	15.7	0.63
77.9	-59	-26.5	-12.3	16.4	0.60
65.7		-26.3	-12.6	16.7	0.61
84.3	-54	-26.0	-5.6	8.7	0.63
72.3		-26.8	-6.2	9.5	0.58
82.1	-60	-25.0	-9.7	13.7	0.70
106.5	-58	-25.2	-10.5	14.6	0.68
x=83.8	-57	-26.1	-10.5	14.4	0.63

LL/4/Q

T_H	T_{FM}	$T_M{}^h$	T_{LM}	%NaCl	XNaCl
69.4	-54	-24.5	-4.6	7.3	0.72
76.2	-52	-25.1	-6.5	9.9	0.69
82.0	-57	-26.0	-6.5	9.9	0.63
85.9		-24.7	-4.9	7.7	0.71
65.5		-24.7	-5.6	8.7	0.71
93.7	-53	-24.2	-6.5	9.9	0.74
97.1	-52	-24.9	-9.9	13.9	0.70
101.5	-54	-25.3	-9.9	13.9	0.68
111.2		-24.9	-10.3	14.4	0.70
80.1		-25.2	-9.2	13.1	0.68
100.5		-25.0	-9.2	13.1	0.70
x=87.6	-54	-25	-7.6	11.1	0.70

SC/1/F-CH

T_H	T_{FM}	$T_M{}^h$	T_{LM}	%NaCl	XNaCl
204.6					
274.3	-72	-26.7	-24.2	25.5	0.59
280.1	-69	-27.0	-24.2	25.5	0.57
298.2	-69	-27.5	-23.8	25.3	0.54
210.2	-67	-26.5	-22.9	24.6	0.60
222.2		-27.5	-20.0	22.7	0.54
279.0		-27.5	-19.9	22.6	0.54
242.2	-52	-37.3	-5.1	8.1	0.18
261.9	-52	-38.0	-5.1	8.1	0.15
238.3	-52	-37.9	-5.2	8.2	0.15
257.3	-52	-37.2	-5.2	8.2	0.18
241.4	-61	-33.3	-22.9	24.6	0.27
262.2	-62	-34.1	-23.6	25.1	0.25
244.6	-61	-42.4	-22.9	24.6	0.13
81.7	-57	-26.5	-11.0	15.0	0.60
78.3	-57	-26.4	-10.0	14.0	0.60

67.3	-59	-26.5	-10.0	14.0	0.60
82.2	-55	-27.3	-6.7	10.1	0.55
135.6	-62	-26.7	-17.1	20.5	0.59
130.6	-62	-26.2	-11.0	15.0	0.62
110.1	-59	-21.7	-25.7	23.3	0.96
130.3	-60	-22.9	-26.4	23.3	0.85
74.2	-51	-0.8	-21.9	26.2	0.96
92.0	-60	-3.7	-22.1	25.7	0.96
91.7	-60	-3.7	-21.9	25.7	0.96

SC/2/F-CH

T_H	T_{FM}	T_{Mh}	T_{LM}	%NaCl	XNaCl
325.8	-57	-26.4	-18.2	21.4	0.60
326.0	-56	-26.6	-18.2	21.4	0.60
326.7	-56	-27.1	-18.3	21.5	0.56
324.8	-72	-29.4	-18.2	21.4	0.43
325.3	-71	-26.9	-17.7	21.0	0.57
325.3	-72	-26.4	-17.7	21.0	0.60
311.6	-60	-26.4	-4.8	7.6	0.60
308.4	-59	-26.5	-4.9	7.7	0.60
314.6	-54	-24.6	-13.8	17.8	0.72
325.8	-67	-5.1	-27.2	25.6	0.62
319.5	-62	-6.5	-26.7	25.4	0.60
324.7	-64	-6.2	-26.6	25.4	0.60
142.3	-67	-4.0	-23.8	25.7	0.78
148.6	-71	4.2	-25.7	26.3	0.68
149.5	-72	4.2	-25.5	26.3	0.74
149.5	-72	4.9	-25.5	26.3	0.74
148.5	-72	6.7	-25.5	26.3	0.74
149.5	-71	4.2	-25.5	26.3	0.74
143.4	-78	-2.7	-23.8	25.9	0.78
152.0	-78	-5.6	-23.6	25.4	0.78

SC/3/F-CH

T_H	T_{FM}	T_{Mh}	T_{LM}	%NaCl	XNaCl
137.4	-55	1.1	-23.2	26.3	0.88
138.6	-55	1.6	-23.2	26.3	0..88
137.4	-55	-1.5	-23.7	26.2	0.79
137.7	-55	-1.5	-23.2	26..2	0.88
138.6	-55	1.1	-23.2	26.3	0.88
136.6	-56	1.4	-23.2	26.3	0.88
136.2	-56	-0.15	-23.2	26.2	0.88
136.7	-56	1.4	-23.4	26.3	0.88
136.7	-56	0.7	-23.7	26.3	0.79
135.9	-56	1.4	-22.7	26.3	0.88
132.5	-56	1.6	-23.5	26.3	0.88
131.8	-56		-23.2	26.3	0.88
131.8	-57	1.0	-23.5	26.3	0.88
131.8	-56	1.6	-23.7	26.3	0.79
132.6	-56	1.6	-23.5	26.3	0.88
131.7	-55	1.1	-23.7	26.3	0.79
136.4	-55	1.0	-23.2	26.2	0.88
137.4	-55	0.7	-23.2	26.3	0.88
133.6	-56	1.1	-23.2	26.3	0.88

135.5	-55	1.1	-23.7	26.3	0.79
x=135.3	-55.5	0.9	-23.3	26.3	0.86

SC/4/F-CH

T_H	T_{FM}	$T_M{}^h$	T_{LM}	%NaCl	XNaCl
101.1	-81	1.5	-26.8	26.3	0.63
93.5	-79	1.2	-26.2	26.3	0.68
83.8					
125.9	-75	0.8	-25.2	26.3	0.74
126.5		3.6	-25.6	26.3	0.68
125.9		1.2	-25.4	26.3	0.74
90.8	-77	-19.9	-24.6	26.4	0.70
113.8	-76	4.0	-25.2	26.3	0.74
135.5	-76	4.3	-24.6	26.3	0.74
113.8	-76	4.1	-24.6	26.3	0.74
100.1	-73	3.5	-25.9	26.3	0.68
112.4	-74	3.5	-25.6	26.3	0.68
113.8	-74	3.5	-25.6	26.3	0.68
116.8	-73	8.2	-25.9	26.3	0.68
x=111.0	-76.0	1.3	-25.5	26.3	0.70
std=15.2	2.5	7.6	0.7		0.04

SC/5/F-CH

T_H	T_{FM}	$T_M{}^h$	T_{LM}	%NaCl	XNaCl
247.8	-61	-24.7	-7.1	10.6	0.71
253.6	-62	-22.7	-6.9	10.4	0.87
246.6	-59	-24.9	-7.0	10.5	0.70
263.5	-61	-24.8	-7.0	10.5	0.71
228.0	-48	-22.0	-4.3	6.9	0.94
220.1	-52	-24.3	-4.5	7.2	0.73
219.9	-51	-22.7	-4.6	7.3	0.87
250.9	-55	-22.1	-6.0	9.2	0.93
275.3	-55	-24.3	-13.7	17..6	0.73
238.8	-63	-22.1	-6.0	9.2	0.93
256.9	-57	-24.6	-5.6	8.7	0.72
277.9	-59	-24.4	-5.6	8.7	0.73
271.5	-61	-22.7	-5.7	8.8	0.87
x=250.1	-57	-23.6	-6.5	9.7	0.80
std=19.5	4.7	1.2	2.4	2.7	0.1

SC/6/F-CH

T_H	T_{FM}	$T_M{}^h$	T_{LM}	%NaCl	XNaCl
105.0	-47	-34.6	-12.6	16.7	0.23
147.2	-47	-36.8	-24.5	26.3	0.17
288.2	-50	-38.8	-13.2	17.2	0.14
281.2	-47	-33.1	-13.0	17.0	0.28
239.9	-50	-35.9	-13.0	17.0	0.20
283.2	-49	-33.1	-13.2	17.2	0.28
295.3	-47	-4.1	-12.2	16.3	0.25
293.9	-49	-35.9	-13.0	17.0	0.20
267.4	-49	-35.0	-12.7	16.8	0.21
272.7	-50	-34.1	-13.2	17.2	0.25
289.3	-49	-33.6	-13.2	17.2	0.27
292.3	-47	-34.1	-13.2	17.2	0.25

282.3	-47	-40.3	-13.2	17.2	0.13
243.9	-22		-0.1	0.1	
264.0	-22		-0.33	0.6	
272.1	-22		-0.1	0.1	
243.9	-22		-0.33	0.6	
262.2	-22		-0.33	0.6	
290.3	-28	-21.5	-3.7	6.0	
x1=257	-48.5	-35.5	-13.9	17.7	0.22
x2=263	-22.9		-0.8	1.6	

SC/7/F-CH

T_H	T_{FM}	$T_M{}^h$	T_{LM}	%NaCl	XNaCl
218.4		-24.0	-11.2	15.3	0.74
225.9		-24.5	-11.3	15.4	0.72
158.0		-25.3	-11.2	115.3	0.68
245.8		-25.0	-11.5	15.6	0.70
218.3		-23.8	-11.6	16.7	0.76
208.5		-22.8	-11.5	15.6	0.86
210.1		-23.0	-11.2	15.3	0.84
193.9		-24.8	-11.1	15.2	0.71
212.0		-25.0	-11.1	15.2	0.70
190.7		-24.6	-11.0	15.1	0.72
267.2		-25.3	-11.7	15.7	0.68
241.4		-25.2	-11.5	15.6	0.68
251.2		-25.6	-11.7	15.7	0.65
227.5		-25.4	-11.5	15.6	0.67
244.2		-26.1	-11.5	15.6	0.62
214.6		-26.1	-11.4	15.5	0.62
x=220.5		-24.8	-11.4	15.4	0.71

SC/1/F-PG

T_H	T_{FM}	$T_M{}^h$	T_{LM}	%NaCl	XNaCl
304.2	-66	-26.0	-17.1	20.5	0.63
277.8	-57	-22.7	-4.2	6.8	0.87
308.3	-67	-26.5	-17.5	20.8	0.60
310.4	-72	-25.7	-17.3	20.7	0.65
289.4	-60	-22.8	-4.3	6.9	0.86
308.3	-63	-25.6	-17.7	21.0	0.65
289.2	-60	-23.8	-6.7	10.2	0.76
287.2	-60	-23.8	-6.5	9.9	0.77
288.0	-63	-23.6	-7.0	10.5	0.78
288.2	-60	-23.7	-6.5	9.9	0.77
290.1	-59	-23.7	-6.5	9.9	0.77
305.5	-71	-25.6	-14.1	18.1	0.65
311.1	-65	-25.5	-14.0	17.9	0.66
306.8	-70	-25.6	-14.0	17.9	0.65
310.5	-66	-26.5	-17.0	20.5	0.60
274.1	-70	-24.9	-7.9	11.6	0.70
292.6	-59	-25.0	-5.9	9.0	0.70
284.5		-22.1	-5.6	8.7	0.93
286.8		-23.2	-5.6	8.7	0.82
280.6		-20.8	-5.6	8.7	0.98
x1=295	-64	-24.3	-10.0	13.4	0.74
107.9	-71	2.1	-22.7	26.3	0.88
113.7	-71	2.1	-22.0	26.3	0.96
105.6	-71	2.1	-21.9	26.3	0.96

105.4	-70	2.1	-22.7	26.3	0.88
105.4	-68	2.1	-22.1	26.3	0.96
108.6	-71	2.2	-22.0	26.3	0.96
113.7	-62	2.1	-21.9	26.3	0.96
111.0	-61	2.1	-23.2	26.3	0.88
108.4	-55	1.6	-22.2	26.3	0.96
109.3	-61	2.0	-22.2	26.3	0.96
x2=109	-66	2.0	-22.3	26.3	0.94

Appendix C

Data from chemical analysis of fluid inclusions

Raw data from D-ICP analysis of fluid inclusions are shown in Table I in the form of atomic ratios. As shown in Chapter 3, replicate D-ICP analyses were performed on several samples; for those cases the mean and the standard deviation of the replicate readings is given. Also included in table I are the Ca/Na atomic ratios calculated from microthermometry following the procedure outlined in Chapter 4 and data set in Appendix B.

Section I, Table I.

Sample	K /Na mean and (std)	n	Li/Na mean and (std)	Ca/Na
AL/1/F	0.059 (0.004)	3	0.019	0.09
AL/2/F	0.050 (0.009)	5	0.0077 (0.0008)	0.09
AL/4/F	0.043	1	0.011	0.17
AL/5/F	0.051 (0.0037)	3	0.0064 (0.0007)	0.17
AL/6/F	0.058 (0.0058)	19	0.0095 (0.0009)	0.13
AL/7/F	0.041	1	0.011	0.13
AL/8/F	0.065 (0.012)	3	0.015 (0.003)	0.11
AL/9/F	0.048 (0.0019)	4	0.010 (0.0004)	0.14
AL/10/F	0.056 (0.0038)	21	0.013 (0.005)	0.14
AL/11/F	0.045	1	0.0076	0.11
AL/12/F	0.057 (0.008)	4	0.006 (0.001)	0.12
AL/13/F	0.055	1	0.0037	0.12
AL/14/F	0.072	1	0.019	0.14
AL/15/F	0.057 (0.01)	3	0.014 (0.002)	0.22
AL/16/F	0.119	3	0.009	0.08
AL/17/F	0.064 (0.007)	2	0.014 (0.0027)	0.14
AL/1/C	0.193	1	0.025	0.3
AL/2/C	0.076	1	0.013	0.12

Section I, Table I (continued)

Sample	K/Na mean and (std)	n	Li/Na mean and (std)	Ca/Na
AS/1/F	0.02 (0.004)	9	0.0023	0.07
AS/2/F	0.036	1	0.0037	0.04
AS/3/F	0.023 (0.004)	8	0.0025 (0.0009)	0.03
AS/4/F	0.023 (0.00027)	4	0.0024 (0.001)	0.09
AS/5/F	0.017	1	0.0025	0.09
AS/6/F	0.026	1	0.005	0.09
AS/7/F	0.017	1	0.0047	0.17
AS/8/F	0.023	1	0.0028	0.18
AS/9/F	0.031	1	0.0029	0.05

Sample	K/Na mean and (std)	n	Li/Na mean and (std)	Ca/Na
DR/1/F	0.038 (0.01)	2	0.0057	
DR/2/F	0.08 (0.014)	2	0.0042	
DR/4/F	0.017	1	0.0018	0.09
DR/6/F	0.014	1	0.0012	0.07
DR/7/F	0.0107 (0.0013)	5	0.0013 (0.00007)	0.05
DR/8/F	0.014 (0.0013)	3	0.0014 (0.00016)	0.08
DR/9/F	0.014 (0.0009)	5	0.0017 (0.00008)	0.05
DR/10/F	0.012 (0.001)	3	0.0011 (0.00012)	0.05
DR/11/F	0.021	1	0.0017	0.19
DR/13/F	0.015	1	0.0016	0.09
DR/15/F	0.018	1	0.0014	0.03
DR/16/F	0.018	1	0.0026	0.12
DR/18/F	0.011 (0.0008)	2	0.0016	0.07
DR/19/F	0.013	1	0.0015	0.06
DR/1/C	0.019	1	0.002	0.11
DR/2/C	0.025	1	0.0032	0.12

Table I (continued)

Sample	K/Na mean and (std)	n	Li/Na mean and (std)	Ca/Na
ECT/1/C	0.034	1	0.0021	0.15
ECT/3/C	0.022	1	0.0015	0.15
ECT/4/C	0.017	1	0.0014	0.15
ECT/5/C	0.041	1	0.0017	0.15
ECT/7/C	0.13	1	0.0022	0.09
ECT/8/C	0.046	1	0.0021	0.16
ECT/9/C	0.021	1	0.0018	0.16
ECT/11/C	0.107	1	0.0035	0.15
ECT/12/C	0.098	1	0.0043	0.15

Sample	Na/K atomic mean and (std)	n	Li/Na atomic mean and (std)	Ca/Na atomic
LL/4/C	0.063	1	0.0026	0.32
LL/5/C	0.125	1	0	0.30
LL/3/Q	0.048	1	0	0.23
LL//4/Q	0.085	1	0.0053	0.18

Sample	K/Na atomic mean and (std)	n	Li/Na atomic mean and (std)	Ca/Na atomic
SC/7/F-CH	0.32	1	0.053	0.22
SC/5/F-CH	0.142	1	0.093	0.13
SC/6/F-CH	0.106	1	0.069	1.8
SC/4/F-CH	0.086	1	0.0235	0.23
SC/3/F-CH	0.086	1	0.013	0.09

Section I, Table IIa. Analysis of variance (ANOVA) for the Na/K (wt) ratios.

sample	a	b	c	d	e	T_i	T_i^2
AL/6/F	8.76	9.35	9.11	9.46	11.19	47.87	2291.537
AS/1/F	30.90	30.50	31.96	32.93	38.46	164.75	27142.56
DR/9/F	41.30	40.50	39.80	42.90	47.50	212	44944

Source of Variance	Sum Squares	Variance	Degrees of Freedom	Mean Squares
Between sample	2855.477	190.3651	2 (h-1)	1427.738
Within sample	82.93812	6.52	12 (N-1)-(h-1)	6.91151
Total	2938.416	195.89	14 (N-1)	

$\Sigma_i T_i^2$=Sum of T_i^2 =74378.1

$\Sigma_i \Sigma_j x_{ij}^2$=sum of squares of all readings=14958.56

n=number of replicates per sample=5

h=number of samples=3

N=nh=15 total number of readings

Between Sample Sum Squares= $\left(\frac{\Sigma_i T_i^2}{n}\right) - \frac{T^2}{N}$=2855.477

Total Sum Squares=$[\Sigma_i \Sigma_j x_{ij}^2] - \frac{T^2}{N}$=2938.416

Within Sample Sum Squares= Total-Between Sample=82.93812

$F_{2,12}$ =Mean Square Between Sample/Mean Square Within Sample

$F_{2,12}$ (calculated) = 206.574

$F_{2,12}$(tabulated) =3.885 (0.05 probability)

$F_{2,12}$ (calculated) > $F_{2,12}$(tabulated)

Table IIb Analysis Of Variance (ANOVA) for the Na/Li(wt) ratios

sample	a	b	c	d	e	T_i	T_i^2
AL/6/F	301.8	318.7	318.1	330.3	342.6	1611.5	2596932
AS/1/F	1255	1217	1221	1261	2500	7454	55562116
DR/9/F	2010	1880	1827	1812	2014	9543	91068849

Source Of Variance	Sum Squares	Variance	Degrees Of Freedom	Mean Squares
between sample	6760494.633	450699	2 (h-1)	3380247.32
within sample	8074273.573	87585.26	12 (N-1)-(h-1)	109481.58
total	1313778.94	538284.9	14 (N-1)	

T=Sum of all readings =18608.5

T^2=3.46×10^8

$\Sigma_i T_i^2$=Sum of T_i^2=1.49×10^8

$\Sigma_i \Sigma_j x_{ij}^2$=sum of squares of all readings=31159358

n=number of replicates per sample=5

h=number of samples=3

N=nh=15 total number of readings

Between Sample Sum Squares= $\left(\frac{\Sigma_i T_i^2}{n}\right) - \frac{T^2}{N} = 6760494.633$

Total Sum Squares= $[\Sigma_i \Sigma_j x_{ij}^2] - \frac{T^2}{N} = 8074273.573$

Within Sample Sum Squares= Total-Between Sample=1313778.94

$F_{2,12}$ calculated=30.87

$F_{2,12}$ tabulated=3.885

$F_{2,12}$ calculated > $F_{2,12}$ tabulated

Section I, Table III.

Cl-Br-Na data from destructive neutron activation analysis are presented in Table II. Raw data were in the form of counts per second. The Cl-Br concentrations (μg) of leachates were calculated using the values obtained from a Cl-Br-Na standard solution which contained 20μgCl, 1μgBr and 12.6μgNa.

Table III. Data from Neutron Activation Analysis.

Sample	Cl μg	Na μg	Br μg
AL/1/F	12.3	5.6	0.059
AL/2/Fa	12.60	3.69	0.059
AL/2/Fb	6.40	1.9	0.028
AL/4/F	17.14	7.73	0.108
AL/5/F	9.28	4.04	0.0604
AL/6/Fa	9.50	3.60	0.046
AL/6/Fb	9.50	4.27	0.057
AL/6/Fc	5.83	2.23	0.031
AL/7/F	24.34	10.17	0.135
AL/8/F	3.79	1.55	0.0203
AL/9/F	15.73	5.34	0.154
AL/10/F	22.84	8.15	0.223
AL/10/Fb	20.45	9.26	0.217
AL/10/Fc	14.55	6.07	0.156
AL/11/Fa	7.34	3.55	0.040
AL/11/Fb	5.66	2.79	0.029

AL/11/Fc	1.45	0.657	0.0087
AL/12/F	1.35	0.70	0.007
AL/13/Fa	7.16	3.35	0.0732
AL/13/Fb	9.87	4.89	0.113
AL/13/Fc	3.67	1.79	0.032
AL/14/F	2.41	0.76	0.0112
AL/15/F	0.82	0.38	0.0047
AL/16/F	1.31	0.60	0.006
AL/17/F	1.94	0.86	0.009
AL/2/C	20.33	7.7	0.214

Table II (continued).

Sample	Cl mg	Na mg	Br mg
AS/1/F	9.51	4.98	0.053
AS/2/F	0.35	0.15	0.0025
AS/3/F	0.98	0.46	0.0053
AS/4/F	1.72	0.78	0.012
AS/5/F	2.81	1.35	0.0158
AS/6/F	1.05	0.53	0.005
AS/7/F			
AS/8/F	2.55	1.25	0.0204
AS/9/F	19.53	10.1	0.099

Sample	Cl µg	Na µg	Br µg
DR/1/Fa	2.34	0.69	0.037
DR/1/Fb	2.14	0.725	0.0304
DR/2/F	14.5	2.31	0.0209
DR/4/F	5.98	2.49	0.04
DR/6/F	0.26	0.13	0.0012
DR/7/F	4.86	1.78	0.0331
DR/8/F	6.6	2.85	0.054
DR/9/F	6.23	2.96	0.0497
DR/10/Fa	8.62	3.64	0.0584
DR/10/fb	8.23	3.77	0.0612

DR/11/F	2.69	0.78	0.0372
DR/13/F	7.16	3.35	0.113
DR/15/F	3.97	2.08	0.024
DR/16/F	3.44	1.76	0.023
DR/18/F	21.12	10.74	0.148
DR/19/F	4.27	2.43	0.037
DR/1/C	24.43	11.29	0.181

Sample	Cl µg	Na µg	Br µg
ECT/1/C	4.87	1.94	0.026
ECT/3/C	4.52	2.10	0.027
ECT/4/C	1.72	0.97	0.0105
ECT/5/C	2.19	0.98	0.0155
ECT/7/F	2.05	1.04	0.0147
ECT/8/C	6.12	3.04	0.055
ECT/9/C	7.00	2.80	0.048
ECT/11/C	7.19	2.86	0.142
ECT/12/C	49.70	15.50	1.228

Sample	Cl µg	Na µg	Br µg
SC/7/F-CH	10.32	3.83	0.012
SC/5/F-CH	8.31	3.07	0.0091
SC/6/F-CH	2.8	1.3	0.0021
SC/4/F-CH	7.03	3.00	0.012
SC/3/F-CH	1.03	0.45	0.0034
LL/4/C	1.17	0.515	0.0068
LL/5/C	0.127	0.08	0.00083
LL/3/Q	0.347	0.142	0.0024
LL/4/Q	0.986	0.389	0.0049

Section II. Calculations of dilution factors and quantification of leachate and decrepitate results.

Data from microthermometry (salinity and Ca/Na ratios) were combined with the

semiquantitative chemical analysis data (D-ICP and Neutron Activation), following a procedure outlined by Shepherd et. al. (1985a) in order to express the chemical analysis data in the form of "true" fluid inclusion concentrations. An example of the calculations and the resulting values for all fluid inclusions analyzed is given below.

If W= weight % NaCl *equivalents* (from thermometric analysis) and M(NaCl)=molecular weight of NaCl then

W/M(NaCl)= number of moles of NaCl *equivalents* in 100g of inclusion solution. Therefore,

$$W/M(NaCl) = n(NaCl)+n(KCl)+1.5n(CaCl_2)+1.5n(LiCl) \quad (1)$$

where n(NaCl), n(KCl), $n(CaCl_2)$ and n(LiCl) are the number of moles of NaCl.etc., in 100g of solution. The number of moles of each of the individual chlorides can be related to each other by the cation atomic ratios obtained from the leachate analysis:

$$n(KCl) = n(NaCl) \times K/Na \quad (2)$$
$$n(CaCl_2) = n(NaCl) \times Ca/Na \quad (3)$$
$$n(LiCl) = n(NaCl) \times Li/Na \quad (4).$$

Therefore, equations (2), (3) and (4) allow the values of n for the other components to be expressed as n(NaCl). If these are substituted back into equation (1) we obtain:

$$W/M(NaCl) = n(NaCl)[1+K/Na+1.5(Ca/Na)+1.5(Li/Na)] \quad (5)$$

The only unknown value is n(NaCl) so substitution of the known values will enable this to be calculated. Once has this been derived it can be put back into equation (2), (3) and (4) to derive n(KCl), $n(CaCl_2)$ and n(LiCl). As n refers to *molarity* (number of n in 100g of solution), the following calculation is undertaken in order to express the values as *molality* (number of moles in 1kg of H_2O). Molality can be expressed as:

$m(NaCl) = 1000n(NaCl)/100-\Sigma_i n_i M_i$, where n_i and M_i are the number of moles and molecular weight respectively for component i.

Therefore the molalities of the chlorides can be calculated. From the m(NaCl), $m(CaCl_2)$, m(KCl) and m(LiCl) values the total Cl content of the fluid inclusions can be calculated. The Cl concentration of the leachate (by neutron activation) can then be used to estimate the dilution factors involved in the analyses. By multiplying the Br and Na value of the leachate with that dilution factor we can calculate the Na and Br concentration of the fluid

inclusion. Then, the concentrations of Ca, K and Li can be estimated from the K/Na, Ca/Na and Li/Na atomic ratios which were determined by D-ICP (Table I) and thermometric analysis (Appendix B). The calculated values are presented in Table IV.

Table IV. Calculated Cl, Na, Ca, K, Br and Li fluid inclusion concentrations(mg/l).

Sample	Cl	Br	Na	Ca	K	Li
AL/1/F	170100	820	77680	12160	7770	420
AL/2/F	170200	790	49690	7780	4130	110
AL/4/F	189700	1200	85570	25300	6240	280
AL/5/F	189800	1240	82650	24430	7150	150
AL/6/F	180500	860	67560	15270	6530	190
AL/7/F	180400	1000	75380	17040	5240	250
AL/8/F	169500	910	69340	13260	8580	270
AL/9/F	186600	1830	63340	15420	5580	190
AL/10/F	186500	1820	66550	16200	6320	260
AL/11/F	176900	960	85560	16370	6530	200
AL/12/F	187400	970	97160	20280	9390	180
AL/13/F	187400	1300	76970	16060	7180	90
AL/14/F	173500	810	55010	13390	6720	310
AL/15/F	179400	1030	83230	31840	8330	450
AL/17/F	189800	880	84140	20490	9130	350
AL/2/C	187300	1970	70570	14730	9090	280

Sample	Cl	Br	Na	Ca	K	Li
AS/1/F	196100	1090	102690	12500	3310	65
AS/2/F						
AS/3/F	185100	1000	86130	4490	3210	68
AS/4/F	189200	1320	86260	13500	3360	55
AS/5/F	189200	1060	90560	14170	2610	68
AS/6/F	190300	910	95320	14920	4200	144
AS/7/F	189900	1340	85440	25260	2460	121
AS/8/F	203100	1620	99860	31260	3890	84
AS/9/F	179400	910	92760	8070	4880	81

Sample	Cl	Br	Na	Ca	K	Li
DR/1/F	11400	180	3360		220	6
DR/2/F	25500	37	4050		540	5
DR/4/F	192500	1290	80140	12540	2310	44
DR/6/F	181100	840	90530	11020	2150	33
DR/7/F	150200	1020	55000	4780	990	22
DR/8/F	179800	1470	77640	10800	1840	33
DR/9/F	150200	1200	71350	6200	1690	37
DR/10/F	150200	1020	63420	5510	1290	21
DR/11/F	227600	3150	66000	21810	2350	34
DR/13/F	200200	3160	93660	14660	2380	45
DR/15/F	164700	995	86270	4500	2630	36
DR/16/F	200600	1340	102640	21420	3130	81
DR/18/F	167800	1180	85320	10390	1590	39
DR/19/F	167300	1450	95200	9930	2100	43
DR/1/C	196400	1450	90770	17360	2920	55

Sample	Cl	Br	Na	Ca	K	Li
ECT/1/C	173400	930	69080	18020	3980	44
ECT/3/C	173400	1040	80570	21020	3000	36
ECT/4/C	173400	1060	97900	25540	2820	41
ECT/5/C	173400	1230	77840	20310	5410	40
ECT/7/C	171600	1230	87070	13630	19190	58
ECT/8/C	173400	1560	86140	22470	6720	55
ECT/9/C	202700	1390	81100	22570	2890	44
ECT/10/C	173400	3420	68980	17990	12510	73
ECT/11/C	173400	4280	54080	14110	8990	70

Sample	Cl	Br	Na	Ca	K	Li
LL//4/C	55300	320	24360	13560	2600	19
LL/5/C	80300	520	50600	26400	10720	
LL/3/Q	111900	770	45800	18320	3730	
LL/4/Q	81300	400	32080	10040	4620	52
SC/7/F-CH	120000	140	44540	17040	24170	710

SC/5/F-CH	68500	75	25300	5720	6090	710
SC6/F-CH	168000	130	78000	253680	14020	1620
SC/4/F-CH	240100	410	102110	40840	14980	720
SC/3/F-CH	228100	750	99670	15600	14530	390

Section III, Charge balance calculations.

The charge balance of the inclusion solutions, or the number of positive charges divided by the number of negative charges, was calculated using the following equation as in Shepherd et. al. (1985a).

$$[\Sigma cZc/(Cc/Ac)]/\ [\Sigma a/Za/(Ca/Aa)]$$

where Zc and Za are the number of charges for individual cations and anions respectively, and C and A represent concentrations and atomic weights of cations (c) and anions (a).

For example, substitution of the chemical analysis results for sample Al/1/F to the above equation yields a charge balance of 0.88. This value which is lower than 1, indicates a slight excess of negative charges in the leachate solution. This however is within the acceptable limits of error (deviation from unity is lower than 0.30) and it is considered reasonable since cations such as Mg and Ba were not incorporated in the calculations.

Section IV, Table IV. Results from whole-rock ICP analysis of fluorites.

Sample	CaO%	SiO_2%	Al_2O_3%	Na_2O%	K_2O%	MgO%	Fe_2O_3%
AL/8/F	69.4	2.01	0.04	0.02	0.03	0.07	0.05
AL/8/F	69.9	2.08	0.03	0.02	0.04	0.08	0.05
DR/1/F	69.1	0.52	0.03	0.05	0.05	0.10	0.05
DR/8/F	71.3	0.59	0.04	0.07	0.04	0.07	0.05
DR/3/F	71.5	0.46	0.03	0.06	0.06	0.09	0.05
AL/6/F	69.5	1.40	0.02	0.12	0.07	0.04	0.03
AL/6/F	70.2	1.37	0.03	0.06	0.06	0.02	-
AS/4/F	70.3	0.60	0.00	0.03	0.02	0.05	0.03
AL/2/F	56.1	22.30	0.04	-	0.04	0.03	-
AL/2/F	54.6	22.75	0.02	-	0.03	0.02	-
AL/14/F	71.5	0.39	0.02	-	-	0.02	-
AL/14/F	70.6	0.34	0.02	-	-	0.02	-
DR/7/F	71.02	0.29	0.02	0.03	0.01	0.02	-
AS/1/F	72.35	0.35	0.02	-	-	0.03	-
AS/1/F	71.24	0.31	0.01	-	-	0.02	-
DR/10/F	71.84	0.44	0.02	0.04	-	0.03	0.01

Sample	Ba(ppm)	Sr(ppm)	Cu(ppm)	Zn(ppm)	La(ppm)	Zr(ppm)	Be(ppm)
AL/8/F	7.51	33.24	4.80	2.07	16.22	45.34	-
AL/8/F	7.46	32.09	4.22	-	20.27	75.19	0.21
DR/1/F	8.40	96.98	5.41	2.60	-	44.63	-
DR/8/F	195.06	66.83	12.31	14.39	-	24.47	-
AS/3/F	102.40	59.64	13.26	7.11	-	46.72	0.24
AL/6/F	3.22	49.33	9.21	8.45	108.35	131.27	2.85
AL/6/F	12.06	52.61	0.63	-	105.05	105.26	3.21
AS/4/F	422.21	67.71	13.56	7.85	-	29.83	-
AL/2/F	13.38	56.87	2.48	17.81	51.25	125.68	1.68
AL/2/F	11.36	55.35	-	-	45.61	59.86	1.53
AL/14/F	10.58	55.59	11.01	30.97	49.76	28.42	0.77
AL/14/F	9.03	55.06	-	-	45.09	57.40	0.76
DR/7/F	32.57	75.23	2.67	2.63	-	48.22	-
AS/1/F	10.95	52.69	6.32	8.40	-	23.46	-
AS/1/F	9.47	50.80	-	-	-	9.20	-
DR/10/F	12.3	67.33	2.77	-	-	26.74	-

Section V, Table V. Results from crush-leach ICP analysis. Standard deviations are given in parentheses where replicate analyses were undertaken.

Sample	K/Na(wt)	Li/Na(wt)
AL/6/F	0.106 (0.007)	0.003 (0.0006)
AL/2/F	0.149	0.0026
AL/1/F	0.121	0.0052
DR/18/F	0.025 (0.0023)	0.00033 (0.0001
DR/19/F	0.025	-
AL/11/F	0.084	0.0025
AL/12/F	0.098	-
AL/17/F	0.149 (0.0034)	0.0030
AS/10/F	0.049	0.0007 (0.0003)
AS/2/F	-	0.00078
AL/5/F	0.085	-
AL/4/F	0.105	0.0015
AL/13/F	0.155	0.0036
AL/7/F	0.095	0.0031
AS/1/F	0.049	0.0007 (0.0002)
AL/9/F	0.105	0.00043 (0.00015)
DR/7/F	0.033 (0.011)	0.00039

Section V, Table VI. Cl/Br data from ion-chromatography and Cl-selective electrode and Na/Br data from crush-leach ICP and ion chromatography.

Sample	Cl/Br (wt)	Na/Br (wt)
AL/9/F	98	23.4
AS/1/F	112 (60)	54 (25)
DR/7/F	263 (21)	96 (21)
DR/8/F	185 (45)	70 (6.1)
DR/10/F	185 (36)	80 (11.5)
DR/1/F	79.2	23.3
DR/2/C	84	29
DR/15/F	280	92
ECT/1/C	282	85

BIBL
LONDON
UNIV